BIOTYPING IN PSYCHIATRY

EDITED BY: Tae Young Lee, Hang Joon Jo, Shinsuke Koike and Andrea Raballo

PUBLISHED IN: Frontiers in Psychiatry

frontiers Research Topics

ISSN 1664-8714
ISBN 978-2-88974-569-2
DOI 10.3389/978-2-88974-569-2

About Frontiers

Frontiers is more than just an open-access publisher of scholarly articles: it is a pioneering approach to the world of academia, radically improving the way scholarly research is managed. The grand vision of Frontiers is a world where all people have an equal opportunity to seek, share and generate knowledge. Frontiers provides immediate and permanent online open access to all its publications, but this alone is not enough to realize our grand goals.

Frontiers Journal Series

The Frontiers Journal Series is a multi-tier and interdisciplinary set of open-access, online journals, promising a paradigm shift from the current review, selection and dissemination processes in academic publishing. All Frontiers journals are driven by researchers for researchers; therefore, they constitute a service to the scholarly community. At the same time, the Frontiers Journal Series operates on a revolutionary invention, the tiered publishing system, initially addressing specific communities of scholars, and gradually climbing up to broader public understanding, thus serving the interests of the lay society, too.

Dedication to Quality

Each Frontiers article is a landmark of the highest quality, thanks to genuinely collaborative interactions between authors and review editors, who include some of the world's best academicians. Research must be certified by peers before entering a stream of knowledge that may eventually reach the public - and shape society; therefore, Frontiers only applies the most rigorous and unbiased reviews.
Frontiers revolutionizes research publishing by freely delivering the most outstanding research, evaluated with no bias from both the academic and social point of view. By applying the most advanced information technologies, Frontiers is catapulting scholarly publishing into a new generation.

What are Frontiers Research Topics?

Frontiers Research Topics are very popular trademarks of the Frontiers Journals Series: they are collections of at least ten articles, all centered on a particular subject. With their unique mix of varied contributions from Original Research to Review Articles, Frontiers Research Topics unify the most influential researchers, the latest key findings and historical advances in a hot research area! Find out more on how to host your own Frontiers Research Topic or contribute to one as an author by contacting the Frontiers Editorial Office: frontiersin.org/about/contact

BIOTYPING IN PSYCHIATRY

Topic Editors:
Tae Young Lee, Pusan National University Yangsan Hospital, South Korea
Hang Joon Jo, Hanyang University, South Korea
Shinsuke Koike, The University of Tokyo, Japan
Andrea Raballo, University of Perugia, Italy

Citation: Lee, T. Y., Jo, H. J., Koike, S., Raballo, A., eds. (2022). Biotyping in Psychiatry. Lausanne: Frontiers Media SA. doi: 10.3389/978-2-88974-569-2

Table of Contents

frontiers in Psychiatry

EDITORIAL
published: 02 February 2022
doi: 10.3389/fpsyt.2022.844206

Editorial: Biotyping in Psychiatry

Tae Young Lee[1,2]*, *Hang Joon Jo*[3,4], *Shinsuke Koike*[5,6] *and Andrea Raballo*[7,8]

[1] Department of Psychiatry, Pusan National University Yangsan Hospital, Yangsan, South Korea, [2] Research Institute for Convergence of Biomedical Science and Technology, Pusan National University Yangsan Hospital, Yangsan, South Korea, [3] Department of Biomedical Engineering, Hanyang University Graduate School of Biomedical Science and Engineering, Seoul, South Korea, [4] Department of Physiology, Hanyang University College of Medicine, Seoul, South Korea, [5] Department of Neuropsychiatry, Graduate School of Medicine, The University of Tokyo, Tokyo, Japan, [6] Center for Evolutionary Cognitive Sciences (ECS), Graduate School of Art and Sciences, The University of Tokyo, Tokyo, Japan, [7] Division of Psychiatry, Department of Medicine, University of Perugia, Perugia, Italy, [8] Center for Translational, Phenomenological and Developmental Psychopathology, Perugia University Hospital, Perugia, Italy

Keywords: biotyping, biomarker, RDoC, psychiatry, NIMH

Editorial on the Research Topic

Biotyping in Psychiatry

Since Wilhelm Griesinger's famous statement that "all mental illnesses are cerebral illnesses" (aka brain mythology), there have been recursive calls for a global revision of psychiatric classifications to better accommodate for mental disorders as disorders of the brain (1). However, the cleavage between current diagnostic systems for mental disorders (which rely upon presenting signs and symptoms) and contemporary neuroscience has not been bridged, to the point that the Research Domain Criteria (RDoC) paradigm was launched as an alternative approach to optimize the identification of relevant neurobiological and behavioral systems involved in the pathogenesis of mental disorders (2). The basic inspiration of the RDoC was to reclassify mental diseases based on biological markers ranging from genes to circuits, physiology, behavior. Specifically, the central heuristic architecture of the RDoC is the deconstruction of human behavior and brain function into neuropsychological "domains" (i.e., "negative valence systems," "positive valence systems," "cognitive systems," "social processes," "arousal and regulatory systems," and "sensorimotor") and related subcomponents, thereby facilitating the identification of multilevel neurobiological substrates.

This move was essentially motivated by the empirical observation that polythetic diagnostic systems for mental disorders, such as the DSM and ICD, are taxed by high degrees of inter-class overlaps, comorbidity and heterogeneity, as well as diverse disease course and response to treatment within the same diagnosis (3). However, although the RDoC initiative was launched by the National Institute of Mental Health more than a decade ago, the gap between traditional research based on syndromic classification and RDoC-based investigation remains monumental and largely unaddressed (4). An obvious, pragmatic strategy to reduce such gap (and finally actualize Griesinger's hope) is to progressively move toward a hybrid system systematically enriching the biological fingerprints of present diagnostic categories, given that a fully biomarker-driven diagnostic system is still a rather distant and futuristic goal. Such a process will necessitate the iterative refinement of interim diagnostic systems and the establishment of standardized methodologies to maximize generalizability. For example, adopting a dimensional, trans-diagnostic perspective to reclassify symptoms could help the understanding of the pathophysiology of psychiatric illnesses in terms of onset, syndromic aggregation of signs and symptoms, and later outcomes. This might also inspire more precise treatment targets or preventive interventions. Therefore, this special Research Topic addresses promising new avenues centered around biotyping in psychiatry. The nine collected studies (2 systematic reviews, 1 mini-review, and 6 original

OPEN ACCESS

Edited and reviewed by:
Ulrich Ettinger,
University of Bonn, Germany

***Correspondence:**
Tae Young Lee
leetaey@gmail.com

Specialty section:
This article was submitted to Neuroimaging and Stimulation, a section of the journal Frontiers in Psychiatry

Received: *27 December 2021*
Accepted: *11 January 2022*
Published: *02 February 2022*

Citation:
Lee TY, Jo HJ, Koike S and Raballo A (2022) Editorial: Biotyping in Psychiatry. Front. Psychiatry 13:844206. doi: 10.3389/fpsyt.2022.844206

investigations) specifically focus on biotyping in order to redefine or reclassify existing mental diseases or to identify biomarkers necessary for such biotyping.

As per the two systematic reviews, first Fatih et al. addressed long-term intracortical inhibition (LICI) as a biomarker in neuropsychiatric disorders. They reviewed 113 articles on psychiatric disorders as well as neurologic disorders. The results indicate that although LICI may have utility as a biomarker of $GABA_B$ functioning, many studies present heterogenous methodology and inconsistent findings, thereby requiring a more substantial effort to increase shared standards in the field. Second, Miranda et al. conducted a systematic review of functional magnetic resonance imaging from the perspective of unsupervised machine learning applications for disease subtyping. However, the results for all explored diseases are inconsistent, indicating the need for concerted, multisite data collection in order to measure the generalizability of results.

The mini-review by Sugiyama et al. addresses the electrophysiological index for sensory processing dysfunctions in psychiatric disorders on the basis of findings of the auditory steady-state response (ASSR). They propose that ASSR amplitude, phase, and resetting responses are sensitive indices for investigating sensory processing dysfunction in psychiatric disorders.

As per the six empirical contributions presented in this topic, two focus on hippocampal subfield studies. Sasabayashi et al. conducted a hippocampal subfield volumetry across illness stages. They suggested that the reduced hippocampal subfield volumes may represent a common biotype associated with psychosis vulnerability. On the other hand, Tai et al. investigated the pathophysiology which protects against progressive hippocampal atrophy by altering neuronal plasticity or inducing neurogenesis. Egger et al. conducted a functional transcranial Doppler study of cerebral blood flow velocity patterns in patients with schizophrenia. The results support the view that schizophrenia, particularly symptom load and thus severity, influences performance in neurocognitive tasks whilst being related to distinct brain hemodynamic patterns. Takahashi et al. conducted an eye movements investigation as a non-invasive potential biomarker for the diagnosis of major depressive disorder. Free-viewing test, Lissajous trajectories of the smooth pursuit eye movement test, and fixation stability test were adopted. They suggested that the detailed parameters of eye movements can assist in differentiating depressive patients from healthy comparisons. Koshiyama et al. investigated an identification of the neural sources and their dynamic interactions using resting-state electroencephalography. This study provides evidence that abnormal resting-state electroencephalography oscillations are driven by patterns of hyper-connectivity across multiple frequency bands and a distributed network of the frontal, temporal and occipital brain regions that are involved in visual and auditory information processing in schizophrenia patients. Dong et al. investigated the prefrontal hemodynamics of patients with major depressive disorders using a head-mounted functional near-infrared spectroscopy.

Taken together, these articles explored state-of-the-art approaches to identify biomarkers or biotypes using a variety of methods, including long-term intracortical inhibition, resting-state or task-based functional connectivity, functional transcranial Doppler. However, to accelerate progress and minimize the risk of inconsistent results and generalizability problems, the next wave of biotyping research should establish standardized methods and adopt transdiagnostic approaches with a sufficient sample size.

AUTHOR CONTRIBUTIONS

TYL and AR wrote the manuscript. All authors provided important intellectual contributions, read, and approved the final version.

FUNDING

This work was supported by the National Research Foundation of Korea (NRF) grant funded by the Korea government (MSIT) (No. 2021R1A2C1006718).

REFERENCES

1. Griesinger W. *Die Pathologie und Therapie der Psychischen Krankheiten Für Aerzte und Studirende*. Stuttgart: Krabbe (1845).
2. Cuthbert BN. The role of RDoC in future classification of mental disorders. *Dialogues Clin Neurosci.* (2020) 22:81–5. doi: 10.31887/DCNS.2020.22.1/bcuthbert
3. Hyman SE. Diagnosing the DSM: diagnostic classification needs fundamental reform. *Cerebrum*. (2011) 2011:6.
4. Maj M. Narrowing the gap between ICD/DSM and RDoC constructs: possible steps and caveats. *World Psychiatry*. (2016) 15:193–4. doi: 10.1002/wps.20370

Conflict of Interest: The authors declare that the research was conducted in the absence of any commercial or financial relationships that could be construed as a potential conflict of interest.

frontiers in Psychiatry

ORIGINAL RESEARCH
published: 27 November 2020
doi: 10.3389/fpsyt.2020.608154

Neurophysiologic Characterization of Resting State Connectivity Abnormalities in Schizophrenia Patients

Daisuke Koshiyama[1], Makoto Miyakoshi[2], Kumiko Tanaka-Koshiyama[1], Yash B. Joshi[1], Juan L. Molina[1], Joyce Sprock[1], David L. Braff[1] and Gregory A. Light[1,3]*

[1] Department of Psychiatry, University of California, San Diego, La Jolla, CA, United States, [2] Swartz Center for Neural Computation, University of California, San Diego, La Jolla, CA, United States, [3] VISN-22 Mental Illness, Research, Education and Clinical Center, VA San Diego Healthcare System, San Diego, CA, United States

OPEN ACCESS

Edited by:
Shinsuke Koike,
The University of Tokyo, Japan

Reviewed by:
Naoya Oribe,
Hizen Psychiatric Center (NHO), Japan
Vicente Molina,
University of Valladolid, Spain

****Correspondence:***
Makoto Miyakoshi
mmiyakoshi@ucsd.edu

Specialty section:
This article was submitted to Schizophrenia, a section of the journal Frontiers in Psychiatry

Received: *19 September 2020*
Accepted: *04 November 2020*
Published: *27 November 2020*

Citation:
Koshiyama D, Miyakoshi M, Tanaka-Koshiyama K, Joshi YB, Molina JL, Sprock J, Braff DL and Light GA (2020) Neurophysiologic Characterization of Resting State Connectivity Abnormalities in Schizophrenia Patients. Front. Psychiatry 11:608154. doi: 10.3389/fpsyt.2020.608154

Background: Patients with schizophrenia show abnormal spontaneous oscillatory activity in scalp-level electroencephalographic (EEG) responses across multiple frequency bands. While oscillations play an essential role in the transmission of information across neural networks, few studies have assessed the frequency-specific dynamics across cortical source networks at rest. Identification of the neural sources and their dynamic interactions may improve our understanding of core pathophysiologic abnormalities associated with the neuropsychiatric disorders.

Methods: A novel multivector autoregressive modeling approach for assessing effective connectivity among cortical sources was developed and applied to resting-state EEG recordings obtained from $n = 139$ schizophrenia patients and $n = 126$ healthy comparison subjects.

Results: Two primary abnormalities in resting-state networks were detected in schizophrenia patients. The first network involved the middle frontal and fusiform gyri and a region near the calcarine sulcus. The second network involved the cingulate gyrus and the Rolandic operculum (a region that includes the auditory cortex).

Conclusions: Schizophrenia patients show widespread patterns of hyper-connectivity across a distributed network of the frontal, temporal, and occipital brain regions. Results highlight a novel approach for characterizing alterations in connectivity in the neuropsychiatric patient populations. Further mechanistic characterization of network functioning is needed to clarify the pathophysiology of neuropsychiatric and neurological diseases.

Keywords: resting-state electroencephalography (EEG), effective connectivity, schizophrenia, source level analysis, biomarker, temporal cortex, frontal cortex

INTRODUCTION

Neurophysiologic abnormalities are commonly studied in patients with schizophrenia in response to experimental stimuli, cognitive, tasks, and even at rest. Neural oscillations play an essential role in cortico-cortical transmission and the integration of information across neural networks supporting critical brain functions, including perception, attention, and other higher-order cognitive functions (1–7).

Neural oscillations can be measured in the scalp electroencephalogram *via* a variety of analytic and experimental settings [e.g., spontaneous, evoked, induced, and emitted (8–10)], which have productively resulted in the identification of abnormalities across a broad range of conditions in schizophrenia patients. Task-related (i.e., evoked and induced) high frequency oscillatory abnormalities in schizophrenia patients, especially for gamma band oscillations (i.e., above 30 Hz), have been consistently reported among the myriad neurophysiological abnormalities seen in schizophrenia (8, 9, 11–17), and are associated with multiple cognitive deficits in patients (18). In contrast to the widely studied stimulus- or task-evoked gamma oscillations, spontaneous oscillatory abnormalities in schizophrenia, particularly in the gamma band, have been relatively less studied.

Resting-state EEG does not require behavioral responses to stimuli or cognitive tasks for elicitation and is already widely used as part of routine neurologic and psychiatric assessments (19). Spontaneous oscillations arise from the synchronous firing of neurons in distributed neuronal networks and are characterized at broadband frequency ranges detectable *via* scalp sensors. Such oscillations can also be characterized *via* the flow of spectral information among their calculated neural sources. Identification of the primary contributing neural sources as well as the dynamic interactions among sources of spontaneous EEG activity may elucidate fundamental pathophysiologic abnormalities associated with the illness which may ultimately yield clinically relevant applications (biomarkers of illness, risk of illness, or sensitivity to therapeutic interventions).

A recent review article reported that schizophrenia patients showed increases in the canonical theta, alpha, and beta bands, but with no difference in the delta band activity in scalp level responses (20). Despite enthusiasm for measures of gamma band phase locking and synchronization to steady-state stimulation (8, 21), resting state gamma band activity has not been commonly studied. Moreover, while such scalp-level responses have been extensively described, the spatial information of neural network dynamics underlying frequency-band specific resting-state EEG activity in schizophrenia patients is largely unknown. To our knowledge, only one paper, by Andreou et al. (22) reported increased resting-state gamma-band functional connectivity across the Rolandic operculum, a region that includes superior temporal and inferior frontal gyri, in schizophrenia patients.

In this study, a novel multivector autoregressive modeling method was developed and applied to assess the effective connectivity of resting-state EEG activity among cortical sources in schizophrenia patients and healthy comparison subjects. This data-driven approach enables an analysis of cortical network dynamics with directed information flow [e.g., Granger causality (23); increased or decreased EEG phase coherence between two cortical regions] using a correlation with a time delay. We hypothesized that patients with schizophrenia would show abnormal increased frequency-specific oscillations (e.g., gamma-band activity) across frontotemporal cortical networks. Furthermore, we aimed to characterize the networks associated with other frequency bands in schizophrenia patients and healthy comparison subjects.

MATERIALS AND METHODS

Subjects

EEG data from $n = 147$ healthy comparison subjects and $n = 159$ schizophrenia patients was processed. Recordings from $n = 2$ healthy comparison subjects and $n = 5$ schizophrenia patients were dropped in the quality control step in the pre-processing of EEG. In the sample of $n = 145$ healthy comparison subjects and $n = 154$ schizophrenia patients, age and sex were significantly different between the groups. Therefore, we removed the subjects of extreme value of age and sex, and used a final sample of $n = 126$ healthy comparison subjects and $n = 139$ schizophrenia patients in the effective connectivity analysis (**Supplementary Method 1**, **Supplementary Table 1**). Resting-state spectral characteristics assessed at a single principal component analysis (PCA)-based composite scalp sensor level were previously reported (24). Antipsychotics, anxiolytics, and anticholinergics were prescribed for 125, 27, and 42 schizophrenia patients, respectively. Since anxiolytics and anticholinergic medications are known to have potential impacts on resting state scalp EEG (25, 26), separate analyses of schizophrenia patients who did not have either anxiolytics nor anticholinergics ($N = 80$) were also conducted. Written informed consent was obtained from each subject. The Institutional Review Board of University of California San Diego approved all experimental procedures (071831, 170147).

Electroencephalography Recording and Pre-processing

Participants sat in a comfortable chair in a quiet room and were instructed to relax and with their eyes open. Subjects were closely monitored *via* a one-way mirror throughout this brief 5 min session. The recording could be paused if subjects appeared to be drowsy either by direct observation or as indicated in their EEG/EOG recordings. The recording would then be resumed after the subject was reminded to keep their eyes open.

EEG was continuously digitized at a rate of 1,000 Hz (nose reference, forehead ground) using a 40-channel Neuroscan system (Neuroscan Laboratories, El Paso, Texas). The electrode montage was based on standard positions in the International 10–5 electrode system (27) fit to the Montreal Neurological Institute template head used in EEGLAB (28). The system acquisition band pass was 0.5–100 Hz. Offline, EEG data were imported to EEGLAB 14.1.2 (29) running under Matlab 2017b (The MathWorks, Natick, MA). Data were high-pass filtered [finite impulse response (FIR), Hamming window, cutoff frequency 0.5 Hz, transition bandwidth 0.5]. EEGLAB plugin *clean_rawdata()* including artifact subspace reconstruction

(ASR) was applied to reduce high-amplitude artifacts (30–35). The parameters used were: flat line removal, 10 s; electrode correlation, 0.7; ASR, 20; window rejection, 0.5. Mean channel rejection rate was 4.2 % [standard deviation (SD) 2.3, range 0–15.8]. Mean data rejection rate was 2.0% (SD 3.5, range 0–22.4). The rejected channels were interpolated using EEGLAB's spline interpolation function. Data were re-referenced to average. Adaptive mixture independent component analysis (ICA) was applied to the pre-processed scalp recording data to obtain temporally maximally independent components (ICs).

Source Localization Using an Equivalent Current Dipole Model

The values in the column of the mixing matrix derived from ICA were mapped on to the scalp electrodes to obtain IC scalp topography, which represents scalp projection of ICA-derived effective EEG sources inside the brain (36). A previous study showed that this scalp topography is modeled well by an equivalent current dipole model, and in fact the "dipolarity" of IC scalp topography correlates with the mutual information reduced by ICA (37). Thus, even though ICA is agnostic on spatial information (electrode locations, electric forward model of the brain, or spatial information about location of the EEG generators), minimizing the mutual information in the decomposed signals naturally achieves a physiologically valid dipolar spatial projection pattern. These findings are often taken as evidence of physiological validity of ICA when applied to scalp-recorded EEG data (independence-dipolarity identity). This estimation of equivalent current dipoles was performed using Fieldtrip functions (38). Two symmetrical dipoles were estimated for scalp topographies (39).

Selection of Independent Components Representing EEG

To select brain ICs among all types of ICs, EEGLAB plugin *ICLabel()* was used (40). The inclusion criteria were (1) "brain" label probability > 0.7 and (2) residual variance i.e., var[(actual scalp topography) – (theoretical scalp projection from the fitted dipole)]/var(actual scalp topography) < 0.15. Seven subjects were removed because they did not have minimum of 4 brain ICs. The mean number of ICs remained was 12.5 (SD 4.5, range 4–25). To ensure consistency across computations, recordings longer than 300 s were truncated to 300 s. Mean data length was 297.7 s (SD 8.9, range 202–300).

Effective Connectivity Analyses

To calculate the grand-mean effective connectivity across ICs for each group, we applied EEGLAB plugin groupSIFT, which recently demonstrated successful application in other neuropsychiatric disorders (41). Renormalized partial directed coherence [RPDC (42)] was calculated across ICs (single window, logarithmically distributing 50 frequency bins from 2 to 55 Hz). This generated a connectivity matrix with the dimension of IC × IC for each participant. The grand-average optimum model order determined *via* the elbow detection method was 7.1 (SD 0.6) i.e. delayed effective connectivity up to about 64 ms was utilized. An autocorrelation function (ACF) test showed that probability for the residual to be white was 0.81 (SD 0.04). Data consistency (43) was 88.2 % (SD 4.3). The estimated equivalent dipole locations of the corresponding ICs were convolved with 3-D Gaussian kernel with 20 mm full width at half maximum (FWHM) to obtain probabilistic dipole density (truncated at 3 σ). The dipole density inside the brain space is segmented into anatomical regions defined by custom automated anatomical labeling [AAL (44)]; the original 88 anatomical regions in AAL were reduced to 76 by summarizing basal and deep limbic regions into two umbrella regions, upper and lower basal. The labels "upper basal" and "lower basal" were originally matched to ventral mid-cingulate, "mid-cingulate" as dorsal mid-cingulate, and "insula" as inferior frontal. The individual IC × IC connectivity matrix was thus mapped to a 76 × 76 connectivity matrix, on which RPDC was also mapped as a weighting factor to modulate pairwise dipole density to calculate graph edges. For both groups (healthy comparison subjects and schizophrenia patients), including a minimum of 70% of unique subjects was set to be an inclusion criterion for each graph node to be analyzed in the next stage. Also, for the group comparison (healthy comparison subjects and schizophrenia patients), 48/76 graph nodes showed overlap between the groups, which explained 82.3% of total dipole density, consistent with findings from Loo et al. (41). For the statistics of RPDC in the frequency domain, a weak family-wise error rate control was applied (45, 46). The brain graphs were visualized using BrainNet Viewer software (47).

RESULTS

The connectivity matrix that represents the group-difference [healthy subjects ($N = 126$) and schizophrenia patients ($N = 139$)] of each EEG band activity [a pre-defined $p < 0.0001$, corrected; two-tailed (48)] is shown in **Supplementary Figure 1**. The results revealed 10 graph edges (effective connectivity, i.e., increased or decreased EEG phase coherence between two cortical regions) for delta band (1–4 Hz), 16 for theta band (4–8 Hz), 14 for alpha band (8–14 Hz), 11 for beta band (14–30 Hz) and 8 for gamma band (30–50 Hz) activity (**Figures 1–3**). The connectivity results of healthy comparison subjects and schizophrenia patients are separately shown in **Supplementary Figure 2**.

The matrix of the group-difference [healthy subjects ($N = 126$) and schizophrenia patients who were not treated with anxiolytics or anticholinergics ($N = 80$)] of each EEG band activity ($p < 0.0001$, corrected; two-tailed) is also shown in **Supplementary Figure 3**. We revealed 10 graph edges for delta band, 14 for theta band, 17 for alpha band, 17 for beta band and 6 for gamma band activity (**Supplementary Figures 4, 5**).

Delta Band Activity (1–4 Hz)

Decreased effective connectivity from a region near the calcarine sulcus to the fusiform, temporal and middle cingulate gyri was detected in delta band in schizophrenia patients compared to healthy subjects (**Figures 1–3**). A bidirectional increased interaction between the right middle temporal gyrus and the right middle cingulate gyrus was also observed. These connectivities were more prominent in the right hemisphere.

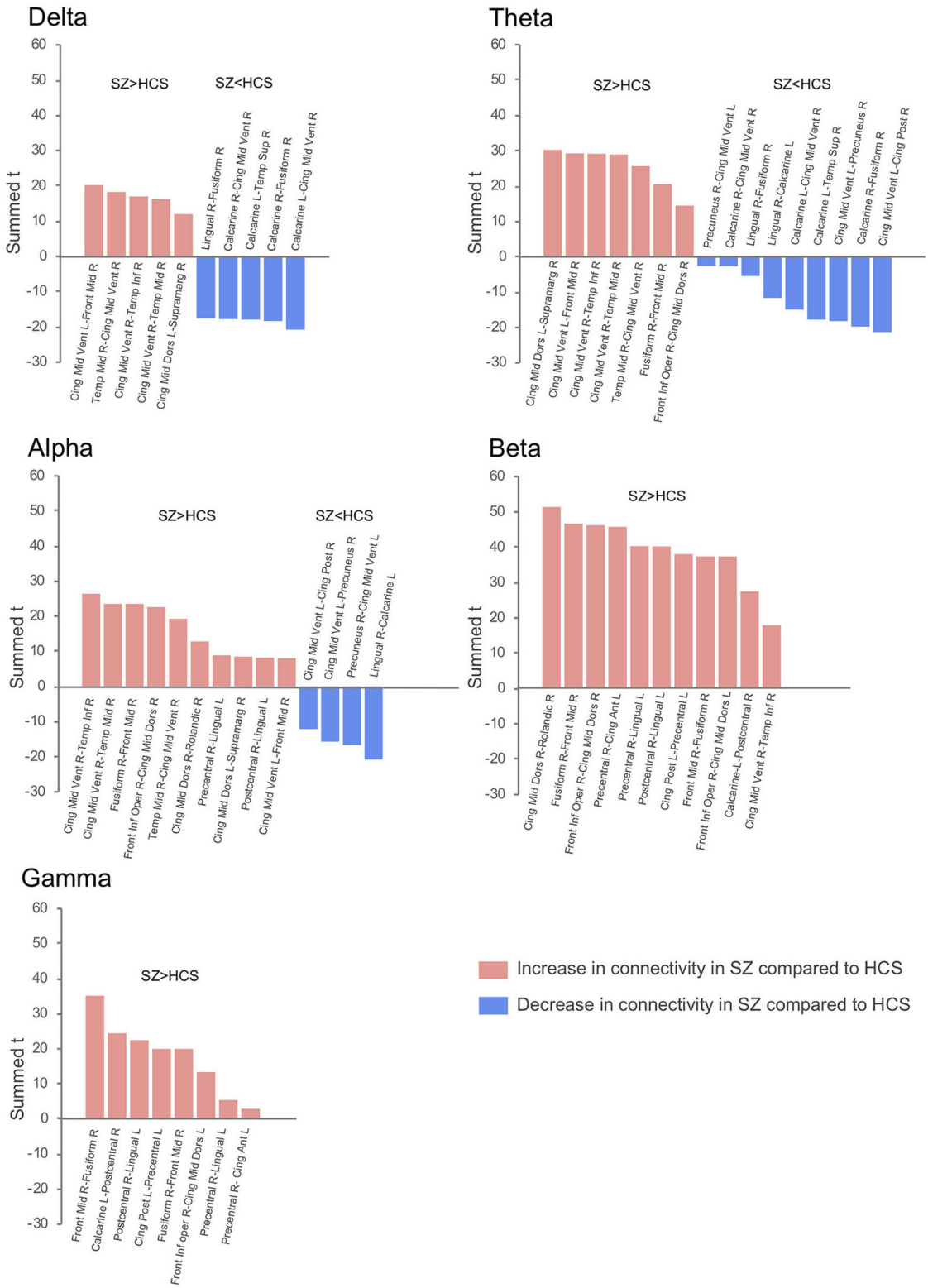

FIGURE 1 | Difference of effective connectivity in each EEG band activity between healthy subjects ($N = 126$) and schizophrenia patients ($N = 139$). SZ, schizophrenia; HCS, healthy comparison subject; L, left; R, right; Front Mid, middle frontal; Front Inf Oper, opercular part of inferior frontal; Cing Ant, anterior cingulate; Cing Mid Dors, dorsal middle cingulate; Cing Mid Vent, ventral middle cingulate; Cing Post, posterior cingulate; Temp Sup, superior temporal; Temp Mid, middle temporal; Temp Inf, inferior temporal; Rolandic, Rolandic operculum; Supramarg, Supramarginal.

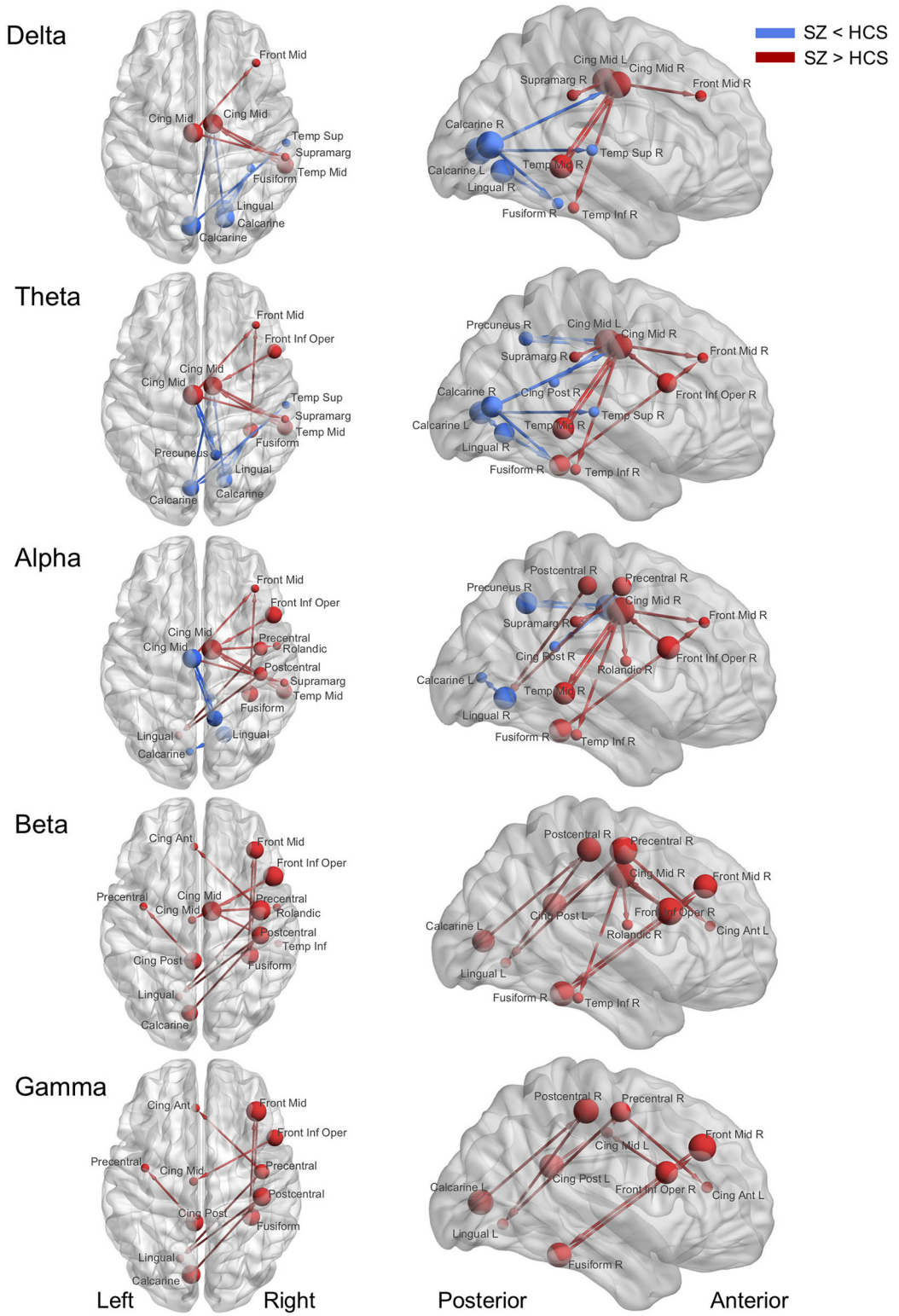

FIGURE 2 | Abnormal effective connectivity of resting-state EEG activity in schizophrenia patients. Red arrow indicates high effective connectivity and blue arrow indicates low connectivity in schizophrenia patients relative to healthy comparison subjects. Sphere size indicate amount of total outflow in each node. SZ, schizophrenia; HCS, healthy comparison subject; Front Mid, middle frontal; Front Inf Oper, opercular part of inferior frontal; Cing Ant, anterior cingulate; Cing Mid Dors, dorsal middle cingulate; Cing Mid Vent, ventral middle cingulate; Cing Post, posterior cingulate; Temp Sup, superior temporal; Temp Mid, middle temporal; Temp Inf, inferior temporal; Rolandic, Rolandic operculum; Supramarg, Supramarginal.

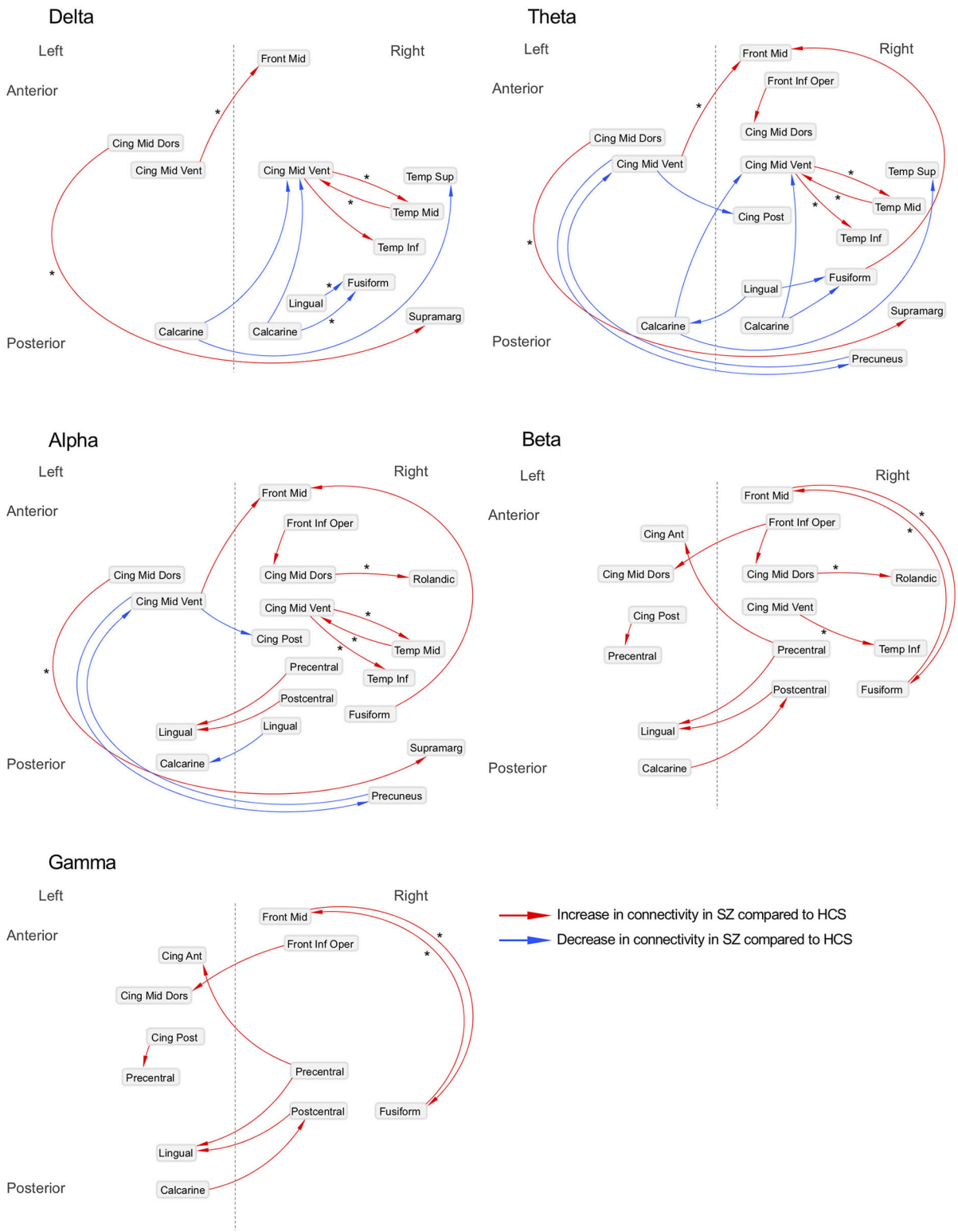

FIGURE 3 | Neural networks underlying resting-state EEG activity in schizophrenia patients. Difference of effective connectivity between healthy subjects ($N = 126$) and schizophrenia patients ($N = 139$) is shown; Asterisks (*) indicate the increased or decreased information flows observed in schizophrenia patients who did not have either anxiolytics nor anticholinergics ($N = 80$) compared to healthy subjects ($N = 126$). SZ, schizophrenia; HCS, healthy comparison subject; Front Mid, middle frontal; Front Inf Oper, opercular part of inferior frontal; Cing Ant, anterior cingulate; Cing Mid Dors, dorsal middle cingulate; Cing Mid Vent, ventral middle cingulate; Cing Post, posterior cingulate; Temp Sup, superior temporal; Temp Mid, middle temporal; Temp Inf, inferior temporal; Rolandic, Rolandic operculum; Supramarg, Supramarginal.

Theta Band Activity (4–8 Hz)

Theta band effective connectivity demonstrated a similar right-sided asymmetry centered on the temporal and middle cingulate gyri in schizophrenia relative to healthy subjects (**Figures 1**–**3**). Decreased effective connectivity from a region near the calcarine sulcus to the fusiform, temporal and middle cingulate gyri was also detected in theta band activity in schizophrenia patients compared to healthy subjects. The bidirectional increased interaction between the right middle cingulate gyrus and right middle temporal gyrus was also seen in theta band activity in schizophrenia patients relative to healthy subjects. Increased effective connectivity from the right fusiform gyrus to the right middle frontal gyrus was seen in schizophrenia relative to healthy subjects.

Alpha Band Activity (8–14 Hz)

The overall pattern of alpha connectivity is similar with those observed in theta band activity (**Figures 1**–**3**). Increased effective connectivity from the right middle cingulate gyrus to the Rolandic operculum (a region that includes auditory cortex and spans Broadmann areas 41 and 42) was detected in schizophrenia relative to healthy subjects. Increased effective connectivity from the right fusiform gyrus to the right middle frontal gyrus and the bidirectional increased interaction between the right middle cingulate gyrus and the right middle temporal gyrus were also seen in schizophrenia relative to healthy subjects.

Beta Band Activity (14–30 Hz)

Abnormal patterns of connectivity were observed among temporal, middle cingulate and occipital regions. These networks overlapped across beta and alpha band activity in schizophrenia patients compared to healthy subjects (**Figures 1**–**3**). Increased effective connectivity from the right middle cingulate gyrus to the Rolandic operculum was also seen in schizophrenia relative to healthy subjects. Increased bidirectional information flows between the right middle frontal gyrus and the right fusiform gyrus were detected in schizophrenia patients compared to healthy subjects.

Gamma Band Activity (30–50 Hz)

The increased bidirectional information flows between the right middle frontal gyrus and the right fusiform gyrus were also detected in gamma band activity in schizophrenia patients compared to healthy subjects (**Figures 1**–**3**). Although the abnormal neural network was overlapped across gamma and beta band activity in patients compared to healthy subjects, the overall structure was simpler and more localized for gamma vs. beta band activity. This relatively simpler structure for gamma band suggests that higher frequency abnormal networks in schizophrenia compared to healthy subjects consisted of more independent local networks that therefore did not connect with other regions.

DISCUSSION

Schizophrenia patients showed broad and widespread hyper-connectivity of cortical networks underlying resting-state EEG activity. Specifically, the following findings were detected; (1) decreased information flows from a region near the right calcarine sulcus to the right fusiform gyrus in delta band activity, and bidirectionally increased interactions between the right fusiform gyrus and the right middle frontal gyrus in beta and gamma band activity (i.e., "visual network"; **Figure 4**); (2) Increased information flow from the right middle cingulate gyrus to the Rolandic operculum across alpha and beta bands in schizophrenia patients compared to healthy subjects (i.e., "auditory network"; **Figure 4**); With few minor exceptions, these results were largely confirmed in a subgroup of schizophrenia patients who were not on anxiolytics or anticholinergics.

The present results replicate abnormal effective connectivity between frontotemporal regions in schizophrenia patients (22). Increased functional connectivity of alpha band activity at the superior parietal and the occipital lobe area at scalp levels of EEG in schizophrenia patients ($N = 28$) were previously reported by Liu et al. (49); we successfully replicate and extended the results showing the involvement of frontotemporal regions. We also previously reported that abnormal spontaneous gamma band activity measured *via* a spatial PCA of scalp channel data was associated with verbal memory performance (24). Although the PCA method used in the prior study provides a data-driven approach for characterizing macroscale/global oscillatory effects at the scalp, the neural interactions among sources were not assessed. The current results suggest that the spontaneous global gamma band abnormalities observed in schizophrenia patients at the scalp level appear to be generated by interactions between prefrontal and temporal regions.

A previous study by Andreou reported increased theta-band resting-state connectivity across midline, sensorimotor, orbitofrontal regions and the left temporoparietal junction in schizophrenia patients ($N = 19$) (50), consistent with our findings of right dominant increased effective connectivity among the temporal and middle cingulate gyri in broad band EEG activity including theta band activity. Inconsistencies in the laterality of effects, however, may be due to the difference of age or clinical severity. For example, the mean age of schizophrenia patients in the Andreou et al. study (50) was 23.5 vs. 44.6 years in the current study. Despite this difference in theta, our finding of increased alpha connectivity at the right temporal region at scalp levels of EEG in schizophrenia patients is fully consistent with the findings of Liu et al. (49).

Of note, despite the temporal differences between neural activity detected by very low frequency blood oxygenation-dependent (BOLD) hemodynamic responses and EEG, our resting-state EEG connectivity findings are also fully compatible with functional magnetic resonance imaging study (fMRI) findings of default mode network abnormalities in schizophrenia patients (51). The present findings of greater connectivity between the middle frontal, anterior cingulate and middle temporal gyri regions, is consistent with greater default mode network activation in schizophrenia (52).

Networks Centered at the Visual Cortex

The effective connectivity networks centered in the calcarine sulcus and the fusiform gyrus in broad band EEG activity

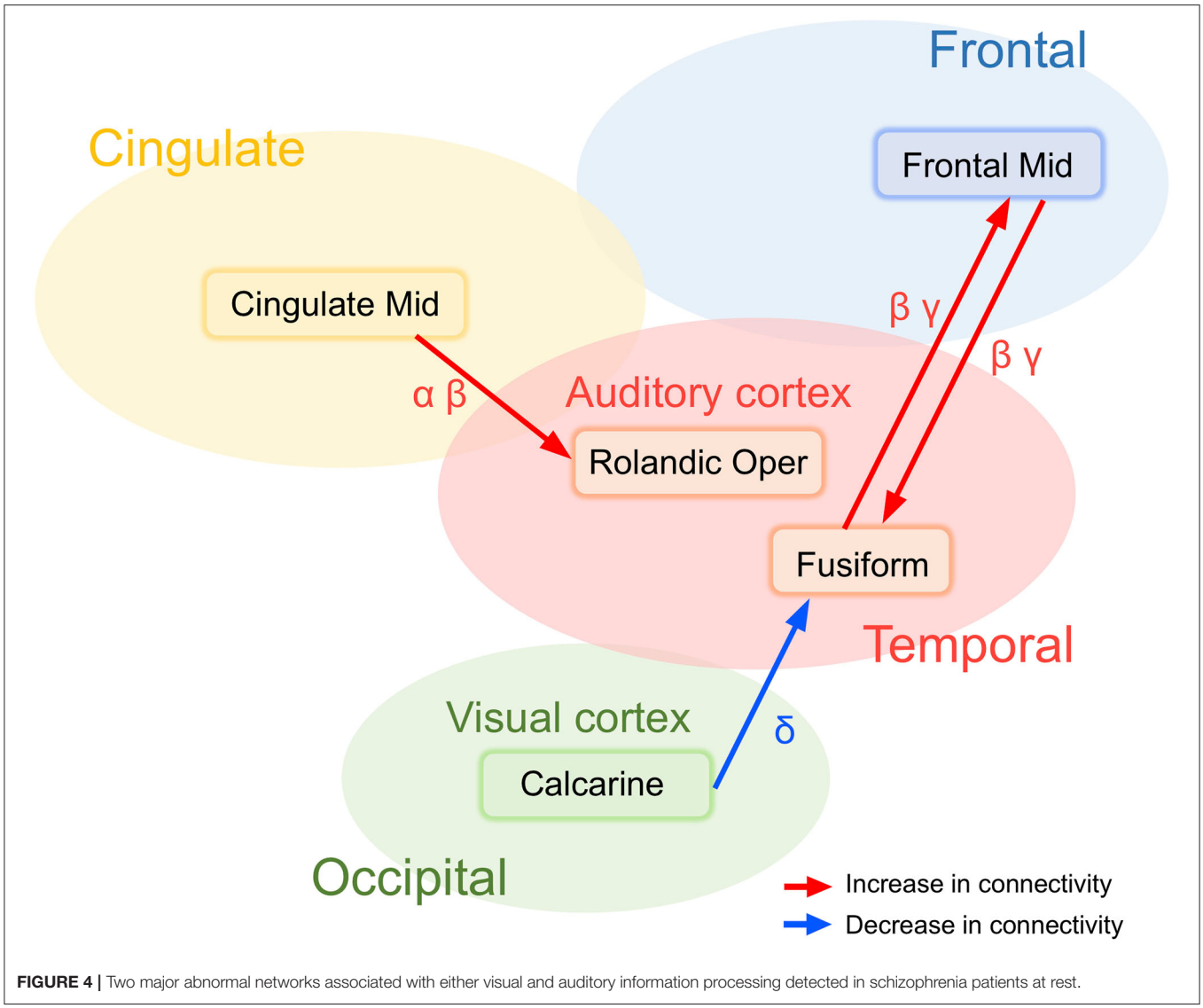

FIGURE 4 | Two major abnormal networks associated with either visual and auditory information processing detected in schizophrenia patients at rest.

were unexpected. The calcarine sulcus is a deep fissure that starts in the temporal lobe that continues into the occipital lobe with the primary visual cortex (V1) centered in this region. The fusiform gyrus is large region in the inferior temporal cortex that also has a functional role in visual information processing (53), including object and face recognition, and the recognition of facial expressions (**Figure 4**). Indeed, despite these unexpected associations, results are consistent with Morita et al. (54) findings of associated eye movement impairments with gray matter cortical thickness in schizophrenia patients in the middle frontal and fusiform gyri and the lateral occipital cortex. Although speculative, patients with schizophrenia may show abnormal excessive simultaneous activation of various perception-related brain regions, which may ultimately contribute to clinical symptoms such as hallucinations, aberrant salience, and delusions.

Networks Centered at the Auditory Cortex

Increased information flows were detected in schizophrenia patients from the right middle cingulate gyrus converging on the right Rolandic operculum (**Figure 4**). In the current analysis, primary auditory cortex is located in the region labeled the Rolandic operculum. Previous studies have demonstrated that deficits in early auditory information processing in schizophrenia patients as indexed by mismatch negativity (48, 55) and gamma-band auditory steady-state responses (9, 56, 57) are supported by distributed networks where the genesis of the responses are detected in the superior temporal gyrus (a region that includes auditory cortex) which subsequently propagate across other temporal and frontal brain regions. The present results suggest that resting state abnormalities in schizophrenia patients are present across multiple frequency bands and over relatively large spatial networks. Measures of network connectivity from cingulate gyrus to the auditory cortex may be therefore

account for multiple neurophysiologic biomarkers and show promise as a future candidate biomarker of abnormalities in schizophrenia patients.

Limitations

Results of this study should be considered in the context of several limitations. First, this is a cross-sectional cohort study of a heterogeneous sample of schizophrenia patients, the majority of whom were prescribed complex medication regimens. While comparisons of patients prescribed vs. not-prescribed medications that are known to impact resting state scalp responses (i.e., anxiolytics or anticholinergics) and healthy subjects showed similar patterns of results, it is possible that other medications including antipsychotics or symptoms may contribute to the observation of abnormal network dynamics. Carefully controlled prospective randomized controlled trials are needed to disentangle medication effects. Despite efforts were made to obtain medical/prescription records for all subjects, self- and informant reports of medication compliance, ultimately medication compliance could not be confirmed for the majority of patients in this study. As such, more rigorous analyses of medication doses and connectivity analyses were not pursued. Second, only 40 EEG channels were used for the analyses in this study. Future studies may benefit from the use of high-density EEG recordings with at least 64 channels (58), individual MRI data, and digitized scalp sensor locations rather than template head models and reliance on standardized electrode locations for potentially improved accuracy of source dynamics. Third, while we believe that elaboration of neural system dynamics reported here will be broadly applicable to multiple neuropsychiatric disorders, we acknowledge the possibility that results from schizophrenia patients with an established illness may not generalize to other populations like clinical high risk or first episode psychosis. Nonetheless, given improvements in medical care and life expectancy, patients with more chronic schizophrenia are likely to represent an increasing proportion of the total schizophrenia population; characterization of abnormal network dynamics among real-world patients *via* data-driven approaches for assessing network dynamics may ultimately be useful for application as biomarkers the development of therapeutics for this largely underserved population.

CONCLUSIONS

Results of this study provide evidence that abnormal resting-state EEG oscillations are driven by patterns of hyper-connectivity across multiple frequency bands and a distributed network of the frontal, temporal and occipital brain regions that are involved in visual and auditory information processing in schizophrenia patients. Future studies of the neural mechanisms underlying the networks detected in this study, in both future clinical and animal studies, are needed to clarify the pathophysiology of neuropsychiatric and neurological diseases in support of the development of novel therapeutic interventions.

DATA AVAILABILITY STATEMENT

The datasets generated for this article are not readily available to third parties. Requests to access the datasets should be directed to Gregory A. Light, glight@health.ucsd.edu.

ETHICS STATEMENT

The studies involving human participants were reviewed and approved by Institutional Review Board of University of California San Diego. The patients/participants provided their written informed consent to participate in this study.

AUTHOR CONTRIBUTIONS

JS and GL collected the data. DK and MM analyzed the data. MM wrote the Matlab code. DK, MM, YJ, JM, KT-K, DB, and GL interpreted the results. DK, MM, and GL designed the study. GL supervised all aspects of collection, analysis, and interpretation of the data. DK, MM, and GL wrote original manuscript. YJ, JM, KT-K, JS, and DB reviewed and edited the manuscript. All authors contributed to and approved the final manuscript.

FUNDING

This study was supported by JSPS Overseas Research Fellowships (DK), the Sidney R. Baer, Jr. Foundation, the Brain and Behavior Research Foundation, and the VISN-22 Mental Illness, Research, Education, and Clinical Center. Swartz Center for Neural Computation is supported by generous gift of Swartz Foundation (New York).

SUPPLEMENTARY MATERIAL

The Supplementary Material for this article can be found online at: https://www.frontiersin.org/articles/10.3389/fpsyt.2020.608154/full#supplementary-material

REFERENCES

1. Joliot M, Ribary U, Llinas R. Human oscillatory brain activity near 40 Hz coexists with cognitive temporal binding. *Proc Natl Acad Sci U S A*. (1994) 91:11748–51. doi: 10.1073/pnas.91.24.11748
2. Traub RD, Whittington MA, Stanford IM, Jefferys JG. A mechanism for generation of long-range synchronous fast oscillations in the cortex. *Nature*. (1996) 383:621–4. doi: 10.1038/383621a0
3. Miltner WH, Braun C, Arnold M, Witte H, Taub E. Coherence of gamma-band EEG activity as a basis for associative learning. *Nature*. (1999) 397:434–6. doi: 10.1038/17126
4. Rodriguez E, George N, Lachaux JP, Martinerie J, Renault B, Varela FJ. Perception's shadow: long-distance synchronization of human brain activity. *Nature*. (1999) 397:430–3. doi: 10.1038/17120
5. Hagoort P, Hald L, Bastiaansen M, Petersson KM. Integration of word meaning and world knowledge in language

comprehension. *Science*. (2004) 304:438–41. doi: 10.1126/science.1095455
6. Spellman T, Rigotti M, Ahmari SE, Fusi S, Gogos JA, Gordon JA. Hippocampal-prefrontal input supports spatial encoding in working memory. *Nature*. (2015) 522:309–14. doi: 10.1038/nature14445
7. Galuske RAW, Munk MHJ, Singer W. Relation between gamma oscillations and neuronal plasticity in the visual cortex. *Proc Natl Acad Sci U S A*. (2019) 116:23317–25. doi: 10.1073/pnas.1901277116
8. Uhlhaas PJ, Singer W. Abnormal neural oscillations and synchrony in schizophrenia. *Nat Rev Neurosci*. (2010) 11:100–13. doi: 10.1038/nrn2774
9. Hirano Y, Oribe N, Kanba S, Onitsuka T, Nestor PG, Spencer KM. Spontaneous gamma activity in schizophrenia. *JAMA Psychiatry*. (2015) 72:813–21. doi: 10.1001/jamapsychiatry.2014.2642
10. Sun Y, Farzan F, Barr MS, Kirihara K, Fitzgerald PB, Light GA, et al. Gamma oscillations in schizophrenia: mechanisms and clinical significance. *Brain Res*. (2011) 1413:98–114. doi: 10.1016/j.brainres.2011.06.065
11. Molina JL, Voytek B, Thomas ML, Joshi YB, Bhakta SG, Talledo JA, et al. Memantine effects on electroencephalographic measures of putative excitatory/inhibitory balance in schizophrenia. *Biol Psychiatry Cogn Neurosci Neuroimaging*. (2020) 5:562–8. doi: 10.1016/j.bpsc.2020.02.004
12. Thune H, Recasens M, Uhlhaas PJ. The 40-Hz auditory steady-state response in patients with schizophrenia: a meta-analysis. *JAMA Psychiatry*. (2016) 73:1145–53. doi: 10.1001/jamapsychiatry.2016.2619
13. Spencer KM, Salisbury DF, Shenton ME, McCarley RW. Gamma-band auditory steady-state responses are impaired in first episode psychosis. *Biol Psychiatry*. (2008) 64:369–75. doi: 10.1016/j.biopsych.2008.02.021
14. Tada M, Kirihara K, Koshiyama D, Fujioka M, Usui K, Uka T, et al. Gamma-band auditory steady-state response as a neurophysiological marker for excitation and inhibition balance: a review for understanding schizophrenia and other neuropsychiatric disorders. *Clin EEG Neurosci*. (2019) 51:234–43. doi: 10.1177/1550059419868872
15. Koshiyama D, Kirihara K, Tada M, Nagai T, Fujioka M, Ichikawa E, et al. Auditory gamma oscillations predict global symptomatic outcome in the early stages of psychosis: a longitudinal investigation. *Clin Neurophysiol*. (2018) 129:2268–75. doi: 10.1016/j.clinph.2018.08.007
16. Koshiyama D, Kirihara K, Tada M, Nagai T, Fujioka M, Ichikawa E, et al. Electrophysiological evidence for abnormal glutamate-GABA association following psychosis onset. *Transl Psychiatry*. (2018) 8:211. doi: 10.1038/s41398-018-0261-0
17. Koshiyama D, Kirihara K, Tada M, Nagai T, Fujioka M, Usui K, et al. Gamma-band auditory steady-state response is associated with plasma levels of d-serine in schizophrenia: an exploratory study. *Schizophr Res*. (2019) 208:467–9. doi: 10.1016/j.schres.2019.02.012
18. Senkowski D, Gallinat J. Dysfunctional prefrontal gamma-band oscillations reflect working memory and other cognitive deficits in schizophrenia. *Biol Psychiatry*. (2015) 77:1010–9. doi: 10.1016/j.biopsych.2015.02.034
19. Feyissa AM, Tatum WO. Adult EEG. *Handb Clin Neurol*. (2019) 160:103–24. doi: 10.1016/B978-0-444-64032-1.00007-2
20. Newson JJ, Thiagarajan TC. EEG frequency bands in psychiatric disorders: a review of resting state studies. *Front Hum Neurosci*. (2018) 12:521. doi: 10.3389/fnhum.2018.00521
21. Uhlhaas PJ, Haenschel C, Nikolic D, Singer W. The role of oscillations and synchrony in cortical networks and their putative relevance for the pathophysiology of schizophrenia. *Schizophr Bull*. (2008) 34:927–43. doi: 10.1093/schbul/sbn062
22. Andreou C, Nolte G, Leicht G, Polomac N, Hanganu-Opatz IL, Lambert M, et al. Increased resting-state gamma-band connectivity in first-episode schizophrenia. *Schizophr Bull*. (2015) 41:930–9. doi: 10.1093/schbul/sbu121
23. Granger CWJ. Investigating causal relations by econometric models and cross-spectral methods. *Econometrica*. (1969) 37:424–38. doi: 10.2307/1912791
24. Tanaka-Koshiyama K, Koshiyama D, Miyakoshi M, Joshi YB, Molina JL, Sprock J, et al. Abnormal spontaneous gamma power is associated with underlying verbal learning and memory dysfunction in schizophrenia. *Front Psychiatry*. (2020) 11:832. doi: 10.3389/fpsyt.2020.00832
25. Buchsbaum MS, Hazlett E, Sicotte N, Stein M, Wu J, Zetin M. Topographic EEG changes with benzodiazepine administration in generalized anxiety disorder. *Biol Psychiatry*. (1985) 20:832–42. doi: 10.1016/0006-3223(85)90208-2
26. Sloan EP, Fenton GW, Standage KP. Anticholinergic drug effects on quantitative electroencephalogram, visual evoked potential, and verbal memory. *Biol Psychiatry*. (1992) 31:600–6. doi: 10.1016/0006-3223(92)90246-V
27. Oostenveld R, Praamstra P. The five percent electrode system for high-resolution EEG and ERP measurements. *Clin Neurophysiol*. (2001) 112:713–9. doi: 10.1016/S1388-2457(00)00527-7
28. Collins DL, Neelin P, Peters TM, Evans AC. Automatic 3D intersubject registration of MR volumetric data in standardized Talairach space. *J Comput Assist Tomogr*. (1994) 18:192–205. doi: 10.1097/00004728-199403000-00005
29. Delorme A, Makeig S. EEGLAB: an open source toolbox for analysis of single-trial EEG dynamics including independent component analysis. *J Neurosci Methods*. (2004) 134:9–21. doi: 10.1016/j.jneumeth.2003.10.009
30. Blum S, Jacobsen NSJ, Bleichner MG, Debener S. A riemannian modification of artifact subspace reconstruction for EEG artifact handling. *Front Hum Neurosci*. (2019) 13:141. doi: 10.3389/fnhum.2019.00141
31. Chang CY, Hsu SH, Pion-Tonachini L, Jung TP. Evaluation of artifact subspace reconstruction for automatic artifact components removal in multi-channel EEG recordings. *IEEE Trans Biomed Eng*. (2020) 67:1114–21. doi: 10.1109/TBME.2019.2930186
32. Chang CY, Hsu SH, Pion-Tonachini L, Jung TP. Evaluation of artifact subspace reconstruction for automatic EEG artifact removal. *Conf Proc IEEE Eng Med Biol Soc*. (2018) 2018:1242–5. doi: 10.1109/EMBC.2018.8512547
33. Gabard-Durnam LJ, Mendez Leal AS, Wilkinson CL, Levin AR. The Harvard automated processing pipeline for electroencephalography (HAPPE): standardized processing software for developmental and high-artifact data. *Front Neurosci*. (2018) 12:97. doi: 10.3389/fnins.2018.00097
34. Kothe CA, Makeig S. BCILAB: a platform for brain-computer interface development. *J Neural Eng*. (2013) 10:056014. doi: 10.1088/1741-2560/10/5/056014
35. Mullen TR, Kothe CA, Chi YM, Ojeda A, Kerth T, Makeig S, et al. Real-time neuroimaging and cognitive monitoring using wearable dry EEG. *IEEE Trans Biomed Eng*. (2015) 62:2553–67. doi: 10.1109/TBME.2015.2481482
36. Onton J, Makeig S. Information-based modeling of event-related brain dynamics. *Prog Brain Res*. (2006) 159:99–120. doi: 10.1016/S0079-6123(06)59007-7
37. Delorme A, Palmer J, Onton J, Oostenveld R, Makeig S. Independent EEG sources are dipolar. *PLoS ONE*. (2012) 7:e30135. doi: 10.1371/journal.pone.0030135
38. Oostenveld R, Fries P, Maris E, Schoffelen JM. FieldTrip: open source software for advanced analysis of MEG, EEG, and invasive electrophysiological data. *Comput Intell Neurosci*. (2011) 2011:156869. doi: 10.1155/2011/156869
39. Piazza C, Miyakoshi M, Akalin-Acar Z, Cantiani C, Reni G, Bianchi AM. An automated function for identifying eeg independent components representing bilateral source activity. In: *XIV Mediterranean Conference on Medical and Biological Engineering and Computing 2016*. Paphos (2016). p. 105–9.
40. Pion-Tonachini L, Kreutz-Delgado K, Makeig S. ICLabel: an automated electroencephalographic independent component classifier, dataset, and website. *Neuroimage*. (2019) 198:181–97. doi: 10.1016/j.neuroimage.2019.05.026
41. Loo SK, Miyakoshi M, Tung K, Lloyd E, Salgari G, Dillon A, et al. Neural activation and connectivity during cued eye blinks in Chronic Tic disorders. *Neuroimage Clin*. (2019) 24:101956. doi: 10.1016/j.nicl.2019.101956
42. Schelter B, Timmer J, Eichler M. Assessing the strength of directed influences among neural signals using renormalized partial directed coherence. *J Neurosci Methods*. (2009) 179:121–30. doi: 10.1016/j.jneumeth.2009.01.006
43. Ding M, Bressler SL, Yang W, Liang H. Short-window spectral analysis of cortical event-related potentials by adaptive multivariate autoregressive modeling: data preprocessing, model validation, and variability assessment. *Biol Cybern*. (2000) 83:35–45. doi: 10.1007/s004229900137
44. Tzourio-Mazoyer N, Landeau B, Papathanassiou D, Crivello F, Etard O, Delcroix N, et al. Automated anatomical labeling of activations in SPM using a macroscopic anatomical parcellation of the MNI MRI single-subject brain. *Neuroimage*. (2002) 15:273–89. doi: 10.1006/nimg.2001.0978

45. Nichols T, Hayasaka S. Controlling the familywise error rate in functional neuroimaging: a comparative review. *Stat Methods Med Res*. (2003) 12:419–46. doi: 10.1191/0962280203sm341ra
46. Groppe DM, Urbach TP, Kutas M. Mass univariate analysis of event-related brain potentials/fields I: a critical tutorial review. *Psychophysiology*. (2011) 48:1711–25. doi: 10.1111/j.1469-8986.2011.01273.x
47. Xia M, Wang J, He Y. BrainNet viewer: a network visualization tool for human brain connectomics. *PLoS ONE*. (2013) 8:e68910. doi: 10.1371/journal.pone.0068910
48. Koshiyama D, Miyakoshi M, Joshi YB, Molina JL, Tanaka-Koshiyama K, Sprock J, et al. Abnormal effective connectivity underlying auditory mismatch negativity impairments in schizophrenia. *Biol Psychiary Cogn Neurosci Neuroimaging*. (2020) 5:1028–39.
49. Liu T, Zhang J, Dong X, Li Z, Shi X, Tong Y, et al. Occipital alpha connectivity during resting-state electroencephalography in patients with ultra-high risk for psychosis and schizophrenia. *Front Psychiatry*. (2019) 10:553. doi: 10.3389/fpsyt.2019.00553
50. Andreou C, Leicht G, Nolte G, Polomac N, Moritz S, Karow A, et al. Resting-state theta-band connectivity and verbal memory in schizophrenia and in the high-risk state. *Schizophr Res*. (2015) 161:299–307. doi: 10.1016/j.schres.2014.12.018
51. Buckner RL, Andrews-Hanna JR, Schacter DL. The brain's default network: anatomy, function, and relevance to disease. *Ann N Y Acad Sci*. (2008) 1124:1–38. doi: 10.1196/annals.1440.011
52. Garrity AG, Pearlson GD, McKiernan K, Lloyd D, Kiehl KA, Calhoun VD. Aberrant "default mode" functional connectivity in schizophrenia. *Am J Psychiatry*. (2007) 164:450–7. doi: 10.1176/ajp.2007.164.3.450
53. Weiner KS, Zilles K. The anatomical and functional specialization of the fusiform gyrus. *Neuropsychologia*. (2016) 83:48–62. doi: 10.1016/j.neuropsychologia.2015.06.033
54. Morita K, Miura K, Fujimoto M, Yamamori H, Yasuda Y, Kudo N, et al. Eye-movement characteristics of schizophrenia and their association with cortical thickness. *Psychiatry Clin Neurosci*. (2019) 73:508–9. doi: 10.1111/pcn.12865
55. Salisbury DF, Kuroki N, Kasai K, Shenton ME, McCarley RW. Progressive and interrelated functional and structural evidence of post-onset brain reduction in schizophrenia. *Arch Gen Psychiatry*. (2007) 64:521–9. doi: 10.1001/archpsyc.64.5.521
56. Koshiyama D, Miyakoshi M, Joshi YB, Molina JL, Tanaka-Koshiyama K, Sprock J, et al. A distributed frontotemporal network underlies gamma-band synchronization impairments in schizophrenia patients. *Neuropsychopharmacology*. (2020) 45:2198–206.
57. Hirano Y, Oribe N, Onitsuka T, Kanba S, Nestor PG, Hosokawa T, et al. Auditory cortex volume and gamma oscillation abnormalities in schizophrenia. *Clin EEG Neurosci*. (2020) 51:244–51. doi: 10.1177/1550059420914201
58. Light GA, Swerdlow NR. Selection criteria for neurophysiologic biomarkers to accelerate the pace of CNS therapeutic development. *Neuropsychopharmacology*. (2020) 45:237–8. doi: 10.1038/s41386-019-0519-0

Conflict of Interest: The authors declare that the research was conducted in the absence of any commercial or financial relationships that could be construed as a potential conflict of interest.

frontiers in Psychiatry

MINI REVIEW
published: 11 March 2021
doi: 10.3389/fpsyt.2021.644541

The Auditory Steady-State Response: Electrophysiological Index for Sensory Processing Dysfunction in Psychiatric Disorders

Shunsuke Sugiyama[1], Kazutaka Ohi[1]*, Ayumi Kuramitsu[1], Kentaro Takai[1], Yukimasa Muto[1], Tomoya Taniguchi[2], Tomoaki Kinukawa[2], Nobuyuki Takeuchi[3], Eishi Motomura[4], Makoto Nishihara[5], Toshiki Shioiri[1] and Koji Inui[6]*

[1] Department of Psychiatry, Gifu University Graduate School of Medicine, Gifu, Japan, [2] Department of Anesthesiology, Nagoya University Graduate School of Medicine, Nagoya, Japan, [3] Depatment of Psychiatry, Aichi Medical University, Nagakute, Japan, [4] Department of Neuropsychiatry, Mie University Graduate School of Medicine, Tsu, Japan, [5] Multidisciplinary Pain Center, Aichi Medical University, Nagakute, Japan, [6] Departmernt of Functioning and Disability, Institute for Developmental Research, Kasugai, Japan

OPEN ACCESS

Edited by:
Shinsuke Koike, The University of Tokyo, Japan

Reviewed by:
Minah Kim, Seoul National University Hospital, South Korea
Mariko Tada, The University of Tokyo, Japan

***Correspondence:**
Shunsuke Sugiyama
s0450032@yahoo.co.jp
Kazutaka Ohi
k_ohi@gifu-u.ac.jp

Specialty section:
This article was submitted to Neuroimaging and Stimulation, a section of the journal Frontiers in Psychiatry

Received: *21 December 2020*
Accepted: *22 February 2021*
Published: *11 March 2021*

Citation:
Sugiyama S, Ohi K, Kuramitsu A, Takai K, Muto Y, Taniguchi T, Kinukawa T, Takeuchi N, Motomura E, Nishihara M, Shioiri T and Inui K (2021) The Auditory Steady-State Response: Electrophysiological Index for Sensory Processing Dysfunction in Psychiatric Disorders. Front. Psychiatry 12:644541. doi: 10.3389/fpsyt.2021.644541

Sensory processing is disrupted in several psychiatric disorders, including schizophrenia, bipolar disorder, and autism spectrum disorder. In this review, we focus on the electrophysiological auditory steady-state response (ASSR) driven by high-frequency stimulus trains as an index for disease-associated sensory processing deficits. The ASSR amplitude is suppressed within the gamma band (≥30 Hz) among these patients, suggesting an imbalance between GABAergic and N-methyl-D-aspartate (NMDA) receptor-mediated neurotransmission. The reduced power and synchronization of the 40-Hz ASSR are robust in patients with schizophrenia. In recent years, similar ASSR deficits at gamma frequencies have also been reported in patients with bipolar disorder and autism spectrum disorder. We summarize ASSR abnormalities in each of these psychiatric disorders and suggest that the observed commonalities reflect shared pathophysiological mechanisms. We reviewed studies on phase resetting in which a salient sensory stimulus affects ASSR. Phase resetting induces the reduction of both the amplitude and phase of ASSR. Moreover, phase resetting is also affected by rare auditory stimulus patterns or superimposed stimuli of other modalities. Thus, sensory memory and multisensory integration can be investigated using phase resetting of ASSR. Here, we propose that ASSR amplitude, phase, and resetting responses are sensitive indices for investigating sensory processing dysfunction in psychiatric disorders.

Keywords: ASSR, gamma-band oscillation, phase resetting, electroencephalography, magnetoencephalography, schizophrenia, bipolar disorder, autism spectral disorder

INTRODUCTION

Recent studies have identified multiple shared genetic associations and other commonalities among psychiatric disorders. For example, genome-wide association studies suggest shared molecular pathomechanisms between schizophrenia and bipolar disorder (1, 2), whereas large-scale imaging analyses have revealed similar white matter abnormalities (3) in patients with

schizophrenia and bipolar disorders. Recent genetic (2, 4) and neuroimaging studies (5, 6) have also demonstrated shared molecular and neurostructural abnormalities between schizophrenia and autism spectrum disorder. Currently, psychiatric disorders continue to be classified based on observed symptoms rather than underlying pathogenic mechanisms. Classifications such as the International Classification of Diseases (ICD) (7) and the Diagnostic and Statistical Manual of Mental Disorders (DSM) (8) have contributed to the standardization of diagnoses and treatment in clinical practice; however, they provide little information regarding neurobiological mechanisms and treatment targets. Indeed, overemphasis on differential diagnosis according to symptom clusters and clinical history has revealed little about the pathological mechanisms underlying these psychiatric disorders. Therefore, it is important to investigate common biological abnormalities across multiple psychiatric disorders. To address this issue, the National Institute of Mental Health is currently attempting to construct a biological framework for understanding the etiology and symptomology of psychiatric disorders (9).

A common symptom of multiple psychiatric disorders is sensory processing dysfunction (10, 11). Neurophysiological approaches such as magnetoencephalography (MEG) and electroencephalography (EEG) can reveal the electrical activity of neuronal ensembles at high temporal resolution, thereby providing quantitative indices of illness that also reflect disease-associated abnormalities at the cellular level. In this review, we focus on the auditory steady-state response (ASSR), an electrophysiological response driven by a train of stimuli delivered at a sufficiently high rate. ASSR recorded using MEG or EEG has been reported to reach maximum amplitude at approximately 40 Hz (12, 13). Previous MEG (14) and positron-emission tomography (15) studies have reported that ASSR originates in the primary auditory cortex and associated subcortical areas (16). The ASSR has been interpreted as a reflection of oscillatory gamma-band activity representing auditory objects (17–19). Moreover, neural oscillations in the gamma frequency band are believed critical for information processing across cortical networks (20, 21). For example, gamma-band activity increases in the visual (22, 23), auditory (24, 25), and somatosensory cortices (26) in response to modality-specific sensory stimuli. Gamma-band activity is also related to working memory and increases in the hippocampus and prefrontal cortex during memory processing (27–29). Therefore, gamma-band activity is involved in a wide range of brain activities, from low-level sensory processing to higher cognitive functions. Further, ASSR amplitude and phase are believed to reflect the balance between inhibitory GABAergic activity and excitatory glutamatergic activity mediated by the N-methyl-D-aspartate (NMDA) receptor (30–32). Thus, ASSR abnormalities as measured by MEG and EEG can reveal aspects of aberrant neurotransmission and neuronal excitation within specific brain circuits.

In 1999, Kwon et al. first demonstrated that patients with schizophrenia showed reduced power and synchronization of the 40-Hz ASSR (33), and subsequent studies by other groups replicated this finding (34–37). A meta-analysis also concluded that 40-Hz ASSR deficits are robust in schizophrenia (38). These ASSR deficits are consistent with anatomic abnormalities of the auditory cortex observed by magnetic resonance imaging (39, 40). Such ASSR deficits at gamma frequencies have also been discovered in bipolar disorder (41–43) and autism spectrum disorder (44). In this review, we first summarize ASSR abnormalities in each of these psychiatric disorders and discuss the potential commonalities in pathophysiology suggested by these observations. Second, we review studies suggesting that modulation of ASSR amplitude and phase by rare auditory patterns or addition of multimodal stimuli, termed phase resetting, also yield useful index for psychiatric disorders. We propose that ASSR is a sensitive index for investigating sensory memory and multisensory integration deficits in psychiatric disorders.

ASSR Deficits in Psychiatric Disorders

Schizophrenia

Most studies documenting ASSR deficits in schizophrenia have been conducted in the chronic disease phase, suggesting a relationship with symptom expression. Intriguingly, however, reduced evoked power and phase locking of the 40-Hz ASSR have also been documented in first-episode patients (35), high-risk individuals before the onset of psychosis (37), and in first-degree relatives (45, 46). In contrast, individuals with schizotypal personality disorder did not exhibit ASSR deficits (46, 47). These findings suggest that these ASSR deficits reflect pathological development independent of disease course or the side effects of long-term antipsychotic medication.

These ASSR deficits are most consistently observed at 40 Hz, whereas responses are usually intact at 20 and 30 Hz [although reduced ASSR at 30 Hz (35) and enhanced ASSR at 20 Hz (48) have been reported]. Recent studies have also reported impaired evoked ASSR power and phase locking at 80 Hz in schizophrenia (36, 49), and these abnormalities were associated with the severity of hallucinations (36) and negative symptoms, such as flat affect, anhedonia, and poverty of speech (49). Tada et al. reported that deficits in the 40-Hz ASSR during a 300–500 ms train were associated with more severe clinical symptoms and cognitive deficits (37). Moreover, patients with schizophrenia taking new generation antipsychotics exhibited significantly increased 40-Hz ASSR synchronization (45). Collectively, these findings indicate that ASSR may also be a useful quantitative index for current clinical symptoms and treatment response.

Bipolar Disorder

Patients with bipolar disorder show a pattern of ASSR deficits similar to that of patients with schizophrenia. To our knowledge, O'Donnell et al. first reported reduced evoked ASSR power at 20, 30, 40, and 50 Hz as well as reduced phase synchronization at 20, 40, and 50 Hz among patients with unmedicated bipolar disorder during manic or mixed episodes using EEG (41). Such ASSR deficits have also been documented in depressive (42), euthymic (43), and manic (41) states in the first episode (35) and the chronic state (41–43) and in both medicated (42, 43) and unmedicated patients (41).

In contrast to a comparative group of patients with bipolar disorder, no ASSR deficits were observed in a parallel group with major depressive disorder (50). In fact, to our knowledge, only one study has reported ASSR deficits in major depressive disorder (51), and reduced ASSR power was found at 30 Hz but not at 40 Hz as observed in patients with bipolar disorder and schizophrenia (51). These findings suggest that major depressive disorder and bipolar disorder have distinct neurophysiological bases and further that 40-Hz ASSR can be used to distinguish bipolar disorder from major depressive disorder (50).

Autism Spectrum Disorder

Wilson et al. first reported reduced 40-Hz ASSR power in 7–17-year-old children and adolescents with autism using MEG (52), with a greater reduction in the left hemisphere. Thereafter, Rojas et al. found reduced evoked power and phase locking of left and right 40-Hz ASSRs among both adults with autism and parents of children with autism (53), suggesting that ASSR is a useful index for diagnosis and risk evaluation. However, utility may be limited to adults as ASSR amplitude increases from childhood through adolescence and plateaus in early adulthood (54). Further, no significant deficits in 20- and 40-Hz ASSRs were found among 5–7-year-old children with autism spectrum disorder (55).

Shared Pathophysiology Among Psychiatric Disorders

Patients with schizophrenia, bipolar disorder, and autism spectrum disorder demonstrate similar patterns of ASSR deficits, suggesting shared neural circuit dysfunction. One emerging hypothesis is that ASSR deficits reflect dysfunction of the GABAergic and/or NMDAergic systems. Blockers of NMDA receptors, such as phencyclidine and ketamine, evoke psychotic symptoms in healthy individuals, exacerbate positive symptoms in patients with schizophrenia, and induce various schizotypic electrophysiological and behavioral abnormalities in experimental animal models (56). For instance, Sohal et al. demonstrated that optogenetic downregulation of parvalbumin-positive GABAergic interneuron activity in mice reduced gamma-band oscillations (57), whereas Sivarao et al. reported that the 40-Hz ASSR in awake rats depended on the degree of NMDA receptor channel blockade (30). Collectively, these findings are consistent with evidence implicating GABA (58) and/or NMDA (59) transmission impairment in schizophrenia.

Post-mortem brain studies of patients with schizophrenia and bipolar disorder have also reported reduced interneuron density in the cerebral cortex and hippocampus (60). Similar to the GABAergic dysfunction in bipolar disorder is the therapeutic efficacy of the mood stabilizer valproate, which has been shown to increase GABA turnover in rat brain (61). Moreover, valproate has been reported to increase GABA levels in human plasma, suggesting that it enhances GABA activity in the central nervous system (62). However, poor understanding of the mechanism of action of valproate in bipolar disorder is a limitation (63), and valproate is not effective in treating schizophrenia or autism spectrum disorder, despite sharing the GABAergic dysfunction hypothesis. A recent study of induced pluripotent stem cell-derived organoids from patients with schizophrenia and bipolar disorder found enhanced GABAergic specification (64), suggesting that the reduction in GABAergic neurons observed after disease onset is a compensatory response to maintain the excitatory/inhibitory balance within neural circuits during cortical development.

Conversely, 40-Hz ASSR deficits have not been observed in patients with major depressive disorder. Hirano et al. showed that spontaneous gamma band activity is high in patients with schizophrenia and that the degree of 40-Hz ASSR deficits was associated with increased spontaneous gamma-band activity (65). Moreover, ketamine, an NMDA receptor antagonist, was effective in treating depression (66) and increases resting-state gamma-band activity (67). Therefore, patients with major depressive disorder, in contrast to those with schizophrenia, may have reduced spontaneous gamma-band activity, and consequently, ASSR deficits may not have been observed. However, spontaneous gamma-band activity has not yet been investigated in patients with major depressive disorder. The number of reports on ASSR in major depressive disorder is small, and similarities and differences with other diseases that have ASSR deficits need to be discussed in the future.

Dysfunction of the GABAergic system has also been implicated in autism spectrum disorder. For example, multiple mouse models of autism established via toxins or manipulation of associated genes exhibit reduced number of neocortical parvalbumin-positive inhibitory neurons (68). A post-mortem study also reported reduced GABA-synthesizing enzymes in parietal and cerebellar cortices of patients with autism spectrum disorder (69), whereas a proton magnetic resonance spectroscopy study reported reduced GABA concentration in the auditory and frontal cortices of living patients (70). These GABAergic deficits may result in a relative excess of glutamatergic activity. Indeed, Fatemi's hyper-glutamatergic hypothesis of autism spectrum disorder posits that deficits in GABA-synthesizing enzymes and increased GABA uptake by astrocytes led to excess cortical glutamate (71).

Autism spectrum disorder and schizophrenia also share behavioral symptoms such as difficulties with social cognition, social interaction, and executive functions (72). In fact, autism spectrum disorder was initially believed to be an early stage of schizophrenia (73). Furthermore, an altered ratio of excitatory to inhibitory cortical activity has been reported in both autism spectrum disorder and schizophrenia (74). Yizhar et al. demonstrated that psychosocial dysfunction, a trait common to both disorders, was associated with increased excitation/inhibition ratio in mouse prefrontal cortex (75). Therefore, understanding the causes of excitation/inhibition imbalance could provide clues to the pathophysiology of these disorders as well as to novel treatment strategies. Further, ASSR could be a sensitive electrophysiological indicator reflecting the excitation/inhibition imbalance common among schizophrenia, bipolar disorder, and autism spectrum disorder.

Perspectives on Neurophysiological Research Using Phase Resetting of ASSR

Phase resetting is a phenomenon that occurs when a stimulus perturbs the phase within a neural oscillation. Resetting the phase of ongoing neural oscillation induces the synchronization of different neurons or brain regions (76). Phase resetting

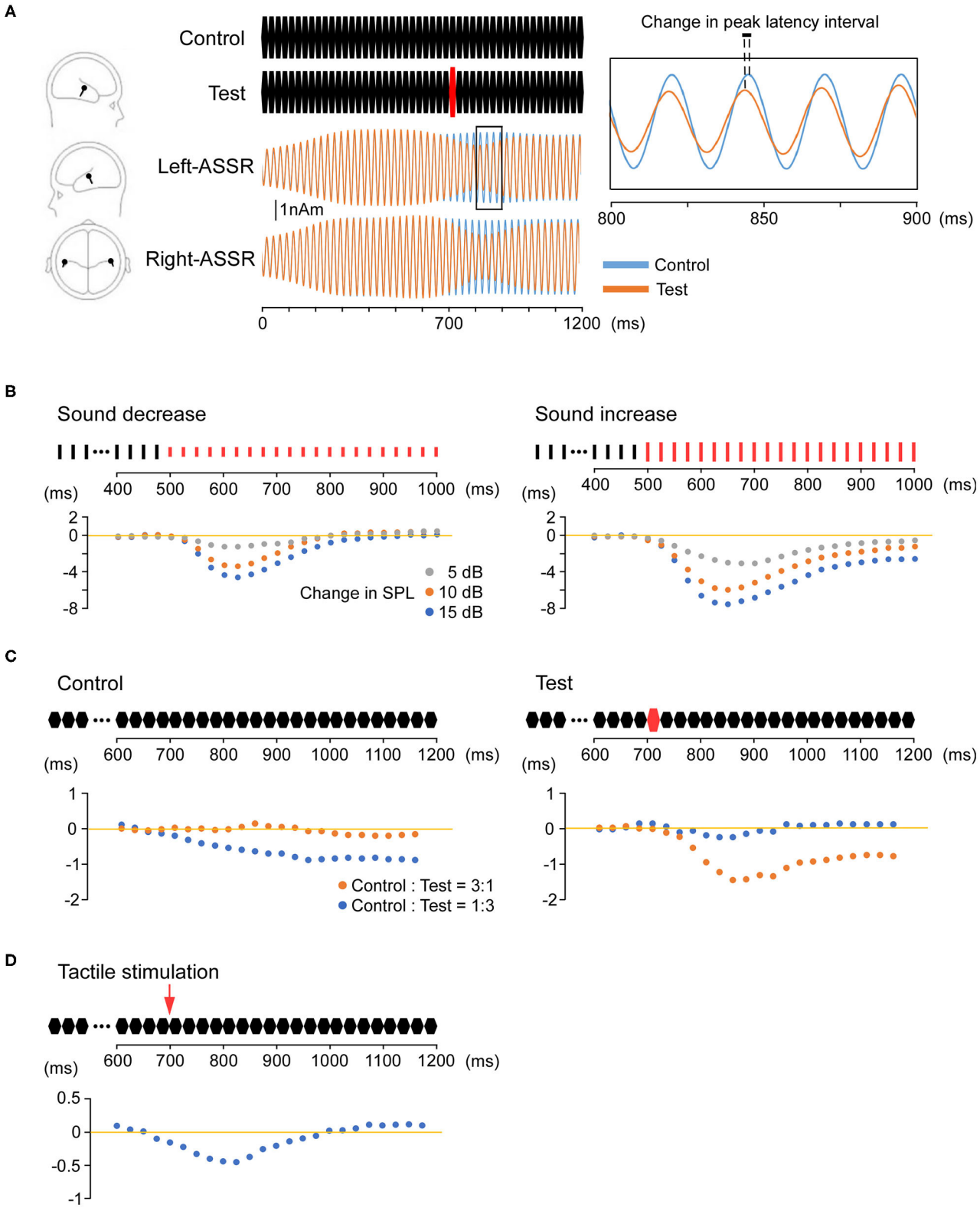

FIGURE 1 | Phase resetting of the auditory steady-state response (ASSR). **(A)** Modulation of the ASSR by stimulus intensity (sound pressure). Repeated presentation of a 25-ms pure tone (upper middle) elicits the 40-Hz ASSR. An abrupt increase in sound pressure at 700 ms causes a reduction in amplitude and phase

(Continued)

FIGURE 1 | (phase resetting). The location of estimated dipoles (left panel), source-strength waveforms (middle), and enlarged waveforms on an expanded time axis (right) are also shown. **(B)** Increasing sound pressure reduces ASSR latency. The Y-axis shows changes in the peak latency interval over time relative to the control condition. The control stimulus is a 1,000-ms train of clicks at 40 Hz. The test stimuli are a 500-ms train of clicks identical to the control stimulus and a subsequent 500-ms click-train of the same frequency but altered sound pressure compared with the control stimulus (−5, −10, −15, 5, 10, or 15 dB). The degree of phase resetting depends on the magnitude of the sound pressure change. **(C)** Modulation of the ASSR by deviant stimuli (odd ball condition). The Y-axis shows changes in the peak latency interval over time compared with the control-only (left) and test-only (right) conditions. The control stimulus is a 1,200-ms train of 25-ms pure tones. The test stimulus is a similar train of pure tones in which the tone sound pressure at 700 ms is increased by 15 dB. Under an oddball paradigm, phase resetting is observed when either the control or test stimulus is rare (deviant). **(D)** Modulation of the ASSR by multimodal stimulation. The Y-axis shows changes in the peak latency interval over time compared with the control condition. As the test stimulus, an electrical pulse is presented to the dorsum of the left or right hand at 700 ms during the train of 25-ms pure tones. Tactile stimulation causes phase resetting of the ASSR, and this cross-modal effect is observed from approximately 50–125 ms after the onset of tactile stimulation.

is the fundamental mechanism underlying synchronization, and neural synchronization is believed to play a role in information processing (77), neuronal communication (78), motor coordination (79), and memory (80). For example, in clinical research, epilepsy is considered a disease that results from neuronal hyper-synchronization (81). The generation of resting tremor in Parkinson's disease has been suggested to be owing to abnormal synchronization of neuronal activity (82). In schizophrenia, the disruption of neural synchronization is believed to be related to fragmented cognitive experience (83).

A salient sensory stimulus on ASSR causes phase resetting that modulates the amplitude and phase (**Figure 1A**) Rohrbaugh et al. first reported that a foreground auditory stimulus reduced both the amplitude and latency of a 40-Hz ASSR evoked by a background rhythmic probe stimulus (84–86). In addition, phase resetting of the 40-Hz ASSR has been reported following a sudden change in stimulus frequency or intensity (87). In a study using an oddball paradigm, button pressing in response to a rare stimulus also caused phase resetting of the 40-Hz ASSR (88). Furthermore, Ross et al. reported that the ASSR was modulated by changing stimulus onset (19), violating the periodicity of a sound stimulus (89), and introducing an interfering stimulus (90). These findings suggest that perturbing stimuli reset the oscillations and shift the ASSR phase back to that of the driving source (90).

Our recent study indicated that increasing the sound pressure can induce a proportionate reduction in ASSR latency (**Figure 1B**) (91). We also demonstrated that ASSR latency can be shortened without changing the physical characteristics of the peripheral input (92). Using an oddball paradigm, we found that a control stimulus with unchanging sequence shortened the ASSR latency when presented with a low probability among other stimulus patterns (**Figure 1C**). These findings indicate that ASSR phase resetting can be induced by an intrinsic comparison process based on sensory memory. Sensory memory impairment has been reported in several neurological and psychiatric disorders, primarily using mismatch negativity (MMN) (93), a negative component of the event-related potential elicited by a deviant stimulus embedded in repetitive stimuli (an oddball paradigm), with maximum negativity at Fz and positivity at the mastoid (94). Mismatch negativity reflects the automatic change detection process based on short-term sensory memory and thus serves as an index of sensory memory disruption (95). For example, patients with schizophrenia (96, 97), autism spectrum disorder (98), and Alzheimer's disease (99) have all demonstrated smaller auditory MMN waveforms than healthy controls. Although previous studies have reported that ASSR is modulated by selective attention (100, 101), our paradigms (91, 92), such as oddball paradigms which are typically used to detect MMN, do not require conditions of attention. Changes in ASSR during such odd ball paradigms (91, 92) may facilitate efficient assessment of sensory memory impairments in psychiatric disorders because such measurements do not require multiple stimulus repetitions, thereby reducing experimental time and patient burden.

We also recently demonstrated reduced ASSR latency by simultaneous tactile stimulation (**Figure 1D**) (102), strongly suggesting that cross-modal input increases the speed of ongoing auditory processing. This cross-modal ASSR paradigm may thus permit the assessment of multimodal sensory integration with high test–retest reliability (103). Moreover, the 40-Hz ASSR is considered superior for providing information on processing speed compared with other sensory paradigms because peak latency can be measured reliably every 12.5 ms. Indeed, our findings of reduced ASSR latency during multimodal stimulation are consistent with previous studies demonstrating faster object recognition using both auditory and visual features compared with either modality alone and with the appearance of unique early-onset multimodal ERP waveforms originating from both sensory and frontal cortex (104, 105). Although previous studies have shown impaired multisensory integration in patients with schizophrenia (106) and autism spectrum disorder (107), psychophysical rather than neurophysiological indicators were assessed. We suggest that the ASSR serves as a robust electrophysiological index of multisensory integration deficits in psychiatric disorders.

CONCLUSION

Patients with schizophrenia, bipolar disorder, and autism spectrum disorder all exhibit deficits in the ASSR at gamma-band frequencies, suggesting shared pathomechanisms including dysregulation of cortical excitatory/inhibitory balance. Moreover, ASSR magnitude and phase reflect auditory memory, multimodal sensory integration, and the comparison of incoming sensory stimuli with previous memory traces. Thus, ASSR could be

a sensitive electrophysiological index for sensory processing deficits in psychiatric disorders.

AUTHOR CONTRIBUTIONS

SS conducted the literature review, SS and KI drafted the manuscript, SS and EM created the figure, AK, KT, YM, TT, TK, NT, MN, and TS provided valuable critical input on the manuscript, and KO edited the final draft. All authors contributed to the article and approved the submitted version.

FUNDING

This study was supported by JSPS KAKENHI Grant Number JP20K16624 to SS.

REFERENCES

1. Lee SH, Ripke SH, Neale BM, Faraone SV, Purcell SM, Perlis RH, et al. Genetic relationship between five psychiatric disorders estimated from genome-wide SNPs. *Nat Genet.* (2013) 45:984–94. doi: 10.1038/ng.2711
2. Cross-Disorder Group of the Psychiatric Genomics Consortium. Identification of risk loci with shared effects on five major psychiatric disorders: a genome-wide analysis. *Lancet.* (2013) 381:1371–9. doi: 10.1016/S0140-6736(12)62129-1
3. Koshiyama D, Fukunaga M, Okada N, Morita K, Nemoto K, Usui K, et al. White matter microstructural alterations across four major psychiatric disorders: mega-analysis study in 2937 individuals. *Mol Psychiatry.* (2020) 25:883–95. doi: 10.1038/s41380-019-0553-7
4. Geschwind DH, Flint J. Genetics and genomics of psychiatric disease. *Science.* (2015) 349:1489–94. doi: 10.1126/science.aaa8954
5. Pinkham AE, Hopfinger JB, Pelphrey KA, Piven J, Penn DL. Neural bases for impaired social cognition in schizophrenia and autism spectrum disorders. *Schizophr Res.* (2008) 99:164–75. doi: 10.1016/j.schres.2007.10.024
6. Sugranyes G, Kyriakopoulos M, Corrigall R, Taylor E, Frangou S. Autism spectrum disorders and schizophrenia: meta-analysis of the neural correlates of social cognition. *PLOS ONE.* (2011) 6:e25322. doi: 10.1371/journal.pone.0025322
7. World Health Organization. *International Classification of Diseases ICD-10.* 10th ed. Geneva: World Health Organization (1992).
8. American Psychiatric Association. *Diagnostic and Statistical Manual of Mental Disorders DSM-5.* Washington, DC: American Psychiatric Association (2013).
9. Insel T, Cuthbert B, Garvey M, Heinssen R, Pine DS, Quinn K, et al. Research domain criteria (RDoC): toward a new classification framework for research on mental disorders. *Am J Psychiatry.* (2010) 167:748–51. doi: 10.1176/appi.ajp.2010.09091379
10. Kas MJ, Fernandes C, Schalkwyk LC, Collier DA. Genetics of behavioural domains across the neuropsychiatric spectrum; of mice and men. *Mol Psychiatry.* (2007) 12:324–30. doi: 10.1038/sj.mp.4001979
11. Harrison LA, Kats A, Williams ME, Aziz-Zadeh L. The importance of sensory processing in mental health: a proposed addition to the research domain criteria (RDoC) and suggestions for RDoC 2.0. *Front Psychol.* (2019) 10:103. doi: 10.3389/fpsyg.2019.00103
12. Galambos R, Makeig S, Talmachoff PJ. A 40-Hz auditory potential recorded from the human scalp. *Proc Natl Acad Sci USA.* (1981) 78:2643–7. doi: 10.1073/pnas.78.4.2643
13. Ross B, Borgmann C, Draganova R, Roberts LE, Pantev C. A high-precision magnetoencephalographic study of human auditory steady-state responses to amplitude-modulated tones. *J Acoust Soc Am.* (2000) 108:679–91. doi: 10.1121/1.429600
14. Ross B. A novel type of auditory responses: temporal dynamics of 40-Hz steady-state responses induced by changes in sound localization. *J Neurophysiol.* (2008) 100:1265–77. doi: 10.1152/jn.00048.2008
15. Pastor MA, Artieda J, Arbizu J, Marti-Climent JM, Peñuelas I, Masdeu JC. Activation of human cerebral and cerebellar cortex by auditory stimulation at 40 Hz. *J Neurosci.* (2002) 22:10501–6. doi: 10.1523/JNEUROSCI.22-23-10501.2002
16. Herdman AT, Lins O, Van Roon P, Stapells DR, Scherg M, Picton TW. Intracerebral sources of human auditory steady-state responses. *Brain Topogr.* (2002) 15:69–86. doi: 10.1023/A:1021470822922
17. Santarelli R, Maurizi M, Conti G, Ottaviani F, Paludetti G, Pettorossi VE. Generation of human auditory steady-state responses (SSRs). II: addition of responses to individual stimuli. *Hear Res.* (1995) 83:9–18. doi: 10.1016/0378-5955(94)00185-S
18. Santarelli R, Conti G. Generation of auditory steady-state responses: linearity assessment. *Scand Audiol Suppl.* (1999) 51:23–32.
19. Ross B, Picton TW, Pantev C. Temporal integration in the human auditory cortex as represented by the development of the steady-state magnetic field. *Hear Res.* (2002) 165:68–84. doi: 10.1016/S0378-5955(02)00285-X
20. Uhlhaas PJ, Haenschel C, Nikolić D, Singer W. The role of oscillations and synchrony in cortical networks and their putative relevance for the pathophysiology of schizophrenia. *Schizophr Bull.* (2008) 34:927–43. doi: 10.1093/schbul/sbn062
21. Bosman CA, Lansink CS, Pennartz CM. Functions of gamma-band synchronization in cognition: from single circuits to functional diversity across cortical and subcortical systems. *Eur J Neurosci.* (2014) 39:1982–99. doi: 10.1111/ejn.12606
22. Gray CM, König P, Engel AK, Singer W. Oscillatory responses in cat visual cortex exhibit inter-columnar synchronization which reflects global stimulus properties. *Nature.* (1989) 338:334–7. doi: 10.1038/338334a0
23. Tallon-Baudry C, Bertrand O. Oscillatory gamma activity in humans and its role in object representation. *Trends Cogn Sci.* (1999) 3:151–62. doi: 10.1016/S1364-6613(99)01299-1
24. Fukushima M, Saunders RC, Leopold DA, Mishkin M, Averbeck BB. Spontaneous high-gamma band activity reflects functional organization of auditory cortex in the awake macaque. *Neuron.* (2012) 74:899–910. doi: 10.1016/j.neuron.2012.04.014
25. Polomac N, Leicht G, Nolte G, Andreou C, Schneider TR, Steinmann S, et al. Generators and connectivity of the early auditory evoked gamma band response. *Brain Topogr.* (2015) 28:865–78. doi: 10.1007/s10548-015-0434-6
26. Faivre N, Dönz J, Scandola M, Dhanis H, Bello Ruiz J, Bernasconi F, et al. Self-grounded vision: hand ownership modulates visual location through cortical β and γ oscillations. *J Neurosci.* (2017) 37:11–22. doi: 10.1523/JNEUROSCI.0563-16.2016
27. Carr MF, Karlsson MP, Frank LM. Transient slow gamma synchrony underlies hippocampal memory replay. *Neuron.* (2012) 75:700–13. doi: 10.1016/j.neuron.2012.06.014
28. Lundqvist M, Rose J, Herman P, Brincat SL, Buschman TJ, Miller EK. Gamma and beta bursts underlie working memory. *Neuron.* (2016) 90:152–64. doi: 10.1016/j.neuron.2016.02.028
29. Yamamoto J, Suh J, Takeuchi D, Tonegawa S. Successful execution of working memory linked to synchronized high-frequency gamma oscillations. *Cell.* (2014) 157:845–57. doi: 10.1016/j.cell.2014.04.009
30. Sivarao DV, Chen P, Senapati A, Yang Y, Fernandes A, Benitex Y, et al. 40 Hz Auditory steady-state response is a pharmacodynamic biomarker for cortical NMDA receptors. *Neuropsychopharmacology.* (2016) 41:2232–40. doi: 10.1038/npp.2016.17
31. Light GA, Zhang W, Joshi YB, Bhakta S, Talledo JA, Swerdlow NR. Single-dose memantine improves cortical oscillatory response dynamics in patients with schizophrenia. *Neuropsychopharmacology.* (2017) 42:2633–9. doi: 10.1038/npp.2017.81
32. Tada M, Kirihara K, Koshiyama D, Fujioka M, Usui K, Uka T, et al. Gamma-band auditory steady-state response as a neurophysiological marker for excitation and inhibition balance: a review for understanding schizophrenia and other neuropsychiatric disorders. *Clin EEG Neurosci.* (2020) 51:234–43. doi: 10.1177/1550059419868872

33. Kwon JS, O'Donnell BF, Wallenstein GV, Greene RW, Hirayasu Y, Nestor PG, et al. Gamma frequency range abnormalities to auditory stimulation in schizophrenia. *Arch Gen Psychiatry.* (1999) 56:1001–5. doi: 10.1001/archpsyc.56.11.1001
34. Light GA, Hsu JL, Hsieh MH, Meyer-Gomes K, Sprock J, Swerdlow NR, et al. Gamma band oscillations reveal neural network cortical coherence dysfunction in schizophrenia patients. *Biol Psychiatry.* (2006) 60:1231–40. doi: 10.1016/j.biopsych.2006.03.055
35. Spencer KM, Salisbury DF, Shenton ME, McCarley RW. Gamma-band auditory steady-state responses are impaired in first episode psychosis. *Biol Psychiatry.* (2008) 64:369–75. doi: 10.1016/j.biopsych.2008.02.021
36. Tsuchimoto R, Kanba S, Hirano S, Oribe N, Ueno T, Hirano Y, et al. Reduced high and low frequency gamma synchronization in patients with chronic schizophrenia. *Schizophr Res.* (2011) 133:99–105. doi: 10.1016/j.schres.2011.07.020
37. Tada M, Nagai T, Kirihara K, Koike S, Suga M, Araki T, et al. Differential alterations of auditory gamma oscillatory responses between pre-onset high-risk individuals and first-episode schizophrenia. *Cereb Cortex.* (2016) 26:1027–35. doi: 10.1093/cercor/bhu278
38. Thuné H, Recasens M, Uhlhaas PJ. The 40-Hz auditory steady-state response in patients with schizophrenia: a meta-analysis. *JAMA Psychiatry.* (2016) 73:1145–53. doi: 10.1001/jamapsychiatry.2016.2619
39. Wright IC, Rabe-Hesketh S, Woodruff PW, David AS, Murray RM, Bullmore ET. Meta-analysis of regional brain volumes in schizophrenia. *Am J Psychiatry.* (2000) 157:16–25. doi: 10.1176/ajp.157.1.16
40. Honea R, Crow TJ, Passingham D, Mackay CE. Regional deficits in brain volume in schizophrenia: a meta-analysis of voxel-based morphometry studies. *Am J Psychiatry.* (2005) 162:2233–45. doi: 10.1176/appi.ajp.162.12.2233
41. O'Donnell BF, Hetrick WP, Vohs JL, Krishnan GP, Carroll CA, Shekhar A. Neural synchronization deficits to auditory stimulation in bipolar disorder. *NeuroReport.* (2004) 15:1369–72. doi: 10.1097/01.wnr.0000127348.64681.b2
42. Oda Y, Onitsuka T, Tsuchimoto R, Hirano S, Oribe N, Ueno T, et al. Gamma band neural synchronization deficits for auditory steady state responses in bipolar disorder patients. *PLOS ONE.* (2012) 7:e39955. doi: 10.1371/journal.pone.0039955
43. Rass O, Krishnan G, Brenner CA, Hetrick WP, Merrill CC, Shekhar A, et al. Auditory steady state response in bipolar disorder: relation to clinical state, cognitive performance, medication status, and substance disorders. *Bipolar Disord.* (2010) 12:793–803. doi: 10.1111/j.1399-5618.2010.00871.x
44. Rojas DC, Wilson LB. γ-band abnormalities as markers of autism spectrum disorders. *Biomark Med.* (2014) 8:353–68. doi: 10.2217/bmm.14.15
45. Hong LE, Summerfelt A, McMahon R, Adami H, Francis G, Elliott A, et al. Evoked gamma band synchronization and the liability for schizophrenia. *Schizophr Res.* (2004) 70:293–302. doi: 10.1016/j.schres.2003.12.011
46. Rass O, Forsyth JK, Krishnan GP, Hetrick WP, Klaunig MJ, Breier A, et al. Auditory steady state response in the schizophrenia, first-degree relatives, and schizotypal personality disorder. *Schizophr Res.* (2012) 136:143–9. doi: 10.1016/j.schres.2012.01.003
47. Brenner CA, Sporns O, Lysaker PH, O'Donnell BF. EEG synchronization to modulated auditory tones in schizophrenia, schizoaffective disorder, and schizotypal personality disorder. *Am J Psychiatry.* (2003) 160:2238–40. doi: 10.1176/appi.ajp.160.12.2238
48. Vierling-Claassen D, Siekmeier P, Stufflebeam S, Kopell N. Modeling GABA alterations in schizophrenia: a link between impaired inhibition and altered gamma and beta range auditory entrainment. *J Neurophysiol.* (2008) 99:2656–71. doi: 10.1152/jn.00870.2007
49. Hamm JP, Gilmore CS, Picchetti NA, Sponheim SR, Clementz BA. Abnormalities of neuronal oscillations and temporal integration to low- and high-frequency auditory stimulation in schizophrenia. *Biol Psychiatry.* (2011) 69:989–96. doi: 10.1016/j.biopsych.2010.11.021
50. Isomura S, Onitsuka T, Tsuchimoto R, Nakamura I, Hirano S, Oda Y, et al. Differentiation between major depressive disorder and bipolar disorder by auditory steady-state responses. *J Affect Disord.* (2016) 190:800–6. doi: 10.1016/j.jad.2015.11.034
51. Chen J, Gong Q, Wu F. Deficits in the 30-Hz auditory steady-state response in patients with major depressive disorder. *NeuroReport.* (2016) 27:1147–52. doi: 10.1097/WNR.0000000000000671
52. Wilson TW, Rojas DC, Reite ML, Teale PD, Rogers SJ. Children and adolescents with autism exhibit reduced MEG steady-state gamma responses. *Biol Psychiatry.* (2007) 62:192–7. doi: 10.1016/j.biopsych.2006.07.002
53. Rojas DC, Maharajh K, Teale P, Rogers SJ. Reduced neural synchronization of gamma-band MEG oscillations in first-degree relatives of children with autism. *BMC Psychiatry.* (2008) 8:66. doi: 10.1186/1471-244X-8-66
54. Rojas DC, Maharajh K, Teale PD, Kleman MR, Benkers TL, Carlson JP, et al. Development of the 40Hz steady state auditory evoked magnetic field from ages 5 to 52. *Clin Neurophysiol.* (2006) 117:110–7. doi: 10.1016/j.clinph.2005.08.032
55. Ono Y, Kudoh K, Ikeda T, Takahashi T, Yoshimura Y, Minabe Y, et al. Auditory steady-state response at 20 Hz and 40 Hz in young typically developing children and children with autism spectrum disorder. *Psychiatry Clin Neurosci.* (2020) 74:354–61. doi: 10.1111/pcn.12998
56. Jentsch JD, Roth RH. The neuropsychopharmacology of phencyclidine: from NMDA receptor hypofunction to the dopamine hypothesis of schizophrenia. *Neuropsychopharmacology.* (1999) 20:201–25. doi: 10.1016/S0893-133X(98)00060-8
57. Sohal VS, Zhang F, Yizhar O, Deisseroth K. Parvalbumin neurons and gamma rhythms enhance cortical circuit performance. *Nature.* (2009) 459:698–702. doi: 10.1038/nature07991
58. Lewis DA, Curley AA, Glausier JR, Volk DW. Cortical parvalbumin interneurons and cognitive dysfunction in schizophrenia. *Trends Neurosci.* (2012) 35:57–67. doi: 10.1016/j.tins.2011.10.004
59. Kantrowitz JT, Javitt DC. N-methyl-D-aspartate (NMDA) receptor dysfunction or dysregulation: the final common pathway on the road to schizophrenia? *Brain Res Bull.* (2010) 83:108–21. doi: 10.1016/j.brainresbull.2010.04.006
60. Benes FM, Berretta S. GABAergic interneurons: implications for understanding schizophrenia and bipolar disorder. *Neuropsychopharmacology.* (2001) 25:1–27. doi: 10.1016/S0893-133X(01)00225-1
61. Löscher W. Valproate enhances GABA turnover in the substantia nigra. *Brain Res.* (1989) 501:198–203. doi: 10.1016/0006-8993(89)91044-5
62. Shiah IS, Yatham LN, Baker GB. Divalproex sodium increases plasma GABA levels in healthy volunteers. *Int Clin Psychopharmacol.* (2000) 15:221–5. doi: 10.1097/00004850-200015040-00005
63. Rosenberg G. The mechanisms of action of valproate in neuropsychiatric disorders: can we see the forest for the trees? *Cell Mol Life Sci.* (2007) 64:2090–103. doi: 10.1007/s00018-007-7079-x
64. Sawada T, Chater TE, Sasagawa Y, Yoshimura M, Fujimori-Tonou N, Tanaka K, et al. Developmental excitation-inhibition imbalance underlying psychoses revealed by single-cell analyses of discordant twins-derived cerebral organoids. *Mol Psychiatry.* (2020) 25:2695–711. doi: 10.1038/s41380-020-0844-z
65. Hirano Y, Oribe N, Kanba S, Onitsuka T, Nestor PG, Spencer KM. Spontaneous gamma activity in schizophrenia. *JAMA Psychiatry.* (2015) 72:813–21. doi: 10.1001/jamapsychiatry.2014.2642
66. Zarate CA Jr, Singh JB, Carlson PJ, Brutsche NE, Ameli R, Luckenbaugh DA, et al. A randomized trial of an N-methyl-D-aspartate antagonist in treatment-resistant major depression. *Arch Gen Psychiatry.* (2006) 63:856–64. doi: 10.1001/archpsyc.63.8.856
67. Rivolta D, Heidegger T, Scheller B, Sauer A, Schaum M, Birkner K, et al. Ketamine dysregulates the amplitude and connectivity of high-frequency oscillations in cortical-subcortical networks in humans: evidence from resting-state magnetoencephalography-recordings. *Schizophr Bull.* (2015) 41:1105–14. doi: 10.1093/schbul/sbv051
68. Gogolla N, Leblanc JJ, Quast KB, Südhof TC, Fagiolini M, Hensch TK, et al. Common circuit defect of excitatory-inhibitory balance in mouse models of autism. *J Neurodev Disord.* (2009) 1:172–81. doi: 10.1007/s11689-009-9023-x
69. Fatemi SH, Halt AR, Stary JM, Kanodia R, Schulz SC, Realmuto GR. Glutamic acid decarboxylase 65 and 67 kDa proteins are reduced in autistic parietal and cerebellar cortices. *Biol Psychiatry.* (2002) 52:805–10. doi: 10.1016/S0006-3223(02)01430-0
70. Rojas DC, Singel D, Steinmetz S, Hepburn S, Brown MS. Decreased left perisylvian GABA concentration in children

with autism and unaffected siblings. *Neuroimage*. (2014) 86:28–34. doi: 10.1016/j.neuroimage.2013.01.045
71. Fatemi SH. The hyperglutamatergic hypothesis of autism. *Prog Neuropsychopharmacol Biol Psychiatry*. (2008) 32:911, author reply 912–3. doi: 10.1016/j.pnpbp.2007.11.005
72. Cheung C, Yu K, Fung G, Leung M, Wong C, Li Q, et al. Autistic disorders and schizophrenia: related or remote? An anatomical likelihood estimation. *PLOS ONE*. (2010) 5:e12233. doi: 10.1371/journal.pone.0012233
73. Kolvin I. Studies in the childhood psychoses. I. Diagnostic criteria and classification. *Br J Psychiatry*. (1971) 118:381–4. doi: 10.1192/bjp.118.545.381
74. Gao R, Penzes P. Common mechanisms of excitatory and inhibitory imbalance in schizophrenia and autism spectrum disorders. *Curr Mol Med*. (2015) 15:146–67. doi: 10.2174/1566524015666150303003028
75. Yizhar O, Fenno LE, Prigge M, Schneider F, Davidson TJ, O'Shea DJ, et al. Neocortical excitation/inhibition balance in information processing and social dysfunction. *Nature*. (2011) 477:171–8. doi: 10.1038/nature10360
76. Varela F, Lachaux JP, Rodriguez E, Martinerie J. The brainweb: phase synchronization and large-scale integration. *Nat Rev Neurosci*. (2001) 2:229–39. doi: 10.1038/35067550
77. Singer W. Synchronization of cortical activity and its putative role in information processing and learning. *Annu Rev Physiol*. (1993) 55:349–74. doi: 10.1146/annurev.ph.55.030193.002025
78. Fries P. A mechanism for cognitive dynamics: neuronal communication through neuronal coherence. *Trends Cogn Sci*. (2005) 9:474–80. doi: 10.1016/j.tics.2005.08.011
79. Schnitzler A, Gross J. Normal and pathological oscillatory communication in the brain. *Nat Rev Neurosci*. (2005) 6:285–96. doi: 10.1038/nrn1650
80. Fell J, Axmacher N. The role of phase synchronization in memory processes. *Nat Rev Neurosci*. (2011) 12:105–18. doi: 10.1038/nrn2979
81. Netoff TI, Clewley R, Arno S, Keck T, White JA. Epilepsy in small-world networks. *J Neurosci*. (2004) 24:8075–83. doi: 10.1523/JNEUROSCI.1509-04.2004
82. Hurtado JM, Lachaux JP, Beckley DJ, Gray CM, Sigvardt KA. Inter- and intralimb oscillator coupling in parkinsonian tremor. *Mov Disord*. (2000) 15:683–91. doi: 10.1002/1531-8257(200007)15:4<683::aid-mds1013>3.0.co;2-#
83. Tononi G, Edelman GM. Schizophrenia and the mechanisms of conscious integration. *Brain Res Brain Res Rev*. (2000) 31:391–400. doi: 10.1016/S0165-0173(99)00056-9
84. Rohrbaugh JW, Varner JL, Paige SR, Eckardt MJ, Ellingson RJ. Event-related perturbations in an electrophysiological measure of auditory function: a measure of sensitivity during orienting? *Biol Psychol*. (1989) 29:247–71. doi: 10.1016/0301-0511(89)90022-7
85. Rohrbaugh JW, Varner JL, Paige SR, Eckardt MJ, Ellingson RJ. Auditory and visual event-related perturbations in the 40 Hz auditory steady-state response. *Electroencephalogr Clin Neurophysiol*. (1990) 76:148–64. doi: 10.1016/0013-4694(90)90213-4
86. Rohrbaugh JW, Varner JL, Paige SR, Eckardt MJ, Ellingson RJ. Event-related perturbations in an electrophysiological measure of auditory sensitivity: effects of probability, intensity and repeated sessions. *Int J Psychophysiol*. (1990) 10:17–32. doi: 10.1016/0167-8760(90)90041-B
87. Makeig S, Galambos R. The CERP: event related perturbation in steady-state responses. In: Basar E, Bullock T, editors. *Brain Dynamics: Progress and Perspectives*. Berlin: Springer. (1989). p. 375–400. doi: 10.1007/978-3-642-74557-7_30
88. Rockstroh B, Müller M, Heinz A, Wagner M, Berg P, Elbert T. Modulation of auditory responses during oddball tasks. *Biol Psychol*. (1996) 43:41–55. doi: 10.1016/0301-0511(95)05175-9
89. Ross B, Pantev C. Auditory steady-state responses reveal amplitude modulation gap detection thresholds. *J Acoust Soc Am*. (2004) 115(5 Pt 1):2193–206. doi: 10.1121/1.1694996
90. Ross B, Herdman AT, Pantev C. Stimulus induced desynchronization of human auditory 40-Hz steady-state responses. *J Neurophysiol*. (2005) 94:4082–93. doi: 10.1152/jn.00469.2005
91. Motomura E, Inui K, Kawano Y, Nishihara M, Okada M. Effects of sound-pressure change on the 40 Hz auditory steady-state response and change-related cerebral response. *Brain Sci*. (2019) 9:203. doi: 10.3390/brainsci9080203
92. Sugiyama S, Kinukawa T, Takeuchi N, Nishihara M, Shioiri T, Inui K. Change-related acceleration effects on auditory steady-state response. *Front Syst Neurosci*. (2019) 13:53. doi: 10.3389/fnsys.2019.00053
93. Bartha-Doering L, Deuster D, Giordano V, am Zehnhoff-Dinnesen A, Dobel C. A systematic review of the mismatch negativity as an index for auditory sensory memory: from basic research to clinical and developmental perspectives. *Psychophysiology*. (2015) 52:1115–30. doi: 10.1111/psyp.12459
94. Näätänen R, Gaillard AW, Mäntysalo S. Early selective-attention effect on evoked potential reinterpreted. *Acta Psychol (Amst)*. (1978) 42:313–29. doi: 10.1016/0001-6918(78)90006-9
95. Näätänen R, Jacobsen T, Winkler I. Memory-based or afferent processes in mismatch negativity (MMN): a review of the evidence. *Psychophysiology*. (2005) 42:25–32. doi: 10.1111/j.1469-8986.2005.00256.x
96. Shelley AM, Ward PB, Catts SV, Michie PT, Andrews S, McConaghy N. Mismatch negativity: an index of a preattentive processing deficit in schizophrenia. *Biol Psychiatry*. (1991) 30:1059–62. doi: 10.1016/0006-3223(91)90126-7
97. Catts SV, Shelley AM, Ward PB, Liebert B, McConaghy N, Andrews S, et al. Brain potential evidence for an auditory sensory memory deficit in schizophrenia. *Am J Psychiatry*. (1995) 152:213–9. doi: 10.1176/ajp.152.2.213
98. Chen TC, Hsieh MH, Lin YT, Chan PS, Cheng CH. Mismatch negativity to different deviant changes in autism spectrum disorders: a meta-analysis. *Clin Neurophysiol*. (2020) 131:766–77. doi: 10.1016/j.clinph.2019.10.031
99. Pekkonen E, Jousmäki V, Könönen M, Reinikainen K, Partanen J. Auditory sensory memory impairment in Alzheimer's disease: an event-related potential study. *NeuroReport*. (1994) 5:2537–40. doi: 10.1097/00001756-199412000-00033
100. Skosnik PD, Krishnan GP, O'Donnell BF. The effect of selective attention on the gamma-band auditory steady-state response. *Neurosci Lett*. (2007) 420:223–8. doi: 10.1016/j.neulet.2007.04.072
101. Bidet-Caulet A, Fischer C, Besle J, Aguera PE, Giard MH, Bertrand O. Effects of selective attention on the electrophysiological representation of concurrent sounds in the human auditory cortex. *J Neurosci*. (2007) 27:9252–61. doi: 10.1523/JNEUROSCI.1402-07.2007
102. Sugiyama S, Kinukawa T, Takeuchi N, Nishihara M, Shioiri T, Inui K. Tactile cross-modal acceleration effects on auditory steady-state response. *Front Integr Neurosci*. (2019) 13:72. doi: 10.3389/fnint.2019.00072
103. Tan HR, Gross J, Uhlhaas PJ. MEG-measured auditory steady-state oscillations show high test–retest reliability: a sensor and source-space analysis. *NeuroImage*. (2015) 122:417–26. doi: 10.1016/j.neuroimage.2015.07.055
104. Giard MH, Peronnet F. Auditory-visual integration during multimodal object recognition in humans: a behavioral and electrophysiological study. *J Cogn Neurosci*. (1999) 11:473–90. doi: 10.1162/089892999563544
105. Senkowski D, Molholm S, Gomez-Ramirez M, Foxe JJ. Oscillatory beta activity predicts response speed during a multisensory audiovisual reaction time task: a high-density electrical mapping study. *Cereb Cortex*. (2006) 16:1556–65. doi: 10.1093/cercor/bhj091
106. Tseng HH, Bossong MG, Modinos G, Chen KM, McGuire P, Allen P. A systematic review of multisensory cognitive-affective integration in schizophrenia. *Neurosci Biobehav Rev*. (2015) 55:444–52. doi: 10.1016/j.neubiorev.2015.04.019
107. Baum SH, Stevenson RA, Wallace MT. Behavioral, perceptual, and neural alterations in sensory and multisensory function in autism spectrum disorder. *Prog Neurobiol*. (2015) 134:140–60. doi: 10.1016/j.pneurobio.2015.09.007

Conflict of Interest: The authors declare that the research was conducted in the absence of any commercial or financial relationships that could be construed as a potential conflict of interest.

frontiers in Psychiatry

ORIGINAL RESEARCH
published: 22 March 2021
doi: 10.3389/fpsyt.2021.642048

Reduced Hippocampal Subfield Volume in Schizophrenia and Clinical High-Risk State for Psychosis

Daiki Sasabayashi[1,2], Ryo Yoshimura[3], Tsutomu Takahashi[1,2], Yoichiro Takayanagi[1,4], Shimako Nishiyama[1,5], Yuko Higuchi[1,2], Yuko Mizukami[1], Atsushi Furuichi[1,2], Mikio Kido[1,2], Mihoko Nakamura[1,2], Kyo Noguchi[6] and Michio Suzuki[1,2]*

[1] Department of Neuropsychiatry, University of Toyama Graduate School of Medicine and Pharmaceutical Sciences, Toyama, Japan, [2] Research Center for Idling Brain Science, University of Toyama, Toyama, Japan, [3] Faculty of Medicine, University of Toyama, Toyama, Japan, [4] Arisawabashi Hospital, Toyama, Japan, [5] Health Administration Center, University of Toyama, Toyama, Japan, [6] Department of Radiology, University of Toyama Graduate School of Medicine and Pharmaceutical Sciences, Toyama, Japan

OPEN ACCESS

Edited by:
Tae Young Lee,
Pusan National University Yangsan Hospital, South Korea

Reviewed by:
Minah Kim,
Seoul National University Hospital, South Korea
Minji Bang,
CHA Bundang Medical Center, South Korea
Na Hu,
Sichuan University, China

***Correspondence:**
Daiki Sasabayashi
ds179@med.u-toyama.ac.jp

Specialty section:
This article was submitted to Neuroimaging and Stimulation, a section of the journal Frontiers in Psychiatry

Received: *15 December 2020*
Accepted: *19 February 2021*
Published: *22 March 2021*

Citation:
Sasabayashi D, Yoshimura R, Takahashi T, Takayanagi Y, Nishiyama S, Higuchi Y, Mizukami Y, Furuichi A, Kido M, Nakamura M, Noguchi K and Suzuki M (2021) Reduced Hippocampal Subfield Volume in Schizophrenia and Clinical High-Risk State for Psychosis. Front. Psychiatry 12:642048. doi: 10.3389/fpsyt.2021.642048

Magnetic resonance imaging (MRI) studies in schizophrenia demonstrated volume reduction in hippocampal subfields divided on the basis of specific cytoarchitecture and function. However, it remains unclear whether this abnormality exists prior to the onset of psychosis and differs across illness stages. MRI (3 T) scans were obtained from 77 patients with schizophrenia, including 24 recent-onset and 40 chronic patients, 51 individuals with an at-risk mental state (ARMS) (of whom 5 subsequently developed psychosis within the follow-up period), and 87 healthy controls. Using FreeSurfer software, hippocampal subfield volumes were measured and compared across the groups. Both schizophrenia and ARMS groups exhibited significantly smaller volumes for the bilateral Cornu Ammonis 1 area, left hippocampal tail, and right molecular layer of the hippocampus than the healthy control group. Within the schizophrenia group, chronic patients exhibited a significantly smaller volume for the left hippocampal tail than recent-onset patients. The left hippocampal tail volume was positively correlated with onset age, and negatively correlated with duration of psychosis and duration of medication in the schizophrenia group. Reduced hippocampal subfield volumes observed in both schizophrenia and ARMS groups may represent a common biotype associated with psychosis vulnerability. Volumetric changes of the left hippocampal tail may also suggest ongoing atrophy after the onset of schizophrenia.

Keywords: hippocampal subfield, hippocampal tail, at-risk mental state, schizophrenia, volumetry, magnetic resonance imaging, CA1, molecular layer of the hippocampus

INTRODUCTION

There is increasing evidence supporting that abnormality of the hippocampus, which subserves a range of roles in learning, memory, and emotional regulation (1, 2), functions in the symptomatology and cognitive impairment of schizophrenia (3, 4). Importantly, the hippocampus is not a uniform structure but rather an aggregate of anatomically and functionally different substructures [e.g., the Cornu Ammonis (CA), dentate gyrus (DG), molecular layers, and subiculum; (5)]. Based on the notion of differently affected hippocampal subfields in schizophrenia

(6–8), an etiological hypothesis claimed that exaggerated pattern completion induced by aberrant dentate-to-CA3 connections generated psychotic associations (9), whereas another hypothesis argued that hippocampal hypermetabolism originating from CA1 was related to acquired psychotic symptoms and mnemonic interference (10). However, much of the hippocampus-mediated mechanism involved in the onset and progress of psychosis remains unknown. Thus, examining functional or structural abnormalities of the hippocampal subfields, and assessing their potential roles as psychosis biotype constructs may be of interest (11).

A hippocampal volume deficit is among the most robust magnetic resonance imaging (MRI) findings in schizophrenia patients (12–14). However, it remains unclear when such hippocampal abnormalities occur, i.e., either before or after onset, or both, due to inconsistent findings in individuals with an at-risk mental state (ARMS) (15) [reduced hippocampal volume (16–18) or no differences (19–24)] and in patients with schizophrenia [progressive volume loss (19, 25, 26) or no atrophy over time (27–30)]. These discrepancies among previous studies may be partly explained by the possibility that hippocampal reduction exists only in specific subfields (16, 21). However, limited studies of hippocampal subfields reported mixed results [reviewed by Haukvik et al. (31) and Hu et al. (32)], with schizophrenia patients having prominent volume reduction in the CA1 (33) or more widespread reductions in the CA2/3, CA4/DG, presubiculum, subiculum, and CA1 (34, 35). Similar findings were reported in a few studies examining hippocampal subfield volumes in ARMS individuals (23, 36). Hippocampal subfield segmentation on the MRI methodology is under development (37), which may partly explain the heterogeneity of the results. Although diverse relationships between severe psychotic symptoms (34, 38, 39) or poor cognitive performance (34, 36, 40) and volume reductions in CA4/DG, CA2/3, CA1, and subiculum has been reported in schizophrenia patients, it remains unknown whether hippocampal abnormalities are related to subclinical psychotic or cognitive manifestation in ARMS individuals. Further studies are required to examine the hippocampal subfield volume changes in psychotic disorders using a more comprehensive and fine-grained segmentation protocol, ideally in multiple disease phases, including the prodromal stage.

This MRI study investigated volumetric alterations of the hippocampal subfield and their relevance to psychotic symptom or cognitive function in schizophrenia patients, including recent-onset and chronic patients, and ARMS individuals compared with healthy controls. We applied a novel segmentation algorithm using an *ex vivo* atlas (41), which was reported to have superior compatibility with existing histopathological information to the conventional one using only an *in vivo* atlas (42, 43), in order to label the hippocampal subfields. Based on recent MRI findings (23, 33, 36, 40), we predicted that both schizophrenia and ARMS subjects have reduced volumes of the specific hippocampal subfields, but that disease chronicity and/or medication may affect the findings. As hippocampal subfield atrophy and clinical symptoms or socio-cognitive deficits in ARMS were reported to be less severe compared to schizophrenia (36, 44), we also predicted their associations predominantly in schizophrenia.

MATERIALS AND METHODS

Study Participants

Seventy-seven patients with schizophrenia, 51 individuals with ARMS, and 87 healthy control subjects were included in the current study (**Table 1**). Between December 2013 and August 2019, the study participants were recruited and examined at the clinics of the Department of Neuropsychiatry, Toyama University Hospital.

The schizophrenia patients were assessed by the Structured Clinical Interview for DSM-IV Axis I Disorders Patient Edition (SCID-I/P) (45) and a detailed chart review, and fulfilled both the DSM-IV-TR (46) and DSM-5 (47) criteria. Recent-onset schizophrenia (ROSz) patients were defined by a duration of psychosis <1 year ($n = 24$, age = 24.5 ± 10.1 years, duration of psychosis = 0.4 ± 0.2 years) (48, 49), whereas chronic schizophrenia patients were defined as those with a duration of psychosis >3 years ($n = 40$, age = 32.4 ± 8.5 years, duration of psychosis = 9.9 ± 6.4 years) (50). As an additional analysis, we also defined the chronic schizophrenia patients as those with a duration of psychosis > 10 years ($n = 16$, age = 36.1 ± 7.2 years, duration of psychosis = 16.2 ± 5.6 years) to limit them to more chronic patients. Sixty-five patients with schizophrenia were receiving antipsychotics at the time of MRI. They were treated with risperidone ($n = 7$), paliperidone ($n = 4$), olanzapine ($n = 25$), quetiapine ($n = 4$), aripiprazole ($n = 17$), perospirone ($n = 6$), blonanserin ($n = 9$), zotepine ($n = 1$), clozapine ($n = 1$), haloperidol ($n = 2$), levomepromazine ($n = 6$), and/or fluphenazine ($n = 1$).

Through a local early intervention service in Toyama (51), ARMS individuals who were diagnosed by the Japanese version of the Comprehensive Assessment of At Risk Mental States (CAARMS) (15, 52) were recruited. All 51 ARMS individuals didn't exceed the threshold for psychosis on the CAARMS at baseline (**Table 1**). The ARMS individuals were prospectively followed (mean = 3.7 years, $SD = 3.0$ years), and subdivided into five individuals (9.6%) who later developed psychosis (ARMS-P) and 28 who did not develop psychosis during clinical follow-up of at least 2 years (ARMS-NP). Based on the DSM-IV-TR criteria, all psychotic disorders in ARMS-P subjects were diagnosed as schizophrenia. Regarding psychiatric comorbidities, ARMS subjects were also diagnosed with pervasive developmental disorders (PDD) ($n = 5$), attention-deficit and disruptive behavior disorders ($n = 1$), depressive disorders ($n = 6$), anxiety disorders ($n = 8$), dissociative disorders ($n = 1$), eating disorders ($n = 1$), adjustment disorders ($n = 9$), schizotypal personality disorders ($n = 3$), or avoidant personality disorders ($n = 1$). At the timing of MRI, 11 subjects (21.6%) were receiving a low dosage of antipsychotics for their severe psychiatric conditions in accordance with the clinical guidelines for early psychosis (53). Simultaneously, 5 subjects (9.8%) were taking antidepressants (imipramine equivalent doses = 112.5 ± 65.0 mg/day), and 14 subjects

TABLE 1 | Demographic and clinical data of the healthy comparison (HC), at-risk mental state (ARMS), and schizophrenia (Sz) groups.

	HC	ARMS	Sz	Statistics
	(*n* = 87)	(*n* = 51)	(*n* = 77)	
Sex, male/female (*n*)	46/41	29/22	39/38	Chi-square = 0.48, $p = 0.788$
Age (years)	26.3 ± 3.9	18.3 ± 4.2	28.8 ± 9.4	$F_{(2, 214)} = 41.59$, $p < 0.001$; ARMS < HC < Sz
Height (cm)	165.7 ± 8.3	164.1 ± 8.0	164.3 ± 8.8	$F_{(2, 214)} = 0.77$, $p = 0.465$
Intracranial volume (ml)	1553 ± 126	1485 ± 144	1501 ± 168	$F_{(2, 214)} = 3.74$, $p = 0.025$[a]; ARMS < HC, Sz
JART-IQ[b]	110.0 ± 6.8	97.3 ± 9.3	101.2 ± 8.7	$F_{(2, 181)} = 43.06$, $p < 0.001$; ARMS < Sz < HC
Handedness (right/left/mixed)	60/8/19	31/3/17	63/2/12	Chi-square = 9.33, $p = 0.053$
Socioeconomic status	6.3 ± 0.8	3.1 ± 1.4	4.4 ± 1.3	$F_{(2, 214)} = 131.15$, $p < 0.001$; ARMS < Sz < HC
Parental socioeconomic status[c]	5.9 ± 0.9	4.9 ± 0.9	4.9 ± 1.3	$F_{(2, 213)} = 21.36$, $p < 0.001$; ARMS, Sz < HC
Age at onset (years)			22.8 ± 8.1	
Duration of psychosis (years)			5.6 ± 6.5	
Medication dose (HPD equivalent, mg/day)		3.0 ± 3.2 (*n* = 11)	10.6 ± 8.3 (*n* = 65)	$F_{(1, 75)} = 8.73$, $p = 0.004$; ARMS < Sz
Medication type (atypical/typical/mixed)		10/1/0	56/0/9	Chi-square = 139.39, $p < 0.001$
Duration of medication (years)		0.6 ± 0.8 (*n* = 6)	6.1 ± 6.8 (*n* = 56)	$F_{(1, 61)} = 3.79$, $p = 0.056$
PANSS positive		12.3 ± 3.4	15.5 ±6.3	$F_{(1, 124)} = 10.47$, $p = 0.002$; ARMS < Sz
PANSS negative		16.4 ± 6.9	18.2 ± 7.5	$F_{(1, 124)} = 1.98$, $p = 0.162$
PANSS general		31.9 ± 7.9	35.0 ± 11.5	$F_{(1, 124)} = 2.71$, $p = 0.102$
CAARMS subscale scores				
Unusual thought global rating scale		3.6 ± 1.4		
Unusual thought frequency scale		3.6 ± 1.9		
Non-Bizarre ideas global rating scale		3.9 ± 1.1		
Non-Bizarre ideas frequency scale		4.4 ± 1.3		
Perceptual abnormalities global rating scale		3.1 ± 1.6		
Perceptual abnormalities frequency scale		3.1 ± 1.9		
Disorganized speech global rating scale		2.5 ± 1.3		
Disorganized speech frequency scale		4.1 ± 2.4		
BACS subdomain z-scores				
Verbal memory		−0.7 ± 1.4	−1.3 ± 1.4	$F_{(1, 112)} = 6.05$, $p = 0.015$; Sz < ARMS
Working memory		−0.8 ± 1.3	−0.9 ± 1.3	$F_{(1, 112)} = 0.16$, $p = 0.692$
Motor function		−0.9 ± 1.3	−2.0 ± 1.5	$F_{(1, 112)} = 19.59$, $p < 0.001$; Sz < ARMS
Verbal fluency		−0.9 ± 1.4	−0.9 ± 1.1	$F_{(1, 112)} = 0.024$, $p = 0.877$
Attention and processing speed		−0.3 ± 1.4	−1.2 ± 1.3	$F_{(1, 112)} = 12.03$, $p < 0.001$; Sz < ARMS
Executive function		−0.4 ± 1.3	−0.7 ± 1.8	$F_{(1, 112)} = 0.87$, $p = 0.354$
BACS mean z-score		−0.7 ± 1.0	−1.2 ± 1.0	$F_{(1, 112)} = 7.13$, $p = 0.009$; Sz < ARMS
SCoRS global rating score		5.3 ± 2.2	5.0 ± 2.5	$F_{(1, 102)} = 0.43$, $p = 0.516$
SOFAS		50.2 ± 10.5	47.3 ± 14.3	$F_{(1, 87)} = 1.19$, $p = 0.279$

Values represent the mean ± SD unless otherwise stated.

ARMS, At-Risk Mental State; BACS, Brief Assessment of Cognition in Schizophrenia; CAARMS, Comprehensive Assessment of At-Risk Mental State; IQ, Intelligence Quotient; JART, Japanese version of National Adult Reading Test; HC, healthy controls; HPD, haloperidol; PANSS, Positive and Negative Syndrome Scale; SCoRS, Schizophrenia Cognition Rating Scale; SOFAS, Social and Occupational Functioning Assessment Scale; Sz, schizophrenia.

[a]*Age was used as a covariate.*

[b]*Data missing for 33 subjects.*

[c]*Data missing for one subject.*

(27.5%) were taking anxiolytics (diazepam equivalent doses = 5.1 ± 2.2 mg/day). Omega-3 fatty acids were not used in any subjects.

Healthy control subjects with no personal or family (first-degree relatives) history of psychiatric diseases who were screened by the SCID-I Non-patient Edition (45) were recruited from hospital staff, University students, and members of the local community.

All participants in the present study were physically healthy at the time of MRI and had no lifetime history of serious head trauma, neurological illness, substance abuse, steroid use, or other serious physical diseases. One hundred and sixty-one of the 216 subjects were also included in our previous study that investigated subregional volumes of the thalamus and basal ganglia in schizophrenia and ARMS (54). The Committee on Medical Ethics of Toyama University approved

this study. Written informed consent was received from all study participants. If the participants were under the age of 20, their parent or guardian also provided written consent.

Clinical Assessment

Clinical symptoms of the schizophrenia and ARMS subjects were rated by the Positive and Negative Syndrome Scale (PANSS) (55), whose scores consisted of the positive items, negative items, and general psychopathology. Cognitive assessments were conducted using the Brief Assessment of Cognition in Schizophrenia (BACS) (56, 57). The BACS scores from their six subdomains (verbal memory, working memory, motor speed, verbal fluency, attention, and executive function) were standardized by calculating z-scores, where the mean score of the healthy Japanese was set to zero and the standard deviation was set to one (58). The Schizophrenia Cognition Rating Scale (SCoRS) (59–61) were also conducted to measure the cognitive abilities related to daily-living functioning or functional capacity. Among 20 items of the SCoRS, global rating scale (range 1–10, higher ratings mean greater impairment in daily living skills) was adapted as a representative value. Social functioning was evaluated by the Social and Occupational Functioning Assessment Scale (SOFAS) (62), whose score (range 0–100, higher ratings mean better functioning) corresponded to the social functioning domain of the Global Assessment of Functioning Scale in the DSM-IV-TR (46). All assessments were administered by experienced psychiatrists and trained psychologists.

MRI

Study participants were scanned using a 3-T Magnetom Verio (Siemens Medical System, Inc., Erlangen, Germany) with a three-dimensional magnetization-prepared rapid gradient echo (MPRAGE) sequence yielding 176 contiguous T1-weighted slices of 1.2-mm thickness in the sagittal plane. The imaging parameters were as follows: repetition time = 2,300 ms, echo time = 2.9 ms, flip angle = 9°, field of view = 256 mm, and matrix size = 256 × 256. The voxel size was 1.0 × 1.0 × 1.2 mm.

Measurement of Hippocampal Subfields

Preprocessing of the T1-weighted images, including the correction for intensity non-uniformity in MRI data (63), was performed using the FreeSurfer pipeline (version 6.0, http://surfer.nmr.mgh.harvard.edu) (64, 65). One trained researcher (RY) blinded to the subjects' identities visually inspected all reconstructed images, and manually edited them to improve their subcortical and temporolimbic segmentations. The hippocampal region was automatically segmented into 12 different subfields using a new algorithm, which was based on a computational atlas assembled from *ex vivo* MRI data of post-mortem medial temporal tissue and *in vivo* MRI data informing about neighboring extrahippocampal structures (41). All subfield outputs were also visually inspected to ensure no robust mislabeling. We measured the intracranial volume (ICV), and volume of the entire hippocampus and 12 hippocampal subfields: hippocampal tail, subiculum, CA1, hippocampal fissure, presubiculum, parasubiculum, molecular layer hippocampus (HP), granule cell and molecular layer of the dentate gyrus (GC-ML-DG), CA3, CA4, fimbria, and hippocampus-amygdala-transition-area (HATA).

Statistical Analysis

Clinical and demographic differences among groups were examined by one-way analysis of variance (ANOVA) or chi-square test.

Absolute regional volumes were analyzed using the repeated measures multivariate analysis of variance (MANCOVA), with age and ICV as covariates, diagnosis (e.g., healthy controls vs. ARMS vs. schizophrenia, ARMS-P vs. ARMS-NP, ROSz vs. chronic schizophrenia, and ARMS vs. ROSz vs. chronic schizophrenia) and sex as between-subject factors, and hemisphere and hippocampal subfields (12 regions) as within-subject variables. We assessed the effects of subfield by lower order MANCOVA only when we detected significant diagnosis-by-subfield-by-hemisphere interactions (**Table 2**) in order to prevent possible type I errors. *Post-hoc* Newman-Keuls tests were employed to follow-up the significant main effects or interactions.

Test-retest reliability of FreeSurfer automated hippocampal subfield segmentation has been established using 3T-MRI data (66, 67). For validation analyses, however, we also combined parts of the subfields to set up the merged hippocampal subfields, such as CA1, subiculum$_{combined}$ (subiculum + presubiculum + parasubiculum), and other (GC-ML-DG + CA3 + CA4) subfields on the basis of previous studies (68, 69). Using the same repeated measures MANCOVA model, absolute regional volumes of these merged subfields were analyzed among the schizophrenia, ARMS, and control groups.

Relationships between the absolute volume of the hippocampal subfields with significant group differences (i.e., hippocampal tail, subiculum, CA1, and molecular layer HP; **Table 2**) and clinical or socio-cognitive variables [e.g., age at onset, duration of psychosis, medication dose, duration of medication, PANSS (positive, negative, and general), BACS (mean z-scores), SCoRS global rating score, and SOFAS] in the schizophrenia and ARMS groups were explored by Pearson's partial correlation coefficients controlled for age, sex, and ICV.

The significance threshold was set at $p < 0.05$ (two-sided). For correlation analyses, a Bonferroni correction was applied to correct for multiple comparisons.

RESULTS

Sample Characteristics

Demographic and clinical characteristics of the sample are summarized in **Table 1**. Groups were matched for sex, height, and handedness, but there were significant differences in age, ICV, premorbid Intelligence Quotient, and personal/parental socioeconomic status. The schizophrenia patients were characterized by higher PANSS positive scores, lower BACS measures, and greater amounts of antipsychotics than ARMS individuals.

TABLE 2 | Absolute volume of the hippocampal subfields in the HC, ARMS, and Sz groups.

Region of Interest (mm^3)	HC ($n = 87$)	ARMS ($n = 51$)	Sz ($n = 77$)	Multivariate analysis of covariates		*Post-hoc* tests	
	(Male 46, Female 41)	(Male 29, Female 22)	(Male 39, Female 38)	Diagnosis × Subfield × Hemisphere		Sz vs. HC	ARMS vs. HC
	Mean ± SD	Mean ± SD	Mean ± SD	$F_{(22,2299)}$	*P*	*P*	*P*
Entire hippocampus				1.79	**0.01**		
Left	3523.5 ± 310.5	3403.5 ± 340.3	3378.0 ± 312.2				
Right	3615.6 ± 343.7	3429.0 ± 312.8	3495.5 ± 361.8				
Hippocampal tail				–	–		
Left	551.8 ± 65.9	522.7 ± 53.6	520.0 ± 58.3			**1.76×10^{-5}**	**5.67×10^{-5}**
Right	570.6 ± 70.5	542.7 ± 67.6	554.6 ± 55.6			0.08	**5.51×10^{-4}**
Subiculum				–	–		
Left	445.5 ± 47.9	430.3 ± 50.8	432.3 ± 47.0			0.12	0.10
Right	454.8 ± 48.3	424.4 ± 48.4	439.9 ± 50.1			0.06	**8.30×10^{-5}**
CA1				–	–		
Left	635.9 ± 72.4	619.8 ± 69.5	612.3 ± 63.5			**1.15×10^{-3}**	**1.54×10^{-2}**
Right	676.9 ± 92.2	643.5 ± 73.5	652.5 ± 75.5			**2.40×10^{-4}**	**2.30×10^{-5}**
Hippocampal fissure							
Left	150.5 ± 25.4	154.0 ± 29.5	153.1 ± 26.6			0.70	0.86
Right	144.8 ± 21.8	143.5 ± 23.1	154.2 ± 26.8			0.62	0.85
Presubiculum				–	–		
Left	320.1 ± 33.6	311.4 ± 41.0	306.3 ± 39.0			0.23	0.38
Right	313.1 ± 35.5	296.4 ± 34.6	299.8 ± 42.2			0.34	0.19
Parasubiculum				–	–		
Left	65.2 ± 10.1	63.6 ± 9.2	60.4 ± 9.9			0.98	0.82
Right	61.3 ± 9.8	59.8 ± 8.2	57.3 ± 9.6			1.00	1.00
Molecular layer HP				–	–		
Left	576.1 ± 56.0	558.4 ± 59.7	552.7 ± 54.8			**7.77×10^{-3}**	0.06
Right	597.6 ± 65.6	563.5 ± 54.8	575.5 ± 60.9			**2.56×10^{-3}**	**1.97×10^{-5}**
GC-ML-DG				–	–		
Left	303.5 ± 33.9	295.3 ± 37.4	291.6 ± 35.6			0.55	0.73
Right	307.8 ± 36.0	292.1 ± 30.4	298.2 ± 40.6			0.60	0.27
CA3				–	–		
Left	200.4 ± 25.8	195.4 ± 27.1	195.4 ± 26.3			0.88	0.74
Right	207.4 ± 29.6	198.8 ± 26.8	206.2 ± 33.4			0.85	0.57
CA4				–	–		
Left	260.1 ± 29.0	253.2 ± 32.7	249.0 ± 29.1			0.34	0.55
Right	260.4 ± 30.0	248.4 ± 26.3	253.8 ± 34.9			0.58	0.46
Fimbria				–	–		
Left	102.8 ± 16.8	94.1 ± 16.8	99.5 ± 20.9			0.62	0.69
Right	103.5 ± 18.1	96.3 ± 17.2	97.9 ± 22.5			0.84	0.82
HATA				–	–		
Left	62.2 ± 7.5	59.2 ± 6.0	58.5 ± 8.4			1.00	1.00
Right	62.3 ± 7.4	59.4 ± 8.0	59.9 ± 9.2			1.00	1.00

ARMS, at-risk mental state; CA, Cornu Ammonis; GC-ML-DG, granule cell and molecular layer of the dentate gyrus; HATA, hippocampus-amygdala-transition-area; HC, healthy controls; HP, hippocampus; Sz, schizophrenia.
Bold font indicates statistical significance.

Volumetric Analyses

On comparison among the schizophrenia, ARMS, and control groups, MANCOVA of the hippocampal volume revealed a significant diagnosis-by-subfield-by-hemisphere interaction. We therefore separately evaluated the group differences in hippocampal subfields for each hemisphere. Compared with controls, the schizophrenia group had a smaller volume in the bilateral CA1, bilateral molecular layer HP, and left hippocampal

tail, and the ARMS group had a smaller volume in the bilateral hippocampal tail, bilateral CA1, right subiculum, and right molecular layer HP (**Table 2**). However, the hippocampal volumes did not differ between the schizophrenia and ARMS groups. ARMS subsample without comorbid PDD diagnosis ($n = 46$) also exhibited a smaller volume in the hippocampal tail ($p = 3.20 \times 10^{-5}$ for left side and $p = 6.78 \times 10^{-5}$ for right side), CA1 ($p = 2.29 \times 10^{-2}$ for left side and $p = 9.54 \times 10^{-6}$ for right side), and subiculum ($p = 3.02 \times 10^{-2}$ for left side and $p = 6.69 \times 10^{-5}$ for right side) bilaterally, as well as in the right molecular layer HP ($p = 1.15 \times 10^{-5}$) compared with controls (**Supplementary Table 1**).

There were no significant differences in the hippocampal volumes between the ARMS-P and -NP groups (**Supplementary Table 2**).

On comparison between the ROSz and chronic schizophrenia groups, a significant diagnosis-by-subfield-by-hemisphere interaction was observed by MANCOVA [$F_{(11, 660)} = 3.58$, $p < 0.001$]. *Post-hoc* analyses demonstrated that the left hippocampal tail was significantly reduced in chronic schizophrenia patients compared with ROSz patients ($p = 1.58 \times 10^{-4}$) (**Supplementary Table 3**). Similarly, re-defined chronic schizophrenia patients (duration of psychosis >10 years) exhibited a significant volume reduction only in the left hippocampal tail compared with ROSz patients ($p = 2.42 \times 10^{-4}$) (**Supplementary Table 4**).

Direct comparison among the ARMS, ROSz, and chronic schizophrenia groups showed a significant diagnosis-by-subfield-by-hemisphere interaction [$F_{(22, 1199)} = 3.19$, $p < 0.001$], and the *post-hoc* tests indicated that the left hippocampal tail was significantly reduced in chronic schizophrenia group compared with ROSz ($p = 2.82 \times 10^{-5}$) and ARMS ($p = 8.28 \times 10^{-3}$) groups, as well as in ARMS group compared with ROSz ($p = 3.81 \times 10^{-2}$) group (**Supplementary Table 5**).

For the analysis of merged hippocampal subfields, a significant diagnosis-by-hemisphere interaction was observed by MANCOVA [$F_{(2, 209)} = 5.12$, $p = 0.01$]. *Post-hoc* analyses demonstrated that sum of the merged hippocampal subfield of the right hemisphere was significantly reduced in ARMS individuals compared with controls ($p = 5.80 \times 10^{-3}$) (**Supplementary Table 6**). However, MANCOVA showed no significant interactions involving diagnosis-by-subfield, supporting the utility of more detailed subfield analyses.

The results of these comparisons remained essentially the same even when medication (dosage and duration) was included as a covariate.

Correlation Analyses

The left hippocampal tail volume was positively correlated with onset age and negatively correlated with duration of psychosis in patients with schizophrenia (**Figure 1**, **Table 3**). In the schizophrenia group, volume reduction of the left hippocampal tail was significantly associated with long-term medication use, whereas the hippocampal subfield volume was not associated with antipsychotic medication dosage (**Figure 1**, **Table 3**). In ARMS individuals, we found no significant relationship between the hippocampal volume and clinical or socio-cognitive variables.

DISCUSSION

In the present MRI study, we have investigated hippocampal subfield volumes based on a reliable *ex vivo* atlas cross-sectionally across multiple stages of psychosis. The schizophrenia and ARMS groups had significantly smaller volumes of the CA1, hippocampal tail, and molecular layer HP than healthy controls, suggesting that hippocampal abnormalities in these specific subfields represent a static vulnerability marker of psychosis. On the other hand, the volume loss in the left hippocampal tail preferentially observed in the chronic stage of psychosis, which was related to early onset age and long-term duration of psychosis, may reflect a regional progressive pathological process after onset.

Our finding of reduced hippocampal volume, especially in the CA1, hippocampal tail, and molecular layer HP, was partly consistent with four previous studies (23, 33, 43, 70) in psychotic disorders that assessed hippocampal subfields using a recent version of segmentation by Iglesias et al. (41). On the other hand, previous studies (34, 35, 39) mainly employing an earlier version of segmentation by Leemput et al. (42) reported widespread volume reductions centered on the CA2/3, CA4/DG, and subiculum. Different segmentation methods among the studies may be partly responsible for these discrepancies; the segmentation protocol by Leemput et al. (42) may have underestimated CA1 volumes and overestimated CA2/3 or subiculum volumes compared with manual demarcation (71, 72). In addition, although the relationship between hippocampal subfield morphology and antipsychotic medication has not been well-documented (31), we cannot exclude the potential confounding effects of antipsychotic medication on the results, in consideration of experimental findings of alterations in hippocampal neurogenesis (73) and hippocampal volumes (74) after antipsychotic treatment. Indeed, we noted a relationship between the hippocampal tail and medication duration, but not medication dosage. The discrepancy might be partly due to the inseparable effects of duration of medication and psychosis, or to the opposite effects of medication dosage on hippocampal anatomy in acute and long-term treatment (75). As the group difference remained significant even when we added medication duration and dosage as covariates in the analytical model, reduced volume of the hippocampal subfields in our schizophrenia cohort cannot be explained only by antipsychotic drug action. Although we failed to detect a significant relationship between hippocampus atrophy and clinical symptoms or cognitive deficits, further studies are required to clarify each specialized role of functional/structural abnormalities of the CA1, molecular layer HP, and hippocampal tail in the pathophysiology of schizophrenia.

Partially consistent with a previous study of an ARMS cohort (23, 36), clinically high-risk subjects for psychosis demonstrated reduced volumes in the CA1, molecular layer HP, hippocampal tail, and subiculum, most of which were also

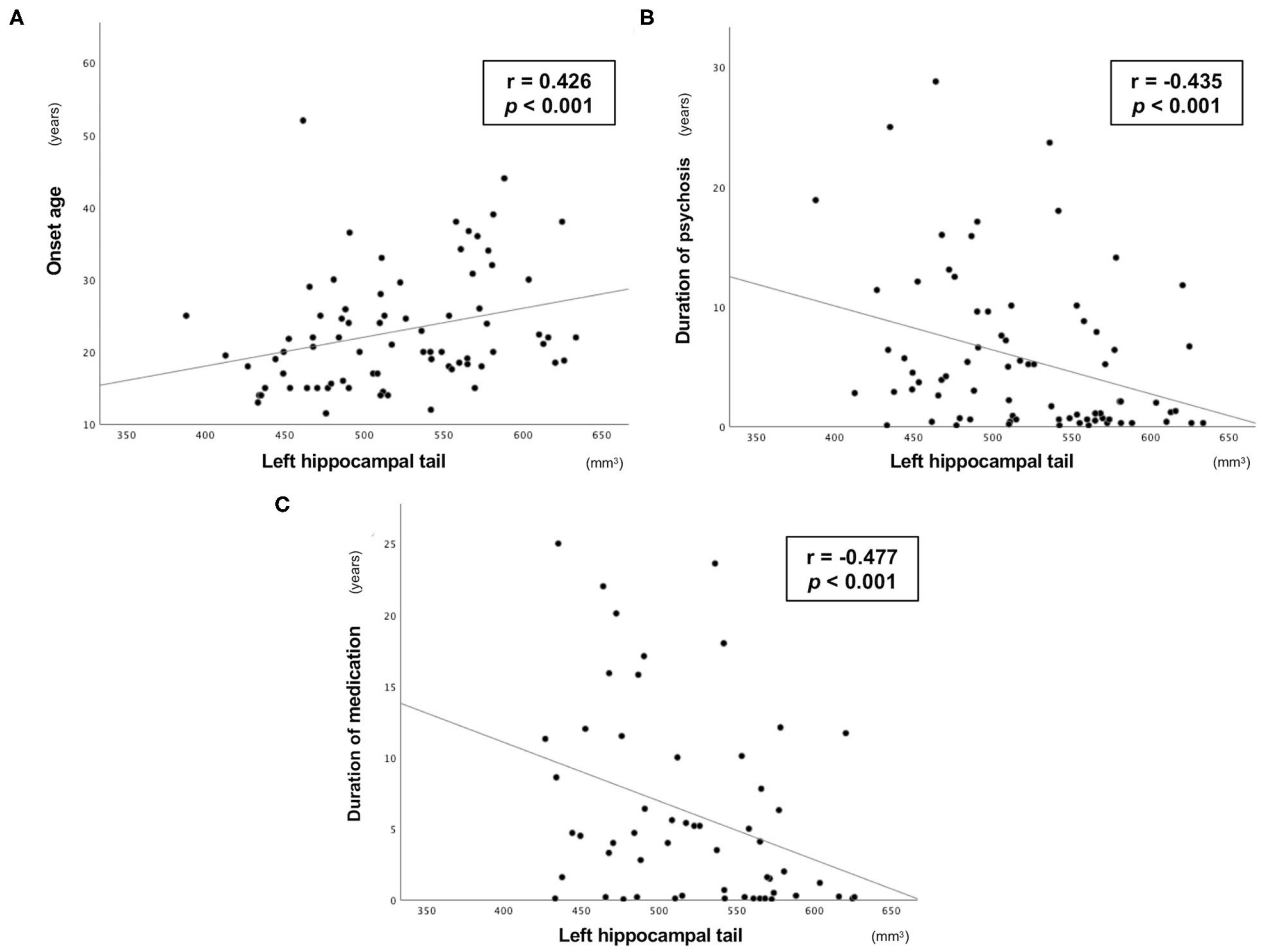

FIGURE 1 | Relationship between the absolute volume of left hippocampal tail and clinical variables in the Sz group. Relationship between the absolute volume of the left hippocampal tail and **(A)** onset age, **(B)** duration of psychosis, and **(C)** duration of medication in patients with schizophrenia.

observed in schizophrenia patients. Because the exclusion of ARMS individuals with PDD diagnosis did not change the conclusion of the study, the hippocampal findings in ARMS may not be explained only by the coexistence of PDD. However, volumes of these subfields did not differ between schizophrenia and ARMS subjects or between ARMS individuals with and without subsequent transition to psychosis in contrast to a few previous findings (36, 76). As rather small sample size of the ARMS-P individuals ($n = 5$) in our cohort could partly explain such discrepancy, their role as a biological discrimination for subsequent psychosis should be further tested in a larger ARMS-P cohort. Reduced hippocampal subfield volumes commonly observed in schizophrenia and ARMS groups should represent a common biotype involved in vulnerability to psychosis. Recently, approaches that can alter some biotypes, such as deficits in hippocampal perfusion or sensory gating (76–78), have been considered as early interventions for psychosis (79, 80). As aerobic exercise and cognitive enhancement therapy can prevent the hippocampal volume decreases over time in early psychosis (81, 82), this biotype may be one of the target candidates for prophylactic treatment in the future.

In contrast to the conventional notion that hippocampal abnormality is a stable feature of schizophrenia (27–30), the combination of the more marked hippocampal tail atrophy in chronic patients relative to recent-onset patients and its relationship with onset age or duration of psychosis suggests a progressive decrease in the hippocampal subfield volume. Direct group comparison also showed the role of illness stages on the hippocampal tail (ROSz > ARMS > chronic schizophrenia), but this result should be interpreted with cautions due to relatively small sample size of ROSz group and significant group difference in age (although statistically controlled). Although the hippocampal tail has not been well-investigated neuroanatomically (41), previous cross-sectional MRI studies reported that reduced volume of this subfield was observed in schizophrenia patients with a longer duration of psychosis (33, 40) in contrast with those with a shorter duration of psychosis (33, 70). Conversely, two longitudinal studies (33, 39) demonstrated that patients with schizophrenia exhibited progressive volume loss in several hippocampal subfields, such as CA1-4, DG, and subiculum, as opposed to putative ongoing atrophy only in the hippocampal tail in this cohort. These studies

TABLE 3 | Relationships between the hippocampal volume and clinical variables in the schizophrenia and ARMS groups.

	ARMS										Sz									
	Left hippocampal tail		Right hippocampal tail		Right subiculum		Left CA1		Right CA1		Right molecular layer HP		Left hippocampal tail		Left CA1		Right CA1		Left molecular layer HP		Right molecular layer HP	
	rho	*p*	*rho*	*p*	*rho*	*p*	*rho*	*p*	*rho*	*p*	*rho*	*p*	*rho*	*p*	*rho*	*p*	*rho*	*p*	*rho*	*p*	*rho*	*p*
Age at onset (years)	–	–	–	–	–	–	–	–	–	–	–	–	0.426	**1.52 × 10^{-4}**	−0.020	0.866	−0.081	0.491	0.040	0.734	0.019	0.872
Duration of psychosis (years)	–	–	–	–	–	–	–	–	–	–	–	–	−0.435	**1.21 × 10^{-4}**	0.009	0.940	0.035	0.772	−0.067	0.573	−0.065	0.587
Medication dose (HPD equiv., mg/day)	0.606	0.111	0.194	0.645	0.084	0.843	−0.056	0.896	−0.381	0.351	−0.189	0.654	0.019	0.882	−0.084	0.516	0.095	0.464	−0.177	0.169	0.035	0.787
Duration of medication (years)	0.007	0.996	0.837	0.369	−0.687	0.518	−0.981	0.126	−0.824	0.384	−0.983	0.119	−0.477	**3.00 × 10^{-4}**	−0.028	0.843	−0.054	0.702	−0.093	0.509	−0.122	0.384
PANSS positive	−0.002	0.987	0.051	0.734	0.101	0.499	−0.018	0.906	0.175	0.240	0.034	0.821	−0.243	0.040	−0.104	0.383	−0.036	0.766	−0.062	0.605	−0.129	0.281
PANSS negative	0.249	0.091	0.193	0.195	0.268	0.069	0.320	0.028	0.286	0.052	0.288	0.049	−0.007	0.956	0.015	0.897	0.123	0.304	0.084	0.482	0.100	0.405
PANSS general	0.010	0.949	0.033	0.827	0.089	0.550	0.167	0.261	0.228	0.123	0.123	0.411	−0.098	0.414	−0.162	0.174	0.058	0.626	−0.059	0.622	−0.023	0.848
BACS mean z-score	−0.056	0.716	−0.176	0.249	−0.001	0.994	−0.271	0.072	0.048	0.755	−0.017	0.913	−0.107	0.410	0.029	0.825	0.006	0.961	−0.099	0.445	−0.004	0.975
SCoRS global rating score	−0.010	0.944	−0.082	0.578	0.145	0.324	0.082	0.581	−0.063	0.668	−0.077	0.604	0.161	0.270	−0.183	0.209	−0.184	0.207	−0.144	0.325	−0.197	0.176
SOFAS	0.002	0.990	−0.086	0.601	0.035	0.831	−0.317	0.049	−0.115	0.485	−0.047	0.777	−0.135	0.387	0.136	0.385	−0.059	0.708	0.084	0.591	−0.061	0.700

ARMS, at-risk mental state; BACS, Brief Assessment of Cognition in Schizophrenia; CA, Cornu Ammonis; HP, hippocampus; HPD, haloperidol; PANSS, Positive and Negative Syndrome Scale; SCoRS, Schizophrenia Cognition Rating Scale; SOFAS, Social and Occupational Functioning Assessment Scale; Sz, schizophrenia.

Bold font indicates statistical significance after Bonferroni's correction for multiple comparisons [seven subfields by 10 clinical variables; $p < 0.000714$ (0.05/70)].

(33, 39) supported the progressive pathology of schizophrenia (19, 25, 26) by confirming that the symptomatic deterioration was synchronized with the decrease in hippocampal volume, although they had limitations; their cohorts were characterized by a relatively small sample size, short-term follow-up period, and mixture of recent-onset and chronic patients. Future large-scale longitudinal studies are required to directly examine the trajectory of the hippocampal subfield atrophy at varying stages of psychotic disorders, focusing on the spatial distribution of subregional deficits.

Although the current MRI study was unable to sufficiently clarify the etiological role of the hippocampus in psychotic disorder, our finding of focal shrinkage in the CA1 and subiculum [molecular layer HP was classified as part of the subiculum or CA fields in most previous segmentations (41, 42)] that developed around onset partly supports the hippocampal hyperactivity models (83, 84). Among them, Small et al. (10) proposed the early involvement of CA1 (and subiculum) in the pathophysiological process responsible for psychosis because it has greater expression of the N-methyl-D-aspartate (NMDA) receptor (85) and may be especially vulnerable to glutamate-mediated neurotoxicity (86). Therefore, excess extracellular glutamate that accumulates preferentially in the CA1/subiculum in the early disease stage affects metabolic demand and blood flow, and causes eventual volume loss in the corresponding region (7, 76, 87). Dysfunction of gamma-aminobutyric acid (GABA)-ergic interneurons, which were proposed to underlie the metabolic and structural alterations in these hippocampal subfields, may propagate to other hippocampal subfields and drive feedforward excitation of the hippocampal trisynaptic circuit (88, 89), leading to the clinical features of schizophrenia and cognitive impairments (90–93). Furthermore, the finding of reduced NMDA receptor related proteins only in the dentate molecular layer in schizophrenia post-mortem brains may imply the specific role of molecular layer in this cascade (94). Alternatively, we previously suggested that only the hippocampal tail exhibits progressive atrophy across the disease stages in contrast to the assumption that hippocampal subfield volume losses extend along the trisynaptic pathway [e.g., CA3-4 and DG; (33)]. In this regard, even though demarcation of the hippocampal tail was slightly different from that in the present study, the cumulative adverse effects of psychotic episodes on the left hippocampal tail have been reported (95). In methylazoxymethanol acetate treated rats as a developmental disruption model of schizophrenia (96), a reduction in synaptic innervation and excitatory synaptic transmission was observed especially in the dorsal hippocampus (97). Thus, the nature of static or progressive structural/functional changes of the hippocampus, particularly in the posterior portion where fewer studies have focused, remains unclear.

Some limitations to the present study should be delineated. First, in order to label the hippocampal subfields, we adopted a new and validated segmentation protocol (41), but it was based on only a T1 sequence, as employed in most previous studies (23, 43, 70). We may be able to obtain more reliable segmentation utilizing an additional T2 sequence (98). Second, hippocampal morphometric changes may be affected not only by intrinsic

factors of psychosis, but also by potential confounding factors such as antipsychotics (99), comorbid anxiety and depression (100), and prolonged stress (101). Future studies should try to replicate the current hippocampal findings in antipsychotic-naïve schizophrenia patients whose comorbid symptoms are well-managed. Thirdly, there are no consensus operational definitions for "resent-onset" or "chronic" schizophrenia [e.g., DSM-IV-TR; (46)]. Although our results did not change significantly between different chronic definitions, potential role of illness stages on the hippocampal volume should be further tested in future longitudinal studies in various illness stages. Fourthly, although the established reliability of automated subfield segmentation (66, 67), our results of significant group difference predominantly in relatively large hippocampal subfields (CA1, molecular layer HP, and hippocampal tail) may raise the possibility of technical issue that prevents accurate group comparison of smaller subfields. Lastly, volume reduction of the hippocampal subfields, especially in the CA1, was also noted in other neuropsychiatric illnesses such as post-traumatic stress disorder, major depressive disorder, and bipolar disorder (102, 103). On the other hand, volume reductions in the CA2/3 and presubiculum were more pronounced in schizophrenia than in bipolar disorder (31), possibly contributing to discrimination among psychiatric disorders. Thus, whether our hippocampal findings belong to a common biotype across psychiatric disorders or a distinct biotype of the schizophrenia spectrum should be investigated.

In conclusion, this MRI study demonstrated that both schizophrenia and ARMS groups exhibit smaller hippocampal volumes, especially in CA1, hippocampal tail, and molecular layer HP subfields. Reduced volume of the left hippocampal tail in schizophrenia was associated with illness chronicity and antipsychotic medication. The hippocampal subfield atrophy may represent a potential biotype that accounts for psychosis vulnerability, but further studies are needed to clarify how it is involved in the formation and development of psychotic disorders.

DATA AVAILABILITY STATEMENT

The datasets utilized for this article are not available immediately because we do not have permission to share them. Requests to access the datasets should be directed to Daiki Sasabayashi, ds179@med.u-toyama.ac.jp.

ETHICS STATEMENT

The studies involving human participants were reviewed and approved by the Committee on Medical Ethics of Toyama University. Written informed consent to participate in this study was provided by the participants' legal guardian/next of kin.

AUTHOR CONTRIBUTIONS

DS, TT, YT, and MS conceived the present study and its methods. DS conducted statistical analyses and wrote the manuscript. DS, SN, YH, YM, AF, MK, and MN recruited participants, and were involved in clinical and diagnostic assessments. DS and RY analyzed MRI data. KN provided technical support for MRI and data processing. DS, AF, MN, and TT managed MRI and clinical data. TT, YT, and MS contributed to the writing and editing of the manuscript. All authors contributed to and approval the final manuscript.

FUNDING

This study was supported by JSPS KAKENHI Grant Numbers JP18K15509, JP19H03579, and JP20KK0193 to DS, JP16K04349 to SN, JP18K07549 to YT, JP18K07550 to TT, and JP20H03598 to MS, the SENSHIN Medical Research Foundation to YT, DS, and YH, THE HOKURIKU BANK Grant-in-Aid for Young Scientists to DS, and by the Health and Labor Sciences Research Grants for Comprehensive Research on Persons with Disabilities from the Japan Agency for Medical Research and Development (AMED) Grant Number 20dk0307094s0201 to MS.

SUPPLEMENTARY MATERIAL

The Supplementary Material for this article can be found online at: https://www.frontiersin.org/articles/10.3389/fpsyt.2021.642048/full#supplementary-material

REFERENCES

1. Kim JJ, Diamond DM. The stressed hippocampus, synaptic plasticity and lost memories. *Nat Rev Neurosci.* (2002) 3:453–62. doi: 10.1038/nrn849
2. Sweeney P, Yang Y. Neural circuit mechanisms underlying emotional regulation of homeostatic feeding. *Trends Endocrinol Metab.* (2017) 28:437–48. doi: 10.1016/j.tem.2017.02.006
3. Harrison PJ. The hippocampus in schizophrenia: a review of the neuropathological evidence and its pathophysiological implications. *Psychopharmacology.* (2004) 174:151–62. doi: 10.1007/s00213-003-1761-y
4. Lieberman JA, Girgis RR, Brucato G, Moore H, Provenzano F, Kegeles L. Hippocampal dysfunction in the pathophysiology of schizophrenia: a selective review and hypothesis for early detection and intervention. *Mol Psychiatry.* (2018) 23:1764–72. doi: 10.1038/mp.2017.249
5. Schultz C, Engelhardt M. Anatomy of the hippocampal formation. *Front Neurol Neurosci.* (2014) 34:6–17. doi: 10.1159/000360925
6. Ghose S, Chin R, Gallegos A, Roberts R, Coyle J, Tamminga C. Localization of NAAG-related gene expression deficits to the anterior hippocampus in schizophrenia. *Schizophr Res.* (2009) 111:131–7. doi: 10.1016/j.schres.2009.03.038
7. Schobel SA, Lewandowski NM, Corcoran CM, Moore H, Brown T, Malaspina D. Differential targeting of the CA1 subfield of the hippocampal formation by schizophrenia and related psychotic disorders. *Arch Gen Psychiatry.* (2009) 66:938–46. doi: 10.1001/archgenpsychiatry.2009.115
8. Talati P, Rane S, Kose S, Blackford JU, Gore J, Donahue MJ. Increased hippocampal CA1 cerebral blood volume in schizophrenia. *Neuroimage Clin.* (2014) 5:359–64. doi: 10.1016/j.nicl.2014.07.004

9. Tamminga CA, Stan AD, Wagner AD. The hippocampal formation in schizophrenia. *Am J Psychiatry.* (2010) 167:1178–93. doi: 10.1176/appi.ajp.2010.09081187
10. Small SA, Schobel SA, Buxton RB, Witter MP, Barnes CA. A pathophysiological framework of hippocampal dysfunction in ageing and disease. *Nat Rev Neurosci.* (2011) 12:585–601. doi: 10.1038/nrn3085
11. Clementz BA, Sweeney JA, Hamm JP, Ivleva EI, Ethridge LE, Pearlson GD. Identification of distinct psychosis biotypes using brain-based biomarkers. *Am J Psychiatry.* (2016) 173:373–84. doi: 10.1176/appi.ajp.2015.14091200
12. Haijma SV, van Haren N, Cahn W, Koolschijn PC, Hulshoff Pol HE, Kahn RS. Brain volumes in schizophrenia: a meta-analysis in over 18 000 subjects. *Schizophr Bull.* (2013) 39:1129–38. doi: 10.1093/schbul/sbs118
13. van Erp TG, Hibar DP, Rasmussen JM, Glahn DC, Pearlson GD, Andreassen OA. Subcortical brain volume abnormalities in 2028 individuals with schizophrenia and 2540 healthy controls via the ENIGMA consortium. *Mol Psychiatry.* (2016) 21:547–53. doi: 10.1038/mp.2015.63
14. Okada N, Fukunaga M, Yamashita F, Koshiyama D, Yamamori H, Ohi K. Abnormal asymmetries in subcortical brain volume in schizophrenia. *Mol Psychiatry.* (2016) 21:1460–6. doi: 10.1038/mp.2015.209
15. Yung AR, Yuen HP, McGorry PD, Phillips LJ, Kelly D, Dell'Olio M. Mapping the onset of psychosis: the Comprehensive Assessment of At-Risk Mental States. *Aust N Z J Psychiatry.* (2005) 39:964–71. doi: 10.1080/j.1440-1614.2005.01714.x
16. Wood SJ, Kennedy D, Phillips LJ, Seal ML, Yücel M, Nelson B. Hippocampal pathology in individuals at ultra-high risk for psychosis: a multi-modal magnetic resonance study. *Neuroimage.* (2010) 52:62–8. doi: 10.1016/j.neuroimage.2010.04.012
17. Dean DJ, Orr JM, Bernard JA, Gupta T, Pelletier-Baldelli A, Carol EE. Hippocampal shape abnormalities predict symptom progression in neuroleptic-free youth at ultrahigh risk for psychosis. *Schizophr Bull.* (2016) 42:161–9. doi: 10.1093/schbul/sbv086
18. Harrisberger F, Buechler R, Smieskova R, Lenz C, Walter A, Egloff L. Alterations in the hippocampus and thalamus in individuals at high risk for psychosis. *NPJ Schizophr.* (2016) 2:16033. doi: 10.1038/npjschz.2016.33
19. Velakoulis D, Wood SJ, Wong MT, McGorry PD, Yung A, Phillips L. Hippocampal and amygdala volumes according to psychosis stage and diagnosis: a magnetic resonance imaging study of chronic schizophrenia, first-episode psychosis, and ultra-high-risk individuals. *Arch Gen Psychiatry.* (2006) 63:139–49. doi: 10.1001/archpsyc.63.2.139
20. Buehlmann E, Berger GE, Aston J, Gschwandtner U, Pflueger MO, Borgwardt SJ. Hippocampus abnormalities in at risk mental states for psychosis? A cross-sectional high resolution region of interest magnetic resonance imaging study. *J Psychiatr Res.* (2010) 44:447–53. doi: 10.1016/j.jpsychires.2009.10.008
21. Witthaus H, Mendes U, Brüne M, Ozgürdal S, Bohner G, Gudlowski Y. Hippocampal subdivision and amygdalar volumes in patients in an at-risk mental state for schizophrenia. *J Psychiatry Neurosci.* (2010) 35:33–40. doi: 10.1503/jpn.090013
22. Klauser P, Zhou J, Lim JK, Poh JS, Zheng H, Tng HY. Lack of evidence for regional brain volume or cortical thickness abnormalities in youths at clinical high risk for psychosis: findings from the longitudinal youth at risk study. *Schizophr Bull.* (2015) 41:1285–93. doi: 10.1093/schbul/sbv012
23. Ho NF, Holt DJ, Cheung M, Iglesias JE, Goh A, Wang M. Progressive decline in hippocampal CA1 volume in individuals at ultra-high-risk for psychosis who do not remit: findings from the longitudinal youth at risk study. *Neuropsychopharmacology.* (2017) 42:1361–70. doi: 10.1038/npp.2017.5
24. Sasabayashi D, Takayanagi Y, Takahashi T, Katagiri N, Sakuma A, Obara C. Subcortical brain volume abnormalities in individuals with an at-risk mental state. *Schizophr Bull.* (2020) 46:834–45. doi: 10.1093/schbul/sbaa011
25. Ebdrup BH, Skimminge A, Rasmussen H, Aggernaes B, Oranje B, Lublin H. Progressive striatal and hippocampal volume loss in initially antipsychotic-naive, first-episode schizophrenia patients treated with quetiapine: relationship to dose and symptoms. *Int J Neuropsychopharmacol.* (2011) 14:69–82. doi: 10.1017/s1461145710000817
26. Rizos E, Papathanasiou MA, Michalopoulou PG, Laskos E, Mazioti A, Kastania A. A longitudinal study of alterations of hippocampal volumes and serum BDNF levels in association to atypical antipsychotics in a sample of first-episode patients with schizophrenia. *PLoS ONE.* (2014) 9:e87997. doi: 10.1371/journal.pone.0087997
27. Lieberman J, Chakos M, Wu H, Alvir J, Hoffman E, Robinson D. Longitudinal study of brain morphology in first episode schizophrenia. *Biol Psychiatry.* (2001) 49:487–99. doi: 10.1016/s0006-3223(01)01067-8
28. Wood SJ, Velakoulis D, Smith DJ, Bond D, Stuart GW, McGorry PD. A longitudinal study of hippocampal volume in first episode psychosis and chronic schizophrenia. *Schizophr Res.* (2001) 52:37–46. doi: 10.1016/s0920-9964(01)00175-x
29. Whitworth AB, Kemmler G, Honeder M, Kremser C, Felber S, Hausmann A. Longitudinal volumetric MRI study in first- and multiple-episode male schizophrenia patients. *Psychiatry Res.* (2005) 140:225–37. doi: 10.1016/j.pscychresns.2005.07.006
30. Mamah D, Harms MP, Barch D, Styner M, Lieberman JA, Wang L. Hippocampal shape and volume changes with antipsychotics in early stage psychotic illness. *Front Psychiatry.* (2012) 3:96. doi: 10.3389/fpsyt.2012.00096
31. Haukvik UK, Tamnes CK, Söderman E, Agartz I. Neuroimaging hippocampal subfields in schizophrenia and bipolar disorder: a systematic review and meta-analysis. *J Psychiatr Res.* (2018) 104:217–26. doi: 10.1016/j.jpsychires.2018.08.012
32. Hu N, Luo C, Zhang W, Yang X, Xiao Y, Sweeney JA. Hippocampal subfield alterations in schizophrenia: a selective review of structural MRI studies. *Biomark Neuropsychiatry.* (2020) 3:100026. doi: 10.1016/j.bionps.2020.100026
33. Ho NF, Iglesias JE, Sum MY, Kuswanto CN, Sitoh YY, De Souza J. Progression from selective to general involvement of hippocampal subfields in schizophrenia. *Mol Psychiatry.* (2017) 22:142–52. doi: 10.1038/mp.2016.4
34. Mathew I, Gardin TM, Tandon N, Eack S, Francis AN, Seidman LJ. Medial temporal lobe structures and hippocampal subfields in psychotic disorders: findings from the Bipolar-Schizophrenia Network on Intermediate Phenotypes (B-SNIP) study. *JAMA Psychiatry.* (2014) 71:769–77. doi: 10.1001/jamapsychiatry.2014.453
35. Haukvik UK, Westlye LT, Mørch-Johnsen L, Jørgensen KN, Lange EH, Dale AM. *In vivo* hippocampal subfield volumes in schizophrenia and bipolar disorder. *Biol Psychiatry.* (2015) 77:581–8. doi: 10.1016/j.biopsych.2014.06.020
36. Vargas T, Dean DJ, Osborne KJ, Gupta T, Ristanovic I, Ozturk S. Hippocampal subregions across the psychosis spectrum. *Schizophr Bull.* (2018) 44:1091–9. doi: 10.1093/schbul/sbx160
37. Wisse LE, Biessels GJ, Geerlings MI. A critical appraisal of the hippocampal subfield segmentation package in FreeSurfer. *Front Aging Neurosci.* (2014) 6:261. doi: 10.3389/fnagi.2014.00261
38. Kuhn S, Musso F, Mobascher A, Warbrick T, Winterer G, Gallinat J. Hippocampal subfields predict positive symptoms in schizophrenia: first evidence from brain morphometry. *Transl Psychiatry.* (2012) 2:e127. doi: 10.1038/tp.2012.51
39. Kawano M, Sawada K, Shimodera S, Ogawa Y, Kariya S, Lang DJ. Hippocampal subfield volumes in first episode and chronic schizophrenia. *PLoS ONE.* (2015) 10:e0117785. doi: 10.1371/journal.pone.0117785
40. Nakahara S, Turner JA, Calhoun VD, Lim KO, Mueller B, Bustillo JR. Dentate gyrus volume deficit in schizophrenia. *Psychol Med.* (2020) 50:1267–77. doi: 10.1017/s0033291719001144
41. Iglesias JE, Augustinack JC, Nguyen K, Player CM, Player A, Wright M. A computational atlas of the hippocampal formation using *ex vivo*, ultra-high resolution MRI: application to adaptive segmentation of *in vivo* MRI. *Neuroimage.* (2015) 115:117–37. doi: 10.1016/j.neuroimage.2015.04.042
42. Leemput KV, Bakkour A, Benner T, Wiggins G, Wald LL, Augustinack J. Automated segmentation of hippocampal subfields from ultra-high resolution *in vivo* MRI. *Hippocampus.* (2009) 19:549–57. doi: 10.1002/hipo.20615
43. Sone D, Sato N, Maikusa N, Ota M, Sumida K, Yokoyama K. Automated subfield volumetric analysis of hippocampus in temporal lobe epilepsy using high-resolution T2-weighed MR imaging. *Neuroimage Clin.* (2016) 12:57–64. doi: 10.1016/j.nicl.2016.06.008
44. Hou CL, Xiang YT, Wang ZL, Everall I, Tang Y, Yang C. Cognitive functioning in individuals at ultra-high risk for psychosis, first-degree relatives of patients with psychosis and

patients with first-episode schizophrenia. *Schizophr Res.* (2016) 174:71–6. doi: 10.1016/j.schres.2016.04.034
45. First MB, Gibbon M, Spitzer RL, Williams JBW. *Structured Clinical Interview for DSM-IV Axis I Disorders*. Washington DC: American Psychiatric Press. (1997).
46. American Psychiatric Association. *Diagnostic and Statistical Manual of Mental Disorders*. 4th ed. Text Revision. Washington DC: American Psychiatric Association Press (2000).
47. American Psychiatric Association. *Diagnostic and Statistical Manual of Mental Disorders.* 5th ed. Washington DC: American Psychiatric Association Press (2013).
48. Flaum MA, Andreasen NC, Arndt S. The Iowa prospective longitudinal study of recent-onset psychoses. *Schizophr Bull.* (1992) 18:481–90. doi: 10.1093/schbul/18.3.481
49. Breitborde NJK, Srihari VH, Wood SW. Review of the operational definition for first-episode psychosis. *Early Interv Psychiatry.* (2009) 3:259–65. doi: 10.1001/archpsyc.57.7.692
50. Takahashi T, Kido M, Sasabayashi D, Nakamura M, Furuichi A, Takayanagi Y. Gray matter changes in the insular cortex during the course of the schizophrenia spectrum. *Front Psychiatry.* (2020) 11:659. doi: 10.3389/fpsyt.2020.00659
51. Mizuno M, Suzuki M, Matsumoto K, Murakami M, Takeshi K, Miyakoshi T. Clinical practice and research activities for early psychiatric intervention at Japanese leading centres. *Early Interv Psychiatry.* (2009) 3:5–9. doi: 10.1111/j.1751-7893.2008.00104.x
52. Miyakoshi T, Matsumoto K, Ito F, Ohmuro N, Matsuoka H. Application of the Comprehensive Assessment of At-Risk Mental States (CAARMS) to the Japanese population: reliability and validity of the Japanese version of the CAARMS. *Early Interv Psychiatry.* (2009) 3:123–30. doi: 10.1111/j.1751-7893.2009.00118.x
53. International Early Psychosis Association Writing Group. International clinical practice guidelines for early psychosis. *Br J Psychiatry Suppl.* (2005) 48:s120–4. doi: 10.1192/bjp.187.48.s120
54. Takahashi T, Tsugawa S, Nakajima S, Plitman E, Chakravarty MM, Masuda F. Thalamic and striato-pallidal volumes in schizophrenia patients and individuals at risk for psychosis: a multi-atlas segmentation study. *Schizophr Res.* (2020). doi: 10.1016/j.schres.2020.04.016. [Epub ahead of print].
55. Kay SR, Fiszbein A, Opler LA. The positive and negative syndrome scale (PANSS) for schizophrenia. *Schizophr Bull.* (1987) 13:261–76. doi: 10.1093/schbul/13.2.261
56. Keefe RS, Goldberg TE, Harvey PD, Gold JM, Poe MP, Coughenour L. The Brief Assessment of Cognition in Schizophrenia: reliability, sensitivity, and comparison with a standard neurocognitive battery. *Schizophr Res.* (2004) 68:283–97. doi: 10.1016/j.schres.2003.09.011
57. Kaneda Y, Sumiyoshi T, Keefe R, Ishimoto Y, Numata S, Ohmori T. Brief assessment of cognition in schizophrenia: validation of the Japanese version. *Psychiatry Clin Neurosci.* (2007) 61:602–9. doi: 10.1111/j.1440-1819.2007.01725.x
58. Kaneda Y, Omori T, Okahisa Y, Sumiyoshi T, Pu S, Ueoka Y. Measurement and treatment research to improve cognition in schizophrenia consensus cognitive battery: validation of the Japanese version. *Psychiatry Clin Neurosci.* (2013) 67:182–8. doi: 10.1111/pcn.12029
59. Keefe RS, Poe M, Walker TM, Kang JW, Harvey PD. The Schizophrenia Cognition Rating Scale: an interview-based assessment and its relationship to cognition, real-world functioning, and functional capacity. *Am J Psychiatry.* (2006) 163:426–32. doi: 10.1176/appi.ajp.163.3.426
60. Kaneda Y, Ueoka Y, Sumiyoshi T, Yasui-Furukori N, Ito T, Higuchi Y. Schizophrenia Cognition Rating Scale Japanese version (SCoRS-J) as a co-primary measure assessing cognitive function in schizophrenia. *Nihon Shinkei Seishin Yakurigaku Zasshi.* (2011) 31:259–62.
61. Higuchi Y, Sumiyoshi T, Seo T, Suga M, Takahashi T, Nishiyama S. Associations between daily living skills, cognition, and real-world functioning across stages of schizophrenia; a study with the Schizophrenia Cognition Rating Scale Japanese version. *Schizophr Res Cogn.* (2017) 7:13–18. doi: 10.1016/j.scog.2017.01.001
62. Goldman HH, Skodol AE, Lave TR. Revising axis V for DSM-IV: a review of measures of social functioning. *Am J Psychiatry.* (1992) 149:1148–56. doi: 10.1176/ajp.149.9.1148
63. Sled JG, Zijdenbos AP, Evans AC. A nonparametric method for automatic correction of intensity nonuniformity in MRI data. *IEEE Trans Med Imaging.* (1998) 17:87–97. doi: 10.1109/42.668698
64. Dale AM, Fischl B, Sereno MI. Cortical surface-based analysis. I. Segmentation and surface reconstruction. *Neuroimage.* (1999) 9:179–94. doi: 10.1006/nimg.1998.0395
65. Fischl B, Sereno MI, Dale AM. Cortical surface-based analysis. II: Inflation, flattening, and a surface-based coordinate system. *Neuroimage.* (1999) 9:195–207. doi: 10.1006/nimg.1998.0396
66. Brown EM, Pierce ME, Clark DC, Fischl BR, Iglesias JE, Milberg WP. Test-retest reliability of FreeSurfer automated hippocampal subfield segmentation within and across scanners. *Neuroimage.* (2020) 210:116563. doi: 10.1016/j.neuroimage.2020.116563
67. Chiappiniello A, Tarducci R, Muscio C, Bruzzone MG, Bozzali M, Tiraboschi P. Automatic multispectral MRI segmentation of human hippocampal subfields: an evaluation of multicentric test-retest reproducibility. *Brain Struct Funct.* (2021) 226:137–50. doi: 10.1007/s00429-020-02172-w
68. Joie RL, Fouquet M, Mezenge F, Landeau B, Villain N, Mevel K. Differential effect of age on hippocampal subfields assessed using a new high-resolution 3T MR sequence. *NeuroImage.* (2010) 53:506–14. doi: 10.1016/j.neuroimage.2010.06.024
69. Flores R, Joie RL, Landeau B, Perrotin A, Mezenge F, Sayette V. Effects of age and Alzheimer's disease on hippocampal subfields: comparison between manual and FreeSurfer volumetry. *Hum Brain Mapp.* (2015) 36:463–74. doi: 10.1002/hbm.22640
70. Baglivo V, Cao B, Mwangi B, Bellani M, Perlini C, Lasalvia A. Hippocampal subfield volumes in patients with first-episode psychosis. *Schizophr Bull.* (2018) 44:552–9. doi: 10.1093/schbul/sbx108
71. Simić G, Kostović I, Winblad B, Bogdanović N. Volume and number of neurons of the human hippocampal formation in normal aging and Alzheimer's disease. *J Comp Neurol.* (1997) 379:482–94. doi: 10.1002/(sici)1096-9861(19970324)379:4<482::aid-cne2>3.0.co;2-z
72. Lim HK, Hong SC, Jung WS, Ahn KJ, Won WY, Hahn C. Automated segmentation of hippocampal subfields in drug-naïve patients with Alzheimer disease. *AJNR Am J Neuroradiol.* (2013) 34:747–51. doi: 10.3174/ajnr.A3293
73. Balu DT, Lucki I. Adult hippocampal neurogenesis: regulation, functional implications, and contribution to disease pathology. *Neurosci Biobehav Rev.* (2009) 33:232–52. doi: 10.1016/j.neubiorev.2008.08.007
74. Schmitt A, Weber S, Jatzko A, Braus DF, Henn FA. Hippocampal volume and cell proliferation after acute and chronic clozapine or haloperidol treatment. *J Neural Transm.* (2004) 111:91–100. doi: 10.1007/s00702-003-0070-2
75. Hu N, Sun H, Fu G, Zhang W, Xiao Y, Zhang L. Anatomic abnormalities of hippocampal subfields in never-treated and antipsychotic-treated patients with long-term schizophrenia. *Neuropsychopharmacol.* (2020) 35:39–48. doi: 10.1016/j.euroneuro.2020.03.020
76. Schobel SA, Chaudhury NH, Khan UA, Paniagua B, Styner MA, Asllani I. Imaging patients with psychosis and a mouse model establishes a spreading pattern of hippocampal dysfunction and implicates glutamate as a driver. *Neuron.* (2013) 78:81–93. doi: 10.1016/j.neuron.2013.02.011
77. Gozzi A, Herdon H, Schwarz A, Bertani S, Crestan V, Turrini G. Pharmacological stimulation of NMDA receptors via co-agonist site suppresses fMRI response to phencyclidine in the rat. *Psychopharmacology.* (2008) 201:273–84. doi: 10.1007/s00213-008-1271-z
78. Javitt DC, Freedman R. Sensory processing dysfunction in the personal experience and neuronal machinery of schizophrenia. *Am J Psychiatry.* (2015) 172:17–31. doi: 10.1176/appi.ajp.2014.13121691
79. Javitt DC. Glycine transport inhibitors for the treatment of schizophrenia: symptom and disease modification. *Curr Opin Drug Discov Devel.* (2009) 12:468–78.
80. Javitt DC. Biotypes in psychosis: has the RDoC era arrived? *Am J Psychiatry.* (2016) 173:313–4. doi: 10.1176/appi.ajp.2016.16020140
81. Eack SM, Hogarty GE, Cho RY, Prasad KM, Greenwald DP, Hogarty SS. Neuroprotective effects of cognitive enhancement therapy against gray matter loss in early schizophrenia: results from a 2-year randomized controlled trial. *Arch Gen Psychiatry.* (2010) 67:674–82. doi: 10.1001/archgenpsychiatry.2010.63

82. Lin J, Chan SK, Lee EH, Chang WC, Tse M, Su WW. Aerobic exercise and yoga improve neurocognitive function in women with early psychosis. *NPJ Schizophr.* (2015) 1:15047. doi: 10.1038/npjschz.2015.47
83. Heckers S, Konradi C. GABAergic mechanisms of hippocampal hyperactivity in schizophrenia. *Schizophr Res.* (2015) 167:4–11. doi: 10.1016/j.schres.2014.09.041
84. Lisman JE, Coyle JT, Green RW, Javitt DC, Benes FM, Heckers S. Circuit-based framework for understanding neurotransmitter and risk gene interactions in schizophrenia. *Trends Neurosci.* (2008) 31:234–42. doi: 10.1016/j.tins.2008.02.005
85. Coultrap SJ, Nixon KM, Alvestad RM, Valenzuela CF, Browning MD. Differential expression of NMDA receptor subunits and splice variants among the CA1, CA3 and dentate gyrus of the adult rat. *Brain Res Mol Brain Res.* (2005) 135:104–11. doi: 10.1016/j.molbrainres.2004.12.005
86. Newell DW, Malouf AT, Franck JE. Glutamate-mediated selective vulnerability to ischemia is present in organotypic cultures of hippocampus. *Neurosci Lett.* (1990) 116:325–30. doi: 10.1016/0304-3940(90)90095-q
87. Kraguljac NV, White DM, Reid MA, Lahti AC. Increased hippocampal glutamate and volumetric deficits in unmedicated patients with schizophrenia. *JAMA Psychiatry.* (2013) 70:1294–302. doi: 10.1001/jamapsychiatry.2013.2437
88. Benes FM. Evidence for altered trisynaptic circuitry in schizophrenic hippocampus. *Biol Psychiatry.* (1999) 46:589–99. doi: 10.1016/s0006-3223(99)00136-5
89. Benes FM, Berretta S. GABAergic interneurons: implications for understanding schizophrenia and bipolar disorder. *Neuropsychopharmacology.* (2001) 25:1–27. doi: 10.1016/s0893-133x(01)00225-1
90. Friston KJ, Liddle PF, Frith CD, Hirsch SR, Frackowiak RS. The left medial temporal region and schizophrenia. *A PET study. Brain.* (1992) 115:367–82. doi: 10.1093/brain/115.2.367
91. Dierks T, Linden DE, Jandl M, Formisano E, Goebel R, Lanfermann H. Activation of Heschl's gyrus during auditory hallucinations. *Neuron.* (1999) 22:615–21. doi: 10.1016/s0896-6273(00)80715-1
92. Schwarcz R, Witter MP. Memory impairment in temporal lobe epilepsy: the role of entorhinal lesions. *Epilepsy Res.* (2002) 50:161–77. doi: 10.1016/s0920-1211(02)00077-3
93. Grimm CM, Aksamaz S, Schulz S, Teutsch J, Sicinski P, Liss B. Schizophrenia-related cognitive dysfunction in the Cyclin-D2 knockout mouse model of ventral hippocampal hyperactivity. *Transl Psychiatry.* (2018) 8:212. doi: 10.1038/s41398-018-0268-6
94. Toro C, Deakin JFW. NMDA receptor subunit NRI and postsynaptic protein PSD-95 in hippocampus and orbitofrontal cortex in schizophrenia and mood disorder. *Schizophr Res.* (2005) 80:323–30. doi: 10.1016/j.schres.2005.07.003
95. Hýža M, Huttlová J, Kerkovský M, Kašpárek T. Psychosis effect on hippocampal reduction in schizophrenia. *Prog Neuropsychopharmacol Biol Psychiatry.* (2014) 48:186–92. doi: 10.1016/j.pnpbp.2013.10.008
96. Lodge DJ, Grace AA. Gestational methylazoxymethanol acetate administration: a developmental disruption model of schizophrenia. *Behav Brain Res.* (2009) 204:306–12. doi: 10.1016/j.bbr.2009.01.031
97. Sanderson TM, Cotel MC, O'Neill MJ, Tricklebank MD, Collingridge GL, Sher E. Alterations in hippocampal excitability, synaptic transmission and synaptic plasticity in a neurodevelopmental model of schizophrenia. *Neuropharmacology.* (2012) 62:1349–58. doi: 10.1016/j.neuropharm.2011.08.005
98. Winterburn JL, Pruessner JC, Chavez S, Schira MM, Lobaugh NJ, Voineskos AN. A novel *in vivo* atlas of human hippocampal subfields using high-resolution 3 T magnetic resonance imaging. *Neuroimage.* (2013) 74:254–65. doi: 10.1016/j.neuroimage.2013.02.003
99. Yang C, Wu S, Lu W, Bai Y, Gao H. Brain differences in first-episode schizophrenia treated with quetiapine: a deformation-based morphometric study. *Psychopharmacology.* (2015) 232:369–77. doi: 10.1007/s00213-014-3670-7
100. Cha J, Greenberg T, Song I, Simpson HB, Posner J, Mujica-Parodi LR. Abnormal hippocampal structure and function in clinical anxiety and comorbid depression. *Hippocampus.* (2016) 26:545–53. doi: 10.1002/hipo.22566
101. Sala M, Perez J, Soloff P, di Nemi SU, Caverzasi E, Soares JC. Stress and hippocampal abnormalities in psychiatric disorders. *Eur Neuropsychopharmacol.* (2004) 14:393–405. doi: 10.1016/j.euroneuro.2003.12.005
102. Chen LW, Sun D, Davis SL, Haswell CC, Dennis EL, Swanson CA. Smaller hippocampal CA1 subfield volume in posttraumatic stress disorder. *Depress Anxiety.* (2018) 35:1018–29. doi: 10.1002/da.22833
103. Han KM, Kim A, Kang W, Kang Y, Kang J, Won E. Hippocampal subfield volumes in major depressive disorder and bipolar disorder. *Eur Psychiatry.* (2019) 57:70–7. doi: 10.1016/j.eurpsy.2019.01.016

Conflict of Interest: The authors declare that the research was conducted in the absence of any commercial or financial relationships that could be construed as a potential conflict of interest.

frontiers in Psychiatry

ORIGINAL RESEARCH
published: 21 May 2021
doi: 10.3389/fpsyt.2021.659814

Prefrontal Functional Connectivity During the Verbal Fluency Task in Patients With Major Depressive Disorder: A Functional Near-Infrared Spectroscopy Study

*Suh-Yeon Dong[1], JongKwan Choi[2], Yeonsoo Park[3], Seung Yeon Baik[4], Minjee Jung[5], Yourim Kim[6] and Seung-Hwan Lee[5,7]**

[1] Department of Information Technology Engineering, Sookmyung Women's University, Seoul, South Korea, [2] OBELAB, Seoul, South Korea, [3] Department of Psychology, University of Notre Dame, Dame, RI, United States, [4] Department of Psychology, Penn State University, State College, PA, United States, [5] Clinical Emotion and Cognition Research Laboratory, Inje University, Goyang, South Korea, [6] Department of Psychology, University of Wisconsin-Milwaukee, Milwaukee, WI, United States, [7] Department of Psychiatry, Inje University Ilsan Paik Hospital, Goyang, South Korea

OPEN ACCESS

Edited by:
Tae Young Lee, Pusan National University Yangsan Hospital, South Korea

Reviewed by:
Sung-Hwa Ko, Pusan National University Yangsan Hospital, South Korea
Junhee Lee, Seoul National University Hospital, South Korea
Wu Jeong Hwang, Seoul National University, South Korea

***Correspondence:**
Seung-Hwan Lee
lshpss@hanmail.net

Specialty section:
This article was submitted to Neuroimaging and Stimulation, a section of the journal Frontiers in Psychiatry

Received: *29 January 2021*
Accepted: *14 April 2021*
Published: *21 May 2021*

Citation:
Dong S-Y, Choi J, Park Y, Baik SY, Jung M, Kim Y and Lee S-H (2021) Prefrontal Functional Connectivity During the Verbal Fluency Task in Patients With Major Depressive Disorder: A Functional Near-Infrared Spectroscopy Study. Front. Psychiatry 12:659814. doi: 10.3389/fpsyt.2021.659814

Deviations in activation patterns and functional connectivity have been observed in patients with major depressive disorder (MDD) with prefrontal hemodynamics of patients compared with healthy individuals. The graph-theoretical approach provides useful network metrics for evaluating functional connectivity. The evaluation of functional connectivity during a cognitive task can be used to explain the neurocognitive mechanism underlying the cognitive impairments caused by depression. Overall, 31 patients with MDD and 43 healthy individuals completed a verbal fluency task (VFT) while wearing a head-mounted functional near-infrared spectroscopy (fNIRS) devices. Hemodynamics and functional connectivity across eight prefrontal subregions in the two groups were analyzed and compared. We observed a reduction in prefrontal activation and weaker overall and interhemispheric subregion-wise correlations in the patient group compared with corresponding values in the control group. Moreover, efficiency, the network measure related to the effectiveness of information transfer, showed a significant between-group difference [t (71.64) = 3.66, corrected $p < 0.001$] along with a strong negative correlation with depression severity (rho = −0.30, $p = 0.009$). The patterns of prefrontal functional connectivity differed significantly between the patient and control groups during the VFT. Network measures can quantitatively characterize the reduction in functional connectivity caused by depression. The efficiency of the functional network may play an important role in the understanding of depressive symptoms.

Keywords: major depressive disorder, fNIRS, functional connectivity, verbal fluency task, efficiency

INTRODUCTION

Impairments in cognitive functions, such as attention, working memory, and executive function, have been reportedly observed in patients with major depressive disorder (MDD). Studies comparing patients and healthy controls have reported that these impairments are associated with abnormal patterns of brain activity. When compared to healthy individuals, patients with MDD have been reported to display aberrant neuropsychological characteristics. Earlier studies have used

functional magnetic resonance imaging (fMRI) to reveal reduced prefrontal activation during digit-sorting tasks (1) and verbal fluency tasks (VFTs) (2), imbalance between left and right prefrontal activation during emotional judgment (3), and reduced activation in the right nucleus accumbens during the monetary incentive delay task (4).

The association between prefrontal cortex (PFC) activation and depressive symptoms has also been investigated using near-infrared spectroscopy (NIRS). Multichannel NIRS is an emerging neuroimaging tool that in addition to detecting the spatiotemporal characteristics of brain function using a non-invasive, portable, and restraint-free technique (5), has been validated in psychiatry patients (6). Recently, studies using NIRS have reported a reduction in prefrontal hemodynamic activation in patients with MDD during the VFT, along with a strong negative correlation between the severity of depression and changes in oxygenated hemoglobin (HbO2) (7–9). However, the functional connectivity has not yet been investigated in depth. Some recent studies have characterized distinct resting-state MRI based-functional connectivity in patients with MDD (10), apathetic depression (11), and remitted MDD (12). Kawano et al. reported a strong negative correlation between the HAMD-21 score and average HbO2 concentration in the frontal lobe (9); however, they did not assess the functional connectivity.

Since the human brain consists of a complex network responsible for its function, considerable attention has been given to the graph theory approach for explaining functional deviations in brain organization resulting from neurological disorders such as schizophrenia (13–15), Alzheimer's disease (16, 17), bipolar disorder (18), attention-deficit hyperactivity disorder (19), and depression (20, 21). Although a majority of the earlier studies on functional connectivity relied on fMRI and electroencephalography (EEG) (21), functional NIRS (fNIRS) can be considered as a reasonable alternative for detecting changes in brain functional networks, owing to its high temporal resolution. A recent review paper on the application of fNIRS in MDD research provided comprehensive evidence that the functional connectivity measured by fNIRS is potentially useful for assessing MDD (22). Zhu et al. reported that patients with affective disorders exhibit significantly reduced connectivity in the PFC using resting-state fNIRS (23). Rosenbaum et al. conducted a functional connectivity analysis on patients with late-life depression (24) and further examined functional connectivity in the cortical areas of the default mode network (25). However, to the best of our knowledge, no studies have investigated the differences in functional connectivity during the VFT task.

In this study, we sought to perform an fNIRS-based functional connectivity analysis to investigate PFC activation patterns during the VFT. Unlike the aforementioned studies, which mainly focused on resting-state functional connectivity, we hypothesized that the functional connectivity elicited by cognitive stimulation (using the VFT in this case) differs between patients with MDD and healthy individuals, and that these differences can be visually described by the prefrontal functional network. As a decrease in verbal fluency has been primarily found in patients with MDD, functional connectivity during the VFT may play an important role in characterizing MDD. Moreover, we calculated graph theory-based connectivity metrics to quantitatively characterize functional connectivity in each group. We identified the measures that demonstrated significant between-group differences based on the connectivity metrics.

TABLE 1 | Participant demographic data ($N = 74$).

Variable	Control ($N = 43$) Mean (SD)	Patient ($N = 31$) Mean (SD)	p-value
Age (years)	34.26 (12.47)	39.48 (13.82)	0.093
HAMD	2.02 (1.99)	23.55 (9.47)	<0.001
HAMA	1.42 (1.67)	22.32 (10.78)	<0.001
BDI-II	5.33 (3.96)	25.48 (12.21)	<0.001
STAI-state	31.44 (6.75)	54.94 (11.98)	<0.001
STAI-trait	35.49 (8.78)	59.58 (11.99)	<0.001

HAMD, hamilton rating scale for depression; HAMA, hamilton rating scale for anxiety; BDI-II, beck depression inventory; STAI, state-trait anxiety inventory.

MATERIALS AND METHODS

Participants

We enrolled 43 healthy participants (age: 34.26 ± 12.47 years, control group) and 31 patients (age: 39.48 ± 13.81 years, patient group) with MDD who were undergoing treatment at the university hospital. The participants in the patient group had already been diagnosed with MDD according to the Diagnostic and Statistical Manual of Mental Disorders, Fifth Edition (26) by a board-certified psychiatrist. The participants' symptoms of depression and anxiety were assessed using the Hamilton Depression Rating Scale (HAMD) (27), Hamilton Anxiety Rating Scale (HAMA) (28), Beck Depression Inventory (BDI-II) (29), and State-Trait Anxiety Inventory (STAI) (30), which was composed of two subscales (STAI-state and STAI-trait, respectively). We excluded patients with an HAMD scores < 8 and healthy individuals with an HAMD scores > 8.

Table 1 represent the demographic data for all enrolled participants. All participants were recruited from the Department of Psychiatry, Inje University Ilsan Paik Hospital. The study was conducted in accordance with the Declaration of Helsinki and was approved by the Institutional Review Board of Inje University Ilsan Paik Hospital (2017–10–013). All the participants provided written informed consent prior to undergoing the fNIRS experiment.

NIRS Device

A head-mounted wireless NIRS system (NIRSIT; OBELAB Inc., Seoul, Korea) was used to obtain HbO2 values from the prefrontal region of the human brain. The NIRS system consists of 24 lasers sources (780/850 nm; maximum power under 1 mW) and 32 photodetectors with multiple source-detector spacing (1.5, 2.12, 3.0, 3.35 cm) resulting in 204 measurement points at a sampling rate of 8.138 Hz (31). We used 48 channels created by a 3.0 cm separation between the source and the detector for further analysis. We aligned the marking point on the front of the device

to the center between the eyes to ensure that the same brain region was recorded. Before wearing the device, the subject's hair were finger-combed away from the forehead to minimize its influence on the measurements. After fixing the device position from the front, the strap and the Velcro hooks on the back were securely fixed to prevent the device from moving while recording.

Activation Task

Participants were instructed to perform the VFT while wearing the wireless head-mounted fNIRS device. The VFT is a type of cognitive assessment, in which participants are asked to produce as many words as possible from a category (semantic or phonemic) in a given period of time. In this study, phonemic VFT was conducted. This task is usually employed in psychological or neuropsychological assessments to detect cognitive impairment (32, 33). The entire procedure consisted of three blocks; each block had a 30-s initial rest and a 60-s VFT (30-s pre-task and 30-s task). Participants were asked to repeat aloud the four Korean consonants, "g," "n," "d," and "r" during the pre-task. During the task, participants were instructed to produce as many Korean words as possible beginning with a designated consonant (randomly presented among the eight consonants, "g," "n," "d," "r," "m," "b," "s," and "h").

Data Analysis

The detected light signals were filtered using high and low-pass filters at 0.005 Hz and 0.1 Hz, respectively, to eliminate cardiovascular artifacts and environmental noise. We rejected poor-quality channels with a signal-to-noise ratio under 30 dB prior to extraction of the hemodynamic data to prevent misinterpretation. The location of the 48 NIRS channels with color-scaled rejection ratios of each subject group are provided in **Supplementary Figure 1**. Subsequently, the hemodynamic responses were extracted using the modified Beer-Lambert law (34) and baseline corrected with the last 5 s of the pre-task as baseline for each block. The average amplitude of the baseline was subtracted. Following baseline correction, we obtained the block averaged responses for each channel. As mentioned in Section 2.2, we only used 48 channels in the prefrontal region. As shown in **Figure 1**, the 48 channels were grouped into eight subregions: the right and left dorsolateral PFC (labeled R1 and L1); the ventrolateral PFC (R2 and L2); the frontopolar PFC (R3 and L3); and the orbitofrontal cortex (R4 and L4). We obtained averaged hemodynamic responses within each subregion, such that each participant's recording became a N-by-8 matrix wherein N indicated time-domain sample numbers and 8 indicated the number of subregions.

The hemodynamic parameters obtained were analyzed to evaluate the functional connectivity. Specifically, functional connectivity was measured using the strength of temporal correlation of hemodynamics between every possible pair of the subregions. Subsequently, computed prefrontal correlation coefficients were used to extract network measures to represent the global network characteristics, such as density, clustering coefficient, and efficiency. We applied weight thresholding to the correlation coefficients to quantitatively measure and compare the functional connectivity between the two groups. Correlations below the threshold value were set to 0 and were assumed to be weak and non-significant links across a threshold range of 0 to 0.95 with increments of 0.05, as they could have been spurious connections. Suprathreshold correlations were set to 1; therefore, we were able to obtain a binary adjacency matrix for each threshold value (35). Subsequently, we calculated the three most commonly used global connectivity measures as functions of the threshold value, namely, density, clustering coefficient, and efficiency. Data processing and analysis were performed using MATLAB 2018b (Mathworks, Inc., Natick, MA) and network measures were extracted using the brain connectivity toolbox, which is built into the MATLAB environment (36).

Statistical Analysis

We used a two-sample *t*-test to assess between-group differences in age, psychological scores, representative means, and functional connectivity measures. Homogeneity of variance was assessed using Levene's test for the equality of variance in a two-sample *t*-test. The degree of freedom was adjusted if the equality of variance was not assumed based on the results of Levene's test. Functional connectivity analysis was performed by calculating Pearson's correlation coefficients between every pair of the represented mean values for the eight subregions. *P*-values obtained from the statistical tests were corrected using the false discovery rate (FDR) for multiple comparisons (37). Following the FDR correction, *p*-values under 0.05 were considered statistically significant. All statistical analyses were performed using IBM SPSS Statistics 23 (IBM Corp. Armonk, NY).

RESULTS

Age and Psychological Test Scores

First of all, the two groups in this study had no significant differences in age [t (72) = −1.701, p = 0.093]. However, the comparison of the five psychological test scores using two-sample *t*-tests revealed statistically significant between-group differences. The HAMD scores in the patient group (mean ± standard deviation: 23.55 ± 9.47) were significantly higher than those in the control group (2.02 ± 2.00) [t (31.93) = −12.46, corrected $p < 0.001$]. Similarly, the HAMA scores in the patient group (22.32 ± 10.78) were significantly higher than those in the control group (1.42 ± 1.67) [t (31.03) = −10.70, corrected $p < 0.001$]. Moreover, the remaining three scores showed statistically significant between-group differences [BDI-II, t (34.59) = −8.86, corrected $p < 0.001$; STAI-state, t (43.66) = −9.85, corrected $p < 0.001$; STAI-trait, t (72) = −9.99, corrected $p < 0.001$].

Task Performance

We measured the number of correct words and the reaction time as task performance metrics during each VFT task. Between-group differences were assessed using two-sample *t*-tests. The word counts in the control group (25.40 ± 6.34) were significantly higher than those in the patient group (19.77 ± 7.53) [t (71) = 3.48, $p = 0.001$]. Similarly, reaction times in the control group (3,257.84 ± 711.64 msec) were significantly lower than those in the patient group (4,368.26 ± 1,995.05 msec) [t (35.54) = −2.97, $p = 0.005$].

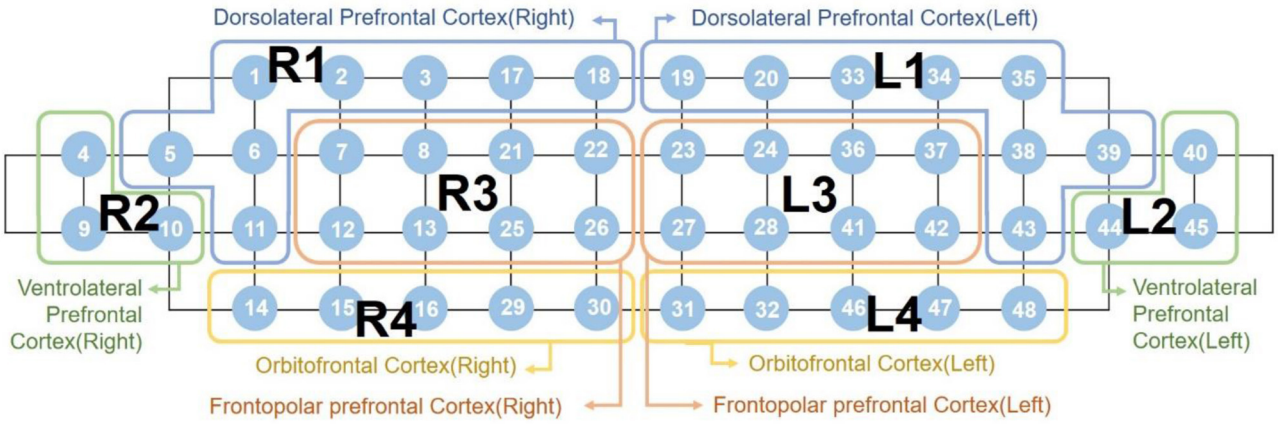

FIGURE 1 | Labeling of the eight subregions mapped by 48 channels "R" indicates the right hemisphere, while "L" indicates the left hemisphere.

fNIRS Activation

Figure 2 shows the average hemodynamic responses during the VFT in each group. As shown in the figure, the HbO2 concentration during the VFT was higher in the control group than in the patient group. **Figure 3** illustrates the transient hemodynamic responses in each subgroup. The transients of the 48 channels are provided in **Supplementary Figure 2**. During the task period, the control group showed significantly higher HbO2 concentrations than the patient group and returned to baseline after the task (not shown in the figure). Moreover, the gap between the two groups was greater in R2, R4, L2, and L4 compared with the other subregions.

Functional Connectivity

The strength of the temporal correlation of hemodynamics between all pairwise combinations of the eight subgroups was calculated using Pearson's correlation coefficient. As shown in **Figure 4A**, the strength of the between-subgroup correlation was higher in the control group than in the patient group. The average of the correlation coefficients of the 28 pairs in the control group (0.68 ± 0.12) was higher than that of the patient group (0.49 ± 0.16). **Figure 4B** shows the spatial distribution of the correlations between each pair of subregions. These figures allow us to observe the areas in which connections are either stronger or weaker. Remarkably, strong interhemispheric connections (e.g., R1-L1, R2-L2, R3-L3, R4-L4) were observed in the control group, but not in the patient group.

We tested the normality of the network measures for each threshold value and evaluated group differences using two-sample *t*-tests. First, a significant difference in the clustering coefficient was observed only at the threshold level of 0.90. The clustering coefficient at 0.9 was significantly larger in the control group (1.01 ± 0.25) than in the patient group (0.76 ± 0.43) [t (44.522) = 2.96, corrected $p = 0.05$] with a difference of 0.17 (95% CI, 0.082 to 0.43). In contrast, density and efficiency exhibited statistically significant between-group differences at all threshold levels ($p < 0.05$). The most significant difference in density was observed at a threshold level of 0.8. At this threshold level, the density in the control group (0.77 ± 0.30) was significantly higher than that in the patient group (0.55 ± 0.21) [t (72) = 3.61, corrected $p = 0.02$] with a difference of 0.22 (95% CI, 0.097 to 0.33). As shown in **Figure 5A**, the most significant difference in efficiency was also found at the threshold level of 0.8. At this threshold level, the efficiency in the control group (0.56 ± 0.28) was significantly higher than that in the patient group (0.34 ± 0.22) [t (71.64) = 3.66, corrected $p < 0.001$], with a difference of 0.058 (95% CI, 0.097 to 0.33). Moreover, we measured the correlation coefficient between the efficiency at this threshold level and the corresponding HAMD scores. A Spearman's correlation revealed a significant negative correlation between these two factors (rho = −0.30, $p = 0.009$), as shown in **Figure 5B**.

DISCUSSION

In this study, we performed functional connectivity-based comparisons between patients with MDD and healthy individuals and calculated the subregional functional connectivity using temporal correlations of the hemodynamics of every pair of subregions of the PFC using a functional connectivity approach. The functional connectivity in each group (control and patient) was visually represented by varying the thickness according to the strength of the subregional functional connectivity. Network measures were calculated to quantitatively evaluate and compare two networks, and the most informative metric was identified as the network measure representing the greatest difference between the two groups (control vs. patient).

The visualization of functional connectivity allowed us to understand subregion-wise functional connection characteristics between the two groups. We observed a clear absence of interhemispheric correlations in patients with MDD. This result is consistent with a previous study indicating that patients with MDD show interhemispheric connectivity deficits in resting-state (38).

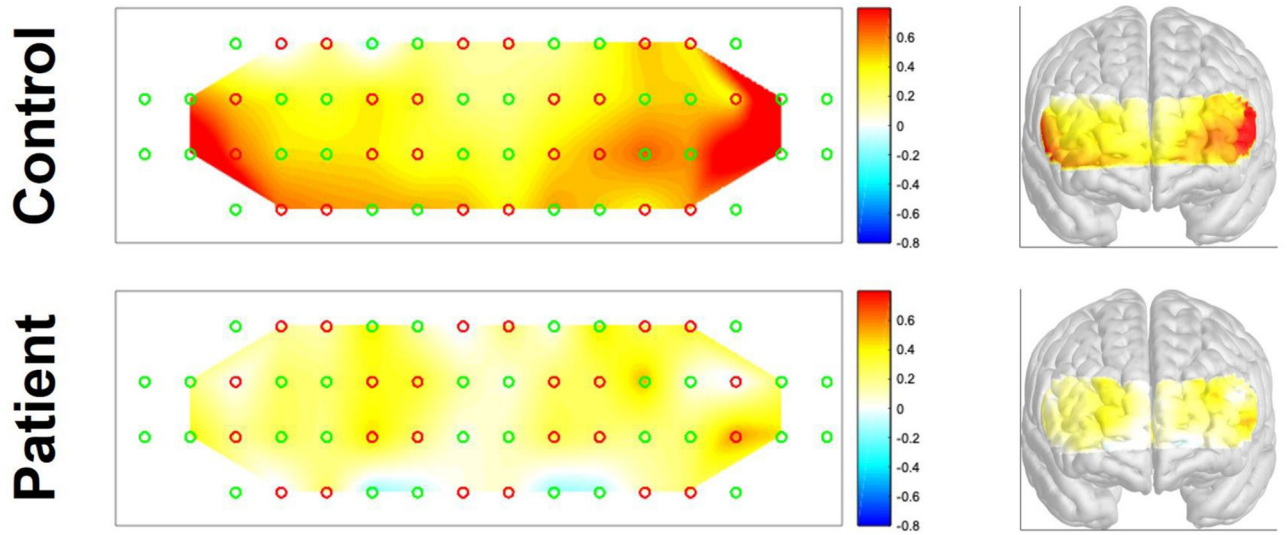

FIGURE 2 | Activation maps of the two groups during the verbal fluency task.

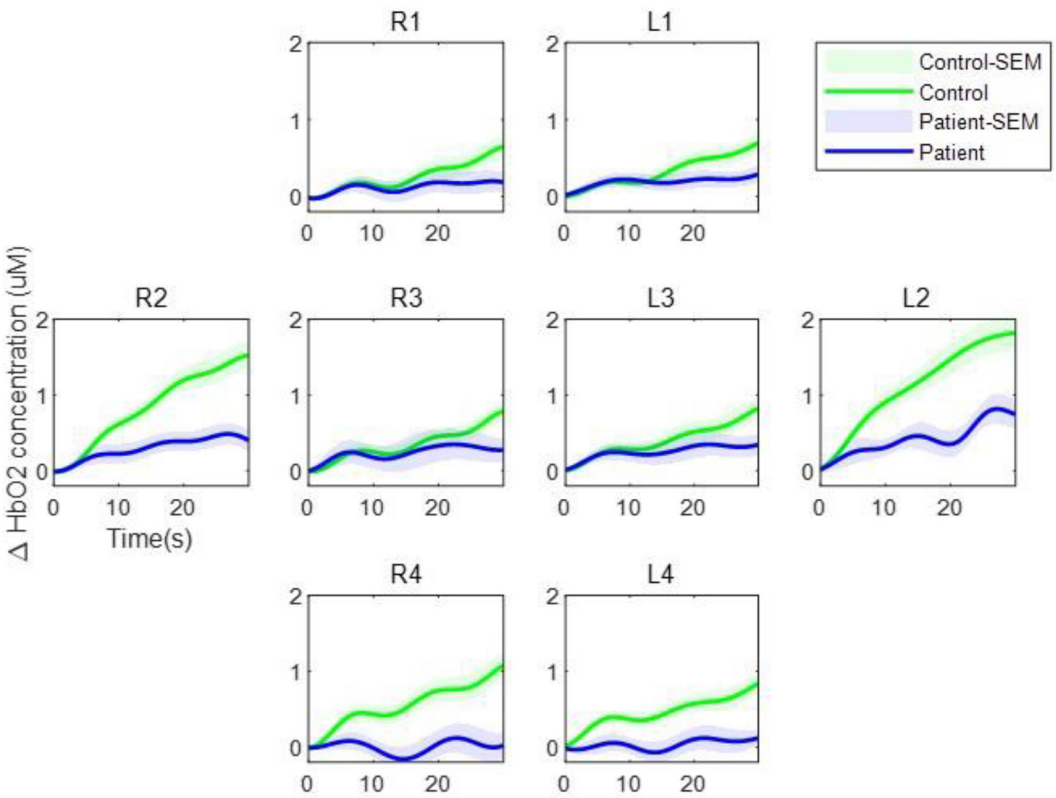

FIGURE 3 | Transient oxygenated hemoglobin concentration during the verbal fluency task. The green line represents the control group while the blue line represents the patient group. The shaded regions represent the standard errors of the mean.

The network measures used in our study are known to characterize basic aspects of network organization (35). Density reflects the overall wiring cost of the network. The clustering coefficient indicates network segregation, while efficiency reflects the network integration (36). Of the two measures, we focused extensively on efficiency, since it showed

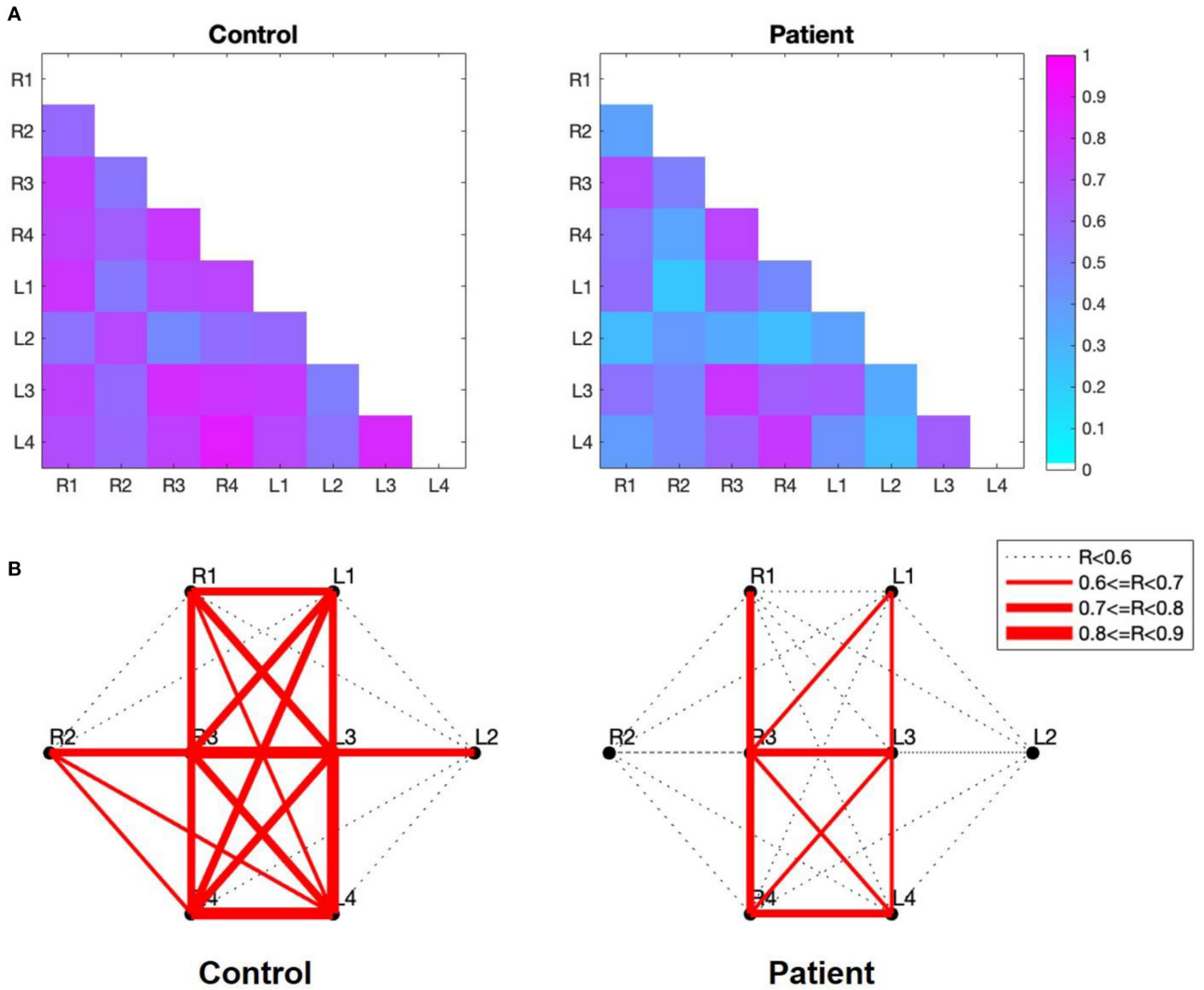

FIGURE 4 | (A) Correlation maps of the verbal fluency task for the two groups. The image shows the lower diagonal of the cross-correlation matrix. The rows and columns of the matrix represent the subgroup, while the cells of the matrix contain the color-coded correlation coefficient of the corresponding pair. The blue cells indicate a lower between-subgroup correlation, while higher between-subgroup correlations are indicated in magenta. **(B)** Subregion-based functional connectivity The line width indicates the strength of the correlation, as determined by the correlation coefficient (R) between each pair of subregions.

a significant between-group difference. We observed a strong negative correlation between fNIRS measures and the severity of depression, which is in line with other two studies (8, 9). Unlike these studies, which calculated correlations based on changes in HbO2 from a single channel (8) or an entire frontal channel (9), we used the network measure instead of HbO2 changes in this study; thus, we were able to offernew interpretations of the relationship between fNIRS measurement and depression severity. As efficiency is a measure of the effectiveness of information transfer, efficiency may play an important role in understanding decreased responsiveness in patients with MDD, including a slower reaction time (4). Although the Spearman's rho between reaction time and efficiency was not statistically significant in our study (rho $= -0.21$, $p = 0.073$), efficiency was the most negatively correlated network metric of the three. Future studies with a larger population may provide experimental evidence. Thus, the results so far demonstrate that these network metrics may be used as valid biomarkers of MDD.

Since most previous studies have focused primarily on resting-state functional connectivity (23–25), this study is distinct in that it suggests task-related functional connectivity. While Rosenbaum et al. have also investigated the functional connectivity during task performance as well as at rest (24, 25), the task adopted in these studies on late-life depression was a trail-making test that is often used for screening visual attention and task switching. This study uses the VFT adopted in the majority of previous studies of MDD. Therefore, we believe that our findings provide meaningful evidence that functional connectivity may be used to understand the behavioral and neurological characteristics of decreased verbal fluency in patients with MDD.

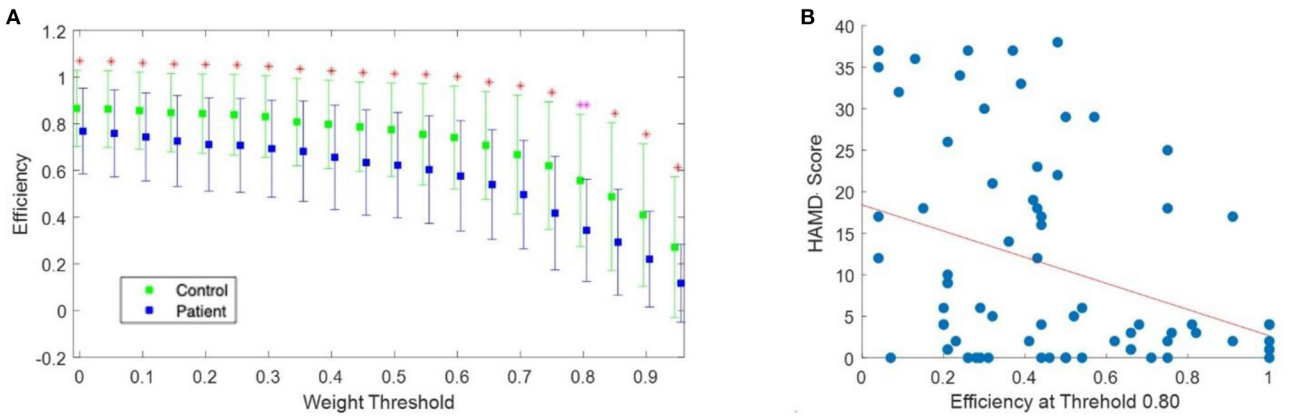

FIGURE 5 | (A) Efficiency as a function of the threshold value. The green squares indicate efficiency in the control group while the blue squares indicate efficiency in the patient group. The error bar indicates the standard deviation. The magenta double asterisk indicates a significant difference at the level of 0.001, while red asterisks indicate a significant difference at the level of 0.05 (*p*-values were FDR-corrected). **(B)** Scatter plot of the efficiency at a threshold of 0.80 vs HAMD scores. The red line indicates the least-squares line. FDR, false discovery rate; HAMD, hamilton depression rating scale.

DATA AVAILABILITY STATEMENT

The datasets generated for this study cannot be made openly available due to ethical concerns. Requests to access the datasets should be directed to Seung-Hwan Lee, lshpss@hanmail.net.

ETHICS STATEMENT

The studies involving human participants were reviewed and approved by Institutional Review Board of Inje University Ilsan Paik Hospital (2017–10–013). The patients/participants provided their written informed consent to participate in this study.

AUTHOR'S NOTE

This study has some limitations. Given that aging is a critical cause of cognitive decline (17) and in light of the potential need to set clinical cut-off points in rating scales for older patients (39), further investigations on age-related functional connectivity in patients with MDD are necessary. Moreover, although depression severity was not the main focus of our study, stricter criteria for enrolling patients with MDD could have provided more accurate results that better represent the characteristics of MDD.

AUTHOR CONTRIBUTIONS

S-YD: conceptualization, data analysis, funding acquisition, and writing – original draft. JC: protocol design, data preprocessing, and writing – review & editing. YP and SB: protocol design, investigation, and writing – review & editing. MJ and YK: data collection, writing – review & editing. S-HL: conceptualization, supervision and writing – review & editing. All authors contributed to the article and approved the submitted version.

FUNDING

This research was supported by the Korea Medical Device Development Fund grant funded by the Korea government (the Ministry of Science and ICT, the Ministry of Trade, Industry and Energy, the Ministry of Health & Welfare, Republic of Korea, the Ministry of Food and Drug Safety) (Grant no. 202013B10), the National Research Foundation of Korea grants (2019R1F1A1058011 and BK21 FOUR), and a research grant from Sookmyung Women's University Research Grants (1-1903-2005).

ACKNOWLEDGMENTS

We would like to thank all study participants. We would also like to thank Ms. Jiyoung Baek of OBELAB for organizing the data for subsequent analysis.

SUPPLEMENTARY MATERIAL

The Supplementary Material for this article can be found online at: https://www.frontiersin.org/articles/10.3389/fpsyt.2021.659814/full#supplementary-material

REFERENCES

1. Siegle GJ, Thompson W, Carter CS, Steinhauer SR, Thase ME. Increased amygdala and decreased dorsolateral prefrontal BOLD responses in unipolar depression: related and independent features. *Biol Psychiatry*. (2007) 61:198–209. doi: 10.1016/j.biopsych.2006.05.048
2. Okada G, Okamoto Y, Yamashita H, Ueda K, Takami H, Yamawaki S. Attenuated prefrontal activation during a verbal fluency task in

remitted major depression. *Psychiatry Clin Neurosci.* (2009) 63:423–5. doi: 10.1111/j.1440-1819.2009.01952.x
3. Grimm S, Beck J, Schuepbach D, Hell D, Boesiger P, Bermpohl F, et al. Imbalance between left and right dorsolateral prefrontal cortex in major depression is linked to negative emotional judgment: an fMRI study in severe major depressive disorder. *Biol Psychiatry.* (2008) 63:369–76. doi: 10.1016/j.biopsych.2007.05.033
4. Carl H, Walsh E, Eisenlohr-Moul T, Minkel J, Crowther A, Moore T, et al. Sustained anterior cingulate cortex activation during reward processing predicts response to psychotherapy in major depressive disorder. *J Affect Disord.* (2016) 203:204–12. doi: 10.1016/j.jad.2016.06.005
5. Scholkmann F, Kleiser S, Metz AJ, Zimmermann R, Mata Pavia J, Wolf U, et al. A review on continuous wave functional near-infrared spectroscopy and imaging instrumentation and methodology. *Neuroimage.* (2014) 85:6–27. doi: 10.1016/j.neuroimage.2013.05.004
6. Lee J, Folley BS, Gore J, Park S. Origins of spatial working memory deficits in schizophrenia: an event-related fMRI and near-infrared spectroscopy study. *PLoS ONE.* (2008) 3:e1760. doi: 10.1371/journal.pone.0001760
7. Pu S, Matsumura H, Yamada T, Ikezawa S, Mitani H, Adachi A, et al. Reduced frontopolar activation during verbal fluency task associated with poor social functioning in late-onset major depression: multi-channel near-infrared spectroscopy study. *Psychiatry Clin Neurosci.* (2008) 62:728–37. doi: 10.1111/j.1440-1819.2008.01882.x
8. Noda T, Yoshida S, Matsuda T, Okamoto N, Sakamoto K, Koseki S, et al. Frontal and right temporal activations correlate negatively with depression severity during verbal fluency task: a multi-channel near-infrared spectroscopy study. *J Psychiatr Res.* (2012) 46:905–12. doi: 10.1016/j.jpsychires.2012.04.001
9. Kawano M, Kanazawa T, Kikuyama H, Tsutsumi A, Kinoshita S, Kawabata Y, et al. Correlation between frontal lobe oxy-hemoglobin and severity of depression assessed using near-infrared spectroscopy. *J Affect Disord.* (2016) 205:154–8. doi: 10.1016/j.jad.2016.07.013
10. Wu X, Lin P, Yang J, Song H, Yang R, Yang J. Dysfunction of the cingulo-opercular network in first-episode medication-naive patients with major depressive disorder. *J Affect Disord.* (2016) 200:275–83. doi: 10.1016/j.jad.2016.04.046
11. Alexopoulos GS, Hoptman MJ, Yuen G, Kanellopoulos D, Seirup JK, Lim KO, et al. Functional connectivity in apathy of late-life depression: a preliminary study. *J Affect Disord.* (2013) 149:398–405. doi: 10.1016/j.jad.2012.11.023
12. DelDonno SR, Jenkins LM, Crane NA, Nusslock R, Ryan KA, Shankman SA, et al. Affective traits and history of depression are related to ventral striatum connectivity. *J Affect Disord.* (2017) 221:72–80. doi: 10.1016/j.jad.2017.06.014
13. Rubinov M, Knock SA, Stam CJ, Micheloyannis S, Harris AWF, Williams LM, et al. Small-world properties of nonlinear brain activity in schizophrenia. *Hum Brain Mapp.* (2009) 30:403–16. doi: 10.1002/hbm.20517
14. Damaraju E, Allen EA, Belger A, Ford JM, McEwen S, Mathalon DH, et al. Dynamic functional connectivity analysis reveals transient states of dysconnectivity in schizophrenia. *NeuroImage Clin.* (2014) 5:298–308. doi: 10.1016/j.nicl.2014.07.003
15. Noda T, Nakagome K, Setoyama S, Matsushima E. Working memory and prefrontal/temporal hemodynamic responses during post-task period in patients with schizophrenia: a multi-channel near-infrared spectroscopy study. *J Psychiatr Res.* (2017) 95:288–98. doi: 10.1016/j.jpsychires.2017.09.001
16. Tijms BM, Wink AM, de Haan W, van der Flier WM, Stam CJ, Scheltens P, et al. Alzheimer's disease: connecting findings from graph theoretical studies of brain networks. *Neurobiol Aging.* (2013) 34:2023–36. doi: 10.1016/j.neurobiolaging.2013.02.020
17. Lin Q, Rosenberg MD, Yoo K, Hsu TW, O'Connell TP, Chun MM. Resting-state functional connectivity predicts cognitive impairment related to Alzheimer's disease. *Front Aging Neurosci.* (2018) 10:94. doi: 10.3389/fnagi.2018.00094
18. Hirose T, Tsujii N, Mikawa W, Shirakawa O. Delayed hemodynamic responses associated with a history of suicide attempts in bipolar disorder: a multichannel near-infrared spectroscopy study. *Psychiatry Res Neuroimaging.* (2018) 280:15–21. doi: 10.1016/j.pscychresns.2018.08.003
19. Ueda S, Ota T, Iida J, Yamamuro K, Yoshino H, Kishimoto N, et al. Reduced prefrontal hemodynamic response in adult attention-deficit hyperactivity disorder as measured by near-infrared spectroscopy. *Psychiatry Clin Neurosci.* (2018) 72:380–90. doi: 10.1111/pcn.12643
20. He H, Yu Q, Du Y, Vergara V, Victor TA, Drevets WC, et al. Resting-state functional network connectivity in prefrontal regions differs between unmedicated patients with bipolar and major depressive disorders. *J Affect Disord.* (2016) 190:483–93. doi: 10.1016/j.jad.2015.10.042
21. Helm K, Viol K, Weiger TM, Tass PA, Grefkes C, Del Monte D, et al. Neuronal connectivity in major depressive disorder: a systematic review. *Neuropsychiatr Dis Treat.* (2018) 14:2715–37. doi: 10.2147/NDT.S170989
22. Ho CSH, Lim LJH, Lim AQ, Chan NHC, Tan RS, Lee SH, et al. Diagnostic and predictive applications of functional near-infrared spectroscopy for major depressive disorder: a Systematic review. *Front Psychiatry.* (2020) 11:378. doi: 10.3389/fpsyt.2020.00378
23. Zhu H, Xu J, Li J, Peng H, Cai T, Li X, et al. Decreased functional connectivity and disrupted neural network in the prefrontal cortex of affective disorders: a resting-state fNIRS study. *J Affect Disord.* (2017) 221:132–44. doi: 10.1016/j.jad.2017.06.024
24. Rosenbaum D, Hagen K, Deppermann S, Kroczek AM, Haeussinger FB, Heinzel S, et al. State-dependent altered connectivity in late-life depression: a functional near-infrared spectroscopy study. *Neurobiol Aging.* (2016) 39:57–68. doi: 10.1016/j.neurobiolaging.2015.11.022
25. Rosenbaum D, Haipt A, Fuhr K, Haeussinger FB, Metzger FG, Nuerk HC, et al. Aberrant functional connectivity in depression as an index of state and trait rumination. *Sci Rep.* (2017) 7:2174. doi: 10.1038/s41598-017-02277-z
26. American Psychiatric Association. *Diagnostic and Statistical Manual of Mental Disorders (DSM-5®).* 5th ed. St. Arlington, VA: American Psychiatric Publishing (2013).
27. Hamilton M. A rating scale for depression. *J Neurol Neurosurg Psychiatry.* (1960) 23:56–62. doi: 10.1136/jnnp.23.1.56
28. Hamilton M. The assessment of anxiety states by rating. *Br J Med Psychol.* (1959) 32:50–55. doi: 10.1111/j.2044-8341.1959.tb00467.x
29. Beck AT, Steer RA, Brown G. *BDI-II, Beck Depression Inventory: Manual.* San Antonio: TX: Psychological Corporation (1996).
30. Spielberger CD, Gorsuch R, Lushene RE, Vagg PR, Jacobs GA. *Manual for the State–Trait Anxiety Inventory.* Palo Alto, CA: Consulting Psychologists Press (1983).
31. Choi JK, Kim JM, Hwang G, Yang J, Choi MG, Bae HM. Time-divided spread-spectrum code-based 400 fW-detectable multichannel fNIRS IC for portable functional brain imaging. *IEEE J Solid State Circuits.* (2016) 51:484–95. doi: 10.1109/JSSC.2015.2504412
32. Takizawa R, Fukuda M, Kawasaki S, Kasai K, Mimura M, Pu S, et al. Neuroimaging-aided differential diagnosis of the depressive state. *Neuroimage.* (2014) 85:498–507. doi: 10.1016/j.neuroimage.2013.05.126
33. Curtis VA, Dixon TA, Bullmore ET, Morris RG, Brammer MJ, Williams SCR, et al. Differential frontal activation in schizophrenic and bipolar patients during verbal fluency. *Neuroimage.* (1999) 9:111–21. doi: 10.1016/S0165-0327(00)00240-8
34. Delpy DT, Cope M, Van Der Zee P, Arridge S, Wray S, Wyatt J. Estimation of optical pathlength through tissue from direct time of flight measurement. *Phys Med Biol.* (1988) 33:1433–42. doi: 10.1088/0031-9155/33/12/008
35. Racz FS, Mukli P, Nagy Z, Eke A. Increased prefrontal cortex connectivity during cognitive challenge assessed by fNIRS imaging. *Biomed Opt Express.* (2017) 8:3842–55. doi: 10.1364/BOE.8.003842

36. Rubinov M, Sporns O. Complex network measures of brain connectivity: uses and interpretations. *Neuroimage.* (2010) 52:1059–69. doi: 10.1016/j.neuroimage.2009.10.003
37. Singh AK, Dan I. Exploring the false discovery rate in multichannel NIRS. *Neuroimage.* (2006) 33:542–9. doi: 10.1016/j.neuroimage.2006.06.047
38. Wang L, Li K, Zhang QE, Zeng YW, Jin Z, Dai WJ, et al. Interhemispheric functional connectivity and its relationships with clinical characteristics in major depressive disorder: A resting state fMRI study. *PLoS ONE.* (2013) 8:e60191. doi: 10.1371/journal.pone.0060191
39. Kogan ES, Kabacoff RI, Hersen M, Van Hasselt VB. Clinical cutoffs for the beck depression inventory and the geriatric depression scale with older adult psychiatric outpatients. *J Psychopathol Behav Assess.* (1994) 16:233–42. doi: 10.1007/BF02229210

Conflict of Interest: JC is the inventor of continuous-wave near infrared spectroscopy technology, licensed to KAIST's spin-off company OBELAB, which focuses on non-invasive, optical brain imaging.

The remaining authors declare that the research was conducted in the absence of any commercial or financial relationships that could be construed as potential conflicts of interest.

frontiers in Psychiatry

SYSTEMATIC REVIEW
published: 02 June 2021
doi: 10.3389/fpsyt.2021.678088

A Systematic Review of Long-Interval Intracortical Inhibition as a Biomarker in Neuropsychiatric Disorders

Parmis Fatih[1]*, *M. Utku Kucuker*[1], *Jennifer L. Vande Voort*[1], *Deniz Doruk Camsari*[1], *Faranak Farzan*[2†] and *Paul E. Croarkin*[1†]

[1] Mayo Clinic Department of Psychiatry and Psychology, Mayo Clinic, Rochester, MN, United States, [2] School of Mechatronic Systems Engineering, Centre for Engineering-Led Brain Research, Simon Fraser University, Surrey, BC, Canada

Long-interval intracortical inhibition (LICI) is a paired-pulse transcranial magnetic stimulation (TMS) paradigm mediated in part by gamma-aminobutyric acid receptor B ($GABA_B$) inhibition. Prior work has examined LICI as a putative biomarker in an array of neuropsychiatric disorders. This review conducted in accordance with the Preferred Reporting Items for Systematic Reviews and Meta-Analyses (PRISMA) sought to examine existing literature focused on LICI as a biomarker in neuropsychiatric disorders. There were 113 articles that met the inclusion criteria. Existing literature suggests that LICI may have utility as a biomarker of $GABA_B$ functioning but more research with increased methodologic rigor is needed. The extant LICI literature has heterogenous methodology and inconsistencies in findings. Existing findings to date are also non-specific to disease. Future research should carefully consider existing methodological weaknesses and implement high-quality test-retest reliability studies.

Keywords: cortical inhibition, electroencephalography, electromyography, long-interval intracortical inhibition, transcranial magnetic stimulation

OPEN ACCESS

Edited by:
Hang Joon Jo,
Hanyang University, South Korea

Reviewed by:
Minah Kim,
Seoul National University Hospital, South Korea
Jennifer Barredo,
Providence VA Medical Center, United States

***Correspondence:**
Parmis Fatih
Fatih.Parmis@mayo.edu

†These authors have contributed equally to this work

Specialty section:
This article was submitted to Neuroimaging and Stimulation, a section of the journal Frontiers in Psychiatry

Received: *08 March 2021*
Accepted: *06 May 2021*
Published: *02 June 2021*

Citation:
Fatih P, Kucuker MU, Vande Voort JL, Doruk Camsari D, Farzan F and Croarkin PE (2021) A Systematic Review of Long-Interval Intracortical Inhibition as a Biomarker in Neuropsychiatric Disorders. Front. Psychiatry 12:678088. doi: 10.3389/fpsyt.2021.678088

INTRODUCTION

Gamma-aminobutyric acid (GABA) is the primary inhibitory neurotransmitter of the central nervous system (1). Cortical inhibition is the physiologic mechanism that modulates cortical excitability and neuroplasticity via the suppression created by the GABAergic neurotransmission (2, 3). Prior studies suggest that GABA and cortical inhibition have a role in the pathophysiology of neuropsychiatric disorders. It has been speculated that GABAergic neurotransmission is altered in various brain based disorders such as mood disorders, psychotic disorders, anxiety, attention-deficit/hyperactivity disorder (ADHD), autism spectrum disorder, neurocognitive disorders, epilepsy, movement disorders, and stroke (4–11). A variety of pre-clinical methods have been used to investigate the role of GABA in the pathophysiology of neuropsychiatric disorders. The safe and non-invasive measurement of GABAergic inhibitory neurotransmission is challenging in clinical studies (12–14).

Transcranial magnetic stimulation (TMS) is a non-invasive brain stimulation technique that utilizes magnetic fields to stimulate nerve cells for the treatment of depression and as a neurophysiological probe (15). Single- and paired-pulse TMS paradigms are frequently used

to assess cortical inhibitory and excitatory mechanisms (16–18). Prior research indicated that the pairing of a conditioning stimulus with a subsequent test stimulus at varying interstimulus intervals generates either intracortical inhibition or facilitation based on the duration of interstimulus interval and intensity of the conditioning stimulus (19, 20). Facilitation and inhibition is measured by either electromyographic (EMG) recordings of motor-evoked potentials or electroencephalography (EEG) recordings (21). TMS-EMG has been used to measure the cortical inhibition in the motor cortex. Subsequent studies with TMS-EEG have facilitated the study of the dorsolateral prefrontal cortex which is implicated in the pathophysiology of neuropsychiatric conditions (22, 23).

Long-interval intracortical inhibition (LICI) is a paired-pulse technique with suprathreshold conditioning and test stimuli applied at interstimulus intervals of 50–200 ms leading to suppression of cortical activity. Prior work suggests that the inhibitory effects of LICI are mediated by $GABA_B$ receptors (24). The interstimulus interval that produces LICI corresponds to the timing of $GABA_B$ inhibitory post-synaptic potentials (25). Furthermore, pharmacological studies demonstrated that $GABA_B$ receptor agonist baclofen, GABA uptake inhibitor tiagabine and GABA structural analog vigabatrin potentiate LICI (26–28). Moreover, short-interval intracortical inhibition (SICI), a TMS paired paradigm mediated by $GABA_A$ activity, is suppressed by LICI which could be explained with pre-synaptic $GABA_B$ mediated inhibition of interneurons (29).

Numerous prior studies have examined cortical excitatory and inhibitory measures using TMS to understand the underlying pathophysiology of neuropsychiatric disorders. Studies of LICI suggest that $GABA_B$ mediated inhibition is altered in various brain based conditions such as mood disorders and psychotic disorders, epilepsy, Parkinson's disease, traumatic brain injury, and dementia. In clinical practice and research, psychiatric disorders are diagnosed based on a checklist approach to symptoms with either Diagnostic and Statistical Manual of Mental Disorders 5th Edition (DSM-5) criteria or structured interviews (30). Treatment response is monitored with interviews and rating scales of symptom severity. Clinical interviews and rating scales have inherent reporting biases. Therefore, the development of non-invasive, quantitative diagnostic, and prognostic biomarkers is essential. Previous studies suggest that LICI might have utility as a diagnostic and prognostic biomarker in neuropsychiatric disorders. There are no prior comprehensive systematic reviews examining studies of LICI. This systematic review sought to summarize the literature examining LICI alterations in brain based disorders. A second goal was to synthesize the existing evidence focused on LICI as a diagnostic and prognostic biomarker for neuropsychiatric disorders. Finally, we review recent work with LICI paradigms related to cognitive neuroscience literature and methodological challenges.

MATERIALS AND METHODS

Search Strategy

This systematic review was conducted according to the guidelines of Preferred Reporting Items for Systematic Reviews and Meta-Analyses (PRISMA) (31, 32). The literature search was performed using the internet databases Embase, EMB Reviews, Medline, APA PsychINFO, Scopus, and Web of Science up to April 8th, 2021. The search strategy was designed in consultation with an experienced medical reference librarian. The full search strategy and search terms used for the literature search are described in the **Supplementary Material**.

Study Selection

Studies were included if the following criteria were met: (a) articles in English; (b) original articles including participants with major neurologic and psychiatric disorders; (c) cortical inhibition was measured with a TMS LICI paradigm. Studies were excluded according to the following criteria: (a) animal studies; (b) review articles, letters to the editor, short communication papers, correspondence articles; (c) published conference abstracts, lectures, and presentations; and (d) study contained only healthy participants. Two authors reviewed articles for inclusion (PF and MK) The articles that met inclusion criteria were included in the review, and the articles that met exclusion criteria were excluded from the review. The senior authors (FF and PC) were consulted for any discrepancies or questions regarding inclusion of articles. The references of the included articles were reviewed, and additional papers fulfilling the eligibility criteria were included in the review.

Data Extraction

The full texts of the eligible articles were reviewed in depth by PF and MK. Data were extracted by PF and the extracted data was verified by MK and PC, JV, and FF. Extracted data included authors, publication year, study design, number of patients and healthy controls, age and sex of control and patient group, stimulation area of cortex, muscle measured [first dorsal interosseous (FDI) and abductor pollicis brevis (APB)], diagnostic assessment instruments (EMG, EEG), stimulation parameters (stimulus intensities, interstimulus interval), medications, interventions, outcomes, and outcome measures.

Outcomes

The primary outcome of this review focused on alterations in LICI in neuropsychiatric disorders in comparison to healthy controls. As mentioned in the introduction, LICI measurements consist of delivering two consecutive TMS pulses that are 50–200 ms apart in which a conditioning stimulus is followed by a test stimulus. LICI is quantified as the ratio of the amplitude of the evoked potential (EP) elicited following a test stimulus to the EP elicited by the conditioning stimulus (conditioned/unconditioned EP). Therefore, an increase in the exact value of the ratio (greater conditioned EP amplitude) implies reduced inhibition or lower cortical inhibition, whereas a decrease in the exact value of the ratio (smaller conditioned EP amplitude) indicates increased inhibition or greater cortical inhibition. To maintain consistent terminology throughout this review for clarity, reduced cortical inhibition will be referred as reduced/decreased LICI or LICI deficit; and increased cortical inhibition will be referred as enhanced/increased LICI. Given that both reduced and enhanced LICI have been reported in the studies included in this review, "LICI impairment" will refer to any significant difference between clinical populations and

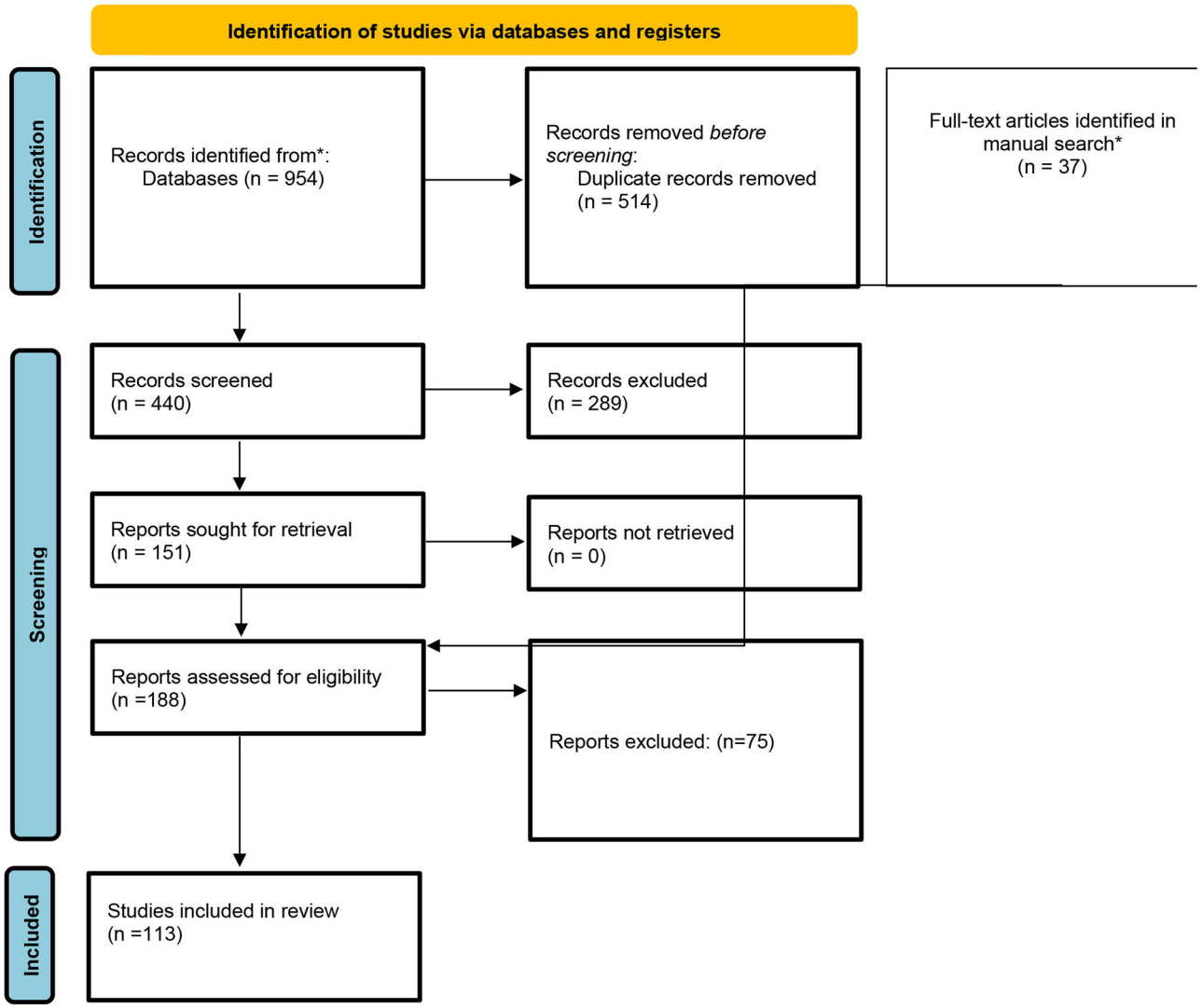

FIGURE 1 | PRISMA diagram. *Records identified from the references of full-text articles.

healthy controls. Additional outcomes examined correlational analyses of LICI and suicidal remission, suicidal severity, symptom severity, functional connectivity, social cognition, cortical silent period (CSP), synaptic plasticity, visuomotor reaction time, motor dexterity, GABA levels measured with proton magnetic resonance spectroscopy (^{1}H-MRS), functional decline, fatigue, and cognitive functioning. The cortical areas of interest were the motor cortex and the dorsolateral pre-frontal cortex (DLPFC). The studies of interest assessed LICI with either EMG or EEG.

RESULTS

Search Results

The detailed description of the search results is shown in the PRISMA flow diagram included in **Figure 1**. A total of 188 articles were selected for full-text inspection after the title and abstracts of all records were screened. The reviewers identified 37 additional studies through checking the quoted references of full texts of the above-mentioned articles. Finally, 113 articles that met inclusion criteria were included and reported in the systematic review. Overall, LICI was investigated in 2 articles for ADHD, 3 articles for bipolar disorder, 9 articles for depression, 4 articles for neurodevelopmental disorders, 9 articles for schizophrenia, 5 articles for substance use, and 3 articles for other psychiatric disorders. Among the articles investigating neurological disorders, LICI was studied in 9 articles for dementia, 20 for epilepsy patients, 21 for movement disorders, 3 for multiple sclerosis, 6 for stroke patients, 12 traumatic brain injury patients and 7 for other neurological disorders. The main findings and full data extraction are summarized in the tables provided in the **Supplementary Material**.

TABLE 1 | LICI in patients with ADHD.

References	Subjects	Method	ISI	LICI
Buchmann et al. (33)	18 ADHD, 18 HC	TMS-EMG	100, 200, 300 ms	↓
Hoeppner et al. (34)	21 ADHD, 21 HC	TMS-EMG	100, 200, 300 ms	↔

ISI, Interstimulus interval; ADHD, Attention deficit hyperactivity disorder; LICI, Long-interval intracortical inhibition; HC, Healthy controls.

TABLE 2 | LICI in patients with bipolar disorder.

References	Subjects	Method	ISI	LICI
Ruiz-Veguilla et al. (35)	19 BD, 28 HC	TMS-EMG	100, 150, 250 ms	↔
Basavaraju et al. (36)	67 BD, 45 HC	TMS-EMG	100 ms	↑
Basavaraju et al. (37)	39 BD, 45 HC	TMS-EMG	100 ms	↑

ISI, Interstimulus interval; BD, Bipolar disorder; LICI, Long-interval intracortical inhibition; HC, Healthy controls. ↑: increased, ↔: no significant difference.

LICI in Psychiatric Disorders

LICI in Patients With ADHD

The LICI paradigm in ADHD patients was investigated with TMS-EMG motor cortical measures in two prior studies. One study enrolled adult subjects and the other enrolled pediatric subjects (**Table 1**). Buchmann et al. examined alterations in LICI among 18 children diagnosed with ADHD compared to 18 healthy control (HC) children. The study evaluated the influence of methylphenidate (MPH) treatment on LICI among children with ADHD. It was shown that baseline LICI was reduced in drug naïve ADHD subjects at an interstimulus interval (ISI) of 100 ms ($p = 0.001$). Treatment with MPH potentiated LICI yielding values similar to healthy controls. For ADHD subjects a reduction in symptoms correlated with LICI improvements following MPH administration ($p < 0.05$) (33). Hoeppner et al. evaluated 21 adult ADHD patients in a cross-sectional study and demonstrated that there was no significant LICI deficit in the patient population compared to age and gender-matched healthy controls (34). These studies indicated significant LICI deficit in children with ADHD, whereas there was no significant LICI difference between adult ADHD patients and healthy controls (33, 34). Therefore, cortical maturation with aging might explain the loss of LICI deficit in the adult ADHD population (34).

LICI in Patients With Bipolar Disorder

Prior studies measuring LICI in patients with bipolar disorder (BD) used TMS-EMG to investigate motor cortex activity (**Table 2**). Ruiz-Veguilla et al. studied trait and state-dependent LICI deficits in 19 adult patients with BD in the depressed phase vs. 28 healthy controls. In the BD sample, 15 patients who were receiving a combination of lithium/valproate plus antipsychotic treatment were assessed 3 months later to evaluate the influence of symptom remission on LICI. Results demonstrated that there was no significant LICI deficit in patients with BD vs. healthy controls at baseline, and LICI did not significantly change with symptom remission at follow-up (35). A cross-sectional study by Basavaraju et al. investigated LICI in 39 medication naïve patients with BD in a manic episode, 28 remitted first-episode mania patients treated with antipsychotic medications or an antipsychotic plus mood stabilizer, and 45 HC. The LICI measures were significantly enhanced in medication naïve patients who were in a manic episode compared to HC ($p = 0.021$). There was no significant difference in LICI between the patients who were in a manic episode and those who remitted, and there was no significant difference in LICI between the remitted patients and HC. Correlation of symptom severity, measured with Young's Mania Rating Scale (YMRS), and LICI was non-significant (36). Another cross-sectional study by Basavaraju et al. evaluated Mirror Neuron Activity (MNA) using LICI, and its correlation with symptom severity in the same group of 39 medication naïve BD patients in a manic episode and 45 HC. MNA was measured while subjects were observing a goal-directed activity. Enhanced MNA assessed with LICI was detected in the medication naïve symptomatic BD patients ($p = 0.033$). LICI mediated putative MNA was significantly correlated with symptom severity ($p = 0.038$) (37).

The studies examining BD patients had varied results demonstrating both normal LICI and enhanced LICI relative to HC. These results are interesting as studies with other neurophysiological paradigms have shown inhibitory deficits in BD (36). Possible explanations and supporting evidence of enhanced LICI in bipolar disorder comes from the studies showing manic symptoms triggered with baclofen and elevated GABA/Creatine ratio in anterior cingulate cortex of patients with BD (38). These results might be affected by study flaws such as larger manic sample and medication naïve condition (36) or small sample size (35).

LICI in Patients With Depression

Seven prior studies in depressed patients examined cortical inhibition measured with TMS-EMG. Two other studies investigated both DLPFC and motor cortex LICI paradigms using EEG (**Table 3**).

Croarkin et al. investigated the association of pre-treatment LICI levels with treatment response in 16 children and adolescents with major depressive disorder (MDD) who were initiated on treatment with fluoxetine. Treatment-resistant subjects had greater LICI deficits at baseline relative to treatment responders at each ISIs of 100, 150, 200 ms ($p = 0.01$, 0.03, 0.01) (39). A cross-sectional study examining the relationship between cortical inhibition and age evaluated LICI in 14 youth with MDD and 19 age-matched HC. Results suggested that increased LICI at 200 ms was associated with older age in depressed youth in both right and left hemispheres ($p = 0.034$, 0.002), whereas there was no significant association with age in the control group (40). LICI was assessed in depressed adolescents with and without a history of suicidal behavior and compared to HC in a study by Lewis et al. Depressed adolescents with a history of suicidal behavior exhibited decreased LICI at interstimulus intervals of 100 ms and 150 ms relative to HC ($p = 0.0002$, 0.0009) and depressed adolescents without suicidal behavior ($p = 0.0049$, 0.0418). Moreover, increased

TABLE 3 | LICI in patients with depression.

References	Subjects	Method	ISI	LICI
Croarkin et al. (39)	8 treatment responder MDD, 8 treatment resistant MDD	TMS-EMG	100, 150, 200 ms	↓ in treatment resistant subjects
Croarkin et al. (40)	14 MDD 19 HC	TMS-EMG	100, 150, 200 ms	↑ with age in adolescents
Sun et al. (41)	33 TRD	TMS-EEG	100 ms	↑ at baseline correlated with decreased suicidality following MST
Sun et al. (42)	23 TRD	TMS-EEG	100 ms	↓ following MST in patient with resolved SI
Lewis et al. (43)	37depressed, 17 depressed + SB, 20 HC	TMS-EMG	100, 150, 200 ms	↓ in depressed subjects with SB
Jeng et al. (44)	20 TRD, 16 non-TRD, 36 HC	TMS-EMG	100, 200 ms	↓ in TRD subjects
Lewis et al. (45)	10 Depressed	TMS-EMG	100, 150 ms	↑ associated with decrease in SI following antidepressant treatment
Balzekas et al. (46)	5 Depressed	TMS-EMG	100, 150, 200 ms	Comparison not measured
Doruk Camsari et al. (47)	15 MDD, 22 HC	TMS-EMG	100, 150, 200 ms	↔

ISI, Interstimulus interval; TRD, Treatment resistant depression; LICI, Long-interval intracortical inhibition; MST, Magnetic seizure therapy; MDD, Major depressive disorder; SI, Suicidal ideation; HC, Healthy controls; SB, Suicidal behavior. ↓: decreased, ↔: no significant difference.

suicidal severity correlated with the reduction in LICI at ISI of 100 and 150 ms (43). Jeng et al. investigated LICI in 20 adult patients with treatment-resistant depression, 16 adult patients who responded to treatment for MDD, and HC to evaluate the utility of LICI as a biomarker in distinguishing treatment response. LICI was significantly reduced in treatment-resistant subjects relative to treatment responders or HC, and decreased LICI was correlated with higher symptom severity ($p < 0.001$). This study also demonstrated a reduction in LICI in treatment after 3 months of SSRI treatment ($p = 0.002$) (44). Lewis et al. examined LICI change and its association with change in suicidal ideation (SI) in depressed adolescents treated with antidepressants and found that decreased SI was associated with enhanced LICI measured at 100 ms when controlling for depression severity ($p = 0.021$). Adolescents with prior suicidal behavior had a greater reduction in follow up LICI relative to those without a previous history of suicidal behavior ($p = 0.038$) (45). In a cross-sectional study by Balzekas et al., the association between LICI and cortical connectivity, measured with resting-state functional magnetic resonance imaging, was found to be non-significant (46). Doruk Camsari et al. investigated the change of LICI with antidepressant treatment and found no significant post-treatment alteration in LICI (47).

Sun et al. investigated pre-treatment LICI in DLPFC and motor cortex, as a biomarker for suicidal remission after Magnetic Seizure Therapy (MST). This study examined 33 treatment-resistant adult depression patients and revealed that remission of suicidal ideation, measured with the Scale for Suicide Ideation (SSI), was correlated with greater LICI in DLPFC at baseline ($p = 0.02$) although pre-treatment LICI in the motor cortex was not significantly correlated with treatment outcome (41). Another study by Sun et al. examined changes in neuroplasticity, using LICI, and suicidal ideation following MST treatment in adults with treatment-resistant depression. Results showed that LICI in DLPFC was reduced following MST treatment in patients with resolved suicidal ideation and that the decrease in LICI was correlated with SSI score reduction ($p = 0.048$, 0.044). There was no significant finding for LICI in the motor cortex (42).

Two studies showed significantly more impaired LICI in treatment-resistant subjects compared to treatment responders. Furthermore, greater LICI deficits in depressed patients with suicidal ideation compared to non-suicidal depressed patients were indicated. Supporting this, enhanced LICI following MST treatment was shown to predict the reduction in suicidal ideation while another study showed the correlation of alteration in LICI and the improvement in suicidal ideation. These results are consistent with the findings showing both $GABA_A$ and $GABA_B$ mediated cortical inhibitory deficits in the pathophysiology of depression (14) in different age groups (48). Moreover, these findings suggest that LICI might be a used as a prognostic biomarker evaluating depressed patients. Regarding suicidal ideation and suicidal behavior, literature was limited to the papers in our review. It is known that impaired behavioral inhibition (i.e., impulsivity) is central to the pathophysiology of suicide. It might be postulated that cognitive and behavioral inhibitory deficits result from cortical inhibition alterations in brain regions vital for inhibitory control, such as the anterior cingulate gyrus (49, 50).

LICI in Patients With Neurodevelopmental Disorders

LICI in neurodevelopmental disorders was investigated in Fragile X and patients with autism spectrum disorder (ASD) using TMS-EMG (**Table 4**). Oberman et al. evaluated LICI in 2 subjects with Fragile X, 2 with ASD, and 5 HC and found no significant LICI difference across these three groups (51). Another study examining LICI alteration in ASD with a larger sample size of 36 patients with ASD and 34 HC had similar results showing no significant LICI deficit in individuals with

TABLE 4 | LICI in patients with neurodevelopmental disorders.

References	Subjects	Method	ISI	LICI
Oberman et al. (51)	2 Fragile X, 2 ASD, 5 HC	TMS-EMG	100 ms	↔
Enticott et al. (52)	36 ASD, 34 HC	TMS-EMG	100 ms	↔
Morin-Parent et al. (53)	18 Fragile X, 18 HC	TMS-EMG	100 ms	↑
Bernardo et al. (54)	14 Rett syndrome, 9 epilepsy control, 11 HC	TMS-EMG	100, 150 ms	↓ in Rett syndrome patients

ISI, Interstimulus interval; ASD, Autism spectrum disorder; LICI, Long-interval intracortical inhibition; HC, Healthy controls. ↑: increased, ↔: no significant difference.

TABLE 5 | LICI in patients with schizophrenia.

References	Subjects	Method	ISI	LICI
Fitzgerald et al. (55)	18 SCZ, 8 HC	TMS-EMG	100 ms	↔
Farzan et al. (56)	14 SCZ, 14 BD, 14 HC	TMS-EEG	100 ms	↓ in DLPFC of SCZ, ↔ in BD
Mehta et al. (57)	54 SCZ, 45 HC	TMS-EMG	100 ms	↔
Mehta et al. (58)	54 SCZ, 45 HC	TMS-EMG	100 ms	↔ MNA
Radhu et al. (59)	38 SCZ, 27 OCD, 46 HC	TMS-EEG	100 ms	↓ in DLPFC of SCZ, ↔ in OCD
Basavaraju et al. (60)	18 SCZ with EBD, 32 SCZ w/o EBD	TMS-EMG	100 ms	↔
Lett et al. (61)	80 SCZ, 115 HC	TMS-EEG	100 ms	↔
Radhu et al. (62)	19 SCZ, 30 FDR of SCZ, 13 OCD, 18 FDR of OCD, 49 HC	TMS-EEG	100 ms	↓ in DLPFC of SCZ, ↔ in OCD
Goodman et al. (63)	12 SCZ with cannabis use, 11 cannabis free SCZ, 10 controls with cannabis use, 13 cannabis free controls	TMS-EMG	100, 150, 200 ms	↔

ISI, Interstimulus interval; HC, Healthy controls; LICI, Long-interval intracortical inhibition; MNA, Mirror neuron activity; DLPFC, Dorsolateral pre-frontal cortex; OCD, Obsessive-compulsive disorder; SCZ, Schizophrenia; EBD, Ego boundary disturbance; BD, Bipolar disorder; FDR, First degree relative. ↓: decreased, ↔: no significant difference.

ASD (52). Morin-Parent et al. studied LICI in 18 individuals with molecular Fragile X diagnosis (7 of them receiving psychotropic medication) and compared these patients to 18 age and gender-matched HC, and results demonstrated that LICI was enhanced in Fragile X subjects relative to HC ($p = 0.011$). When the analysis was limited to only non-medicated Fragile X individuals, results demonstrated a similar trend of enhanced LICI although, the significance was lost ($p = 0.060$) (53). Bernardo et al. investigated LICI in Rett syndrome patients comparing them to non-Rett syndrome epilepsy patients and health controls. LICI was reduced in the Rett syndrome patients relative to epilepsy and healthy controls ($p = 0.002$). Furthermore, impaired motor performance was significantly associated with decreased LICI ($p = 0.003$) (54).

LICI in Patients With Schizophrenia Spectrum Disorders

Five prior studies examined the motor cortex, TMS-EMG LICI in patients with schizophrenia (SCZ). Three studies focused on both DLPFC and motor cortex, and 1 study focused on only DLPFC using EEG (**Table 5**).

In a study including 18 SCZ patients (9 were medicated with antipsychotics) and 18 HC, Fitzgerald et al. demonstrated that there was no significant difference across groups regarding LICI (55). A cross-sectional study by Mehta et al. examined a larger sample size of 54 SCZ patients and 45 HC, and they also found no significant LICI difference in SCZ patients relative to HC. There was also no significant correlation between social cognition measures and LICI in both groups (57). Another study by Mehta et al. evaluated MNA using LICI in the same group of above-mentioned subjects and showed that action observation did not have a significant effect on LICI. Further, there was no significant correlation between MNA and social cognition in both SCZ patients and HC (58). Basavaraju et al. examined LICI to investigate MNA with a sample of 50 SCZ patients, 18 with ego boundary disturbances (EBD) and 32 without EBD, and demonstrated no significant MNA difference between groups (60). Goodman et al. examined the effect of cannabis use on LICI in SCZ patients in a study involving 4 groups of subjects: 12 cannabis dependent SCZ patients, 11 cannabis free SCZ patients, 10 cannabis dependent controls, and 13 cannabis free controls. The findings demonstrated that cannabis use did not significantly alter LICI in either the SCZ group or control group; likewise, LICI was not significantly different in SCZ subjects and controls (63).

Farzan et al. investigated alterations in LICI assessed with gamma oscillations in DLPFC and motor cortex of 14 patients with SCZ, 14 patients with BD, and 14 HC. The study revealed that SCZ patients had significantly impaired cortical inhibition of gamma oscillations in DLPFC relative to BD patients and HC ($p < 0.01$, $p < 0.01$), whereas there was no significant difference between BD subjects and HC. Notably, in this study, LICI measured from the motor cortex did not differ significantly across SCZ patients, BD patients, and HC (56). Another study targeting DLPFC in SCZ patients as compared to OCD patients

and HC demonstrated that SCZ patients had significantly greater LICI reduction relative to OCD group and HC (p = 0.0465, 0.004, respectively). There were no significant differences between the OCD and HC samples. Once again there were no significant differences in LICI measures from the motor cortex among the three groups. However, the study revealed that SCZ symptom severity, measured with the Brief Psychiatric Rating Scale (BPRS), was correlated with a deficit in LICI ($p = 0.0457$) (59). Radhu et al. examined LICI in SCZ and OCD patients and their unaffected first-degree relatives compared to HC. Results exhibited that SCZ patients had greater LICI deficit in the DLPFC relative to first-degree relatives ($p = 0.03$) and HC (p = 0.032). First degree relatives had impaired LICI compared to HC patients, but this was not statistically significant. LICI measures in the motor cortex did not differ across SCZ patients, first-degree relatives, and HC. Likewise, there was no significant difference across OCD patients, first-degree relatives, and HC in either the motor cortex or DLPFC (62).

Lett et al. investigated LICI in the DLPFC using TMS-EEG and examined the correlation between GAD glutamic acid decarboxylase 1 (GAD1) variant and LICI in SCZ patients and HC. It was shown that GAD1 T allele carrier healthy controls had greater LICI cluster size ($p = 0.003$), whereas patients with SCZ who were allele carriers had a lower cluster size (0.04) (61).

The studies examining LICI in motor cortex of SCZ patients failed to show any significant correlation between LICI alterations and neural correlates of SCZ symptoms (i.e., MNA for ego boundary disturbances). Whereas, studies investigating LICI in DLFPC of SCZ demonstrated significant findings. The dysfunctional frontal inhibitory neurotransmission might be underlying the cognitive function deficits present in SCZ principally the working memory performance (59, 64, 65).

LICI in Patients With Substance Use Disorder

Prior studies examined LICI in nicotine, cocaine, alcohol, and cannabis users (**Table 6**). Four of those studies examined the motor cortex using TMS-EMG, whereas one study investigated the DLPFC using TMS-EEG. Another study investigating the effects of cannabis use on LICI in SCZ patients is mentioned above in the "LICI in patients with Schizophrenia Spectrum Disorders" section.

In a cross-sectional study involving 10 abstinent cocaine-dependent subjects and 10 HC, results demonstrated no significant LICI deficit in cocaine users relative to the control group (66). Gjini et al. confirmed the same finding, showing no significant difference of LICI, in their study evaluating 52 abstinent cocaine-dependent subjects and 42 HC (69). Lang et al. demonstrated that there were no differences in LICI among subjects using nicotine and subjects who were not using nicotine (67). Fitzgerald et al. investigated LICI alterations in 42 chronic cannabis users and showed that there was no significant difference in LICI relative to the non-user control group (68).

Naim-Feil et al. investigated the alteration of LICI in DLPFC of 12 alcohol-dependent subjects post-detoxification and 14 HC. Results revealed that the alcohol-dependent group had greater reduction in LICI in both left and right DLPFC relative to the control group ($p = 0.003$, $p = 0.006$) (70).

The studies regarding substance use disorders suggested that LICI measurements from DLPFC tend to reveal more significant differences than LICI measurements from motor cortex. The prior negative findings with LICI paradigms in substance use disorders are important to ponder and reconcile with pre-clinical studies showing the alterations in the GABAergic changes of brain after chronic cocaine administration (71, 72) as well as modulatory effects of GABAergic agents in cocaine addiction treatment (73, 74). As mentioned in the above studies alterations in GABAergic circuits were in the relative brain regions for addiction, such as the DLPFC [59]. Collectively, these findings suggest that patients with substance use disorders may have underlying GABAergic deficits in pre-frontal neurocircuitry. Further studies utilizing TMS-EEG to investigate the cortical inhibition in potentially affected brain regions are essential to explicate the role of LICI in substance use disorders.

LICI in Patients With Other Psychiatric Disorders

A study investigating LICI over DLPFC and motor cortex in psychopathic offenders through TMS-EEG indicated that LICI was impaired in DLPFC ($p = 0.005$) but not in the motor cortex relative to healthy subjects (**Table 7**). Moreover, psychopathic offenders displayed worse working memory performance (p = 0.005), measured with the letter-number sequencing test, which demonstrated a non-significant but trending correlation with LICI in DLPFC ($p = 0.069$). Healthy subjects showed better working memory performance associated with greater LICI in DLPFC ($p = 0.005$) (75). Salas et al. showed that there were no abnormalities of motor cortex LICI in individuals with chronic insomnia relative to good sleepers (76). LICI alteration was

TABLE 6 | LICI in patients with substance use.

References	Subjects	Method	ISI	LICI
Sundaresan et al. (66)	10 cocaine users, 10 HC	TMS-EMG	50, 100 ms	↔
Lang et al. (67)	19 nicotine users, 19 HC	TMS-EMG	50, 100, 150 ms	↔
Fitzgerald et al. (68)	42 cannabis user, 19 HC	TMS-EMG	100 ms	↔
Gjini et al. (69)	52 cocaine users, 42 HC	TMS-EMG	50, 100 ms	↔
Naim-Feil et al. (70)	12 alcohol dependent, 14 HC	TMS-EEG	100 ms	↓ in DLPFC

ISI, Interstimulus interval; HC, Healthy controls; LICI, Long-interval intracortical inhibition; DLPFC, Dorsolateral pre-frontal cortex. ↓: decreased, ↔: no significant difference.

TABLE 7 | LICI in patients with other psychiatric disorders.

References	Subjects	Method	ISI	LICI
Hoppenbrouwers et al. (75)	13 psychopathic offenders, 15 HC	TMS-EEG	100, 150, 250 ms	↓ in DLPFC
Salas et al. (76)	18 chronic insomnia, 10 HC	TMS-EMG	100 ms	↔
Li et al. (77)	26 GAD, 35 HC	TMS-EMG	100 ms	↔

ISI, Interstimulus interval; HC, Healthy controls; LICI, Long-interval intracortical inhibition; DLPFC, Dorsolateral pre-frontal cortex; GAD, Generalized anxiety disorder. ↓: decreased, ↔: no significant difference.

TABLE 8 | LICI in patients with dementia.

References	Subjects	Method	ISI	LICI
Brem et al. (78)	16 AD, 13 HC	TMS-EMG	100 ms	↓
Benussi et al. (79)	27 FTD, 24 HC	TMS-EMG	50, 100, 150 ms	↔
Benussi et al. (80)	79 AD, 61 FTD, 32 HC	TMS-EMG	50, 100, 150 ms	↓ in FTD, ↔ in AD
Fried et al. (81)	9 AD, 15 DM, 12 HC	TMS-EMG	100 ms	High reproducibility of LICI indicated
Benussi et al. (82)	113 FTD mutation carrier FDR, 75 mutation non-carrier FDR	TMS-EMG	50, 100, 150 ms	↓ in FTD mutation carriers
Assogna et al. (83)	17 probable FTD	TMS-EMG	50, 100, 150 ms	↑ following palmitoylethanolamide luteoline administration
Benussi et al. (84)	186 FTD	TMS-EMG	50, 100, 150 ms	↓ in GRN mutation carriers
Benussi et al. (85)	171 FTD, 74 HC	TMS-EMG	50, 100, 150 ms	↓
Benussi et al. (86)	66 FTD	TMS-EMG	50, 100, 150 ms	↔ no association with whole brain fluidity

ISI, Interstimulus interval; HC, Healthy controls; LICI, Long-interval intracortical inhibition; FTD, Frontotemporal dementia; AD, Alzheimer's disease; GRN, Granulin; FDR, First degree relative.

investigated by Li et al. evaluating 26 patients with generalized anxiety disorder who were medication naive and 35 age and sex-matched controls, and it was demonstrated that LICI did not differ significantly in patients with anxiety relative to HC. Nevertheless, decrements in LICI correlated with higher symptom scores measured with the Hamilton Anxiety Rating Scale ($p = 0.020$) (77).

LICI in Neurologic Disorders

LICI in Patients With Dementia

Among 9 studies investigating the role of LICI in dementia, 6 studied subjects with frontotemporal dementia (FTD), 2 with Alzheimer's disease (AD), and 1 investigated both disorders (**Table 8**). The motor cortex was the area of interest for all the studies. Brem et al. studied LICI alterations in 7 AD patients taking acetylcholinesterase inhibitor (AChEI) medication, 9 AD patients taking AChEI medication with memantine, and 13 HC. The study demonstrated reductions in LICI in the group receiving AChEI medications and those receiving AChEI medication+memantine relative to HC subjects ($p = 0.025$, 0.015). Impairments in cognitive functioning, measured with Alzheimer's Disease Assessment Scale-Cognitive Subscale (ADAS-Cog), were significantly associated with LICI deficit ($p = 0.010$) (78). Benussi et al. examined the LICI alterations in FTD mutation carriers, 13 pre-symptomatic and 14 symptomatic, relative to HC. Although there was no significant LICI deficit in FTD mutation carriers, symptomatic carriers had greater LICI deficit compared to the other groups (79). In a study investigating the role of LICI as a biomarker distinguishing AD from FTD ($n = 79$ AD, $n = 61$ FTD, $n = 32$ HC) Benussi et al. did not detect any significant difference of LICI between AD and FTD patients or AD patients and HC. The LICI impairment in the FTD group was significantly greater relative to controls at ISI of 150 ms (80). Fried et al. demonstrated LICI's high reproducibility in AD patients and HC with a prospective cohort study ($\alpha = 0.88$, 0.98) (81). Another study by Benussi et al. examined LICI as a disease progression biomarker in FTD mutation carriers and non-carrier at-risk individuals. 113 subjects carrying monogenic FTD mutation and 75 non-carriers with affected first-degree relatives were evaluated, and years from symptom onset were determined by subtracting the age of the participant from mean familial age at symptom onset. Reduced LICI was detected in mutation carriers relative to non-carriers at 20 years before expected symptom onset ($p < 0.001$) (82). Assogna et al. examined change in LICI following palmitoylethanolamide luteoline (PEA-LUT) administration and found that LICI was increased after PEA-LUT (83). In another cross-sectional study the same group demonstrated that LICI was more reduced in GRN mutation carriers relative to non-carrier first-degree relatives and there was no significant association of LICI with behavioral symptoms (84). LICI alteration in different phenotypes of FTD and its correlation with functional decline and symptom severity were studied in another study of Benussi et al. LICI was demonstrated to be impaired in all phenotypes (behavioral variant of FTD,

agrammatic variant of Primary Progressive Aphasia, semantic variant of PPA) of FTD relative to HC ($p < 0.05$). Disease duration, functional decline, and increased symptom severity were significantly associated with LICI deficit in FTD patients ($p < 0.001$) (85). LICI's association with brain network connectivity and fluidity was examined by Benussi et al. and they indicated that there was no significant relation (86).

These studies of LICI have examined Alzheimer's disease and Frontotemporal Dementia. Alzheimer studies have presented varied results. Several prior studies have shown the modulatory effect of $GABA_B$ stimulation in Alzheimer's disease (87). Interaction between the cholinergic and GABAergic systems as well as inhibitory interactions between SAI and LICI might explain the difference between AD group and HC. However, the findings in FTD patients were quite consistent, showing LICI deficits in the patient population. The results showing LICI deficit detected before symptom onset in FTD mutations carriers and LICI's correlation with functional decline underlie the potential utility of LICI as a biomarker estimating the disease progression.

LICI in Patients With Epilepsy

LICI in epilepsy was studied in 20 studies (**Table 9**). Brodtmann et al. demonstrated reduced LICI at ISI of 200–300 ms in idiopathic generalized epilepsy (IGE) patients, and significant facilitation instead of inhibition was observed at the same intervals in the IGE group ($p < 0.05$) (88). Valzania et al. demonstrated impaired LICI in progressive myoclonic epilepsy patients relative to HC at the ISI of 100–150 ms and facilitation of motor evoked potential at 50 ms ISI ($p < 0.001$) (89). Manganotti et al. studied juvenile myoclonic epilepsy patients and found no significant LICI difference relative to HC (90). Molnar et al. did not find any significant effect of bilateral anterior thalamus deep brain stimulation (DBS) on LICI in epilepsy patients, and LICI was impaired in all DBS stimulus conditions (off, cycling, and continuous) at ISI of 50 ms ($p = 0.0003$, 0.0015, 0.0001) (91). Badawy et al. demonstrated facilitation instead of inhibition in both hemispheres of IGE patients using the LICI paradigm; thus, LICI was reduced relative to HC ($p < 0.01$ at ISI of 250 ms). Similar findings were also demonstrated with

TABLE 9 | LICI in patients with epilepsy.

References	Subjects	Method	ISI	LICI
Brodtmann et al. (88)	7 IGE, 16 HC	TMS-EMG	50–400 ms	↓
Valzania et al. (89)	12 IGE, 8 HC	TMS-EMG	50, 100, 150, 250 ms	↓
Manganotti et al. (90)	15 JME, 12 HC	TMS-EMG	30–400 ms	↔
Molnar et al. (91)	5 Epilepsy, 9 HC	TMS-EMG	50–200 ms	↓
Badawy et al. (92)	35 IGE, 27 focal epilepsy, 29 HC	TMS-EMG	200–400 ms	↓ in IGE and focal epilepsy
Badawy et al. (93)	59 IGE, 47 focal epilepsy, 32 HC	TMS-EMG	50–300 ms	↓ at baseline, ↑ following AED treatment in seizure free subjects
Badawy and Jackson (94)	26 migraine, 22 focal epilepsy, 28 IGE 19 HC	TMS-EMG	50–400 ms	↓ in migraine, IGE and focal epilepsy
Badawy et al. (95)	11 focal epilepsy, 13 IGE, 17 HC	TMS-EMG	50–400 ms	↓ IGE and focal epilepsy
Badawy et al. (96)	30 refractory epilepsy, 35 seizure free on monotherapy, 12 seizure free on dual therapy	TMS-EMG	100–300 ms	↓
Badawy et al. (97)	46 JME, 41 JAE, 50 GE-TCS, 20 HC	TMS-EMG	100–300 ms	↓
Badawy et al. (98)	85 TLE, 20 HC	TMS-EMG	100–300 ms	↔
Badawy et al. (99)	11 IGE, 11 focal epilepsy, 10 HC	TMS-EMG	100–400 ms	↓
Badawy et al. (100)	21 isolated seizure, 20 IGE, 18 focal epilepsy, 20 HC	TMS-EMG	100–300 ms	↓ in IGE and focal epilepsy
Badawy et al. (101)	46 TLE, 39 Extra-TLE, 20 HC	TMS-EMG	100–300 ms	↓ at baseline, ↑ following AED treatment in seizure free subjects
Silbert et al. (102)	10 IGE, 12 HC	TMS-EMG	100–350 ms	↓ in migraine, IGE, and focal epilepsy
Pawley et al. (103)	28 moderately controlled epilepsy, 40 poorly controlled epilepsy, 28 HC	TMS-EMG	50–250 ms	↓ IGE and focal epilepsy
Bauer et al. (104)	40 IGE, 69 focal epilepsy, 95 HC	TMS-EMG	50–250 ms	↓
Bolden et al. (105)	30 IGE, 24 HC	TMS-EEG	50–200 ms	↓
Bolden et al. (106)	30 IGE, 22 HC	TMS-EEG	50–200 ms	↔
Huang et al. (107)	41 poorly controlled TLE, 71 well-controlled TLE, 44 HC	TMS-EMG	50–300 ms	↓

ISI, Interstimulus interval; JAE, juvenile absence epilepsy; LICI, Long-interval intracortical inhibition; GE-TCS, Generalized epilepsy with tonic-clonic seizures; IGE, Idiopathic generalized epilepsy; TLE, Temporal lobe epilepsy; HC, Healthy controls; AED, Antiepileptic drug; JME, Juvenile myoclonic epilepsy; PME, Progressive myoclonic epilepsy.

ipsilateral LICI measures of focal epilepsy patients ($p < 0.01$ at ISI of 250 ms) but there was no significant impairment in the contralateral hemisphere relative to HC (92). Additionally, Badawy et al. examined the effect of the antiepileptic drug treatment in epilepsy patients and showed that in seizure-free IGE patients, LICI was restored post-treatment in the dominant hemisphere at interstimulus intervals of 50, 150, 250, and 300 ms ($p < 0.01$). Focal epilepsy patients who were seizure-free post-treatment also had restored LICI in the ipsilateral hemisphere at interstimulus intervals of 250–300 ms ($p < 0.05$). IGE and focal epilepsy patients with ongoing seizures did not have any significant change in LICI post-treatment (93). Badawy and Jackson examined LICI in migraine and epilepsy patients and demonstrated LICI impairment in migraine, IGE, and focal epilepsy patients relative to HC at the interstimulus interval of 250 ms ($p < 0.05$). Results showed that LICI had greater reduction in focal epilepsy ($p < 0.05$) and IGE patients ($p < 0.01$) relative to migraine patients (94). In a prospective cohort study, the reproducibility of LICI in drug naïve epilepsy patients was investigated by measuring LICI in two separate sessions 4–20 weeks apart. Results suggested that LICI was reduced in epilepsy patients relative to HC at baseline, and there was no significant intersession variability in both patient and control groups (95). In another longitudinal study, Badawy et al. investigated the effect of the antiepileptic drug on LICI over time by evaluating epilepsy patients in 4 phases 1–2 weeks, 2–6, 12–18, and 30–36 months apart. Results showed that refractory IGE and focal epilepsy patients demonstrated worsening LICI over time whereas in seizure-free IGE and focal epilepsy patients, significant improvement of LICI and decreased cortical excitability was observed with antiepileptic medications (96). In a cross-sectional study, Badawy et al. compared patients with juvenile myoclonic epilepsy (JME), juvenile absence epilepsy (JAE), and generalized epilepsy with tonic-clonic seizures (GE-TCS). All drug naïve patients (JME, JAE, and GE-TCS) groups demonstrated lower LICI relative to HC ($p < 0.01$). JME patients had greater impairment in LICI compared to JAE and GE-TCS subjects ($p < 0.05$) (97). Temporal lobe epilepsy (TLE) patients were examined for LICI in a cross-sectional study by Badawy et al. and results revealed that LICI in the ipsilateral hemisphere of drug naïve TLE patients was reduced relative to HC ($p < 0.01$). Refractory TLE subjects demonstrated the same findings but LICI impairment also applied for the contralateral hemisphere, and the refractory group demonstrated more reduced LICI compared to seizure-free and drug naïve TLE patients (98). Another cross-sectional study evaluated the role of glucose levels in LICI alteration and found that in both healthy controls and epilepsy patients (IGE and focal epilepsy) LICI in both hemispheres was reduced in the fasting state relative to the postprandial state ($p < 0.05$) (99). In another study, Badawy et al. included patients having isolated unprovoked seizures and revealed this sample of patients had reduced LICI relative to HC ($p < 0.01$), though impairment in LICI was lower compared to IGE patients ($p < 0.01$) and focal epilepsy patients ($p < 0.05$) (100). Focal epilepsy patients with different epileptogenic regions were examined in a cross-sectional study, and it was demonstrated that LICI was reduced in drug naïve, refractory, and seizure-free TLE and extra-TLE patients relative HC ($p < 0.05$). Notably, in drug naïve and seizure-free patients significant LICI impairment was only seen in the ipsilateral hemisphere. Refractory groups demonstrated lower LICI relative to seizure-free and drug naïve TLE and extra-TLE patients ($p < 0.05$) (101). Silbert et al. studied IGE patients and found that LICI was not significantly different between unmedicated IGE patients and HC, whereas IGE patients on antiepileptic drug treatment had enhanced LICI relative to unmedicated IGE patients ($p < 0.001$) and HC ($p = 0.003$) (102). Pawley et al. investigated LICI in longstanding uncontrolled epilepsy patients and revealed that LICI in poorly controlled or moderately controlled generalized epilepsy patients did not differ significantly from HC. In focal epilepsy patients, poorly controlled and moderately controlled epilepsy was associated with enhanced LICI compared to HC ($p = 0.040$) (103). Bauer et al. demonstrated similar findings showing no significant LICI differences across HC, IGE, and focal epilepsy patients (104). Bolden et al. also found that controlled IGE patients, treatment resistant IGE patients, and HC did not have a significantly different LICI. Nevertheless, results demonstrated that patients with lower LICI performed worse in attention tasks (105). A companion study by the same research group found that participants with the excitatory response on LICI demonstrated greater mood disturbance relative to participants with the inhibitory response (106). In a cross-sectional study, Huang et al. studied TLE patients and demonstrated that LICI was stronger in poorly controlled and well-controlled TLE patients relative to HC at interstimulus intervals of 50, 100, and 200 ms ($p = 0.026$, 0.002, 0.001) (107).

The majority of the studies demonstrated reduced LICI in patients with various seizure disorders. However, some studies demonstrated normal or increased LICI in patients with epilepsy. It would be anticipated that patients with seizure disorders have GABAergic inhibitory deficits, as this is supported by previous studies that have consistently shown the alterations in GABAergic transmission, especially in patients with absence seizures as well as in mouse models of generalized and focal seizures (108). The non-significant findings in studies of LICI with epilepsy patients might related to small intertrial intervals, the selection of the hemisphere (i.e., dominant vs. ipsilateral) examined in analyses (104) or the criteria used to classify participants as treatment-refractory (105).

LICI in Patients With Movement Disorders

LICI was investigated in dystonia, Huntington's disease, and Parkinson's disease patients (**Table 10**). Chen et al. studied 8 patients with writer's cramp and 18 HC in a cross-sectional study and showed that LICI measured from the left (symptomatic) hemisphere at 50–80 ms interstimulus interval was reduced in dystonia patients relative to HC during voluntary muscle contraction ($p = 0.02$) (111). The study did not find any significant results for LICI alteration at rest and in the right hemisphere. In another cross-sectional study, Espay et al. compared LICI in psychogenic dystonia, organic dystonia patients, and HC during rest and active muscle contraction.

TABLE 10 | LICI in patients with movement disorders.

References	Subjects	Method	ISI	LICI
Berardelli et al. (109)	20 PD, 11 HC	TMS-EMG	100–250 ms	↑
Tegenthoff et al. (110)	13 HD, 21 HC	TMS-EMG	1–999 ms	Prolonged in classical HD patients
Chen et al. (111)	8 Dystonia, 18 HC	TMS-EMG	20–200 ms	↓ during voluntary contraction, ↔ at rest
Valzania et al. (112)	13 PD, 12 HC	TMS-EMG	40–300 ms	↑
Romeo et al. (113)	10 ET, 8 HC	TMS-EMG	100, 150, 200 ms	↔
Rona et al. (114)	10 Dystonia, 11 HC	TMS-EMG	100–250 ms	↑
Priori et al. (115)	16 HD, 28 HC	TMS-EMG	100–250 ms	↔
Chen et al. (116)	7 HD, 7 HC	TMS-EMG	50–200 ms	↔
Pierantozzi et al. (117)	29 PD, 29 HC	TMS-EMG	20–200 ms	↓, restored following Apomorphine
Cunic et al. (118)	12 PD, 8 HC	TMS-EMG	50–200 ms	↔
Bares et al. (119)	12 PD, 10 HC	TMS-EMG	200–250 ms	↔
Sailer et al. (120)	10 PD, 10 HC	TMS-EMG	100 ms	↔
Espay et al. (121)	18 dystonia, 12 HC	TMS-EMG	50–200 ms	↓
Cantello et al. (122)	18 PD, 12 HC	TMS-EMG	50–300 ms	↑
Fierro et al. (123)	14 PD, 8 HC	TMS-EMG	80 ms	↓ in non-medicated PD patients
Chu et al. (124)	11 PD, 9 HC	TMS-EMG	100, 150 ms	↓
Meunier et al. (125)	17 dystonia, 19 HC	TMS-EMG	90 ms	↔
Barbin et al. (126)	20 PD, 10 HC	TMS-EEG	100 ms	↓ in dyskinetic PD patients
Lu et al. (127)	12 PD, 12 ET, 12 HC	TMS-EEG	100 ms	Comparison not measured
Philpott et al. (128)	28 HD, 17 HC	TMS-EMG	100 ms	↓
Latorre et al. (129)	10 DTS, 7 PWT, 10 ET, 10 HC	TMS-EEG	100 ms	↔ baseline, PAS induced LICI ↓ in ET and HC

ISI, Interstimulus interval; ET, Essential tremor; LICI, Long-interval intracortical inhibition; PWT, Primary writing tremor; PD, Parkinson's Disease; DTS, Dystonic syndrome; HC, Healthy controls; PAS, Paired associative stimulation; HD, Huntington's disease. ↑: increased, ↓: decreased, ↔: no significant difference.

The results indicated that organic dystonia patients had an impaired LICI relative to healthy controls at rest ($p = 0.009$). Psychogenic dystonia patients did not differ significantly from controls at rest. However, psychogenetic dystonia patients demonstrated significantly greater LICI compared to patients with organic dystonia. Results for LICI measured during active muscle contraction were not significant (121). Meunier et al. examined the influence of paired associative stimulation and motor learning on LICI in dystonia patients. It was demonstrated that LICI decreased following learning of simple motor tasks and paired associative stimulation in HC ($p < 0.01$), but both did not have a significant effect in dystonia patients (125). In a cross-sectional study Latorre et al. examined LICI alteration in dystonic syndrome, primary writing tremor and essential tremor patients relative to HC. Baseline LICI was not significantly different across groups but paired associative plasticity induced LICI was significantly decreased in essential tremor patients and HC whereas it did not change in dystonic syndrome and primary writing tremor patients (129).

LICI alteration in Huntington's disease (HD) was investigated by Tegenthoff et al. and the results of their study demonstrated that LICI was prolonged in classical hypotonic-hyperkinetic HD patients relative to HC. In contrast, Westphal variant HD patients had a shortened LICI relative to classical type HD patients ($p < 0.05$) (110). A cross-sectional study by Priori et al. indicated that there were no significant LICI differences across HD patients and HC (115). Philpott et al. compared asymptomatic HD patients, symptomatic HD patients, and HC and found that both patient groups had a significantly impaired LICI relative to controls ($p = 0.02$). In pre-HD patients, LICI deficit was correlated with the number of CAG repeats ($p = 0.01$), and LICI was negatively correlated with behavioral symptoms in both groups (128).

Berardelli et al. examined LICI measures in Parkinson's disease (PD) and the potential impact of L-dopa treatment on LICI. The results revealed that PD patients had an enhanced LICI relative to HC at interstimulus intervals of 150 and 200 ms ($p < 0.05$). Following L-dopa treatment, LICI values were restored approaching healthy subjects ($p = 0.01$) (109). Valzania et al. demonstrated similar findings showing enhanced LICI in PD patients relative to HC at interstimulus intervals of 40, 50, and 75 ms ($p < 0.01$) (112). Chen at al. studied 7 PD patients with Globus Pallidus internus (GPi) stimulators and did not show any significant difference in LICI between PD patients and HC. Additionally, there was no difference in LICI in patients with PD when the GPi stimulator was turned on, off, or to half the amplitude (116). Pierantozzi et al. investigated the effect of apomorphine infusion on LICI in PD patients and demonstrated that baseline LICI was reduced in PD patients relative to HC and

apomorphine infusion enhanced and restored LICI (117). Cunic et al. studied PD patients with subthalamic nucleus stimulators and showed that there was no significant LICI difference between patients and HC at baseline, and stimulation conditions did not affect LICI levels in PD patients (118). In a cross-sectional study, Bares et al. did not find any significant LICI impairment in L-dopa or dopamine agonist naïve PD patients relative to HC (119). Sailer et al. presented similar findings in their study, showing no significant LICI alteration in PD patients relative to HC both in the presence or absence of dopaminergic medications (120). Cantello et al. had contradictory results demonstrating enhanced LICI in PD patients relative to HC in both affected and less affected hemispheres at only 250 ms interstimulus interval (122). Fierro et al. collected LICI measures in PD patients with and without L-dopa treatment and following rTMS. LICI was reduced in patients with PD who were not taking L-dopa relative to those who were taking L-dopa ($p = 0.005$) and HC ($p < 0.016$). LICI improved following rTMS in PD patients without L-dopa ($p < 0.01$), but there was no significant effect of rTMS in PD patients who were taking L-dopa (123). LICI reduction in PD patients both on and off medication relative to HC was demonstrated by Chu et al. at interstimulus intervals of 100–150 ms ($p = 0.035$) (124). Barbin et al. compared dyskinetic PD patients to non-dyskinetic PD patients on and off L-dopa treatment. The results revealed that among medication and unmedicated PD subjects, dyskinetic PD patients had a reduced LICI relative to HC ($p < 0.05$). Conversely, there was no significant difference between non-dyskinetic PD patients and controls. LICI was only significantly different between dyskinetic and non-dyskinetic patients when L-dopa was present ($p < 0.05$) (126). Lu et al. examined the effect of paired associative stimulation (PAS) on LICI in Essential Tremor (ET), PD patients, and HC and demonstrated that PAS induced a reduction in LICI irrespective of group ($p < 0.01$) (127). Patients with essential tremor were investigated by Remeo et al. and there was no significant difference in LICI between the patient group and HC (113).

Studies examining LICI in patients with Parkinson's disease have presented mixed results. Several studies have shown enhanced LICI in the patient population. One suggested mechanism for this difference was larger motor-evoked potentials (MEPs) of conditioning stimulus (109). Conversely, several other studies have shown impairment in LICI, which is consistent with repeated findings of a shorter silent period in patients with Parkinson's disease (16, 130). Decreased MEP facilitation of test stimulus in patients due to increased tonic activity might explain the impairments in LICI (122). Studies have varied in their methodology in terms of the Parkinson's disease treatment and TMS protocol, which might also contribute to the discrepancies in findings. Findings also varied in Huntington's disease some results indicating normal LICI and some showing reduced LICI in HD patients. Inhibition impairments in HD have been shown before and might be attributed to increased excitability and constant preparation for movement (128). Discrepancies between findings could be related to the methodologic issues that might confound the results such as coil type and active contraction vs. resting muscle. In dystonia, studies have shown LICI impairment in dystonic patients compared to healthy controls. Previous studies showing the effectiveness of $GABA_B$ receptor agonist baclofen also support our findings (131, 132).

LICI in Patients With Multiple Sclerosis

Three prior studies examined LICI in the context of Multiple Sclerosis (MS) (**Table 11**). In a cross-sectional study, Mori et al. examined the correlation between disability scores and LICI levels in MS patients, and the study did not result in any significant findings for LICI (133). Nantes et al. compared MS patients with HC and examined the association between LICI and cortical damage measured with MRI. It was demonstrated that LICI did not differ across relapsing-remitting MS patients, progressive MS patients, and HC. Additionally, there was no significant correlation between measures of cortical damage and LICI in MS patients (134). Squintani et al. investigated the role of LICI in the improvement of spastic hypertonia in MS patients following 9-tetrahydrocannabinol and cannabidiol (THC: CBD) oromucosal spray treatment. The results showed that LICI impairment in MS patients relative to HC ($p < 0.05$) significantly improved after THC: CBD treatment for 4 weeks ($p < 0.05$) (135).

Findings have varied with respect to multiple sclerosis. The dysfunctional GABAergic transmission and cortical inhibition in MS patients have been demonstrated in the literature and baclofen, which acts on $GABA_B$ receptors, is known as a reliable agent in treating spasticity, which is a common debilitating symptom in patients with MS (136, 137). The study included in our review presented significant LICI deficit in MS patients with treatment resistant spasticity (135). Therefore, stratified analysis, according to spasticity, might be required to reveal the association between LICI and MS symptoms.

LICI in Patients With Stroke

LICI in stroke patients was studied in 6 studies (**Table 12**). LICI and its evolvement over time were examined in post-stroke patients by Swayne et al. Results demonstrated no significant change in LICI over time measured at 1, 3, and 6 months following stroke. LICI in the affected hemisphere was reduced in the patient group relative to healthy controls ($p = 0.029$), and it was correlated with poorer clinical scores in the acute period and 3 months post-stroke but not at 6 months (138). In a cross-sectional study, Kuppuswamy et al. investigated the association between post-stroke fatigue and LICI and did not demonstrate any significant relation (139). Schambra et al. failed to demonstrate any significant LICI difference across acute and chronic stroke patients and controls (140). In a double-blinded placebo-controlled randomized cross over study, the same group examined the effect of theophylline treatment on LICI in 18 chronic stroke patients. There was no significant LICI change in the theophylline group relative to placebo in chronic stroke patients (141). Mooney et al. compared chronic stroke patients and HC based on LICI and investigated its correlation with GABA concentration measured with magnetic resonance spectroscopy. LICI was found to be enhanced in chronic stroke patients relative to HC in the ipsilesional motor cortex ($p <$

TABLE 11 | LICI in patients with multiple sclerosis.

References	Subjects	Method	ISI	LICI
Mori et al. (133)	89 MS	TMS-EEG	100 ms	Comparison not measured
Nantes et al. (134)	36 MS, 18 HC	TMS-EMG	100 ms	↔
Squintani et al. (135)	19 MS, 19 HC	TMS-EMG	100 ms	↓

ISI, Interstimulus interval; MS, Multiple Sclerosis; LICI, Long-interval intracortical inhibition; HC, Healthy controls. ↓: decreased, ↔: no significant difference.

TABLE 12 | LICI in patients with stroke.

References	Subjects	Method	ISI	LICI
Swayne et al. (138)	10 stroke patients, 10 HC	TMS-EMG	100 ms	↓
Kuppuswamy et al. (139)	70 stroke patients	TMS-EMG	100 ms	Comparison not measured
Schambra et al. (140)	41 stroke patients, 21 HC	TMS-EMG	100 ms	↔
Schambra et al. (141)	18 stroke patients	TMS-EMG	150–250 ms	Comparison not measured
Mooney et al. (142)	12 stroke patients, 16 HC	TMS-EEG	100 ms	↑
Mooney et al. (143)	10 stroke patients, 12 HC	TMS-EMG	100, 150	↑

ISI, Interstimulus interval; HC, Healthy controls; LICI, Long-interval intracortical inhibition. ↑: increased, ↓: decreased, ↔: no significant difference.

0.001), whereas there was no significant association between LICI and metabolite concentrations in stroke patients and HC (142). Another study by the same group confirmed the same finding by demonstrating greater LICI in the ipsilesional motor cortex of chronic stroke patients relative to HC at the ISI of 150 ms and indicated that LICI did not change significantly following motor skill learning task in both chronic stroke patients and HC (143).

Studies have presented mixed results in stroke. Studies that found alterations in LICI discussed the methodological differences (using single ISI vs. using range of ISI) as an explanation for the discrepancy between studies (142). On the other hand, it has been consistently shown that LICI has not changed after interventions. Animal studies demonstrated the importance of $GABA_B$ mediated inhibitory transmission in post-stroke recovery (144). Baclofen was also shown to be effective compared to conventional medical management in increasing quality of life in patients with post-stroke spasticity (145). Stratified analysis of patients, according to spasticity, might reveal differences in LICI between patients with a history of stroke and healthy controls.

LICI in Patients With Traumatic Brain Injury

Most prior studies examining LICI alteration after traumatic brain injury (TBI) focused on the motor cortex and used EMG measures except for one prior TMS-EEG study (**Table 13**). Tremblay et al. investigated LICI in 12 football players with concussion history that occurred more than a year ago and 14 non-concussed players. The findings demonstrated that athletes with concussion history had a significantly enhanced LICI relative to non-concussed ($p = 0.05$) (146). De Beaumont et al. confirmed the same finding showing enhanced LICI in concussed football players ($p < 0.03$), which was found to be correlated with the number of previous concussions ($p < 0.05$) (147). Another study by De Beaumont et al. examined the effect of LICI on synaptic plasticity, measured with paired associative stimulation (PAS) inducing long-term potentiation (LTP)/ long-term depression (LTD) effects in concussed football players and non-concussed control groups. Results indicated enhanced LICI in the concussed group at baseline, which was correlated with suppressed synaptic plasticity ($p = 0.037$) (148). A study including 40 retired concussed Australian football players and 20 HC, presented contradictory results relative to previous findings indicating that concussed athletes had reduced LICI relative to HC ($p > 0.001$). Additionally, reduction in LICI was associated with poorer performance in finer motor dexterity ($p = 0.049$) (149). Tremblay et al. assessed LICI and its association with metabolic disruption after TBI, ^{1}H-MRS. Unlike previous studies, results demonstrated that there was no significant LICI difference in concussed players relative to non-concussed. Nevertheless, GABA levels measured with ^{1}H-MRS were positively correlated with LICI in concussed players ($p = 0.001$) (150). Another study investigating cortical inhibition in concussed football players examined LICI during the acute asymptomatic phase following concussion (1–4 weeks after), and results indicated that there was no significant LICI alteration in concussed players relative to non-concussed (151). Lewis et al. compared retired elite rugby players, community-level rugby players, and non-contact sport players as controls and found that LICI was enhanced in elite players relative to controls, whereas there was no significant difference between community-level players and controls (152). Seeger et al. evaluated children 4-weeks after mild TBI (mTBI), which included 35 symptomatic and 27 asymptomatic subjects, all with mTBI, and 28 HC. Findings indicated that the symptomatic mTBI group had reduced LICI relative to HC, and reduction in LICI was associated with increased post-concussion symptom severity ($p = 0.027, 0.012$). This study was different from previous TBI studies as it contained both female and male subjects, and results demonstrated that females had more pronounced

TABLE 13 | LICI in patients with traumatic brain injury.

References	Subjects	Method	ISI	LICI
Tremblay et al. (146)	12 concussed, 14 HC	TMS-EMG	100 ms	↑
De Beaumont et al. (147)	21 concussed, 15 HC	TMS-EMG	100 ms	↑
De Beaumont et al. (148)	13 concussed, 19 HC	TMS-EMG	100 ms	↑
Pearce et al. (149)	40 concussed, 20 HC	TMS-EMG	100 ms	↓
Tremblay et al. (150)	16 concussed, 14 HC	TMS-EMG	100 ms	↔
Powers et al. (151)	8 concussed, 8 HC	TMS-EMG	100 ms	↔
Lewis et al. (152)	51 concussed, 22 HC 62 with TBI, 22 HC	TMS-EMG	99 ms	↑ in elite players, ↔ in community players ↓ in symptomatic patients
Seeger et al. (153)	25 concussed, 25 HC	TMS-EMG	100 ms	↓
Pearce et al. (154)	20 PCS, 20 recovered concussed, 20 HC	TMS-EMG	100 ms	↑ in PCS patients, ↔ in recovered patients
Pearce et al. (155)	17 TBI, 15 HC	TMS-EMG	100 ms	↑ measured with EMG, ↔ measured with EEG
Opie et al. (156)	78 PPCS, 29 asymptomatic TBI, 26 HC	TMS-EEG	100 ms	↔
King et al. (157)	12 concussed, 14 HC	TMS-EMG	100 ms	↑

ISI, Interstimulus interval; TBI, traumatic brain injury; LICI, Long-interval intracortical inhibition; PCS, Post-concussion syndrome; HC, Healthy controls; PPCS, Persistent post-concussive symptoms. ↑: increased, ↓: decreased, ↔: no significant difference.

TABLE 14 | LICI in patients with other neurologic disorders.

References	Subjects	Method	ISI	LICI
Salerno et al. (159)	21 ALS, 12 HC	TMS-EMG	55–255 ms	↓
Zanette et al. (160)	35 ALS, HC	TMS-EMG	50–300 ms	↓
Tamburin et al. (161)	8 cerebellar syndrome, 14 HC	TMS-EMG	30–500 ms	↑
Kang et al. (162)	12 PKD, 10 HC	TMS-EMG	80 ms	↓
Siniatchkin et al. (163)	16 migraine, 15 HC	TMS-EEG	60–120 ms	↔
Canafoglia et al. (164)	10 ULD, 5 LBD, 16 HC	TMS-EMG	30–100 ms	↓ in LBD patients
Cosentino et al. (165)	24 migraine, 24 HC	TMS-EMG	100 ms	Comparison not measured

ISI, Interstimulus interval; PKD, Paroxysmal kinesigenic dyskinesia; LICI, Long-interval intracortical inhibition; ULD, Unverricht-Lundborg Disease (ULD); ALS, Amyotrophic lateral sclerosis; LBD, Lafora body disease; HC, Healthy controls. ↑: increased, ↓: decreased, ↔: no significant difference.

LICI ($p = -0.016$) (153). A cross-sectional study by Pearce et al. showed reduced LICI in concussed rugby players, 15–21 years after the injury, relative to HC, and LICI alteration was associated with slower motor dexterity ($p = 0.03$, $p < 0.01$) (154). In another study by Pearce et al. LICI alteration in post-concussion syndrome (PCS) was investigated evaluating 20 concussed subjects with PCS, 20 asymptomatic subjects with a history of concussion, and 20 HC. Results indicated that LICI was enhanced in the PCS group relative to recovered subjects and controls ($p < 0.001$); furthermore, worsened fatigue and poorer amplitude discrimination was associated with altered LICI ($p < 0.001$, 0.02) (155). A prospective cohort study by King et al. involving 78 children with persistent post-concussive symptoms, 29 asymptomatic with TBI history, and 26 age and gender-matched HC, examined LICI alteration 1 and 2 months post-injury and its association with the persistence of symptoms. It was shown that LICI did not differ across groups at 1 and 2 months post-injury; likewise, it did not significantly change over time (157). Opie et al. examined LICI in the motor cortex of adult subjects with history of mTBI and HC using both EMG and EEG. Results demonstrated that LICI measured with EMG was enhanced in subjects with a history of mTBI relative to healthy controls ($p < 0.0001$) whereas TMS-EEG measures for LICI did not significantly differ across groups (156).

The majority of the studies have shown enhanced LICI in groups with a history of concussion compared to healthy controls or non-concussed athletes. However, several studies showed reduction in LICI in patients with a history of concussion. Authors discussed that the etiology of the trauma (American football vs. Australian football), number of concussions, and severity of the injury might be confounding the results (149). Excessive GABAergic activity that occurs after a concussion is thought to be a protective mechanism against the excessive

glutamatergic activity, which is thought to be an initial response to brain injury (146). Nevertheless, animal studies pointed out that excess GABAergic inhibition might be responsible for TBI instead (158). Therefore, regardless of the timeline after the trauma, excessive GABAergic activity seemed to be associated with TBI.

LICI in Patients With Other Neurological Disorders

Two prior studies examined LICI paradigms in patients with Amyotrophic Lateral Sclerosis (ALS). Salerno et al. demonstrated that LICI was reduced in bulbar ALS ($p = 0.01$) and spinal ALS ($p = 0.02$) relative to HC at the ISI of 155 ms (159) (**Table 14**). However, the difference between the two ALS groups was not significant. Zanette et al. confirmed the same results showing reduced LICI in ALS patients ($p < 0.01$), specifically in those with upper motor neuron involvement ($p < 0.05$) (160). Tamburin et al. studied ataxic patients with pure cerebellar syndrome and demonstrated that LICI was enhanced in the patient group relative to HC at ISI of 200–500 ms ($p = 0.007$) (161). In a cross-sectional study, Kang et al. revealed that LICI was reduced in drug naïve paroxysmal kinesigenic dyskinesia patients relative to HC (162). Patients with migraines were studied by Siniatchkin et al. and results showed no significant LICI alteration in migraine without aura patients (163). Cosentino et al. indicated that there was a correlation between impaired LICI measured with test stimulus of 150% resting motor threshold and increased migraine disease duration (165). Canafoglia et al. investigated LICI in genetically different progressive myoclonus epilepsy syndromes. They found that LICI was significantly impaired in Lafora Body Disease (LBD) relative to HC at ISI of 80–100 ms, but the LICI difference between LBD and Unverricht-Lundborg Disease was not significant (164).

DISCUSSION

The search for biomarkers in neuropsychiatric disorders spans several decades and arguably has progressed slower for psychiatric disorders as compared to neurological disorders. The interest for ongoing research in neuropsychiatric biomarkers is catalyzed by concern for poor clinical outcomes, enhanced diagnostics, and interventional development. Descriptive diagnostic approaches to psychiatric disorders are necessary clinical realities that often fail to provide valid neurophysiological constructs of disease. In general, psychiatric research is plagued by variable methodologies, meager effect sizes, and limited replications.

This was the first systematic review of LICI as a putative biomarker in neuropsychiatric disorders. Broadly, present LICI findings are somewhat mixed and not disease specific. Impairments of LICI have been demonstrated in ADHD, depression, schizophrenia, epilepsy, ALS, and dementia. There were mixed and inconsistent findings in bipolar disorder, neurodevelopment disorders, substance use disorders, multiple sclerosis, stroke, and TBI. Among the studies, LICI has been investigated as a diagnostic and prognostic biomarker, a predictor of treatment response, and a marker of symptom severity. Few studies investigated the reproducibility of LICI. It is also important to highlight that many of the studies focused on bipolar disorder, depression, schizophrenia, dementia, epilepsy, and TBI had overlapping samples among separate manuscripts (36, 37, 39–42, 57, 79, 80, 85, 97, 99). This creates additional challenges in considering the validity, reliability, and synthesis of existing neuropsychiatric LICI literature.

Impairment in LICI in neuropsychiatric diseases has been mostly demonstrated in the direction of reduced cortical inhibition, however, increased cortical inhibition (increased LICI) has also been shown, especially in bipolar disorder, TBI, and Parkinson's disease. It is possible that the disruption of the networks directly associated with the inhibitory GABAergic activity results in reduced LICI whereas, an insult to the networks associated with increased excitatory activity leads to a compensatory increase in GABAergic activity resulting in increased cortical inhibition (increased LICI). Even though there is not sufficient evidence to suggest whether the disruption of inhibitory/excitatory balance in neuropsychiatric disorders is state or trait dependent, several studies have shown restoration of LICI following symptoms remission (93, 155). It is important to highlight a substantial limitation of the present review. A number of studies that were included examined the response to paired-pulse stimulation with ISIs of 200–300 ms and were referred to as LICI. However, work by Cash et al. suggests that stimulation with ISIs at these durations produces a period of late cortical disinhibition that is distinct from LICI (166). These studies were included as the intent was to provide and exhaustive review of prior work with LICI and many of the studies included measurements with ISIs above and below 200 ms. This is an important confound in interpreting the results and could explain some of the broad discrepant findings.

Broadly, TMS-EMG and TMS-EEG measures of LICI are appealing from a practical standpoint. Cortical inhibition measures with TMS are relatively inexpensive, easy to collect, straight forward to analyze, and have demonstrated high test-retest reliability. The prior work focused on LICI has important methodologic limitations to consider for future studies. Medication regimens in clinical populations must be carefully considered with respect to both safety and as confounds. These factors must be characterized and accounted for in future research. When ethically and pragmatically feasible, medicated and unmedicated patient populations should be tested. Disease progression or staging should be carefully described in future studies. Methodology to standardize TMS coil orientation and stimulus intensity is an important future consideration. Electrical field modeling and stereotactic neuronavigation are invaluable tools in establishing reliable study protocols. Further considerations include an online inspection of MEP or TMS-evoked potential data to monitor for artifact and signal-to-noise ratio. Standardized pre-processing and post-processing methodology with detailed published descriptions are additional considerations. Studies with TMS-EEG present unique challenges as recent work has advocated for careful peripheral sensory controls as peripheral effects may have presented confounds in prior TMS-EEG work. Experts have advocated for standardized approaches, the methodology that controls for peripheral effects, and data sharing.

CONCLUSION

Current studies with LICI have methodologic weaknesses and discordant findings. Future study, with rigorous methodology is needed to develop LICI paradigms for risk assessment, screening, diagnosis, prognosis, and monitoring treatment effects in neuropsychiatric disorders. With further work, measures of LICI could be rapidly translated into clinical settings.

DATA AVAILABILITY STATEMENT

The original contributions presented in the study are included in the article/**Supplementary Material**, further inquiries can be directed to the corresponding author/s.

AUTHOR CONTRIBUTIONS

All authors made contributions to the conception and design of the study, assisted with the acquisition and review of articles, contributed to the interpretation of findings, drafted the article, assisted with revisions, and approved the final version of the manuscript prior to submission.

FUNDING

The research reported in this publication was supported by the National Institutes of Health (NIH) awards R01 MH113700 and R01 MH124655. FF was supported by Michael Smith Foundation for Health Research Scholar Award (Award No. 17727), Natural Sciences and Engineering Research Council (RGPIN-05783), and CIHR (Funding Reference No. 165863). The supporters had no role in the design, analysis, interpretation, or publication of the study.

SUPPLEMENTARY MATERIAL

The Supplementary Material for this article can be found online at: https://www.frontiersin.org/articles/10.3389/fpsyt.2021.678088/full#supplementary-material

REFERENCES

1. Krnjevic K. Role of GABA in cerebral cortex. *Can J Physiol Pharmacol.* (1997) 75:439–51.
2. DeFelipe J, Fariñas I. The pyramidal neuron of the cerebral cortex: morphological and chemical characteristics of the synaptic inputs. *Progr Neurobiol.* (1992) 39:563–607.
3. Daskalakis ZJ, Fitzgerald PB, Christensen BK. The role of cortical inhibition in the pathophysiology and treatment of schizophrenia. *Brain Res Rev.* (2007) 56:427–42. doi: 10.1016/j.brainresrev.2007.09.006
4. Krystal JH, Sanacora G, Blumberg H, Anand A, Charney DS, Marek G, et al. Glutamate and GABA systems as targets for novel antidepressant and mood-stabilizing treatments. *Mol Psychiatry.* (2002) 7:S71–80. doi: 10.1038/sj.mp.4001021
5. Benes FM, McSparren J, Bird ED, SanGiovanni JP, Vincent SL. Deficits in small interneurons in prefrontal and cingulate cortices of schizophrenic and schizoaffective patients. *Arch Gen Psychiatry.* (1991) 48:996–1001. doi: 10.1001/archpsyc.1991.01810350036005
6. Kalueff AV, Nutt DJ. Role of GABA in anxiety and depression. *Depress Anxiety.* (2007) 24:495–517. doi: 10.1002/da.20262
7. Edden RAE, Crocetti D, Zhu H, Gilbert DL, Mostofsky SH. Reduced GABA concentration in attention-deficit/hyperactivity disorder. *Arch Gen Psychiatry.* (2012) 69:750–3. doi: 10.1001/archgenpsychiatry.2011.2280
8. Schür RR, Draisma LW, Wijnen JP, Boks MP, Koevoets MG, Joëls M, et al. Brain GABA levels across psychiatric disorders: a systematic literature review and meta-analysis of (1) H-MRS studies. *Hum Brain Mapp.* (2016) 37:3337–52. doi: 10.1002/hbm.23244
9. Treiman DM. GABAergic mechanisms in epilepsy. *Epilepsia.* (2001) 42:8–12. doi: 10.1046/j.1528-1157.2001.042suppl.3008.x
10. Boecker H. Imaging the role of GABA in movement disorders. *Curr Neurol Neurosci Rep.* (2013) 13:385. doi: 10.1007/s11910-013-0385-9
11. Davalos A, Leira R, Serena J, Castellanos M, Aneiros A, Castillo J. The role of gama aminobutyric acid (GABA) in acute ischemic stroke. *Stroke.* (2001) 32:370. doi: 10.1161/str.32.suppl_1.370-b
12. Sanacora G, Mason GF, Krystal JH. Impairment of GABAergic transmission in depression: new insights from neuroimaging studies. *Crit Rev Neurobiol.* (2000) 14:23–45. doi: 10.1615/critrevneurobiol.v14.i1.20
13. Luscher B, Shen Q, Sahir N. The GABAergic deficit hypothesis of major depressive disorder. *Mol Psychiatry.* (2011) 16:383–406. doi: 10.1038/mp.2010.120
14. Radhu N, de Jesus DR, Ravindran LN, Zanjani A, Fitzgerald PB, Daskalakis ZJ. A meta-analysis of cortical inhibition and excitability using transcranial magnetic stimulation in psychiatric disorders. *Clin Neurophysiol.* (2013) 124:1309–20. doi: 10.1016/j.clinph.2013.01.014
15. Barker AT, Jalinous R, Freeston IL. Non-invasive magnetic stimulation of human motor cortex. *Lancet.* (1985) 325:1106–7.
16. Cantello R, Gianelli M, Civardi C, Mutani R. Magnetic brain stimulation: the silent period after the motor evoked potential. *Neurology.* (1992) 42:1951–9. doi: 10.1212/wnl.42.10.1951
17. Nakamura H, Kitagawa H, Kawaguchi Y, Tsuji H. Intracortical facilitation and inhibition after transcranial magnetic stimulation in conscious humans. *J Physiol.* (1997) 498 (Pt. 3):817–23. doi: 10.1113/jphysiol.1997.sp021905
18. van der Kamp W, Zwinderman AH, Ferrari MD, van Dijk JG. Cortical excitability and response variability of transcranial magnetic stimulation. *J Clin Neurophysiol.* (1996) 13:164–71. doi: 10.1097/00004691-199603000-00007
19. Kujirai T, Caramia MD, Rothwell JC, Day BL, Thompson PD, Ferbert A, et al. Corticocortical inhibition in human motor cortex. *J Physiol.* (1993) 471:501–19. doi: 10.1113/jphysiol.1993.sp019912
20. Valls-Solé J, Pascual-Leone A, Wassermann EM, Hallett M. Human motor evoked responses to paired transcranial magnetic stimuli. *Electroencephalogr Clin Neurophysiol.* (1992) 85:355–64. doi: 10.1016/0168-5597(92)90048-g
21. Fitzgerald PB, Brown TL, Daskalakis ZJ. The application of transcranial magnetic stimulation in psychiatry and neurosciences research. *Acta Psychiatr Scand.* (2002) 105:324–40. doi: 10.1034/j.1600-0447.2002.1r179.x
22. Daskalakis ZJ, Farzan F, Barr MS, Maller JJ, Chen R, Fitzgerald PB. Long-Interval cortical inhibition from the dorsolateral prefrontal cortex: a TMS–EEG study. *Neuropsychopharmacology.* (2008) 33:2860–9. doi: 10.1038/npp.2008.22
23. Noda Y. Toward the establishment of neurophysiological indicators for neuropsychiatric disorders using transcranial magnetic stimulation-evoked potentials: a systematic review. *Psychiatry Clin Neurosci.* (2020) 74:12–34. doi: 10.1111/pcn.12936
24. Florian J, Müller-Dahlhaus M, Liu Y, Ziemann U. Inhibitory circuits and the nature of their interactions in the human motor cortex a pharmacological TMS study. *J Physiol.* (2008) 586:495–514. doi: 10.1113/jphysiol.2007.142059
25. McCormick DA. GABA as an inhibitory neurotransmitter in human cerebral cortex. *J Neurophysiol.* (1989) 62:1018–27. doi: 10.1152/jn.1989.62.5.1018
26. McDonnell MN, Orekhov Y, Ziemann U. The role of GABAB receptors in intracortical inhibition in the human motor cortex. *Exp Brain Res.* (2006) 173:86–93. doi: 10.1007/s00221-006-0365-2

27. Werhahn KJ, Kunesch E, Noachtar S, Benecke R, Classen J. Differential effects on motorcortical inhibition induced by blockade of GABA uptake in humans. *J Physiol.* (1999) 517 (Pt. 2):591–7. doi: 10.1111/j.1469-7793.1999.0591t.x
28. Pierantozzi M, Marciani MG, Palmieri MG, Brusa L, Galati S, Caramia MD, et al. Effect of vigabatrin on motor responses to transcranial magnetic stimulation: an effective tool to investigate *in vivo* GABAergic cortical inhibition in humans. *Brain Res.* (2004) 1028:1–8. doi: 10.1016/j.brainres.2004.06.009
29. Sanger TD, Garg RR, Chen R. Interactions between two different inhibitory systems in the human motor cortex. *J Physiol.* (2001) 530:307–17. doi: 10.1111/j.1469-7793.2001.0307l.x
30. Association AP. *Diagnostic and Statistical Manual of Mental Disorders (DSM-5®)*. Arlington, TX: American Psychiatric Pub (2013).
31. Moher D, Liberati A, Tetzlaff J, Altman DG, Group P. Preferred reporting items for systematic reviews and meta-analyses: the PRISMA statement. *PLoS Med.* (2009) 6:e1000097. doi: 10.1371/journal.pmed.1000097
32. Page MJ, McKenzie JE, Bossuyt PM, Boutron I, Hoffmann TC, Mulrow CD, et al. The PRISMA 2020 statement: an updated guideline for reporting systematic reviews. *BMJ.* (2021) 372:n71. doi: 10.1136/bmj.n71
33. Buchmann J, Gierow W, Weber S, Hoeppner J, Klauer T, Benecke R, et al. Restoration of disturbed intracortical motor inhibition and facilitation in attention deficit hyperactivity disorder children by methylphenidate. *Biol Psychiatry.* (2007) 62:963–9. doi: 10.1016/j.biopsych.2007.05.010
34. Hoeppner J, Neumeyer M, Wandschneider R, Herpertz SC, Gierow W, Haessler F, et al. Intracortical motor inhibition and facilitation in adults with attention deficit/hyperactivity disorder. *J Neural Transm.* (2008) 115:1701–7. doi: 10.1007/s00702-008-0091-y
35. Ruiz-Veguilla M, Martín-Rodríguez JF, Palomar FJ, Porcacchia P, Álvarez de Toledo P, Perona-Garcelán S, et al. Trait- and state-dependent cortical inhibitory deficits in bipolar disorder. *Bipolar Disord.* (2016) 18:261–71. doi: 10.1111/bdi.12382
36. Basavaraju R, Sanjay TN, Mehta UM, Muralidharan K, Thirthalli J. Cortical inhibition in symptomatic and remitted mania compared to healthy subjects: a cross-sectional study. *Bipolar Disord.* (2017) 19:698–703. doi: 10.1111/bdi.12546
37. Basavaraju R, Mehta UM, Pascual-Leone A, Thirthalli J. Elevated mirror neuron system activity in bipolar mania: evidence from a transcranial magnetic stimulation study. *Bipolar Disord.* (2019) 21:259–69. doi: 10.1111/bdi.12723
38. Brady RO Jr, McCarthy JM, Prescot AP, Jensen JE, Cooper AJ, et al. Brain gamma-aminobutyric acid (GABA) abnormalities in bipolar disorder. *Bipolar Disord.* (2013) 15:434–9. doi: 10.1111/bdi.12074
39. Croarkin PE, Nakonezny PA, Husain MM, Port JD, Melton T, Kennard BD, et al. Evidence for pretreatment LICI deficits among depressed children and adolescents with nonresponse to fluoxetine. *Brain Stimul.* (2014) 7:243–51. doi: 10.1016/j.brs.2013.11.006
40. Croarkin PE, Nakonezny PA, Lewis CP, Zaccariello MJ, Huxsahl JE, Husain MM, et al. Developmental aspects of cortical excitability and inhibition in depressed and healthy youth: an exploratory study. *Front Hum Neurosci.* (2014) 8:669. doi: 10.3389/fnhum.2014.00669
41. Sun Y, Farzan F, Mulsant BH, Rajji TK, Fitzgerald PB, Barr MS, et al. Indicators for remission of suicidal ideation following magnetic seizure therapy in patients with treatment-resistant depression. *JAMA Psychiatry.* (2016) 73:337–45. doi: 10.1001/jamapsychiatry.2015.3097
42. Sun Y, Blumberger DM, Mulsant BH, Rajji TK, Fitzgerald PB, Barr MS, et al. Magnetic seizure therapy reduces suicidal ideation and produces neuroplasticity in treatment-resistant depression. *Transl Psychiatry.* (2018) 8:253. doi: 10.1038/s41398-018-0302-8
43. Lewis CP, Nakonezny PA, Blacker CJ, Vande Voort JL, Port JD, Worrell GA, et al. Cortical inhibitory markers of lifetime suicidal behavior in depressed adolescents. *Neuropsychopharmacology.* (2018) 43:1822–31. doi: 10.1038/s41386-018-0040-x
44. Jeng JS, Li CT, Lin HC, Tsai SJ, Bai YM, Su TP, et al. Antidepressant-resistant depression is characterized by reduced short- and long-interval cortical inhibition. *Psychol Med.* (2019) 50:1285–91. doi: 10.1017/s0033291719001223
45. Lewis CP, Camsari DD, Sonmez AI, Nandakumar AL, Gresbrink MA, Daskalakis ZJ, et al. Preliminary evidence of an association between increased cortical inhibition and reduced suicidal ideation in adolescents treated for major depression. *J Affect Disord.* (2019) 244:21–4. doi: 10.1016/j.jad.2018.09.079
46. Balzekas I, Lewis CP, Shekunov J, Port JD, Worrell GA, Joon Jo H, et al. A pilot study of GABA(B) correlates with resting-state functional connectivity in five depressed female adolescents. *Psychiatry Res Neuroimaging.* (2018) 279:60–3. doi: 10.1016/j.pscychresns.2018.05.013
47. Doruk Camsari D, Lewis CP, Sonmez AI, Nandakumar AL, Gresbrink MA, Daskalakis ZJ, et al. Transcranial magnetic stimulation markers of antidepressant treatment in adolescents with major depressive disorder. *Int J Neuropsychopharmacol.* (2019) 22:435–44. doi: 10.1093/ijnp/pyz021
48. Lissemore JI, Bhandari A, Mulsant BH, Lenze EJ, Reynolds CF 3rd, Karp JF, et al. Reduced GABAergic cortical inhibition in aging and depression. *Neuropsychopharmacology.* (2018) 43:2277–84. doi: 10.1038/s41386-018-0093-x
49. Pan LA, Batezati-Alves SC, Almeida JR, Segreti A, Akkal D, Hassel S, et al. Dissociable patterns of neural activity during response inhibition in depressed adolescents with and without suicidal behavior. *J Am Acad Child Adolesc Psychiatry.* (2011) 50:602–11.e603. doi: 10.1016/j.jaac.2011.03.018
50. Zhao J, Verwer RWH, Gao SF, Qi XR, Lucassen PJ, Kessels HW, et al. Prefrontal alterations in GABAergic and glutamatergic gene expression in relation to depression and suicide. *J Psychiatr Res.* (2018) 102:261–74. doi: 10.1016/j.jpsychires.2018.04.020
51. Oberman L, Ifert-Miller F, Najib U, Bashir S, Woollacott I, Gonzalez-Heydrich J, et al. Transcranial magnetic stimulation provides means to assess cortical plasticity and excitability in humans with fragile x syndrome and autism spectrum disorder. *Front Synapt Neurosci.* (2010) 2:26. doi: 10.3389/fnsyn.2010.00026
52. Enticott PG, Kennedy HA, Rinehart NJ, Tonge BJ, Bradshaw JL, Fitzgerald PB. GABAergic activity in autism spectrum disorders: an investigation of cortical inhibition via transcranial magnetic stimulation. *Neuropharmacology.* (2013) 68:202–9. doi: 10.1016/j.neuropharm.2012.06.017
53. Morin-Parent F, Champigny C, Lacroix A, Corbin F, Lepage J-F. Hyperexcitability and impaired intracortical inhibition in patients with fragile-X syndrome. *Transl Psychiatry.* (2019) 9:312. doi: 10.1038/s41398-019-0650-z
54. Bernardo P, Cobb S, Coppola A, Tomasevic L, Di Lazzaro V, Bravaccio C, et al. Neurophysiological signatures of motor impairment in patients with rett syndrome. *Ann Neurol.* (2020) 87:763–73. doi: 10.1002/ana.25712
55. Fitzgerald PB, Brown TL, Marston NA, Oxley TJ, de Castella A, Daskalakis ZJ, et al. A transcranial magnetic stimulation study of abnormal cortical inhibition in schizophrenia. *Psychiatry Res.* (2003) 118:197–207. doi: 10.1016/s0165-1781(03)00094-5
56. Farzan F, Barr MS, Levinson AJ, Chen R, Wong W, Fitzgerald PB, et al. Evidence for gamma inhibition deficits in the dorsolateral prefrontal cortex of patients with schizophrenia. *Brain.* (2010) 133:1505–14. doi: 10.1093/brain/awq046
57. Mehta UM, Thirthalli J, Basavaraju R, Gangadhar BN. Association of intracortical inhibition with social cognition deficits in schizophrenia: findings from a transcranial magnetic stimulation study. *Schizophr Res.* (2014) 158:146–50. doi: 10.1016/j.schres.2014.06.043
58. Mehta UM, Thirthalli J, Basavaraju R, Gangadhar BN, Pascual-Leone A. Reduced mirror neuron activity in schizophrenia and its association with theory of mind deficits: evidence from a transcranial magnetic stimulation study. *Schizophr Bull.* (2014) 40:1083–94. doi: 10.1093/schbul/sbt155
59. Radhu N, Garcia Dominguez L, Farzan F, Richter MA, Semeralul MO, Chen R, et al. Evidence for inhibitory deficits in the prefrontal cortex in schizophrenia. *Brain.* (2015) 138:483–97. doi: 10.1093/brain/awu360
60. Basavaraju R, Mehta UM, Thirthalli J, Gangadhar BN. Mirror neuron dysfunction and ego-boundary disturbances in schizophrenia: a transcranial magnetic stimulation study. *Indian J Psychol Med.* (2015) 37:58–65. doi: 10.4103/0253-7176.150821
61. Lett TA, Kennedy JL, Radhu N, Dominguez LG, Chakravarty MM, Nazeri A, et al. Prefrontal white matter structure mediates the influence of

GAD1 on working memory. *Neuropsychopharmacology.* (2016) 41:2224–31. doi: 10.1038/npp.2016.14
62. Radhu N, Dominguez LG, Greenwood TA, Farzan F, Semeralul MO, Richter MA, et al. Investigating cortical inhibition in first-degree relatives and probands in schizophrenia. *Sci Rep.* (2017) 7:43629. doi: 10.1038/srep43629
63. Goodman MS, Bridgman AC, Rabin RA, Blumberger DM, Rajji TK, Daskalakis ZJ, et al. Differential effects of cannabis dependence on cortical inhibition in patients with schizophrenia and non-psychiatric controls. *Brain Stimul.* (2017) 10:275–82. doi: 10.1016/j.brs.2016.11.004
64. Daskalakis ZJ, Farzan F, Barr MS, Rusjan PM, Favalli G, Levinson AJ, et al. Evaluating the relationship between long interval cortical inhibition, working memory and gamma band activity in the dorsolateral prefrontal cortex. *Clin EEG Neurosci.* (2008) 39:150–5. doi: 10.1177/155005940803900310
65. Potkin SG, Turner JA, Brown GG, McCarthy G, Greve DN, Glover GH, et al. Working memory and DLPFC inefficiency in schizophrenia: the FBIRN study. *Schizophr Bull.* (2009) 35:19–31. doi: 10.1093/schbul/sbn162
66. Sundaresan K, Ziemann U, Stanley J, Boutros N. Cortical inhibition and excitation in abstinent cocaine-dependent patients: a transcranial magnetic stimulation study. *Neuroreport.* (2007) 18:289–92. doi: 10.1097/WNR.0b013e3280143cf0
67. Lang N, Hasan A, Sueske E, Paulus W, Nitsche MA. Cortical hypoexcitability in chronic smokers? A transcranial magnetic stimulation study. *Neuropsychopharmacology.* (2008) 33:2517–23. doi: 10.1038/sj.npp.1301645
68. Fitzgerald PB, Williams S, Daskalakis ZJ. A transcranial magnetic stimulation study of the effects of cannabis use on motor cortical inhibition and excitability. *Neuropsychopharmacology.* (2009) 34:2368–75. doi: 10.1038/npp.2009.71
69. Gjini K, Ziemann U, Napier TC, Boutros N. Dysbalance of cortical inhibition and excitation in abstinent cocaine-dependent patients. *J Psychiatr Res.* (2012) 46:248–55. doi: 10.1016/j.jpsychires.2011.10.006
70. Naim-Feil J, Bradshaw JL, Rogasch NC, Daskalakis ZJ, Sheppard DM, Lubman DI, et al. Cortical inhibition within motor and frontal regions in alcohol dependence post-detoxification: a pilot TMS-EEG study. *World J Biol Psychiatry.* (2016) 17:547–56. doi: 10.3109/15622975.2015.1066512
71. Kushner SA, Unterwald EM. Chronic cocaine administration decreases the functional coupling of GABAB receptors in the rat ventral tegmental area as measured by baclofen-stimulated 35S-GTPγS binding. *Life sciences.* (2001) 69:1093–102. doi: 10.1016/s0024-3205(01)01203-6
72. Frankowska M, Wydra K, Faron-Gorecka A, Zaniewska M, Kusmider M, Dziedzicka-Wasylewska M, et al. Neuroadaptive changes in the rat brain GABA(B) receptors after withdrawal from cocaine self-administration. *Eur J Pharmacol.* (2008) 599:58–64. doi: 10.1016/j.ejphar.2008.09.018
73. Brebner K, Childress AR, Roberts DC. A potential role for GABA(B) agonists in the treatment of psychostimulant addiction. *Alcohol Alcohol.* (2002) 37:478–84. doi: 10.1093/alcalc/37.5.478
74. Sofuoglu M, Kosten TR. Novel approaches to the treatment of cocaine addiction. *CNS Drugs.* (2005) 19:13–25. doi: 10.2165/00023210-200519010-00002
75. Hoppenbrouwers SS, De Jesus DR, Stirpe T, Fitzgerald PB, Voineskos AN, Schutter DJ, et al. Inhibitory deficits in the dorsolateral prefrontal cortex in psychopathic offenders. *Cortex.* (2013) 49:1377–85. doi: 10.1016/j.cortex.2012.06.003
76. Salas RE, Galea JM, Gamaldo AA, Gamaldo CE, Allen RP, Smith MT, et al. Increased use-dependent plasticity in chronic insomnia. *Sleep.* (2014) 37:535–44. doi: 10.5665/sleep.3492
77. Li CT, Lu CF, Lin HC, Huang YZ, Juan CH, Su TP, et al. Cortical inhibitory and excitatory function in drug-naive generalized anxiety disorder. *Brain Stimul.* (2017) 10:604–8. doi: 10.1016/j.brs.2016.12.007
78. Brem A-K, Atkinson N, Seligson E, Pascual-Leone A. Differential pharmacological effects on brain reactivity and plasticity in Alzheimer's disease. *Front Psychiatry.* (2013) 4:124. doi: 10.3389/fpsyt.2013.00124
79. Benussi A, Cosseddu M, Filareto I, Dell'Era V, Archetti S, Cotelli MS, et al. Impaired LTP-like cortical plasticity and intra-cortical facilitation in presymptomatic FTLD mutation carriers. *J Neurochem.* (2016) 138 (Suppl. 1):308. doi: 10.1002/ana.24731
80. Benussi A, Di Lorenzo F, Dell'Era V, Cosseddu M, Alberici A, Caratozzolo S, et al. Transcranial magnetic stimulation distinguishes Alzheimer disease from frontotemporal dementia. *Neurology.* (2017) 89:665–72. doi: 10.1212/wnl.0000000000004232
81. Fried PJ, Jannati A, Davila-Pérez P, Pascual-Leone A. Reproducibility of single-pulse, paired-pulse, and intermittent theta-burst TMS measures in healthy aging, type-2 diabetes, and alzheimer's disease. *Front Aging Neurosci.* (2017) 9:263. doi: 10.3389/fnagi.2017.00263
82. Benussi A, Gazzina S, Premi E, Cosseddu M, Archetti S, Dell'Era V, et al. Clinical and biomarker changes in presymptomatic genetic frontotemporal dementia. *Neurobiology of Aging.* (2019) 76:133–140. doi: 10.1016/j.neurobiolaging.2018.12.018
83. Assogna M, Casula EP, Borghi I, Bonnì S, Samà D, Motta C, et al. Effects of palmitoylethanolamide combined with luteoline on frontal lobe functions, high frequency oscillations, and GABAergic transmission in patients with frontotemporal dementia. *J Alzheimers Dis.* (2020) 76:1297–308. doi: 10.3233/jad-200426
84. Benussi A, Dell'Era V, Cantoni V, Cotelli MS, Cosseddu M, Spallazzi M, et al. Neurophysiological correlates of positive and negative symptoms in frontotemporal dementia. *J Alzheimers Dis.* (2020) 73:1133–42. doi: 10.3233/JAD-190986
85. Benussi A, Dell'Era V, Cantoni V, Cotelli MS, Cosseddu M, Spallazzi M, et al. TMS for staging and predicting functional decline in frontotemporal dementia. *Brain Stimul.* (2020) 13:386–92. doi: 10.1016/j.brs.2019.11.009
86. Benussi A, Premi E, Gazzina S, Cantoni V, Cotelli MS, Giunta M, et al. Neurotransmitter imbalance dysregulates brain dynamic fluidity in frontotemporal degeneration. *Neurobiol Aging.* (2020) 94:176–84. doi: 10.1016/j.neurobiolaging.2020.05.017
87. Li Y, Sun H, Chen Z, Xu H, Bu G, Zheng H. Implications of GABAergic neurotransmission in alzheimer's disease. *Front Aging Neurosci.* (2016) 8:31. doi: 10.3389/fnagi.2016.00031
88. Brodtmann A, Macdonell RA, Gilligan A, Curatolo J, Berkovic SF. Cortical excitability and recovery curve analysis in generalized epilepsy. *Neurology.* (1999) 53:1347.
89. Valzania F, Strafella A, Tropeani A, Rubboli G, Nassetti S, Tassinari C. Facilitation of rhythmic events in progressive myoclonus epilepsy: a transcranial magnetic stimulation study. *Clin Neurophysiol.* (1999) 110:152–7.
90. Manganotti P, Bongiovanni LG, Zanette G, Fiaschi A. Early and late intracortical inhibition in juvenile myoclonic epilepsy. *Epilepsia.* (2000) 41:1129–38. doi: 10.1111/j.1528-1157.2000.tb00318.x
91. Molnar G, Sailer A, Gunraj C, Cunic D, Wennberg R, Lozano A, et al. Changes in motor cortex excitability with stimulation of anterior thalamus in epilepsy. *Neurology.* (2006) 66:566–71. doi: 10.1212/01.wnl.0000198254.08581.6b
92. Badawy RA, Curatolo JM, Newton M, Berkovic SF, Macdonell RA. Changes in cortical excitability differentiate generalized and focal epilepsy. *Ann Neurol.* (2007) 61:324–31. doi: 10.1002/ana.21087
93. Badawy RA, Macdonell RA, Berkovic SF, Newton MR, Jackson GD. Predicting seizure control: cortical excitability and antiepileptic medication. *Ann Neurol.* (2010) 67:64–73. doi: 10.1002/ana.21806
94. Badawy RA, Jackson GD. Cortical excitability in migraine and epilepsy: a common feature? *J Clin Neurophysiol.* (2012) 29:244–9. doi: 10.1097/WNP.0b013e3182570fee
95. Badawy RA, Jackson GD, Berkovic SF, Macdonell RA. Inter-session repeatability of cortical excitability measurements in patients with epilepsy. *Epilepsy Res.* (2012) 98:182–6. doi: 10.1016/j.eplepsyres.2011.09.011
96. Badawy RA, Jackson GD, Berkovic SF, Macdonell RA. Cortical excitability and refractory epilepsy: a three-year longitudinal transcranial magnetic stimulation study. *Int J Neural Syst.* (2013) 23:1250030. doi: 10.1142/S012906571250030X
97. Badawy RA, Vogrin SJ, Lai A, Cook MJ. Patterns of cortical hyperexcitability in adolescent/adult-onset generalized epilepsies. *Epilepsia.* (2013) 54:871–8. doi: 10.1111/epi.12151
98. Badawy RA, Vogrin SJ, Lai A, Cook MJ. The cortical excitability profile of temporal lobe epilepsy. *Epilepsia.* (2013) 54:1942–9. doi: 10.1111/epi.12374
99. Badawy RA, Vogrin SJ, Lai A, Cook MJ. Cortical excitability changes correlate with fluctuations in glucose levels in patients with epilepsy. *Epilepsy Behav.* (2013) 27:455–60. doi: 10.1016/j.yebeh.2013.03.015

100. Badawy RA, Vogrin SJ, Lai A, Cook MJ. On the midway to epilepsy: is cortical excitability normal in patients with isolated seizures? *Int J Neural Syst.* (2014) 24:1430002. doi: 10.1142/S0129065714300022
101. Badawy RA, Vogrin SJ, Lai A, Cook MJ. Does the region of epileptogenicity influence the pattern of change in cortical excitability? *Clin Neurophysiol.* (2015) 126:249–56.
102. Silbert BI, Heaton AE, Cash RF, James I, Dunne JW, Lawn ND, et al. Evidence for an excitatory GABAA response in human motor cortex in idiopathic generalised epilepsy. *Seizure.* (2015) 26:36–42. doi: 10.1016/j.seizure.2015.01.014
103. Pawley AD, Chowdhury FA, Tangwiriyasakul C, Ceronie B, Elwes RD, Nashef L, et al. Cortical excitability correlates with seizure control and epilepsy duration in chronic epilepsy. *Ann Clin Transl Neurol.* (2017) 4:87–97. doi: 10.1002/acn3.383
104. Bauer PR, de Goede AA, Stern WM, Pawley AD, Chowdhury FA, Helling RM, et al. Long-interval intracortical inhibition as biomarker for epilepsy: a transcranial magnetic stimulation study. *Brain.* (2018) 141:409–21. doi: 10.1093/brain/awx343
105. Bolden LB, Griffis JC, Nenert R, Allendorfer JB, Szaflarski JP. Cortical excitability and seizure control influence attention performance in patients with idiopathic generalized epilepsies (IGEs). *Epilepsy Behav.* (2018) 89:135–42. doi: 10.1016/j.yebeh.2018.10.026
106. Bolden LB, Griffis JC, Nenert R, Allendorfer JB, Szaflarski JP. Cortical excitability affects mood state in patients with idiopathic generalized epilepsies (IGEs). *Epilepsy Behav.* (2019) 90:84–9. doi: 10.1016/j.yebeh.2018.11.001
107. Huang HW, Tsai JJ, Su PF, Mau YL, Wu YJ, Wang WC, et al. Cortical excitability by transcranial magnetic stimulation as biomarkers for seizure controllability in temporal lobe epilepsy. *Neuromodulation.* (2020) 23:399–406. doi: 10.1111/ner.13093
108. Joshi K, Cortez MA, Snead OC. Targeting the GABA B receptor for the treatment of epilepsy. In: *GABAB Receptor*. Cham: Humana Press (2016). p. 175–95.
109. Berardelli A, Rona S, Inghilleri M, Manfredi M. Cortical inhibition in Parkinson's disease. A study with paired magnetic stimulation. *Brain.* (1996) 119 (Pt. 1):71–7. doi: 10.1093/brain/119.1.71
110. Tegenthoff M, Vorgerd M, Juskowiak F, Roos V, Malin JP. Postexcitatory inhibition after transcranial magnetic single and double brain stimulation in Huntington's disease. *Electroencephalogr Clin Neurophysiol.* (1996) 101:298–303. doi: 10.1016/0924-980x(96)94645-7
111. Chen R, Wassermann EM, Caños M, Hallett M. Impaired inhibition in writer's cramp during voluntary muscle activation. *Neurology.* (1997) 49:1054–9.
112. Valzania F, Strafella A, Quatrale R, Santangelo M, Tropeani A, Lucchi D, et al. Motor evoked responses to paired cortical magnetic stimulation in Parkinson's disease. *Electroencephalogr Clin Neurophysiol.* (1997) 105:37–43
113. Romeo S, Berardelli A, Pedace F, Inghilleri M, Giovannelli M, Manfredi M. Cortical excitability in patients with essential tremor. *Muscle Nerve.* (1998) 21:1304–8. doi: 10.1002/(sici)1097-4598(199810)21:10<1304::aid-mus9>3.0.co;2-f
114. Rona S, Berardelli A, Vacca L, Inghilleri M, Manfredi M. Alterations of motor cortical inhibition in patients with dystonia. *Mov Disord.* (1998) 13:118–24. doi: 10.1002/mds.870130123
115. Priori A, Polidori L, Rona S, Manfredi M, Berardelli A. Spinal and cortical inhibition in Huntington's chorea. *Mov Disord.* (2000) 15:938–46. doi: 10.1002/1531-8257(200009)15:5<938::aid-mds1026>3.0.co;2-q
116. Chen R, Garg RR, Lozano AM, Lang AE. Effects of internal globus pallidus stimulation on motor cortex excitability. *Neurology.* (2001) 56:716–23. doi: 10.1212/wnl.56.6.716
117. Pierantozzi M, Palmieri MG, Marciani MG, Bernardi G, Giacomini P, Stanzione P. Effect of apomorphine on cortical inhibition in Parkinson's disease patients: a transcranial magnetic stimulation study. *Exp Brain Res.* (2001) 141:52–62. doi: 10.1007/s002210100839
118. Cunic D, Roshan L, Khan FI, Lozano AM, Lang AE, Chen R. Effects of subthalamic nucleus stimulation on motor cortex excitability in Parkinson's disease. *Neurology.* (2002) 58:1665–72. doi: 10.1212/wnl.58.11.1665
119. Bares M, Kanovsky P, Klajblova H, Rektor I. Intracortical inhibition and facilitation are impaired in patients with early Parkinson's disease: a paired TMS study. *Eur J Neurol.* (2003) 10:385–9. doi: 10.1046/j.1468-1331.2003.00610.x
120. Sailer A, Molnar GF, Paradiso G, Gunraj CA, Lang AE, Chen R. Short and long latency afferent inhibition in Parkinson's disease. *Brain.* (2003) 126:1883–94. doi: 10.1093/brain/awg183
121. Espay AJ, Morgante F, Purzner J, Gunraj CA, Lang AE, Chen R. Cortical and spinal abnormalities in psychogenic dystonia. *Ann Neurol.* (2006) 59:825–34. doi: 10.1002/ana.20837
122. Cantello R, Tarletti R, Varrasi C, Cecchin M, Monaco F. Cortical inhibition in Parkinson's disease: new insights from early, untreated patients. *Neuroscience.* (2007) 150:64–71. doi: 10.1016/j.neuroscience.2007.08.033
123. Fierro B, Brighina F, D'Amelio M, Daniele O, Lupo I, Ragonese P, et al. Motor intracortical inhibition in PD: L-DOPA modulation of high-frequency rTMS effects. *Exp Brain Res.* (2008) 184:521–8. doi: 10.1007/s00221-007-1121-y
124. Chu J, Wagle-Shukla A, Gunraj C, Lang AE, Chen R. Impaired presynaptic inhibition in the motor cortex in Parkinson disease. *Neurology.* (2009) 72:842–9. doi: 10.1212/01.wnl.0000343881.27524.e8
125. Meunier S, Russmann H, Shamim E, Lamy JC, Hallett M. Plasticity of cortical inhibition in dystonia is impaired after motor learning and paired-associative stimulation. *Eur J Neurosci.* (2012) 35:975–86. doi: 10.1111/j.1460-9568.2012.08034.x
126. Barbin L, Leux C, Sauleau P, Meyniel C, Nguyen JM, Pereon Y, et al. Non-homogeneous effect of levodopa on inhibitory circuits in Parkinson's disease and dyskinesia. *Parkinsonism Relat Disord.* (2013) 19:165–70. doi: 10.1016/j.parkreldis.2012.08.012
127. Lu MK, Chen CM, Duann JR, Ziemann U, Chen JC, Chiou SM, et al. Investigation of motor cortical plasticity and corticospinal tract diffusion tensor imaging in patients with parkinsons disease and essential tremor. *PLoS ONE.* (2016) 11:e0162265. doi: 10.1371/journal.pone.0162265
128. Philpott AL, Cummins TDR, Bailey NW, Churchyard A, Fitzgerald PB, Georgiou-Karistianis N. Cortical inhibitory deficits in premanifest and early Huntington's disease. *Behav Brain Res.* (2016) 296:311–7. doi: 10.1016/j.bbr.2015.09.030
129. Latorre A, Rocchi L, Batla A, Berardelli A, Rothwell JC, Bhatia KP. The signature of primary writing tremor is dystonic. *Mov Disord.* (2021). doi: 10.1002/mds.28579. [Epub ahead of print].
130. Priori A, Berardelli A, Inghilleri M, Accornero N, Manfredi M. Motor cortical inhibition and the dopaminergic system. Pharmacological changes in the silent period after transcranial brain stimulation in normal subjects, patients with Parkinson's disease and drug-induced parkinsonism. *Brain.* (1994) 117 (Pt. 2):317–23. doi: 10.1093/brain/117.2.317
131. Cloud LJ, Jinnah HA. Treatment strategies for dystonia. *Expert Opin Pharmacother.* (2010) 11:5–15. doi: 10.1517/14656560903426171
132. Leland Albright A, Barry MJ, Shafron DH, Ferson SS. Intrathecal baclofen for generalized dystonia. *Dev Med Child Neurol.* (2001) 43:652–7. doi: 10.1017/s0012162201001190
133. Mori F, Kusayanagi H, Monteleone F, Moscatelli A, Nicoletti CG, Bernardi G, et al. Short interval intracortical facilitation correlates with the degree of disability in multiple sclerosis. *Brain Stimul.* (2013) 6:67–71. doi: 10.1016/j.brs.2012.02.001
134. Nantes JC, Zhong J, Holmes SA, Narayanan S, Lapierre Y, Koski L. Cortical damage and disability in multiple sclerosis: relation to intracortical inhibition and facilitation. *Brain Stimul.* (2016) 9:566–73. doi: 10.1016/j.brs.2016.01.003
135. Squintani G, Donato F, Turri M, Deotto L, Teatini F, Moretto G, et al. Cortical and spinal excitability in patients with multiple sclerosis and spasticity after oromucosal cannabinoid spray. *J Neurol Sci.* (2016) 370:263–8. doi: 10.1016/j.jns.2016.09.054
136. Feldman RG, Kelly-Hayes M, Conomy JP, Foley JM. Baclofen for spasticity in multiple sclerosis. Double-blind crossover and three-year study. *Neurology.* (1978) 28:1094–8. doi: 10.1212/wnl.28.11.1094
137. Gao F, Yin X, Edden RAE, Evans AC, Xu J, Cao G, et al. Altered hippocampal GABA and glutamate levels and uncoupling from functional connectivity in multiple sclerosis. *Hippocampus.* (2018) 28:813–23. doi: 10.1002/hipo.23001
138. Swayne OB, Rothwell JC, Ward NS, Greenwood RJ. Stages of motor output reorganization after hemispheric stroke suggested by longitudinal studies of cortical physiology. *Cereb Cortex.* (2008) 18:1909–22. doi: 10.1093/cercor/bhm218

139. Kuppuswamy A, Clark EV, Turner IF, Rothwell JC, Ward NS. Post-stroke fatigue: a deficit in corticomotor excitability? *Brain.* (2015) 138:136–48. doi: 10.1093/brain/awu306
140. Schambra HM, Ogden RT, Martínez-Hernández IE, Lin X, Chang YB, Rahman A, et al. The reliability of repeated TMS measures in older adults and in patients with subacute and chronic stroke. *Front Cell Neurosci.* (2015) 9:335. doi: 10.3389/fncel.2015.00335
141. Schambra HM, Martinez-Hernandez IE, Slane KJ, Boehme AK, Marshall RS, Lazar RM. The neurophysiological effects of single-dose theophylline in patients with chronic stroke: a double-blind, placebo-controlled, randomized cross-over study. *Restor Neurol Neurosci.* (2016) 34:799–813. doi: 10.3233/RNN-160657
142. Mooney RA, Ackerley SJ, Rajeswaran DK, Cirillo J, Barber PA, Stinear CM, et al. The influence of primary motor cortex inhibition on upper limb impairment and function in chronic stroke: a multimodal study. *Neurorehabil Neural Repair.* (2019) 33:130–40. doi: 10.1177/1545968319826052
143. Mooney RA, Cirillo J, Stinear CM, Byblow WD. Neurophysiology of motor skill learning in chronic stroke. *Clin Neurophysiol.* (2020) 131:791–8. doi: 10.1016/j.clinph.2019.12.410
144. Kokinovic B, Medini P. Loss of GABA B -mediated interhemispheric synaptic inhibition in stroke periphery. *J Physiol.* (2018) 596:1949–64. doi: 10.1113/JP275690
145. Creamer M, Cloud G, Kossmehl P, Yochelson M, Francisco GE, Ward AB, et al. Effect of intrathecal baclofen on pain and quality of life in poststroke spasticity. *Stroke.* (2018) 49:2129–37. doi: 10.1161/STROKEAHA.118.022255
146. Tremblay S, de Beaumont L, Lassonde M, Theoret H. Evidence for the specificity of intracortical inhibitory dysfunction in asymptomatic concussed athletes. *J Neurotrauma.* (2011) 28:493–502. doi: 10.1089/neu.2010.1615
147. De Beaumont L, Mongeon D, Tremblay S, Messier J, Prince F, Leclerc S, et al. Persistent motor system abnormalities in formerly concussed athletes. *J Athl Train.* (2011) 46:234–40. doi: 10.4085/1062-6050-46.3.234
148. De Beaumont L, Tremblay S, Poirier J, Lassonde M, Theoret H. Altered bidirectional plasticity and reduced implicit motor learning in concussed athletes. *Cereb Cortex.* (2012) 22:112–21. doi: 10.1093/cercor/bhr096
149. Pearce AJ, Hoy K, Rogers MA, Corp DT, Maller JJ, Drury HG, et al. The long-term effects of sports concussion on retired Australian football players: a study using transcranial magnetic stimulation. *J Neurotrauma.* (2014) 31:1139–45. doi: 10.1089/neu.2013.3219
150. Tremblay S, Beaule V, Proulx S, Tremblay S, Marjanska M, Doyon J, et al. Multimodal assessment of primary motor cortex integrity following sport concussion in asymptomatic athletes. *Clin Neurophysiol.* (2014) 125:1371–9. doi: 10.1016/j.clinph.2013.11.040
151. Powers KC, Cinelli ME, Kalmar JM. Cortical hypoexcitability persists beyond the symptomatic phase of a concussion. *Brain Inj.* (2014) 28:465–71. doi: 10.3109/02699052.2014.888759
152. Lewis GN, Hume PA, Stavric V, Brown SR, Taylor D. New Zealand rugby health study: motor cortex excitability in retired elite and community level rugby players. *NZ Med J.* (2017) 130:34–44.
153. Seeger TA, Kirton A, Esser MJ, Gallagher C, Dunn J, Zewdie E, et al. Cortical excitability after pediatric mild traumatic brain injury. *Brain Stimul.* (2017) 10:305–14. doi: 10.1016/j.brs.2016.11.011
154. Pearce AJ, Rist B, Fraser CL, Cohen A, Maller JJ. Neurophysiological and cognitive impairment following repeated sports concussion injuries in retired professional rugby league players. *Brain Inj.* (2018) 32:498–505. doi: 10.1080/02699052.2018.1430376
155. Pearce AJ, Tommerdahl M, King DA. Neurophysiological abnormalities in individuals with persistent post-concussion symptoms. *Neuroscience.* (2019) 408:272–81. doi: 10.1016/j.neuroscience.2019.04.019
156. Opie GM, Foo N, Killington M, Ridding MC, Semmler JG. Transcranial magnetic stimulation-electroencephalography measures of cortical neuroplasticity are altered after mild traumatic brain injury. *J Neurotrauma.* (2019) 36:2774–84. doi: 10.1089/neu.2018.6353
157. King R, Kirton A, Zewdie E, Seeger TA, Ciechanski P, Barlow KM. Longitudinal assessment of cortical excitability in children and adolescents with mild traumatic brain injury and persistent post-concussive symptoms. *Front Neurol.* (2019) 10:451. doi: 10.3389/fneur.2019.00451
158. Kobori N, Dash PK. Reversal of brain injury-induced prefrontal glutamic acid decarboxylase expression and working memory deficits by D1 receptor antagonism. *J Neurosci.* (2006) 26:4236–46. doi: 10.1523/JNEUROSCI.4687-05.2006
159. Salerno A, Georgesco M. Double magnetic stimulation of the motor cortex in amyotrophic lateral sclerosis. *Electroencephalogr Clin Neurophysiol.* (1998) 107:133–9. doi: 10.1016/s0013-4694(98)00054-6
160. Zanette G, Tamburin S, Manganotti P, Refatti N, Forgione A, Rizzuto N. Different mechanisms contribute to motor cortex hyperexcitability in amyotrophic lateral sclerosis. *Clin Neurophysiol.* (2002) 113:1688–97. doi: 10.1016/s1388-2457(02)00288-2
161. Tamburin S, Fiaschi A, Marani S, Andreoli A, Manganotti P, Zanette G. Enhanced intracortical inhibition in cerebellar patients. *J Neurol Sci.* (2004) 217:205–10. doi: 10.1016/j.jns.2003.10.011
162. Kang SY, Sohn YH, Kim HS, Lyoo CH, Lee MS. Corticospinal disinhibition in paroxysmal kinesigenic dyskinesia. *Clin Neurophysiol.* (2006) 117:57–60. doi: 10.1016/j.clinph.2005.09.007
163. Siniatchkin M, Kroner-Herwig B, Kocabiyik E, Rothenberger A. Intracortical inhibition and facilitation in migraine–a transcranial magnetic stimulation study. *Headache.* (2007) 47:364–70. doi: 10.1111/j.1526-4610.2007.00727.x
164. Canafoglia L, Ciano C, Visani E, Anversa P, Panzica F, Viri M, et al. Short and long interval cortical inhibition in patients with Unverricht-Lundborg and Lafora body disease. *Epilepsy Res.* (2010) 89:232–7. doi: 10.1016/j.eplepsyres.2010.01.006
165. Cosentino G, Di Marco S, Ferlisi S, Valentino F, Capitano WM, Fierro B, et al. Intracortical facilitation within the migraine motor cortex depends on the stimulation intensity. A paired-pulse TMS study. *J Headache Pain.* (2018) 19:65. doi: 10.1186/s10194-018-0897-4
166. Cash RF, Ziemann U, Murray K, Thickbroom GW. Late cortical disinhibition in human motor cortex: a triple-pulse transcranial magnetic stimulation study. *J Neurophysiol.* (2010) 103:511–8. doi: 10.1152/jn.00782.2009

Disclaimer: The content of this publication is solely the responsibility of the authors and does not necessarily represent the official views of the NIH.

Conflict of Interest: PC has received research support from Neuronetics, NeoSync, and Pfizer. He has received in-kind support from AssureRx, MagVenture, and Neuronetics. He has provided consultation for Myriad Genetics Procter & Gamble Co., and Sunovion. JV has received in-kind support from AssureRx.

The remaining authors declare that the research was conducted in the absence of any commercial or financial relationships that could be construed as a potential conflict of interest.

frontiers in Psychiatry

ORIGINAL RESEARCH
published: 25 June 2021
doi: 10.3389/fpsyt.2021.679021

Psychopathological Symptom Load and Distinguishable Cerebral Blood Flow Velocity Patterns in Patients With Schizophrenia and Healthy Controls: A Functional Transcranial Doppler Study

Stephan T. Egger[1,2], Julio Bobes[2], Katrin Rauen[3,4], Erich Seifritz[1], Stefan Vetter[1†] and Daniel Schuepbach[5,6†]*

[1] Department of Psychiatry, Psychotherapy and Psychosomatics, Faculty of Medicine, University Hospital of Zurich, University of Zürich, Zurich, Switzerland, [2] Department of Psychiatry, Faculty of Medicine, University of Oviedo, Oviedo, Spain, [3] Department of Geriatric Psychiatry, Faculty of Medicine, Psychiatric University Hospital of Zurich, University of Zürich, Zurich, Switzerland, [4] Institute for Stroke and Dementia Research, Ludwig Maximilian University Munich, University Hospital, Munich, Germany, [5] Department of General Psychiatry, Center of Psychosocial Medicine, University of Heidelberg, Heidelberg, Germany, [6] Klinikum am Weissenhof, Weinsberg, Germany

OPEN ACCESS

Edited by:
Shinsuke Koike,
The University of Tokyo, Japan

Reviewed by:
Jill R. Glausier,
University of Pittsburgh, United States
Rita Bella,
University of Catania, Italy

***Correspondence:**
Stephan T. Egger
stephan.egger@pukzh.ch

† These authors have contributed equally to this work

Specialty section:
This article was submitted to Schizophrenia, a section of the journal Frontiers in Psychiatry

Received: 10 March 2021
Accepted: 21 May 2021
Published: 25 June 2021

Citation:
Egger ST, Bobes J, Rauen K, Seifritz E, Vetter S and Schuepbach D (2021) Psychopathological Symptom Load and Distinguishable Cerebral Blood Flow Velocity Patterns in Patients With Schizophrenia and Healthy Controls: A Functional Transcranial Doppler Study. Front. Psychiatry 12:679021. doi: 10.3389/fpsyt.2021.679021

Introduction: Schizophrenia is a severe psychiatric disorder, with executive dysfunction and impaired processing speed playing a pivotal role in the course of the disease. In patients with schizophrenia, neurocognitive deficits appear to be related to alterations in cerebral hemodynamics. It is not fully understood if psychopathological symptom load (i.e., presence and severity of symptoms) is also related to alterations in cerebral hemodynamics. We aim to study the relationship between psychopathological symptom load and cerebral hemodynamics in the Middle Cerebral Artery (MCA) during a cognitive task in patients with schizophrenia and healthy controls.

Methodology: Cerebral hemodynamics in the MCA were examined in 30 patients with schizophrenia and 15 healthy controls using functional Transcranial Doppler (fTCD) during the Trail Making Test (TMT). Psychopathological symptoms were measured using the Brief Psychiatric Rating Scale (BPRS). Patients were dichotomized according to BPRS scores: mild-moderate (BPRS < 41, $n = 15$) or marked-severe (BPRS $\geqq 41$, $n = 15$). Mean blood flow velocity (MFV) in the MCA and processing speed of the TMT were analyzed. Cerebral hemodynamics were analyzed using the general additional model (GAM) with a covariate analysis of variance (ANCOVA) for group comparisons.

Results: Patients and healthy controls were comparable regarding demographics. Patients had a slower processing speed for the TMT-A (patients-severe: 52s, patients-moderate: 40s, healthy-controls: 32s, $p = 0.019$) and TMT-B [patients-severe: 111s, patients-moderate: 76s, healthy-controls: 66s, $p < 0.001$)]. Patients demonstrated differing hemodynamic profiles in both TMTs: TMT- A [$F_{(6,\ 1,792)} = 17$, $p < 0.000$); TMT-B [$F_{(6,\ 2,692)} = 61.93$, $p < 0.000$], with a delay in increase in MFV and a failure to return to baseline values.

Conclusions: Patients with schizophrenia demonstrated slower speeds of processing during both the TMT-A and TMT-B. The speed of processing deteriorated with increasing psychopathological symptom load, additionally a distinct cerebral hemodynamic pattern in the MCA was observed. Our results further support the view that severity of schizophrenia, particularly psychopathological symptom load, influences performance in neurocognitive tasks and is related to distinct patterns of brain hemodynamics.

Keywords: transcranial doppler, schizophrenia, symptomalogy, trail making test, cognition, hemodynamics

INTRODUCTION

Schizophrenia is a severe psychiatric disorder which is characterized by hallucinations, delusions and blunted affect (1). Although not part of the diagnostic criteria, cognitive impairment is also a common feature of schizophrenia, often occurring before the onset of the first psychotic episode and continuing throughout the course of the disease (2, 3), with cognitive impairment and executive functions playing a pivotal role for outcome and prognosis, as well as being major determinants of quality of life and well-being (4, 5).

Cognitive impairment and executive function are measured by numerous neuropsychological assessment tools, including the Trail Making Test (TMT)-A and TMT-B. In contrast to other neuropsychological instruments, the TMTs are easy to use; their interpretation is straightforward. Consequently, they are widely used in both research and clinical practice (6, 7). The TMTs are considered to be sensitive to cognitive dysfunction and frontal lobe integrity, assessing graphomotor activity, visual scanning, selective attention, mental flexibility and executive functioning (6, 7). Patients with schizophrenia show impaired performance in the TMT, with deficits in processing speed and inefficient simultaneous processing strategies (6, 8). There is evidence that in patients with schizophrenia, the frontal lobes, particularly the dorsolateral prefrontal cortex (DLPFC), play a pivotal role in executing the TMTs (9, 10).

Cognitive performance is partly determined by the brain's ability to increase blood supply to the areas activated during a cognitive task. Due to the skull's anatomic conditions, the increase in diameter of the cerebral arteries is limited; an increase in cerebral blood supply is achieved by increasing blood flow velocity in the cerebral arteries. Therefore, we consider Mean Flow Velocity (MFV) a valid indicator for brain activity (11, 12). Transcranial Doppler (TCD) is a versatile, non-invasive method for assessing the cerebral arteries' functioning and hemodynamic characteristics (11, 13). TCD provides a continuous measurement of blood flow velocity with high temporal resolution. However, TCD has low anatomical resolution and is not able to deliver a direct brain image. Despite this limitation, TCD has been used to study physiological and hemodynamic conditions in several neurological diseases and psychiatric disorders (11, 13, 14). The neurocognitive impairment in schizophrenia appears to be related to alterations in blood flow in several brain areas, including the DLPFC (15–18).

The middle cerebral arteries (MCA) irrigate the brain's lateral hemispheres, including the DLPFC, subcortical structures, basal ganglia and the striatum (19). A number of these structures, principally the DLPFC, striatum and thalamus, are activated during the TMT (17), making fTCD a suitable method for the physiological and hemodynamic assessment of brain activity in these areas during a neurocognitive task (20). Previous studies using functional TCD (fTCD) in patients with schizophrenia and healthy controls showed clear differences in the MCA hemodynamic pattern during the TMT (14); to what extent there are also hemodynamic differences between those affected with schizophrenia, in relation to the number and severity of symptoms (i.e., symptom load) is thus far unexplored.

Our study aims to determine the relationship between psychopathological symptom load (in healthy controls and patients with schizophrenia) and cerebral hemodynamics in the MCA during a neurocognitive task. New results may contribute to increased use of fTCD as an assessment tool in neuropsychiatric disorders, particularly schizophrenia. We examined cerebral blood flow velocity during the TMT in patients with schizophrenia and healthy controls, using a visuomotor control task to compensate for hemodynamic changes resulting solely from the motor and visual activities during the TMT.

MATERIALS AND METHODS

Subjects

Thirty patients fulfilling the WHO-ICD 10 (21) criteria for schizophrenia participated in this study; they were age and sex-matched with 15 healthy controls. The healthy controls had no medical, neurological or psychiatric condition at the time of examination; they were recruited for a previous study conducted by our research group, using the same examination protocol and equipment (14). All participants were right-handed. All patients with schizophrenia were taking antipsychotic medication. The following exclusion criteria applied to patients: 1. affective disorder (according to ICD-10: F3); 2. organic brain disorder (according to ICD-10: F0); 3. active substance abuse disorder (according to ICD-10: F1) in the 3 months before inclusion; 4. unstable neurological; or 5. medical condition. Basic demographic characteristics of the participants were collected. Besides the participants' education, we included the mean education of their parents to disentangle poor educational performance attributable to early onset of the disorder or familial accumulation. The competent ethics committee approved the study, all participants provided written informed consent.

Clinical Assessment and Psychometric Measurements

Within 24 h of the fTCD measurement, psychopathological symptoms were assessed using the Brief Psychiatric Rating Scale (BPRS) (22), overall clinical severity of symptoms was assessed using the Clinical Global Impression Scale (CGI) (23). For this study, the daily antipsychotic dose was converted to chlorpromazine equivalents according to current guidelines (24, 25). Effects of antipsychotics on the extrapyramidal system were examined using the Simpson- Angus Scale (SAS) (26) and the Barnes Akathisia Scale (BAS) (27, 28).

The BPRS is one of the most frequently used scales to measure psychopathology in patients with schizophrenia, systematically assessing the presence and severity of symptoms. It consists of 18 single items assessing different symptoms. Each item is evaluated according to a seven-item Likert scale, ranging from "1" (not present) to "7" (extremely severe). Thus, the sum score ranges from 18 to 126. We used the BPRS sum score as a measure of the psychopathological symptom load. Participants were classified according to BPRS sum scores, as "non-affected" or healthy controls; those with a diagnosis of schizophrenia and a BPRS score below 41 points were classified as "mild-moderate," those with a BPRS score of 41 points or more were classified as "marked- severe"(29).

Equipment and Cerebral Blood Flow Measurements

Doppler measurements were performed using a Multi-Dop X instrument (DWL Elektronische Systeme GmbH, Sipplingen-Germany). Two dual 2 MHz transducers were attached and fixed with a headband. Both MCAs were insonated at depths of 48–55 mm through the temporal bone window. The 2 MHz transducers were fixed with a headband, so motion artifacts of the head did not alter the position of the transducers. This approach is supported by published evidence demonstrating that functional transcranial Doppler is fairly robust to movement artifacts (30). As indicated by measurement artifact data, we screened for MFV values outside the 60–150% range of the mean MFV recording of a subject before, after and during the cognitive task.

Cerebral Hemodynamics and Cognitive Task

Subjects were asked to abstain from caffeine and nicotine consumption 2 h prior to the examination (31). MFV data were continuously recorded during the psychological paradigm, integrating MFV data for each cardiac cycle. Participants underwent a standardized briefing. They were instructed about the nature of the study and the psychological paradigm. To reduce learning effects, the cognitive task was presented only once. We administered the TMTs as a paper and pencil test. In the TMT-A, subjects had to connect 25 numbers in ascending order (i.e., 1, 2, 3,..., 25). In the TMT-B, participants had to connect numbers (1–13) and letters (A–L) alternately in ascending order (i.e., 1, A, 2, B, 3, C,..., 13, L). Subjects had to solve the TMTs as quickly and accurately as possible. In the control task participants were asked to randomly connect circles placed in a 10 by 10 cm square. Lines had to be drawn at a pace of 1.0 or 0.5 Hz to simulate the pace of the TMT-A (0.89+−0.21 Hz) and the TMT-B (0.46+−0.15Hz). The control task simulates visuomotor scanning during the TMTs. The control task was placed randomly before or after each TMT, with a break of 60 s between each task.

Statistical Analysis

Data are presented in tables using simple descriptive statistics (mean, standard deviation, percentages). For the analysis of group differences, specific statistical tests were performed. Continuous data were analyzed using a univariate analysis of variance (ANOVA), with a secondary *t*-test to evaluate model differences. The chi-square test was applied to categorical data. A *post hoc* power analysis was conducted, using the effect sizes for differences in completion time between the TMT-A and TMT-B.

For the purposes of analysis, the MFV consisted of the following elements, following procedures used in a previous study (20): (a). integration of MFV from 100 Hz sampling to 1 Hz; (b). normalization of digitized data with reference to pre-and post-task rest phases (60s intervals of rest with 30s between the first and last 15s); and (c) relative MFV (relative to resting state) values, averaged and converted to percentage values. All MFV values in this paper are relative MFV, i.e., cerebral blood flow velocity change compared with resting phase values. For analysis of the TMT-A and B, the time to be analyzed was dictated by the time required by the fastest participant to complete the task.

The general additional model (GAM); was used for graphical representation, as well as to statistically evaluate the change in mean flow velocity over time (in seconds), controlled for side and sex. The advantage of non-parametric tests, such as the general additional model, lies in their greater flexibility regarding assumptions about data (32–34). The GAM allows for regression and weight analysis at both fixed and random variable level (or for discrete and continuous variables) (33). Using a non-parametric test allows for a realistic visual comparison of flow velocity, facilitating the inference of its clinical relevance (35, 36). Accordingly, a better representation of dynamic and inter-dependent results such as blood flow is provided. However, the mathematical and statistical analysis and consequently, comparison of the GAMs outcomes is more complex (34, 37). Therefore, a covariate analysis of variance (ANCOVA) was used to evaluate differences in the GAM of blood flow velocity obtained for each group and side. Thus, allowing us to determine whether a statistical difference between the hemodynamic curves was demonstrated., A pairwise-comparison was conducted to determine the time frames in which the curves differed from one another.

RESULTS

Demographics and Clinical Characteristics

Patients and control subjects were comparable regarding age, sex and years of parent's education. Years of own education for those with schizophrenia was significantly shorter than healthy controls, with no difference between severity groups. Patients with a marked-severe psychopathological symptom

load obtained significantly higher CGI-S scores than those with moderate symptomatology [3.60 ± 1.06 vs. 5.20 ± 0.68, $F_{(1, 28)} = 24.44$, $p < 0.001$]. The duration of illness and hospitalization rates did not differ significantly between patient groups. Each participant with a diagnosis of schizophrenia had an antipsychotic prescribed, some two. Most antipsychotics prescribed were second-generation antipsychotics. There were no significant differences regarding the antipsychotics prescribed (data not shown) and dose (as chlorpromazine equivalents). Furthermore, the rate of extrapyramidal motor symptoms and akathisia was also similar (see **Table 1**). The *post hoc* power analysis reached a power of 1-ß of 0.99.

TMT Performance

In comparison to healthy controls, patients with schizophrenia required significantly more time to complete both TMTs. Furthermore, more severely ill patients took significantly longer to complete the test than those classified as mild-moderately ill; TMT-A [patients-severe: 52.3 ± 30.8; patients-moderate: 40.2 ± 12.7; healthy-controls: 31.0 ± 7.4, $F_{(2, 42)} = 4.38$, $p = 0.019$] and TMT-B [patients-severe: 66.2 ± 18.9; patients-moderate: 75.5 ± 22.9; healthy-controls: 111.1 ± 20.9, $F_{(2, 42)} = 19.08$, $p < 0.001$]. Since the fastest performance on the TMT-A was 20s, and for the TMT-B 30s, these are the time periods considered for statistical analysis. There was no statistically significant difference between groups regarding the rate of errors on the TMTs (see **Table 1**).

Mean Cerebral Blood Flow Velocity During the TMT-A

For healthy-controls, there was a significant change in MFV over time [$F(s)_{(3.991, 4.912)} = 15.43$, $p < 0.001$], with a hemispheric difference in MFV [$F_{(1, 266)} = 10.55$, $p = 001$]; in the *post hoc* pairwise analysis we identified that the hemispheric (right > left) difference was only significant for the first 10 s of the measurement period. For those mildly-moderately affected, there was also a change of MFV over time [$F(s)_{(7.403, 8.356)} = 6.707$, $p < 0.001$], we did not find a hemispheric difference in the MFV [$F_{(1, 266)} = 0.979$, $p = 0.323$]; with the *post hoc* pairwise analysis also demonstrating no hemispheric differences at any time point. Finally, in those with higher psychopathological symptom load, we found a change in MFV over time [$F(s)_{(8.087, 8.767)} = 9.746$, $P < 0.001$], with a hemispheric difference (left > right) in the MFV [$F_{(1, 266)} = 7.71$, $p < 0.001$]; the *post hoc* pairwise comparison indicating that this difference was only significant during the middle phase of the measurement (s 9 to 14). There is a statistically significant difference between the curves of the three groups under comparison [$F_{(6, 1,792)} = 17, p < 0.000$].

Group differences and hemispheric differences in MFV during the TMT-A are graphically represented (**Figure 1**). The mean flow velocity in both middle cerebral arteries shows a similar pattern for all three groups during the TMT-A; in the first 5–10 s, there is an increase in blood flow followed by a steady decrease. Healthy controls reached the peak of blood flow 2 s faster than those with schizophrenia. Furthermore, those with marked-severe psychopathological symptom load show a delayed and higher increase and a slighter decrease in the blood blow velocity in the left MCA.

Mean Cerebral Blood Flow Velocity During the TMT-B

Healthy controls demonstrate a change of MFV over time [$F(s)_{(4.890, 5.952)} = 23.04$, $p < 0.001$], without a hemispheric difference in MFV [$F_{(1, 406)} = 0.693$, $p = 0.405$] during the TMT-B. Those mild-moderately affected also showed a change in MFV over time [$F(s)_{(8.106, 8.779)} = 18.62$, $p < 0.001$], without a hemispheric difference in MFV [$F_{(1, 406)} = 1.117$, $p = 0.291$], the *post hoc* pairwise comparison, however, demonstrated a difference for the first eight s of the measurement period. Those more severely affected also demonstrated a change in MFV over time [$F(s)_{(5.750, 6.882)} = 3.888$, $p < 0.001$], and a hemispheric difference in MFV [$F_{(1, 406)} = 28.42$, $p < 0.001$]; with the pairwise *post hoc* comparison revealing a significant difference for the first 5 s and in the middle phase of the measurement period (s 18 to 21). There is a statistically significant difference between the curves of the three comparison groups [$F_{(6, 2,692)} = 61.93, p < 0.000$).

Group differences and hemispheric differences in MFV during the TMT-B are graphically represented (**Figure 2**). Healthy controls reach a peak in blood flow after 5 s, with a continuous decrease. Those with mild-moderate psychopathological symptom load also reach the first peak after 7 s, followed by a slight decrease and a second lower peak. Finally, those with more severe schizophrenia show a discrepancy between both MCAs. Both MCAs form two peaks, the first just a few seconds after beginning the task, the second after 20 s. The right MCA shows a lower increased MFV, demonstrating a lower initial peak than the left MCA 20 s after beginning the task.

DISCUSSION

Using an age and gender-balanced sample population, including patients with schizophrenia and healthy controls, we examined the mean blood flow velocity during the TMT-A and TMT-B in the middle cerebral artery using functional transcranial doppler. In our study, participants with a higher psychopathological symptom load (represented by higher BPRS scores) demonstrated slower processing speed (with similar accuracy) during the TMT-A and TMT-B, compared with participants with fewer symptoms and healthy controls. The hemodynamic pattern also demonstrated a clearly distinguishable profile between patients with schizophrenia and healthy controls. The differences were more marked in those with higher symptom severity and when the complexity of the cognitive task increased (i.e., TMT-B over TMT-A). In summary, our results demonstrate a relationship between psychopathological symptom load, cognitive demand, decreased processing speed and distinct hemodynamic patterns in the MCA during the TMT-A and TMT-B.

Healthy controls in our study demonstrate in both the TMT-A and TMT-B, an initial increase in cerebral blood flow, which returns smoothly to baseline values, thus reproducing previous

TABLE 1 | Demographic and clinical characteristics of the sample.

	Non- affected *N* = 15	Mild-moderate *N* = 15	Marked-severe *N* = 15		
Demographic Variables				Statistics	*p*
Age (in years)	33.87 (7.68)	34.05 (7.73)	32.40 (5.38)	$F_{(2, 42)} = 0.222$	0.80
Sex (male/female)	10/5	10/5	12/3	$X^2_{(2, 45)} = 0.865$	0.65
Education (in years)	19.17 (4.17)[a]	13.07 (2.60)[a]	13.10 (2.48)[a]	$F_{(2, 42)} = 18.313$	<0.001
Parents' Education (in years)	15.47 (3.83)	14.70 (3.00)	13.97 (3.03)	$F_{(2, 42)} = 0.769$	0.47
Clinical variables					
BPRS	–	30.27 (4.91)[b]	43.73 (3.67)[b]	$F_{(1, 28)} = 72.421$	<0.001
CGI-S	–	3.60 (1.06)[b]	5.20 (0.68)[b]	$F_{(1, 28)} = 24.436$	<0.001
Chlorpromazine equivalent dosage (mg/d)		531.67 (165.69)	543.33 (176.14)	$F_{(1, 28)} = 0.035$	0.85
EPS	–	3.47 (2.10)	4.93(7.91)	$F_{(1, 28)} = 0.481$	0.49
BAS	–	0.53 (0.74)	1.07 (0.96)	$F_{(1, 28)} = 2.89$	0.10
Duration of illness (in years)	–	8.67 (6.91)	12.20 (4.04)	$F_{(1, 28)} = 2.922$	0.09
Number of hospitalizations	–	3.47 (2.03)	5.13 (4.70)	$F_{(1, 28)} = 1.587$	0.22
Cognitive performance					
TMT-A (duration in seconds)	31.00 (7.43)[c]	40.20 (12.66)[c]	52.27 (30.84)[c]	$F_{(2, 42)} = 4.388$	0.019
TMT-B (duration in seconds)	66.20 (18.89)[c]	75.53 (22.98)[c]	111.13 (20.99)[c]	$F_{(2, 42)} = 19.085$	<0.001

Pairwise comparison: [a]non-affected > mild-moderate and marked-severe; [b]marked-severe > mild-moderate: [c]marked-severe < mild-moderate < non-affected.

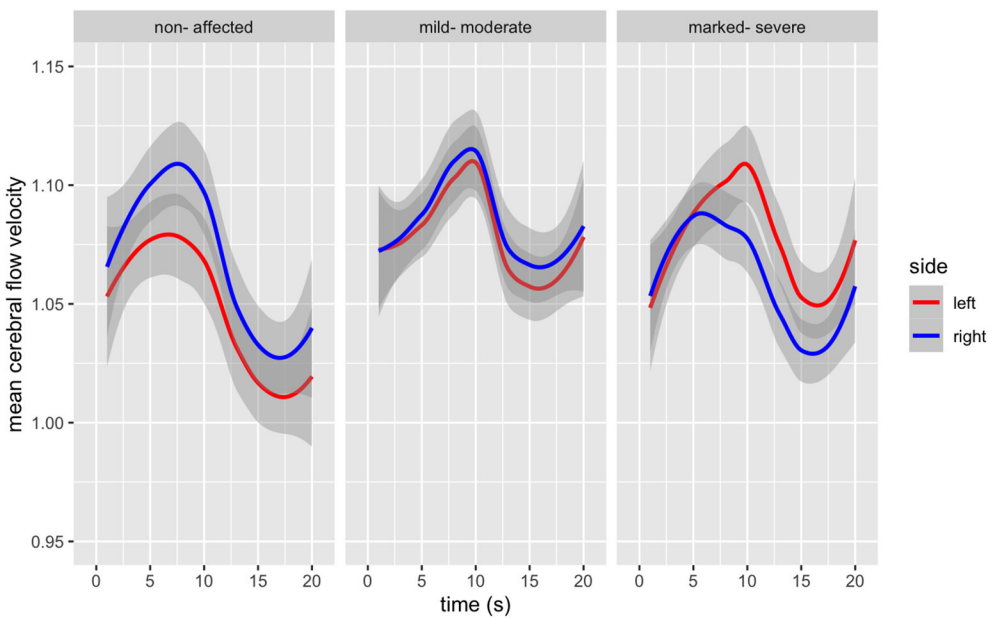

FIGURE 1 | Bilateral Mean Flow Velocity changes from baseline in the Middle Cerebral Artery during the duration of the TMT-A (in seconds), according to psychopathological symptom load [$F_{(6, 1,792)} = 17$, $p < 0.000$].

findings in healthy subjects (38). Patients with schizophrenia fail to reproduce this pattern. Firstly, the increase in MFV is delayed; secondly, the MFV fails to return to baseline values. The differences in the hemodynamic pattern for patients with schizophrenia are accentuated, as psychopathological symptom load and cognitive demand increases (i.e., TMT-B over TMT-A). Processing speed may mediate the demonstrated differences in hemodynamic pattern according to symptom severity and cognitive demand for the TMT-A and TMT-B. This lends further support to the notion that neuronal activity and cerebral blood flow are closely coupled; with MFV resulting from the activation of (or correspondingly the failure to deactivate) cortical areas in the MCA's irrigation territory (9, 12, 19, 39, 40). Patients with schizophrenia demonstrate increased brain activity (as indicated by a higher MFV) for lower performance (i.e., slower processing speed) compared to healthy controls (16).

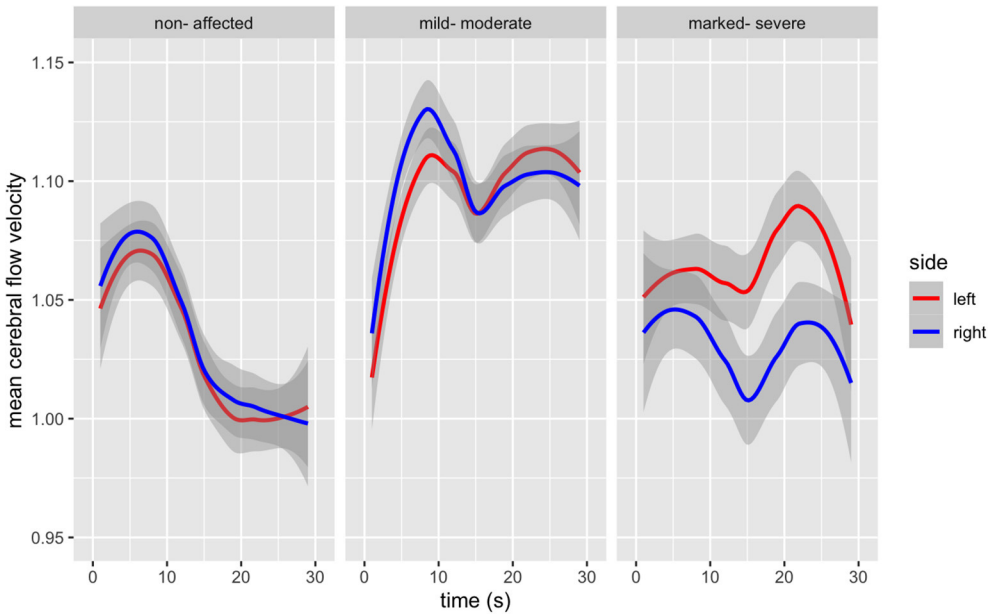

FIGURE 2 | Bilateral Mean Flow Velocity changes from baseline in the Middle Cerebral Artery during the duration of the TMT-B (in seconds), according to psychopathological symptom load [$F_{(6,\ 2,692)} = 61.93$, $p < 0.000$].

Neuroimaging studies demonstrate different brain activation patterns for the TMT-A and TMT-B. In the case of the TMT-A, areas involved in graphomotor speed, visual scanning, and selective attention are activated, whereas for the TMT-B, activated areas relate to mental flexibility and executive functioning (8). Previous findings also report a positive correlation between the TMT-B and hemodynamic activity in the MCA; this may be due to activation of the DLPFC, temporal cortex, basal ganglia and the thalamus during the TMT-B (17, 18). Several of these neuroanatomical areas are also involved in psychopathology and the neurocognitive anomalies related to schizophrenia (14, 41). Studies (including ours) using fTCD demonstrate a correlation between performance and hemodynamic patterns (14–16). This lends support to the view that factors inherent to schizophrenia as well as to other conditions characterized by executive dysfunction, such as dysfunctional neuronal integrity, accelerated white matter aging, hypoperfusion and increased vascular resistance (42–45) may play a role. Since our sample was matched for age and gender, we cannot make any inferences regarding the effects of aging on our results. In the absence of a direct anatomical image, taking into account that the irrigation territory of the MCA is extensive, our findings in this respect are not conclusive.

Our study has some other limitations which must be taken into account in order to better understand and interpret our findings. The lack of further neurocognitive assessments limits our results to the cognitive abilities measured by the TMTs. Taking into account that patients and healthy controls showed similar error rates (i.e., both were accurate), the main difference between the subsamples is processing speed. Medication, particularly antipsychotics, can impair cognitive performance, whether directly or through side effects (46–50), Furthermore, they can also influence hemodynamics (47). In our design, we did not directly control for this potentially confounding factor. Nonetheless, we did not find a difference regarding the dose and side effects of antipsychotics among patients with schizophrenia. Those with a higher psychopathological symptom load had a longer course of the disease with higher rates of hospitalization, which may be related to more severely impaired cognitive performance (51, 52). The influence of systemic circulation on cerebral blood flow, especially heart rate and arterial blood pressure, is controlled for using a random motor activity (53, 54). The control task aims to compensate for subtle alterations in circulation and other confounding factors through relative values compared to resting phase values before and after the paradigm (53). Furthermore, all participants were medically and neurologically stable, with no circulatory anomalies at the time of the study. Other potential confounders, such as anxiety, hypo- or hyperventilation (55), were not observed during the measurement procedure.

In summary, patients with schizophrenia performed less satisfactorily on both TMTs. Performance deteriorated with increasing symptom load, parallel with a distinct cerebral blood flow pattern in the MCA. Our results further support the view that schizophrenia, particularly symptom load and thus severity, influences performance in neurocognitive tasks, whilst being related to distinct brain hemodynamic patterns. Furthermore, these results support the use of fTCD as a brain imaging

technique capable of studying brain hemodynamics during neurocognitive tasks.

DATA AVAILABILITY STATEMENT

The raw data supporting the conclusions of this article will be made available by the authors, without undue reservation.

ETHICS STATEMENT

The studies involving human participants were reviewed and approved by Kantonale Ethikkommission of Zurich. The patients/participants provided their written informed consent to participate in this study.

AUTHOR CONTRIBUTIONS

SE and DS conceived the presented idea, carried out the experiment, and analyzed the results and prepared the manuscript. JB and ES aided in interpreting the results and supervised the manuscript. KR and SV contributed to the interpretation of the results. All authors contributed to the article and approved the submitted version.

ACKNOWLEDGMENTS

With thanks to Mrs. Lorna McBroom for proofreading and language editing of the manuscript.

REFERENCES

1. Marder SR, Cannon TD. Schizophrenia. *N Engl J Med.* (2019) 381:1753–61. doi: 10.1056/NEJMra1808803
2. Zanelli J, Mollon J, Sandin S, Morgan C, Dazzan P, Pilecka I, et al. Cognitive change in schizophrenia and other psychoses in the decade following the first episode. *Am J Psychiatry.* (2019) 176:811–9. doi: 10.1176/appi.ajp.2019.18091088
3. Shahab S, Mulsant BH, Levesque ML, Calarco N, Nazeri A, Wheeler AL, et al. Brain structure, cognition, and brain age in schizophrenia, bipolar disorder, and healthy controls. *Neuropsychopharmacology.* (2019) 44:898–906. doi: 10.1038/s41386-018-0298-z
4. Eisenberg DP, Berman KF. Executive function, neural circuitry, and genetic mechanisms in schizophrenia. *Neuropsychopharmacology.* (2010) 35:258–77. doi: 10.1038/npp.2009.111
5. Green MF, Harvey PD. Cognition in schizophrenia: past, present, and future. *Schizophr Res Cogn.* (2014) 1:e1–9. doi: 10.1016/j.scog.2014.02.001
6. Bowie CR, Harvey PD. Administration and interpretation of the trail making test. *Nat Protoc.* (2006) 1:2277–81. doi: 10.1038/nprot.2006.390
7. Tombaugh T. Trail making test A and B: normative data stratified by age and education. *Arch Clin Neuropsychol.* (2004) 19:203–14. doi: 10.1016/S0887-6177(03)00039-8
8. Heinrichs RW, Zakzanis KK. Neurocognitive deficit in schizophrenia: a quantitative review of the evidence. *Neuropsychology.* (1998) 12:426. doi: 10.1037/0894-4105.12.3.426
9. Fujiki R, Morita K, Sato M, Kamada Y, Kato Y, Inoue M, et al. Reduced prefrontal cortex activation using the trail making test in schizophrenia. *Neuropsychiatr Dis Treat.* (2013) 9:675–85. doi: 10.2147/NDT.S43137
10. Stuss DT. Functions of the frontal lobes: relation to executive functions. *J Int Neuropsychol Soc.* (2011) 17:759–65. doi: 10.1017/S1355617711000695
11. Stroobant N, Vingerhoets G. Transcranial doppler ultrasonography monitoring of cerebral hemodynamics during performance of cognitive tasks: a review. *Neuropsychol Rev.* (2000) 10:213–31. doi: 10.1023/A:1026412811036
12. Wolf ME. Functional TCD: regulation of cerebral hemodynamics–cerebral autoregulation, vasomotor reactivity, and neurovascular coupling. *Front Neurol Neurosci.* (2015) 36:40–56. doi: 10.1159/000366236
13. Duschek S, Schandry R. Functional transcranial doppler sonography as a tool in psychophysiological research. *Psychophysiology.* (2003) 40:436–54. doi: 10.1111/1469-8986.00046
14. Schuepbach D, Egger ST, Boeker H, Duschek S, Vetter S, Seifritz E, et al. Determinants of cerebral hemodynamics during the trail making test in schizophrenia. *Brain Cogn.* (2016) 109:96–104. doi: 10.1016/j.bandc.2016.09.002
15. Liddle P, Friston K, Frith C, Hirsch S, Jones T, Frackowiak R. Patterns of cerebral blood flow in schizophrenia. *Br J Psychiatry.* (1992) 160:179–86. doi: 10.1192/bjp.160.2.179
16. Kekin I, Bosnjak D, Makaric P, Bajic Z, Rossini Gajsak L, Malojcic B, et al. Significantly lower right middle cerebral artery blood flow velocity in the first episode of psychosis during neurocognitive testing. *Psychiatr Dan.* (2018) 30:172–82. doi: 10.24869/spsih.2018.172
17. Zakzanis KK, Mraz R, Graham SJ. An fMRI study of the trail making test. *Neuropsychologia.* (2005) 43:1878–86. doi: 10.1016/j.neuropsychologia.2005.03.013
18. Kubo M, Shoshi C, Kitawaki T, Takemoto R, Kinugasa R, Yoshida H, et al. Increase in prefrontal cortex blood flow during the computer version trail making test. *Neuropsychobiology.* (2008) 58:200–10. doi: 10.1159/000201717
19. Tatu L, Moulin T, Bogousslavsky J, Duvernoy H. Arterial territories of the human brain: cerebral hemispheres. *Neurology.* (1998) 50:1699–708. doi: 10.1212/WNL.50.6.1699
20. Misteli M, Duschek S, Richter A, Grimm S, Rezk M, Kraehenmann R, et al. Gender characteristics of cerebral hemodynamics during complex cognitive functioning. *Brain Cogn.* (2011) 76:123–30. doi: 10.1016/j.bandc.2011.02.009
21. World Health Organization. *WHO: The ICD-10 Classification of Mental and Behavioural Disorders: Clinical Descriptions and Diagnostic Guidelines*. Geneva: World Health Organization (1992).
22. Overall JE, Gorham DR. The brief psychiatric rating scale. *Psychol Rep.* (1962) 10:799–812. doi: 10.2466/pr0.1962.10.3.799
23. Guy W. *ECDEU Assessment Manual For Psychopharmacology*. Rockville: US Department of Health, Education, and Welfare, Public Health Service, Alcohol, Drug Abuse, and Mental Health Administration, National Institute of Mental Health, Psychopharmacology Research Branch, Division of Extramural Research Programs (1976).
24. Woods SW. Chlorpromazine equivalent doses for the newer atypical antipsychotics. *J Clin Psychiatry.* (2003) 64:663–7. doi: 10.4088/JCP.v64n0607
25. Rey MJ, Schulz P, Costa C, Dick P, Tissot R. Guidelines for the dosage of neuroleptics. I: Chlorpromazine equivalents of orally administered neuroleptics. *Int Clin Psychopharmacol.* (1989) 4:95–104. doi: 10.1097/00004850-198904000-00001
26. Simpson GM, Angus JW. A rating scale for extrapiramidal side effects. *Acta Psychiatr Scandinav.* (1970) 45(S212):11–19. doi: 10.1111/j.1600-0447.1970.tb02066.x
27. Barnes TR. A rating scale for drug-induced akathisia. *Br J Psychiatry.* (1989) 154:672–676. doi: 10.1192/bjp.154.5.672
28. Barnes TR. The Barnes Akathisia rating scale–revisited. *J Psychopharmacol.* (2003) 17:365–70. doi: 10.1177/0269881103174013
29. Leucht S, Kane JM, Kissling W, Hamann J, Etschel E, Engel R. Clinical implications of brief psychiatric rating scale scores. *Br J Psychiatry.* (2005) 187:366–71. doi: 10.1192/bjp.187.4.366
30. Lohmann H, Ringelstein EB, Knecht S. Functional transcranial doppler sonography. *Front Neurol Neurosci.* (2006) 21:251–60. doi: 10.1159/000092437
31. Brodie FG, Atkins ER, Robinson TG, Panerai RB. Reliability of dynamic cerebral autoregulation measurement using spontaneous fluctuations in blood pressure. *Clin Sci.* (2009) 116:513–20. doi: 10.1042/CS20080236

32. Sejdic E, Kalika D, Czarnek N. An analysis of resting-state functional transcranial doppler recordings from middle cerebral arteries. *PLoS ONE.* (2013) 8:e55405. doi: 10.1371/journal.pone.0055405
33. Larsen K. GAM: the predictive modeling silver bullet. Multithreaded. *Stitch Fix.* (2015) 30:196–223.
34. van Oijen M. Linear modelling: LM, GLM, GAM and mixed models. In: van Oijen M, editors. *Bayesian Compendium*. Springer (2020).
35. Rigby RA, Stasinopoulos DM. Generalized additive models for location, scale and shape. *J Royal Stat Soc Series C.* (2005) 54:507–54. doi: 10.1111/j.1467-9876.2005.00510.x
36. Agarwal R, Frosst N, Zhang X, Caruana R, Hinton GE. Neural additive models: interpretable machine learning with neural nets. *Arxiv Prep Arxiv*. (2020).
37. Sørensen Ø, Brandmaier AM, Macià D, Ebmeier K, Ghisletta P, Kievit RA, et al. Meta-analysis of generalized additive models in neuroimaging studies. *NeuroImage.* (2021) 224:117416. doi: 10.1016/j.neuroimage.2020.117416
38. Boban M, Crnac P, Junakovic A, Malojcic B. Hemodynamic monitoring of middle cerebral arteries during cognitive tasks performance. *Psychiatry Clin Neurosci.* (2014) 68:795–803. doi: 10.1111/pcn.12191
39. Phillips AA, Chan FH, Zheng MMZ, Krassioukov AV, Ainslie PN. Neurovascular coupling in humans: physiology, methodological advances and clinical implications. *J Cereb Blood Flow Metab.* (2016) 36:647–64. doi: 10.1177/0271678X15617954
40. Mikadze YV, Lysenko ES, Bogdanova MD, Abuzaid SM, Shakhnovich AR. Interhemispheric differences observed during the performance of cognitive tasks using doppler ultrasound. *Human Physiol.* (2018) 44:170–4. doi: 10.1134/S0362119718020135
41. Henseler I, Falkai P, Gruber O. A systematic fMRI investigation of the brain systems subserving different working memory components in schizophrenia. *Eur J Neurosci.* (2009) 30:693–702. doi: 10.1111/j.1460-9568.2009.06850.x
42. Puglisi V, Bramanti A, Lanza G, Cantone M, Vinciguerra L, Pennisi M, et al. Impaired cerebral haemodynamics in vascular depression: insights from transcranial doppler ultrasonography. *Front Psychiatry.* (2018) 9:316. doi: 10.3389/fpsyt.2018.00316
43. Vinciguerra L, Lanza G, Puglisi V, Pennisi M, Cantone M, Bramanti A, et al. Transcranial doppler ultrasound in vascular cognitive impairment-no dementia. *PLoS ONE.* (2019) 14:e0216162. doi: 10.1371/journal.pone.0216162
44. Wright S, Kochunov P, Chiappelli J, McMahon R, Muellerklein F, Wijtenburg SA, et al. Accelerated white matter aging in schizophrenia: role of white matter blood perfusion. *Neurobiol Aging.* (2014) 35:2411–8. doi: 10.1016/j.neurobiolaging.2014.02.016
45. Kochunov P, Chiappelli J, Wright SN, Rowland LM, Patel B, Wijtenburg SA, et al. Multimodal white matter imaging to investigate reduced fractional anisotropy and its age-related decline in schizophrenia. *Psychiatry Res.* (2014) 223:148–56. doi: 10.1016/j.pscychresns.2014.05.004
46. Lee SM, Chou YH, Li MH, Wan FJ, Yen MH. Effects of antipsychotics on cognitive performance in drug-naive schizophrenic patients. *Prog Neuropsychopharmacol Biol Psychiatry.* (2007) 31:1101–7. doi: 10.1016/j.pnpbp.2007.03.016
47. Lee SM, Chou YH, Li MH, Wan FJ, Yen MH. Effects of haloperidol and risperidone on cerebrohemodynamics in drug-naive schizophrenic patients. *J Psychiatr Res.* (2008) 42:328–35. doi: 10.1016/j.jpsychires.2007.02.007
48. Fervaha G, Agid O, Takeuchi H, Lee J, Foussias G, Zakzanis KK, et al. Extrapyramidal symptoms and cognitive test performance in patients with schizophrenia. *Schizop Res.* (2015) 161:351–6. doi: 10.1016/j.schres.2014.11.018
49. Mentzel CL, Bakker PR, Van Os J, Drukker M, Matroos GE, Hoek HW, et al. Effect of antipsychotic type and dose changes on tardive dyskinesia and parkinsonism severity in patients with a serious mental illness: the curacao extrapyramidal syndromes study XII. *J Clin Psychiatry.* (2017) 78:279–85. doi: 10.4088/JCP.16m110491
50. Schuepbach D, Michel M, Wagner G, Duschek S, Herpertz SC. Extrapyramidal symptoms in schizophrenia: evidence of blunted cerebral hemodynamics during a planning task. *Int Clin Psychopharmacol.* (2017) 32:225–30. doi: 10.1097/YIC.0000000000000171
51. Herold CJ, Schmid LA, Lässer MM, Seidl U, Schröder J. Cognitive performance in patients with chronic schizophrenia across the lifespan. *GeroPsych.* (2017) 30:35–44. doi: 10.1024/1662-9647/a000164
52. Sørup FKH, Brunak S, Eriksson R. Association between antipsychotic drug dose and length of clinical notes: a proxy of disease severity? *BMC Med Res Methodol.* (2020) 20:1–7. doi: 10.1186/s12874-020-00993-1
53. Duschek S, Heiss H, Schmidt MF, Werner NS, Schuepbach D. Interactions between systemic hemodynamics and cerebral blood flow during attentional processing. *Psychophysiology.* (2010) 47:1159–66. doi: 10.1111/j.1469-8986.2010.01020.x
54. Panerai RB, Eyre M, Potter JF. Multivariate modeling of cognitive-motor stimulation on neurovascular coupling: transcranial doppler used to characterize myogenic and metabolic influences. *Am J Physiol Regul Integr Comp Physiol.* (2012) 303:R395–407. doi: 10.1152/ajpregu.00161.2012
55. Van den Bergh O, Zaman J, Bresseleers J, Verhamme P, Van Diest I. Anxiety, pCO2 and cerebral blood flow. *Int J Psychophysiol.* (2013) 89:72–7. doi: 10.1016/j.ijpsycho.2013.05.011

Conflict of Interest: The authors declare that the research was conducted in the absence of any commercial or financial relationships that could be construed as a potential conflict of interest.

frontiers in Psychiatry

ORIGINAL RESEARCH
published: 10 August 2021
doi: 10.3389/fpsyt.2021.673443

Eye Movement Abnormalities in Major Depressive Disorder

Junichi Takahashi[1], Yoji Hirano[1,2], Kenichiro Miura[3], Kentaro Morita[4,5], Michiko Fujimoto[3,6], Hidenaga Yamamori[3,6,7], Yuka Yasuda[3,8], Noriko Kudo[3,9], Emiko Shishido[10], Kosuke Okazaki[11], Tomoko Shiino[12,13], Tomohiro Nakao[1], Kiyoto Kasai[5,14], Ryota Hashimoto[3,6] and Toshiaki Onitsuka[1]**

[1] Department of Neuropsychiatry, Graduate School of Medical Sciences, Kyushu University, Fukuoka, Japan, [2] Institute of Industrial Science, The University of Tokyo, Tokyo, Japan, [3] Department of Pathology of Mental Diseases, National Institute of Mental Health, National Center of Neurology and Psychiatry, Kodaira, Japan, [4] Department of Rehabilitation, The University of Tokyo Hospital, Tokyo, Japan, [5] Department of Neuropsychiatry, Graduate School of Medicine, The University of Tokyo, Tokyo, Japan, [6] Department of Psychiatry, Graduate School of Medicine, Osaka University, Suita, Japan, [7] Japan Community Health Care Organization Osaka Hospital, Osaka, Japan, [8] Life Grow Brilliant Mental Clinic, Osaka, Japan, [9] Graduate School of Science and Technology, Nara Institute of Science and Technology, Ikoma, Japan, [10] Division of Cerebral Integration, Department of System Neuroscience, National Institute for Physiological Sciences, Okazaki, Japan, [11] Department of Psychiatry, Nara Medical University, Kashihara, Japan, [12] Division of Developmental Emotional Intelligence, Research Center for Child Mental Development, University of Fukui, Fukui, Japan, [13] United Graduate School of Child Development, Osaka University, Kanazawa University, Hamamatsu University School of Medicine, Chiba University and University of Fukui, Suita, Japan, [14] The International Research Center for Neurointelligence (WPI-IRCN), The University of Tokyo Institutes for Advanced Study, Tokyo, Japan

OPEN ACCESS

Edited by:
Tae Young Lee,
Pusan National University Yangsan Hospital, South Korea

Reviewed by:
Nikolaos Smyrnis,
National and Kapodistrian University of Athens, Greece
Missal Marcus,
Catholic University of Louvain, Belgium
Pedro E. Maldonado,
University of Chile, Chile
Elisa C. Dias,
Nathan Kline Institute for Psychiatric Research, United States

***Correspondence:**
Yoji Hirano
yhouji@mac.com
Toshiaki Onitsuka
onitsuka.toshiaki.939@m.kyushu-u.ac.jp

Specialty section:
This article was submitted to Neuroimaging and Stimulation, a section of the journal Frontiers in Psychiatry

Received: 27 February 2021
Accepted: 14 July 2021
Published: 10 August 2021

Citation:
Takahashi J, Hirano Y, Miura K, Morita K, Fujimoto M, Yamamori H, Yasuda Y, Kudo N, Shishido E, Okazaki K, Shiino T, Nakao T, Kasai K, Hashimoto R and Onitsuka T (2021) Eye Movement Abnormalities in Major Depressive Disorder. Front. Psychiatry 12:673443. doi: 10.3389/fpsyt.2021.673443

Background: Despite their high lifetime prevalence, major depressive disorder (MDD) is often difficult to diagnose, and there is a need for useful biomarkers for the diagnosis of MDD. Eye movements are considered a non-invasive potential biomarker for the diagnosis of psychiatric disorders such as schizophrenia. However, eye movement deficits in MDD remain unclear. Thus, we evaluated detailed eye movement measurements to validate its usefulness as a biomarker in MDD.

Methods: Eye movements were recorded from 37 patients with MDD and 400 healthy controls (HCs) using the same system at five University hospitals. We administered free-viewing, fixation stability, and smooth pursuit tests, and obtained 35 eye movement measurements. We performed analyses of covariance with group as an independent variable and age as a covariate. In 4 out of 35 measurements with significant group-by-age interactions, we evaluated aging effects. Discriminant analysis and receiver operating characteristic (ROC) analysis were conducted.

Results: In the free-viewing test, scanpath length was significantly shorter in MDD ($p = 4.2 \times 10^{-3}$). In the smooth pursuit test, duration of saccades was significantly shorter and peak saccade velocity was significantly lower in MDD ($p = 3.7 \times 10^{-3}$, $p = 3.9 \times 10^{-3}$, respectively). In the fixation stability test, there were no significant group differences. There were significant group differences in the older cohort, but not in the younger cohort, for the number of fixations, duration of fixation, number of saccades, and fixation density in the free-viewing test. A discriminant analysis using scanpath length in the free-viewing test and peak saccade velocity in the smooth pursuit showed MDD could be distinguished from HCs with 72.1% accuracy. In the ROC analysis,

the area under the curve was 0.76 (standard error = 0.05, $p = 1.2 \times 10^{-7}$, 95% confidence interval = 0.67–0.85).

Conclusion: These results suggest that detailed eye movement tests can assist in differentiating MDD from HCs, especially in older subjects.

Keywords: major depressive disorder, free-viewing test, fixation stability test and smooth pursuit test, alerted aging effect, discriminant analysis, eye movements

INTRODUCTION

Major depressive disorder (MDD) is a common global disorder that affects over 264 million people (1). Depression is ranked as the single largest contributor to global disability (7.5% of all years lived with a disability) (2) and has been one of the top three leading causes of health loss for nearly three decades (3). The lifetime prevalence of MDD was reported to be 14–17% with a 1-year prevalence of 4–8% (WHO, 2020). Many studies have attempted to elucidate the pathophysiology of depression; however, it remains poorly understood. Stressful events, genetic vulnerability, environmental interactions, abnormalities in several neurotransmitters, inflammation, as well as alterations in neuropeptides and hormones have been investigated as causes of MDD (4–6). Natural disasters (7), pandemics such as COVID-19 (8–10), and cultural differences (11–14) also have a huge impact on the development of MDD.

Clinically, it is difficult to diagnose mood disorders in patients with MDD and bipolar disorder (15). For example, during the initial evaluation, patients with bipolar disorder sometimes show only depressive symptoms and thus receive antidepressants based on a diagnosis of MDD, which may cause several critical problems (16, 17). For this reason, objective indices for MDD are needed; however, to date, none have been established.

Eye movements are considered a potential biomarker for the diagnosis of mental illness (18, 19). We previously showed an integrated score using three measurements (scanpath length during a free-viewing test, horizontal position gain during the fast Lissajous paradigm in a smooth pursuit test, and the duration of fixations during the far distractor paradigm of a fixation stability test) could distinguish between patients with schizophrenia (SZ) and HCs with 82% accuracy (20). A recent review has provided convincing evidence of eye-movement abnormalities in SZ (21, 22). However, Smyrnis et al. (23) noted that the sensitivity of eye movement deficits to differentiate psychiatric patients from healthy controls (HCs) was not high enough to be clinically relevant for diagnostic purposes. In the previous study (20), our group reported that eye movement can be a useful biomarker for schizophrenia. In order to use eye movements as a diagnostic tool, it is necessary to discriminate schizophrenia from other psychiatric disorders. Therefore, we conducted the same tasks used in the previous studies.

As listed in **Table 1**, several studies have used different methods to evaluate eye movements in MDD. Iacono et al. (24) reported that the performance of the MDD group was not significantly different from that of the HC group regarding smooth-pursuit eye movement (SPEM), but smooth-pursuit tracing errors were greater for those with a higher frequency of episodes of the disorder. Abel et al. (25) studied smooth pursuit gain and catch-up saccade (CUS) in affective disorders and found that when the constant stimulus velocity was 5°/s, but not 20°/s, MDD patients had higher CUS rates than HCs. Malaspina et al. (26) studied the effects of electroconvulsive therapy (ECT) on SPEM with severe MDD and reported that SPEM was transiently disrupted but pursuit performances were improved after two sessions of ECT and at 2 months follow-up. They concluded that SPEM abnormalities may be a state marker in severe MDD. Flechtner et al. (27) explored SPEM in thirty-four MDD patients and found they exhibited lower pursuit gain and higher CUS rates than HCs. Flechtner et al. (28) also reported that SPEM performance was not influenced by medication or clinical state in a test-retest study. Fabisch et al. (29) reported no significant difference between unipolar depressed patients and HCs. Li et al. (31) reported that compared with the HC group, the MDD group had a significantly shorter duration and more saccades in a fixation stability test. Taken together, these studies indicate inconsistent findings regarding eye movement abnormalities in MDD.

In the present study, we recorded eye movements and determined the detailed characteristics of eye movements in MDD patients at multiple facilities. We then examined how eye movements might be useful for differentiating between MDD and HCs.

MATERIALS AND METHODS

Subjects

Patients with MDD recruited from Kyushu University Hospital, Osaka University Hospital, The University of Tokyo Hospital, and Nagoya University Hospital were diagnosed by two or more trained psychiatrists according to criteria from the DSM-IV based on the Structured Clinical Interview for DSM-IV (SCID). All subjects were biologically unrelated, were of Japanese descent, and had no history of ophthalmologic disease, or neurological/medical conditions that might influence the central nervous system. Specific exclusion criteria included atypical headaches, head trauma with loss of consciousness, thyroid disease, epilepsy, seizures, substance-related disorders, or intellectual disability. HCs were recruited through regional advertisements and were evaluated for psychiatric, medical, and neurological concerns using the non-patient version of the SCID to exclude individuals with current or past contact with psychiatric services or who had received psychiatric medication. Eye movements were recorded

TABLE 1 | Demographic and clinical characteristics of the study subjects and major findings of patients with MDD in eight eye movement studies.

		MDD patients							Healthy controls						
			Age (years)		Male		Currently on medication			Age (years)		Male			
Study	**Task**	***N***	**Mean**	**SD**	***N***	**%**	***N***	**%**	***N***	**Mean**	**SD**	***N***	**%**	**Parameters**	**Major findings in MDD**
Iacono et al. (24)[a]	SPEM	25	37.9	12.9	5	20	N/A	N/A	46	35.0	11.9	8	22.9	RT, RMSE	All variables: no significance
Abel et al. (25)[b]	SPEM	16	48.4	12.4	16	100	4	25	21	37.5	10.9	21	100	TWAG, CUS rates, CUS amplitude	Higher CUS rates in 5°/s SPEM
Malaspina et al. (26)	SPEM	18	28.9	5.6	N/A	N/A	0	0	20	30.6	7	N/A	N/A	% abn, Large saccades	All variables: no significance
Flechtner et al. (27)	SPEM	34	46.9	11	9	26.5	30	88.2	42	34.3	10.9	20	47.6	Pursuit gain, CUS, Anticipatory saccade, BUS, SWJ	Lower pursuit gain
Flechtner et al. (28)[c]	SPEM	34	46.9	11	9	26.5	34	100	42	34.3	10.9	20	47.6	Pursuit gain, CUS, Anticipatory saccade, BUS, SWJ	All variables: no significant difference between all time
Fabisch et al. (29)	SPEM	19	34.4	8.3	19	100	19	100	21	37.8	5.9	21	100	Peak gain, CUS error, CUS velocities	All variables: no significance
Chen et al. (30)	FVT	19	28.3	4.7	N/A	N/A	0	0	19	27.9	4.6	N/A	N/A	NF, tFD, aFD	More NF, longer tFD and aFD
Li et al. (31)	FST	60	25.4	7.2	N/A	N/A	0	0	60	24.2	6.1	N/A	N/A	NF, FD, Number of saccades, Saccade path	More NF and number of saccades, shorter FD, longer saccade path
	FVT													NF, Duration of saccade, Saccade amplitude, mFD, Saccade path	Shorter duration of saccade, longer mFD

SPEM, Smooth pursuit eye movement; FVT, Free-viewing test; FST, Fixation stability test; RT, Reaction time; RMSE, Root mean square error; TWAG, Time-weight average gain; CUS, Catch-up saccade; BUS, Back-up saccade; SWJ, Square wave jerk, NF, number of fixations; tFD, total fixation duration; aFD, average fixation duration; FD, fixation duration; mFD, mean fixation duration.

[a] *This study analyzed remitted MDD.*

[b] *This study analyzed affective disorders (MDD non-psychotic = 10, MDD psychotic = 1, bipolar depression non-psychotic = 4, schizoaffective disorder = 1).*

[c] *A longitudinal study by Flechtner et al. (27).*

TABLE 2 | Demographics of the HC and MDD groups.

	HCs	MDD	χ^2 or *t*	*p*-value
Male/female	201/199	18/19	0.04	0.85
Age (years)	35.3 ± 14.8	49.5 ± 11.6	−7.0	$8.6 \times 10^{-9*}$
Education (years)	15.4 ± 2.3	14.5 ± 2.4	2.1	0.41
Premorbid IQ	107.7 ± 8.1	106.9 ± 10.9	0.38	0.71
Current IQ	107.1 ± 12.0	100.4 ± 13.5	2.7	$6.7 \times 10^{-3*}$
Onset age (years)		36.9 ± 13.6		
Duration of illness (years)		13.0 ± 8.4		
HAM-D		12.0 ± 6.3		
IMP (mg)		187.9 ± 150.4		
DZP (mg)		6.0 ± 5.9		
CPZ (mg)		61.9 ± 117.1		

Premorbid IQ was estimated using the Japanese Adult Reading Test.
Current IQ was estimated using the Wechsler Intelligence Scale short form.
HAM-D, Hamilton Depression Rating Scale; IMP, imipramine; DZP, diazepam; CPZ, chlorpromazine.
$^*p < 0.05$.

from 51 patients with MDD and 519 HCs, who were recruited from Kyushu University (28 MDD, 29 HCs), Osaka University (15 MDD, 333 HCs), The University of Tokyo (6 MDD, 70 HCs), Nagoya University (2 MDD, 48 HCs), and Nara Medical University (0 MDD, 40 HCs). Each facility used a common protocol and analysis manual, and quality control was performed every 2 months to ensure uniformity of the data. We used the data from 37 patients with MDD and 400 HCs, for which the quality of the data was ensured by rigorous quality checks. Current symptoms of depression were evaluated using the Hamilton Depression Scale (HAM-D) (32) and the total dosages of prescribed the antidepressant benzodiazepine or antipsychotics were calculated using imipramine (IMP), diazepam (DZP), and chlorpromazine (CPZ) equivalents (mg/day) (33). The demographic information of the study subjects is shown in **Table 2**. Based on the criteria for depression (34), 15 patients showed mild depression, 9 showed moderate depression, 1 showed severe depression and 9 were euthymic. HAM-D scores of the three patients were unknown.

The study was performed in accordance with the World Medical Association's Declaration of Helsinki and was approved by the Research Ethical Committees of Kyushu University, Osaka University, The University of Tokyo, Nagoya University, and Nara Medical University. All participants provided written consent to the study after a full explanation of the study procedures. Anonymity was preserved for all participants.

Eye Movement Recordings and Processing of Eye Movement Data

The subjects faced a 19-inch liquid crystal display monitor placed 70 cm from the observers' eyes. Visual stimuli were presented using MATLAB (The Mathworks, Natick, MA, USA) *via* the Psychophysics Toolbox extension (35). The eye movements and pupil areas of the left eye were measured at 1 kHz using the EyeLink1000 Plus (SR Research, Ontario, Canada) system.

Eye position data were smoothed with a digital FIR filter (−3 dB at 30 Hz), and the eye velocity and acceleration traces were obtained using a two-point forward difference algorithm to identify saccadic eye movements. Eye movement records were segmented into the blink, the saccade, and the fixation periods. Further details are described in **Supplementary Methods**.

Eye Movement Paradigms and Extracted Measurements

We administered 3 eye movement paradigms (free-viewing test, fixation stability test, and smooth pursuit test) and obtained 35 eye movement measurements comprising 13 measurements from the free viewing test, 16 measurements from the smooth pursuit test, and 6 measurements from the fixation stability test. We chose the examinations of eye movements used in the previously published reports (18, 36, 37). Examples of eye movement examinations are shown in **Figure 1**. Each paradigm is discussed in detail below.

The free-viewing test was performed using images from five categories that involved buildings, everyday items, foods, fractal patterns, and noise (four images for each category). The subjects were instructed to freely view the presented image for 8 s (**Figure 1A**). We measured the number and the median duration of the fixations, the number of saccades, the median durations, the amplitude, the mean and the peak velocity of saccades, the scanpath length, and the fixation density (38). The medians over each image were calculated for each eye movement measurement. In addition, we examined the main sequence relation of the saccades of individual subjects (for details, see **Supplementary Methods**).

In the smooth pursuit eye movement test, subjects were required to track a moving target for 20 s. The target moved horizontally and vertically with a Lissajous trajectory (**Figure 1B**) and the trial was repeated twice. We measured the number and the median duration of fixations, along with the number, median

FIGURE 1 | Eye movement paradigms. **(A)** Free-viewing test*. **(B)** Lissajous trajectories of the smooth pursuit eye movement test. **(C)** Fixation stability test. The fixed target (center) and a distracter stimulus (right). *This image example is a photo taken by the author which is not the actual one used for the test.

duration, amplitude, mean, and peak velocities of saccades. In addition, we measured the position gain, the velocity gain, the common logarithm of the signal-to-noise ratio (SNR), and the root mean square error (RMSE) for the horizontal and vertical eye movements separately in each trial.

For the fixation stability test, subjects were required to maintain their gaze on a fixed target presented at the center of the monitor (**Figure 1C**). A few seconds (1–2 s randomly) after the central fixed target was continually presented, a distracter stimulus appeared at 3° right or left of the central fixed target and presented for 5 s. We measured the number of fixations, the median duration of fixations, the number of saccades, the number of microsaccades, and the scanpath length for each trial. The trial was repeated four times, and we calculated the mean of each eye movement measure over all the trials.

Because some eye movement measurements are influenced by optical devices (39), we divided subjects into naked eye, glasses, and soft contact lens groups and normalized the measurements. Z-scores are dimensionless mathematical tools that allow for the mean-normalization of results within groups. Z-scores are standardized scores (by the group mean and group standard deviation) and no normal assumption is made. They indicate how many standard deviations (σ) an observation (X) is above or below the mean of a control group (μ).

$$z = \frac{X - \mu}{\sigma},$$

where X represents individual data for the observed measurement and μ and σ represent the mean and the standard deviation for the control group, respectively.

Statistical Analysis

All statistical analyses were performed using SPSS 26.0 (IBM Corp., Armonk, NY, USA). Group comparisons of demographic variables were performed using a two-tailed t-test or a χ^2-test when appropriate.

Because we previously reported that age should be considered when investigating eye movements (40) and other studies also indicated significant effects of age on saccadic eye movements and smooth pursuit eye movements (41, 42), we performed analyses of covariance (ANCOVAs) with the group factor as an independent variable and age as a covariate for z score of each eye measurement. We performed a correction with a false discovery rate (FDR) of 0.05 (Benjamini–Hochberg procedure) for each measurement, considering the nature of multiple comparisons. When significant group-by-age interactions were observed, to evaluate the age effect, we divided MDD and HCs into two cohorts (younger and older cohorts) stratified by the median age of MDD, 48 years [HC group: younger cohort ($N = 314$), older cohort ($N = 86$); MDD group: younger cohort ($N = 19$), older cohort ($N = 18$)]. Then, we examined the simple main effects of group in younger and older cohorts using a general linear model.

For associations between eye movement measurements and demographics, we conducted multiple regression analyses using the stepwise method with eye movement measurements, which showed a significant difference between groups, where eye movement measurements were dependent variables, and age, medication (CPZ, DZP, and IMP equivalents), and HAM-D scores were independent variables. The significance level was set at $p < 0.05$.

A linear discriminant analysis was performed using statistically significant measurements as independent valuables between groups. After the discriminant analysis, the discriminant score was calculated. Optimal sensitivity and specificity of the discriminant score to differentiate between MDD and HCs were determined *via* receiver operating characteristic (ROC) curve analysis using a non-parametric approach. We calculated the Youden index for each cutoff value [(sensitivity + specificity) – 1] to find the cutoff values that maximized the discriminating power.

In addition, 37 HCs were randomly selected to match ages between groups by a technician who was unrelated to this study, and we performed t-tests to evaluate age-matched group differences in eye movement measurements. A linear discriminant analysis was also performed.

TABLE 3 | Results of ANCOVA.

	HCs ($n = 400$)		MDD ($n = 37$)			Age-by-group interaction		Effect of group	
	Median	**SD**	**Median**	**SD**	***df***	***F*-value**	***p*-value**	***F*-value**	***p*-value**
Free-viewing test									
Number of fixations	23.00	3.32	21.50	4.93	1,433	5.07	$2.5 \times 10^{-2*}$	N/A	N/A
Duration of fixation	254.50	46.30	267.00	86.41	1,433	5.51	$1.9 \times 10^{-2*}$	N/A	N/A
Number of saccades	21.00	3.80	20.00	5.33	1,433	7.19	$7.6 \times 10^{-3*}$	N/A	N/A
Duration of saccades	42.38	5.59	42.50	6.65	1,433	0.10	0.75	0.91	0.34
Saccade amplitude	4.00	1.17	3.60	0.99	1,433	0.00	0.99	0.66	0.42
Average saccade velocity	93.94	19.25	81.99	17.50	1,433	0.12	0.73	2.51	0.11
Peak saccade velocity	185.10	44.55	181.81	43.85	1,433	0.73	0.39	0.01	0.91
Scanpath length	110.70	28.81	92.56	34.98	1,433	2.19	0.14	8.30	$4.2 \times 10^{-3**}$
Fixation density	0.88	0.39	0.92	0.51	1,433	9.58	$2.1 \times 10^{-3*}$	N/A	N/A
Main sequence v_{max}	436.81	119.83	419.68	107.90	1,433	0.39	0.53	0.41	0.52
Main sequence s	9.29	4.40	7.63	3.95	1,433	0.00	0.95	0.13	0.72
Main sequence v_0	33.93	9.88	32.60	10.27	1,433	0.57	0.45	0.01	0.94
Number of blinks	1.00	1.49	1.00	1.31	1,433	3.64	0.06	0.45	0.50
Smooth pursuit test									
Horizontal SNR	2.03	0.16	2.02	0.18	1,433	2.74	0.10	0.00	0.95
Horizontal position gain	1.01	0.03	1.00	0.03	1,433	0.93	0.33	0.34	0.56
Horizontal RMSE	8.35	4.18	8.78	4.11	1,433	2.30	0.13	0.39	0.53
Vertical SNR	1.84	0.20	1.80	0.20	1,433	1.22	0.27	0.27	0.60
Vertical position gain	0.96	0.07	0.95	0.09	1,433	0.67	0.41	1.18	0.28
Vertical RMSE	14.03	7.94	13.83	9.69	1,433	1.56	0.21	0.15	0.70
Number of fixations	58.25	13.77	60.00	13.99	1,433	0.17	0.68	1.00	0.32
Duration of fixations	259.88	69.00	250.75	79.92	1,433	1.29	0.26	4.27	0.04
Number of saccades	56.00	15.71	59.50	13.85	1,433	0.16	0.69	0.73	0.39
Duration of saccades	30.13	5.63	34.50	9.41	1,433	3.62	0.06	8.54	$3.7 \times 10^{-3**}$
Saccade amplitude	1.94	0.62	2.38	0.71	1,433	3.22	0.07	5.40	0.02
Average saccade velocity	65.13	11.71	70.80	9.85	1,433	0.00	0.96	1.42	0.23
Peak saccade velocity	98.05	38.71	136.46	46.52	1,433	2.32	0.13	8.41	$3.9 \times 10^{-3**}$
Horizontal velocity gain	0.85	0.11	0.77	0.14	1,433	0.85	0.36	4.60	0.03
Vertical velocity gain	0.76	0.13	0.70	0.16	1,433	0.59	0.44	1.43	0.23
Number of blinks	1.00	4.00	1.00	2.57	1,433	0.10	0.76	0.24	0.62
Fixation stability test									
Number of fixations	3.00	2.46	3.25	2.71	1,433	0.25	0.62	0.10	0.75
Duration of fixation	2057.19	1492.87	1422.50	1558.35	1,433	0.21	0.64	0.50	0.48
Number of saccades	1.50	2.30	2.00	2.53	1,433	0.91	0.34	0.04	0.85
Scanpath length	1.13	2.21	1.36	2.43	1,433	0.23	0.63	0.02	0.89
Number of microsaccades	6.25	3.51	6.50	4.17	1,433	0.46	0.50	0.13	0.72
Number of blinks	0.00	0.97	0.00	0.70	1,433	2.68	0.10	0.04	0.84

RMSE, Root mean square error; SNR, signal-to-noise ratio; N/A, not applicable.
*$p < 0.05$.
***Represents significant after false discovery rate correction.*

RESULTS

Demographics and Eye Movement Measurements

The demographics of both groups are shown in **Table 2**. There was no difference in the sex ratio between the two groups ($p = 0.85$) or years of education ($p = 0.41$); however, age was significantly different ($p = 8.6 \times 10^{-9}$).

Overall, 35 eye movement measurements were obtained in this study. In the HC group, 189 subjects were naked eyes, 124 wore glasses, and 87 had soft contact lenses, whereas 20, 14, and 3 were naked eyes, wore glasses, or had soft contact lenses in the MDD group, respectively (**Supplementary Table 1**).

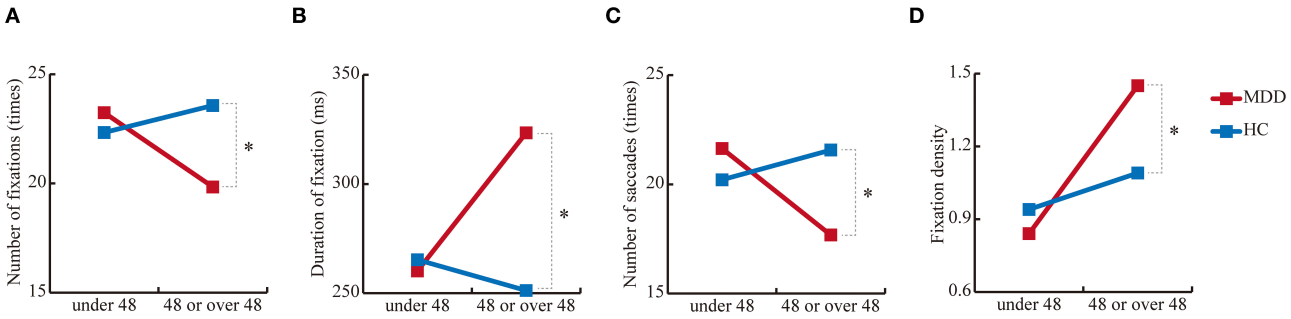

FIGURE 2 | Simple main effects of group. **(A)** Number of fixations, **(B)** duration of fixation, **(C)** number of saccades, and **(D)** fixation density in the free-viewing test. *$p < 0.01$.

Differences Between Groups

Table 3 shows the mean ± SD of 35 measurements for both groups. In the free-viewing test, there was a significant group difference in scanpath length [$F_{(1, 433)} = 8.3$, $p = 4.2 \times 10^{-3}$] but the other measurements were not significantly different ($0.11 < p < 0.94$). In the smooth pursuit test, there were significant group differences in duration of saccades [$F_{(1, 433)} = 8.5$, $p = 3.7 \times 10^{-3}$] and peak saccade velocity [$F_{(1, 433)} = 8.4$, $p = 3.9 \times 10^{-3}$] but the other measurements were not significantly different ($0.02 < p < 0.95$). There were no significant group differences in the fixation stability test ($0.48 < p < 0.89$).

Differences in Younger and Older Cohorts

In 4 out of 35 measurements, there were significant interactions between age and group [$F_{(1, 433)} = 5.1$, $p = 2.5 \times 10^{-2}$) for number of fixations; $F_{(1, 433)} = 5.5$, $p = 1.9 \times 10^{-2}$ for duration of fixation; $F_{(1, 433)} = 7.2$, $p = 7.6 \times 10^{-3}$ for number of saccades; and $F_{(1, 433)} = 9.6$, $p = 2.1 \times 10^{-3}$ for fixation density) (**Table 3**). For the number of fixations, the group effect was significant in the older cohort [$F_{(1, 433)} = 17.8$, $p = 2.9 \times 10^{-5}$] but not in the younger cohort [$F_{(1, 433)} = 1.3$, $p = 0.26$]. For the duration of fixation, the group effect was also significant in the older cohort [$F_{(1, 433)} = 30.7$, $p = 5.3 \times 10^{-8}$] but not in the younger cohort [$F_{(1, 433)} = 0.19$, $p = 0.67$]. For the number of saccades, the group effect was significant in the older cohort [$F_{(1, 433)} = 15.0$, $p = 1.2 \times 10^{-4}$] but not in the younger cohort [$F_{(1, 433)} = 2.4$, $p = 0.12$]. Finally, for the fixation density, the group effect was significant in the older cohort [$F_{(1, 433)} = 12.4$, $p = 4.8 \times 10^{-4}$] but not the younger cohort [$F_{(1, 433)} = 1.3$, $p = 0.26$], which suggests altered aging effects in MDD (**Figure 2**).

Correlations Between Eye Movement Measurements and Demographics

No correlations were statistically significant with scanpath length in the free-viewing test. The duration of saccades and peak saccade velocity in the smooth pursuit test had no correlations other than age ($R = 0.44$, $p = 0.02$, $R = 0.47$, $p = 0.01$, respectively).

Discriminant Analysis and ROC Analysis

Significant group differences were observed in scanpath length in the free-viewing test, and duration of saccades and peak saccade velocity in the smooth pursuit test. We selected scanpath length of the free-viewing test and peak saccade velocity of the smooth pursuit test for the discriminant analysis using z score for each parameter, because these values were statistically significant between groups and were obtained by independent tests. According to the linear discriminant analysis, we correctly classified 72.1% of the subjects using the resubstitution method and correctly classified 71.9% of the subjects using the leave-one-out cross-validation method. The discriminant score was calculated using the following formula: discriminant score = – 0.52 × (z score of scanpath length) + 0.83 × (z score of peak saccade velocity). **Figure 3** shows the ROC curve of the discriminant score between the MDD and HC groups. The area under the curve (AUC) of the ROC analysis in MDD vs. HCs was 0.76 (standard error = 0.05, $p = 1.2 \times 10^{-7}$, 95% CI = 0.67 – 0.85), indicating that the discriminant score for the scanpath length in the free-viewing test and the peak saccade velocity in the smooth pursuit test could be used to differentiate between MDD and HC subjects with moderate accuracy. The Youden index indicated a favorable cutoff point of 0.39, which resulted in 81% sensitivity and 69% specificity.

Age-Matched Group Analysis

The results of the *t*-test are shown in **Supplementary Table 2**. These were: the scanpath length for the free viewing test (raw $p = 0.01$, $d = 0.6$); the duration of saccades and peak saccade velocity for the smooth pursuit test (raw $p = 3.9 \times 10^{-3}$, $d = -0.7$; raw $p = 1.5 \times 10^{-3}$, $d = -0.8$, respectively), but none of them were significant after FDR correction. According to the linear discriminant analysis, we correctly classified 75.7% of the subjects using the resubstitution method and correctly classified 73.0% of the subjects using the leave-one-out cross-validation method. The discriminant score was calculated using the following formula: discriminant score = – 0.63 × (scanpath length) + 0.80 × (peak saccade velocity). **Supplementary Figure 1** shows the ROC curve of the discriminant score between the MDD and HC groups in age-matched group analysis. AUC of the ROC analysis in MDD vs.

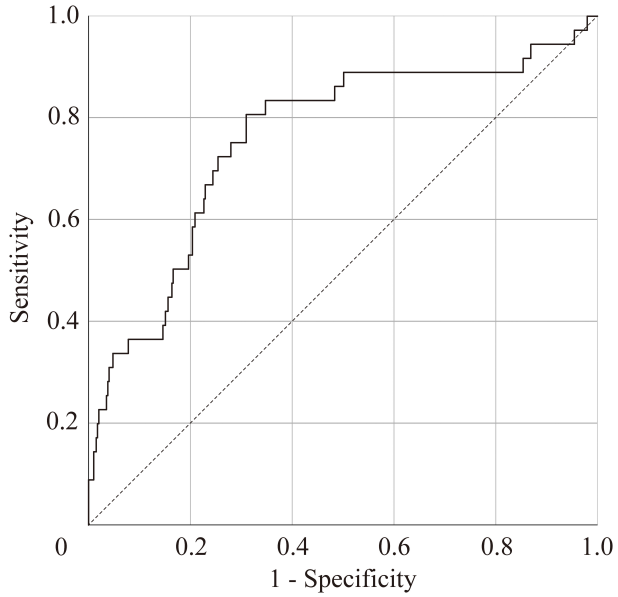

FIGURE 3 | Receiver-operator curve (ROC) to predict patients with major depressive disorder. Area under the ROC = 0.76 (standard error = 0.05, $p = 1.2 \times 10^{-7}$, 95% confidence interval, 0.67–0.85).

HCs was 0.77 (standard error = 0.06, $p = 6.5 \times 10^{-5}$, 95% CI = 0.66 – 0.88). The Youden index indicated a favorable cutoff point of 0.03, which resulted in 73% sensitivity and 81% specificity.

DISCUSSION

The present study investigated eye movement measurements of MDD using free-viewing, fixation stability, and smooth pursuit tests. The results are as follows: (1) MDD showed a significantly shortened scanpath length in the free-viewing test and a longer duration of saccades and higher peak saccade velocity in the smooth pursuit test compared with HCs; (2) altered aging effects of MDD were observed for the number of fixations, duration of fixation, number of saccades, and fixation density; and (3) the AUC of the ROC analysis was 0.76 (standard error = 0.05, $p = 1.2 \times 10^{-7}$, 95% CI = 0.67 – 0.85).

The current findings are partially consistent with a previous study (31) that reported MDD patients exhibited fewer saccades and a shortened scanpath length in the free-viewing task compared with HCs. In addition, they found that MDD patients had a significantly shorter gaze time and more saccades in the fixation stability test. However, in the present study, there were no significant differences in the fixation stability test between MDD and HC subjects. These differences between studies might be because the previous study by Li et al. (31) did not compensate for multiple tests, and thus their results should be interpreted carefully. Hsu et al. (43) investigated temporal preparation in MDD using a saccadic eye movement task where subjects were required to make a saccade between a central and an eccentric visual target. Patients with MDD showed a larger number of saccades initiated prior to the appearance of the expected stimulus, indicating reduced temporal preparation in MDD. In addition, the authors reported that oculomotor impulsivity interacted with temporal preparation. In our study, there were no significant differences in the duration of fixation and the number of saccades in the fixation stability test between groups, suggesting that oculomotor impulsivity was not observed in MDD. However, differences in experimental design may account for the reported discrepancies.

Our previous study (20) reported that during the free-viewing test, patients with SZ also had a significantly shortened scanpath length compared with HCs. Based on this result, it appears that the decline in the scanpath length in MDD may be less severe than that in SZ. Egaña et al. (44) reported significant shortened scanpath in SZ compared with HCs was resulted from the increasing occurrence of undetected microsaccades. Our future study will examine this issue for shortened scanpath length in MDD. In the smooth pursuit test, there were significant declines in horizontal and vertical position gains in SZ, but there were no significant changes in position gain in MDD. However, there were significant differences in the duration of saccades and peak saccade velocity, which may indicate that patients with MDD compensate with position error by catch-up saccade. It will be necessary to clarify the commonality and heterogeneity of eye movement parameters in psychiatric disorders in future studies.

Altered aging effects of MDD including the number of fixations, duration of fixation, number of saccades, and fixation density are also of particular interest. Indeed, accelerated brain aging was reported in MDD patients (45). In terms of symptoms, Dunlop et al. (46) suggested that accelerated aging was associated with greater impulsivity and depression severity. A genetic study by Han et al. reported that patients with MDD had a degree of epigenetic and methylation change that was reflective of an older age. In particular, they suggested that MDD patients were 8 months biologically older than people without MDD (47). The current finding on different patterns of aging effects between MDD and HCs suggests that MDD patients may show different age-related changes from HCs, which could relate to disease characteristics. We hope to confirm these findings in a larger cohort in the future.

The results of discriminant analysis and ROC analysis suggest that the combination of scanpath length by free-viewing test and peak saccade velocity by smooth pursuit test are potential biomarkers to differentiate between MDD and HCs. In the present study, we also performed age-matched group analysis and found no significant differences after FDR correction in the eye movement variables that were significantly different in the main ANCOVA. However, in terms of effect sizes comparing MDD and HCs, the impacts of eye movements seem to be more significant compared to other indices. For example, in a structural brain imaging study with mega-analysis methods (48), patients with MDD had a significantly thinner cortical gray matter in the orbitofrontal cortex, anterior cingulate gyrus, posterior cingulate gyrus, insula, and temporal lobes compared to HCs (Cohen's d effect size: −0.10 to

−0.14), whereas the effect sizes of our present study were 0.60–0.77. In addition, the study using MRI as a biomarker reported that patients with MDD were distinguished from HCs with a sensitivity of 77% and specificity of 78% (49), which was comparable to the present results. Therefore, it may be reasonable to select variables of eye movements as potential biomarkers. It will be important to utilize the same measurements for the differentiation of other psychiatric disorders. Further study of the eye movement measurements in psychiatric disorders other than SZ and MDD, such as bipolar disorder, anxiety disorder, obsessive-compulsive disorder, and autism spectrum disorder may identify eye movement-related biological differences across psychiatric disorders. In future clinical applications, it may be necessary to narrow down the parameters to be used.

Several limitations of this study must be considered. First, differences in group age might have influenced the discrimination analysis because we used the peak saccade velocity in the smooth pursuit test as an independent variable, which is associated with age. To obtain more accurate results, demographically-matched groups should be used in future analyses. Second, patients with MDD had various disease status including mild-to-moderate severity and remission with medication. Furthermore, the sample size was relatively small. Thus, larger numbers of samples with all types of depressive states ranging from mild to severe will be required to determine whether the abnormalities are traits or a state of the disorder. As shown in age-matched group analyses, although the effect sizes were large, significant differences would only be found with larger sample sizes in an exploratory study. Therefore, we need to confirm further our results in another extensive age-matched data set as a confirmatory study. Third, the current study cannot answer the question of whether the current findings are specific to MDD or not. It will thus be important to investigate other psychiatric disorders such as bipolar disorder. Our future study will perform direct comparisons among disorders, including schizophrenia, with larger sample size. Finally, the neural basis of these age-related eye-movement abnormal changes remains poorly understood. Thus, to determine the neural basis of these age-related eye-movement abnormalities, functional neuroimaging studies including functional magnetic resonance imaging, electroencephalography, or magnetoencephalography should be combined during the eye-movement tasks.

CONCLUSION

In the current study, MDD patients had a significantly shortened scanpath length in the free-viewing test and a longer duration of saccades and higher peak saccade velocity in the smooth pursuit test compared with HCs. In addition, altered aging effects of MDD were detected for the number of fixations, duration of fixation, number of saccades, and fixation density. The discriminant score calculated by the scanpath length in the free-viewing test and peak saccade velocity in the smooth pursuit test might be used to differentiate between MDD and HCs with moderate accuracy. These results suggest that detailed eye movement tests can assist in differentiating MDD from HCs, especially in older subjects.

DATA AVAILABILITY STATEMENT

The raw data supporting the conclusions of this article will be made available by the authors, without undue reservation.

ETHICS STATEMENT

The studies involving human participants were reviewed and approved by Research Ethical Committees of Kyushu University, Osaka University, The University of Tokyo, Nagoya University, and Nara Medical University. The patients/participants provided their written informed consent to participate in this study.

AUTHOR CONTRIBUTIONS

JT, KMi, RH, YH, and TO designed the study. JT, KMi, KMo, MF, HY, YY, NK, ES, KO, and TS collected and analyzed the data. JT prepared the first draft of the manuscript and created the figures. KMi, YH, RH, and TO assisted with data analyses and supervised the research. KMi, KMo, MF, HY, YY, NK, ES, KO, TS, TN, KK, RH, and TO edited the manuscript. All authors contributed to and have approved the final manuscript.

FUNDING

This research was supported, in part, by the Japan Agency for Medical Research and Development under grant numbers JP21dm0207069 (TO, KK, and KMi) and GAJJ020620 (JP19dm0107124h0004) (YH), JP18dm0207006 (RH), JP20dm0307002 (RH), JP20lm0203007 (RH); a Grant-in-Aid for Young Scientists B JP22791129 (YH); a Grant-in-Aid for Scientific Research C: JP 16K10217 (TO), JP 15K09836 (YH), JP 18K07604 (YH), JP 19H03579 (YH), B: 20H03611 (RH) and Fund for the Promotion of Joint International Research (Fostering Joint International Research B): JP20KK0193 (YH) from the Japan Society for the Promotion of Science; Medical Research Fund (YH) from Takeda Science Foundation; Research Fund Award (YH) from the Brain Science Foundation; 60th Research Grant Award (YH) from UBE Industries Foundation; SIRS Research Fund Award (YH) from the Schizophrenia International Research Society and The Grand Prize Young Investigator Program Award 2020 (YH) from the Japanese Society of Biological Psychiatry. This work was supported in part by UTokyo Center for Integrative Science of Human Behavior (CiSHuB), and by the International Research Center for Neurointelligence (WPI-IRCN) at The University of Tokyo Institutes for Advanced Study (UTIAS) (KK). The funding sources had no further role in study design, in the collection, analysis, interpretation of data, in

writing the report, or in the decision to submit the paper for publication.

ACKNOWLEDGMENTS

The authors gratefully acknowledge the administrative support of Motoko Soya and Maiko Kawasoe. We thank J. Ludovic Croxford, PhD, from Edanz Group (https://en-author-services.edanz.com/ac) for editing a draft of this manuscript.

SUPPLEMENTARY MATERIAL

The Supplementary Material for this article can be found online at: https://www.frontiersin.org/articles/10.3389/fpsyt.2021.673443/full#supplementary-material

Supplementary Figure 1 | Receiver-operator curve (ROC) to predict patients with major depressive disorder. Area under the ROC = 0.77 (standard error = 0.06, $p = 6.5 \times 10^{-5}$, 95% confidence interval, 0.66–0.88).

Supplementary Table 1 | Eye movement measurements of HCs and MDD subjects.

Supplementary Table 2 | Results of *t*-tests between age-matched groups.

REFERENCES

1. World Health Organization. *Depression*. (2020). Available online at: https://www.who.int/news-room/fact-sheets/detail/depression
2. World Health Organization. *Depression and Other Common Mental Disorders: Global Health Estimates*. World Health Organization (2017). Available online at: https://apps.who.int/iris/handle/10665/254610
3. GBD 2017 Disease and Injury Incidence and Prevalence Collaborators. Global, regional, and national incidence, prevalence, and years lived with disability for 354 diseases and injuries for 195 countries and territories, 1990-2017: a systematic analysis for the Global Burden of Disease Study 2017. *Lancet*. (2018) 392:1789–858. doi: 10.1016/S0140-6736(18)32279-7
4. Kupfer DJ, Frank E, Phillips ML. Major depressive disorder: new clinical, neurobiological, and treatment perspectives. *Lancet*. (2012) 379:1045–55. doi: 10.1016/S0140-6736(11)60602-8
5. Boku S, Nakagawa S, Toda H, Hishimoto A. Neural basis of major depressive disorder: beyond monoamine hypothesis. *Psychiatry Clin Neurosci*. (2018) 72:3–12. doi: 10.1111/pcn.12604
6. Hashimoto K. Rapid-acting antidepressant ketamine, its metabolites and other candidates: a historical overview and future perspective. *Psychiatry Clin Neurosci*. (2019) 73:613–27. doi: 10.1111/pcn.12902
7. North CS, Baron D, Chen AF. Prevalence and predictors of postdisaster major depression: convergence of evidence from 11 disaster studies using consistent methods. *J Psychiatr Res*. (2018) 102:96–101. doi: 10.1016/j.jpsychires.2017.12.013
8. Taquet M, Luciano S, Geddes JR, Harrison PJ. Bidirectional associations between COVID-19 and psychiatric disorder: retrospective cohort studies of 62 354 COVID-19 cases in the USA. *Lancet Psychiatry*. (2021) 8:130–40. doi: 10.1016/S2215-0366(20)30462-4
9. Shigemura J, Ursano RJ, Morganstein JC, Kurosawa M, Benedek DM. Public responses to the novel 2019 coronavirus (2019-nCoV) in Japan: mental health consequences and target populations. *Psychiatry Clin Neurosci*. (2020) 74:281–2. doi: 10.1111/pcn.12988
10. Stavridou A, Stergiopoulou AA, Panagouli E, Mesiris G, Thirios A, Mougiakos T, et al. Psychosocial consequences of COVID-19 in children, adolescents and young adults: a systematic review. *Psychiatry Clin Neurosci*. (2020) 74:615–6. doi: 10.1111/pcn.13134
11. Kashihara J, Yamakawa I, Kameyama A, Muranaka M, Taku K, Sakamoto S. Perceptions of traditional and modern types of depression: a cross-cultural vignette survey comparing Japanese and American undergraduate students. *Psychiatry Clin Neurosci*. (2019) 73:441–7. doi: 10.1111/pcn.12838
12. Kobayashi D, First MB, Shimbo T, Kanba S, Hirano Y. Association of self-reported religiosity with the development of major depression in multireligious country Japan. *Psychiatry Clin Neurosci*. (2020) 74:535–41. doi: 10.1111/pcn.13087
13. Scalabrini A, Xu J, Northoff G. What COVID-19 tells us about the self: the deep intersubjective and cultural layers of our brain. *Psychiatry Clin Neurosci*. (2021) 75:37–45. doi: 10.1111/pcn.13185
14. Fekadu N, Shibeshi W, Engidawork E. Major depressive disorder: pathophysiology and clinical management. *J Depress Anxiety*. (2017) 6:255. doi: 10.4172/2167-1044.1000255
15. Osório FL, Loureiro SR, Hallak JEC, Machado-de-Sousa JP, Ushirohira JM, Baes CVW, et al. Clinical validity and intrarater and test-retest reliability of the Structured Clinical Interview for DSM-5 - Clinician Version (SCID-5-CV). *Psychiatry Clin Neurosci*. (2019) 73:754–60. doi: 10.1111/pcn.12931
16. Williams AJ, Lai Z, Knight S, Kamali M, Assari S, McInnis MG. Risk factors associated with antidepressant exposure and history of antidepressant-induced mania in bipolar disorder. *J Clin Psychiatry*. (2018) 79:17m11765. doi: 10.4088/JCP.17m11765
17. Goldberg JF, Nierenberg AA, Iosifescu DV. Wrestling with antidepressant use in bipolar disorder: the ongoing debate. *J Clin Psychiatry*. (2021) 82:19ac13181. doi: 10.4088/JCP.19ac13181
18. Benson PJ, Beedie SA, Shephard E, Giegling I, Rujescu D, St Clair D. Simple viewing tests can detect eye movement abnormalities that distinguish schizophrenia cases from controls with exceptional accuracy. *Biol Psychiatry*. (2012) 72:716–24. doi: 10.1016/j.biopsych.2012.04.019
19. Brakemeier S, Sprenger A, Meyhöfer I, McDowell JE, Rubin LH, Hill SK, et al. Smooth pursuit eye movement deficits as a biomarker for psychotic features in bipolar disorder-Findings from the PARDIP study. *Bipolar Disord*. (2020) 22:602–11. doi: 10.1111/bdi.12865
20. Morita K, Miura K, Fujimoto M, Yamamori H, Yasuda Y, Iwase M, et al. Eye movement as a biomarker of schizophrenia: using an integrated eye movement score. *Psychiatry Clin Neurosci*. (2017) 71:104–14. doi: 10.1111/pcn.12460
21. Wolf A, Ueda K, Hirano Y. Recent updates of eye movement abnormalities in patients with schizophrenia: a scoping review. *Psychiatry Clin Neurosci*. (2021) 75:82–100. doi: 10.1111/pcn.13188
22. Hashimoto R. Do eye movement abnormalities in schizophrenia cause Praecox Gefühl? *Psychiatry Clin Neurosci*. (2021) 75:79–80. doi: 10.1111/pcn.13197
23. Smyrnis N, Amado I, Krebs MO, Sweeney JA. Eye movements in psychiatry. In: Klein C, Ettinger U, editors. *Eye Movement Research. Studies in Neuroscience, Psychology and Behavioral Economics*. Cham: Springer (2019). p. 703–48. doi: 10.1007/978-3-030-20085-5_16
24. Iacono WG, Peloquin LJ, Lumry AE, Valentine RH, Tuason VB. Eye tracking in patients with unipolar and bipolar affective disorders in remission. *J Abnorm Psychol*. (1982) 91:35–44. doi: 10.1037/0021-843X.91.1.35
25. Abel LA, Friedman L, Jesberger J, Malki A, Meltzer HY. Quantitative assessment of smooth pursuit gain and catch-up saccades in schizophrenia and affective disorders. *Biol Psychiatry*. (1991) 29:1063–72. doi: 10.1016/0006-3223(91)90248-K
26. Malaspina D, Amador XF, Coleman EA, Mayr TL, Friedman JH, Sackeim HA. Smooth pursuit eye movement abnormality in severe major depression: effects of ECT and clinical recovery. *J Neuropsychiatry Clin Neurosci*. (1994) 6:36–42.
27. Flechtner KM, Steinacher B, Sauer R, Mackert A. Smooth pursuit eye movements in schizophrenia and affective disorder. *Psychol Med*. (1997) 27:1411–9. doi: 10.1017/S0033291797005709
28. Flechtner KM, Steinacher B, Sauer R, Mackert A. Smooth pursuit eye movements of patients with schizophrenia and affective disorder during

clinical treatment. *Eur Arch Psychiatry Clin Neurosci*. (2002) 252:49–53. doi: 10.1007/s004060200011
29. Fabisch K, Fitz W, Fabisch H, Haas-Krammer A, Klug G, Zapotoczky S, et al. Sinusoidal smooth pursuit eye tracking at different stimulus frequencies: position error and velocity error before catch-up saccades in schizophrenia and in major depressive disorder. *Aust N Z J Psychiatry*. (2009) 43:855–65. doi: 10.1080/00048670903107542
30. Chen S, Zhou R, Cui H, Chen X. Deficits in cue detection underlie event-based prospective memory impairment in major depression: an eye tracking study. *Psychiatry Res*. (2013) 209:453–8. doi: 10.1016/j.psychres.2013.01.015
31. Li Y, Xu Y, Xia M, Zhang T, Wang J, Liu X, et al. Eye movement indices in the study of depressive disorder. *Shanghai Arch Psychiatry*. (2016) 28:326–34.
32. Hamilton M. A rating scale for depression. *J Neurol Neurosurg Psychiatry*. (1960) 23:56–62. doi: 10.1136/jnnp.23.1.56
33. Inada T, Inagaki A. Psychotropic dose equivalence in Japan. *Psychiatry Clin Neurosci*. (2015) 69:440–7. doi: 10.1111/pcn.12275
34. Zimmerman M, Martinez JH, Young D, Chelminski I, Dalrymple K. Severity classification on the Hamilton Depression Rating Scale. *J Affect Disord*. (2013) 150:384–8. doi: 10.1016/j.jad.2013.04.028
35. Brainard DH. The psychophysics toolbox. *Spat Vis*. (1997) 10:433–6. doi: 10.1163/156856897X00357
36. Miura K, Hashimoto R, Fujimoto M, Yamamori H, Yasuda Y, Ohi K, et al. An integrated eye movement score as a neurophysiological marker of schizophrenia. *Schizophr Res*. (2014) 160:228–9. doi: 10.1016/j.schres.2014.10.023
37. Arolt V, Teichert HM, Steege D, Lencer R, Heide W. Dis- tinguishing schizophrenic patients from healthy controls by quantitative measurement of eye movement para- meters. *Biol Psychiatry*. (1998) 44:448–58. doi: 10.1016/S0006-3223(97)00479-4
38. Over EA, Hooge IT, Erkelens CJ. A quantitative measure for the uniformity of fixation density: the Voronoi method. *Behav Res Methods*. (2006) 38:251–61. doi: 10.3758/BF03192777
39. Müller C, Stoll W, Schmäl F. The effect of optical devices and repeated trials on the velocity of saccadic eye movements. *Acta Otolaryngol*. (2003) 123:471–6. doi: 10.1080/00016480300684
40. Takahashi J, Miura K, Morita K, Fujimoto M, Miyata S, Okazaki K, et al. Effects of age and sex on eye movement characteristics. *Neuropsychopharmacol Rep*. (2021) 41:152–8. doi: 10.1002/npr2.12163
41. Irving EL, Steinbach MJ, Lillakas L, Babu RJ, Hutchings N. Horizontal saccade dynamics across the human life span. *Invest Ophthalmol Vis Sci*. (2006) 47:2478–84. doi: 10.1167/iovs.05-1311
42. de Hemptinne C, Ivanoiu A, Lefèvre P, Missal M. How does Parkinson's disease and aging affect temporal expectation and the implicit timing of eye movements? *Neuropsychologia*. (2013) 51:340–8. doi: 10.1016/j.neuropsychologia.2012.10.001
43. Hsu TY, Lee HC, Lane TJ, Missal M. Temporal preparation, impulsivity and short-term memory in depression. *Front Behav Neurosci*. (2019) 13:258. doi: 10.3389/fnbeh.2019.00258
44. Egaña JI, Devia C, Mayol R, Parrini J, Orellana G, Ruiz A, et al. Small saccades and image complexity during free viewing of natural images in schizophrenia. *Front Psychiatry*. (2013) 4:1–13. doi: 10.3389/fpsyt.2013.00037
45. Wolkowitz OM, Epel ES, Reus VI, Mellon SH. Depression gets old fast: do stress and depression accelerate cell aging? *Depress Anxiety*. (2010) 27:327–38. doi: 10.1002/da.20686
46. Dunlop K, Victoria LW, Downar J, Gunning FM, Liston C. Accelerated brain aging predicts impulsivity and symptom severity in depression. *Neuropsychopharmacology*. (2021) 46:911–19. doi: 10.1038/s41386-021-00967-x
47. Han LKM, Aghajani M, Clark SL, Chan RF, Hattab MW, Shabalin AA, et al. Epigenetic aging in major depressive disorder. *Am J Psychiatry*. (2018) 175:774–82. doi: 10.1176/appi.ajp.2018.17060595
48. Schmaal L, Hibar DP, Sämann PG, Hall GB, Baune BT, Jahanshad N, et al. Cortical abnormalities in adults and adolescents with major depression based on brain scans from 20 cohorts worldwide in the ENIGMA Major Depressive Disorder Working Group. *Mol Psychiatry*. (2017) 22:900–9. doi: 10.1038/mp.2016.60
49. Kambeitz J, Cabral C, Sacchet MD, Gotlib IH, Zahn R, Serpa MH, et al. Detecting neuroimaging biomarkers for depression: a meta-analysis of multivariate pattern recognition studies. *Biol Psychiatry*. (2017) 82:330–8. doi: 10.1016/j.biopsych.2016.10.028

Conflict of Interest: The authors declare that the research was conducted in the absence of any commercial or financial relationships that could be construed as a potential conflict of interest.

Publisher's Note: All claims expressed in this article are solely those of the authors and do not necessarily represent those of their affiliated organizations, or those of the publisher, the editors and the reviewers. Any product that may be evaluated in this article, or claim that may be made by its manufacturer, is not guaranteed or endorsed by the publisher.

frontiers in Psychiatry

SYSTEMATIC REVIEW
published: 22 October 2021
doi: 10.3389/fpsyt.2021.665536

Systematic Review of Functional MRI Applications for Psychiatric Disease Subtyping

Lucas Miranda[1]*, *Riya Paul*[2,3], *Benno Pütz*[1], *Nikolaos Koutsouleris*[2,3] and *Bertram Müller-Myhsok*[1,4]

[1] Department of Statistical Genetics, Max Planck Institute of Psychiatry, Munich, Germany, [2] Department of Precision Psychiatry, Max Planck Institute of Psychiatry, Munich, Germany, [3] Department of Psychiatry and Psychotherapy, Section for Neurodiagnostic Applications, Ludwig-Maximilian University, Munich, Germany, [4] Department of Health Data Science, Institute of Translational Medicine, University of Liverpool, Liverpool, United Kingdom

Background: Psychiatric disorders have been historically classified using symptom information alone. Recently, there has been a dramatic increase in research interest not only in identifying the mechanisms underlying defined pathologies but also in redefining their etiology. This is particularly relevant for the field of personalized medicine, which searches for data-driven approaches to improve diagnosis, prognosis, and treatment selection for individual patients.

Methods: This review aims to provide a high-level overview of the rapidly growing field of functional magnetic resonance imaging (fMRI) from the perspective of unsupervised machine learning applications for disease subtyping. Following the PRISMA guidelines for protocol reproducibility, we searched the PubMed database for articles describing functional MRI applications used to obtain, interpret, or validate psychiatric disease subtypes. We also employed the active learning framework ASReview to prioritize publications in a machine learning-guided way.

Results: From the 20 studies that met the inclusion criteria, five used functional MRI data to interpret symptom-derived disease clusters, four used it to interpret clusters derived from biomarker data other than fMRI itself, and 11 applied clustering techniques involving fMRI directly. Major depression disorder and schizophrenia were the two most frequently studied pathologies (35% and 30% of the retrieved studies, respectively), followed by ADHD (15%), psychosis as a whole (10%), autism disorder (5%), and the consequences of early exposure to violence (5%).

Conclusions: The increased interest in personalized medicine and data-driven disease subtyping also extends to psychiatric disorders. However, to date, this subfield is at an incipient exploratory stage, and all retrieved studies were mostly proofs of principle where further validation and increased sample sizes are craved for. Whereas results for all explored diseases are inconsistent, we believe this reflects the need for concerted, multisite data collection efforts with a strong focus on measuring the generalizability of results. Finally, whereas functional MRI is the best way of measuring brain function available to date, its low signal-to-noise ratio and elevated monetary cost make it a poor

OPEN ACCESS

Edited by:
Shinsuke Koike,
The University of Tokyo, Japan

Reviewed by:
Gregory Neal Barnes,
University of Louisville, United States
Manpreet Kaur Singh,
Stanford University, United States

***Correspondence:**
Lucas Miranda
lucas_miranda@psych.mpg.de

Specialty section:
This article was submitted to Computational Psychiatry, a section of the journal Frontiers in Psychiatry

Received: *08 February 2021*
Accepted: *07 September 2021*
Published: *22 October 2021*

Citation:
Miranda L, Paul R, Pütz B, Koutsouleris N and Müller-Myhsok B (2021) Systematic Review of Functional MRI Applications for Psychiatric Disease Subtyping. Front. Psychiatry 12:665536. doi: 10.3389/fpsyt.2021.665536

clinical alternative. Even with technology progressing and costs decreasing, this might incentivize the search for more accessible, clinically ready functional proxies in the future.

Keywords: functional MRI (fMRI), personalized medicine, disease subtyping, biotypes, machine learning, unsupervised learning, clustering, translational psychiatry

INTRODUCTION

Psychiatric Disease Prevalence

Psychiatric disorders have a long history of being classified based solely on their associated symptoms, with the first systematic analysis attempts dating back as far as the late 1800s (1). Since the introduction of the Diagnostic Manual of Mental Disorders (DSM) back in 1952 (2), and most notably since the inclusion of operationalized criteria in 1978 in the DSM-III (3), statistics on discrete pathological entities and their combination began to accumulate, yielding the potential of understanding psychiatric epidemiology in a consistent way. The last version of the DSM manual (DSM-5), published in 2013 (4), contains 297 discrete disorders categorized into 11 broad classes, grouped by evidence of co-occurring symptoms. Current prevalence estimates indicate that, on average, more than one in six individuals (17.6%) have experienced at least one common psychiatric disorder within the last year and almost three in ten (29.2%) during their lifetime (5). In an attempt to assess both the severity of the disorders and the response after individual treatment, several standardized symptom scores have been developed, including the Hamilton Depression Rating Scale (HAM-D) for Major Depression Disorder and the Positive and Negative Syndrome Scale (PANSS) for Schizophrenia, among others.

Heterogeneity and Alternatives to Symptom-Based Diagnosis

Symptoms and clinical information can be relatively easy to acquire, and their analysis can be useful to understand the symptom prevalence in the population and assess the effectiveness of treatment on a broad scale (6). They do not, however, necessarily reflect anything about the underlying mechanisms causing them. Furthermore, given the complexity of the genetic and environmental factors at play, the same set of symptoms can arise from different causes, while the same biological causes may lead to different symptoms or phenotypes (7, 8). This is particularly important when analyzing the response to treatment, where the outcome is challenging to predict based on the symptoms alone, and response to medication is vastly heterogeneous, being treatment-resistant variants of disease not uncommon (9). For example, current estimates indicate that about 30 and 34% of medicated patients diagnosed with depression and schizophrenia, respectively, do not respond to treatment even after trying two or more drugs (10, 11). This can be interpreted as an indication of the underlying mechanistic heterogeneity of these symptom-defined disorders. In light of this concern and with the advantage of new technologies and an increasing amount of related data, several initiatives have embarked on the quest to find data-driven mechanistic disease definitions that may aid the issue. One of the most important to date has been the Research Domain Criteria (RDoC), which was introduced by the NIH (National Institute of Health) in 2009 as a framework to guide research projects in the understanding of mental disorders from a combination of different perspectives, including not only self-reported symptoms but also genomics, circuits, and behavior, among others (12). The ideas behind these mechanistic-based classifications have the potential of expanding our knowledge of mental disorders themselves, advancing biomarker discovery, and helping improve prognosis prediction and identify the best treatments for individual patients whose overlapping symptoms have distinct etiological causes, in a notion that is very much in line with those of personalized medicine (13).

Functional MRI for Disease Subtyping

The idea of using multivariate pattern analysis to unravel the heterogeneity mentioned above and unveil subgroups of patients within already defined diseases is not new (12, 14, 15). However, the advent of massive biological related datasets (the so-called *high-throughput biology*) in areas such as genomics, transcriptomics, and proteomics, and the newly available techniques to study the brain in a non-invasive way, opened a whole new field of possibilities to study not only the underlying mechanisms of symptom-related clusters but to search for biologically defined subtypes of disease (or *biotypes*) as well. Although initial hopes were put mainly on genetics, over the years an increasing number of Genome-Wide Association Studies (GWAS) have revealed that brain disorders tend to be associated with a high number of genetic variants with tiny effect sizes (16–18). Furthermore, individual genetic alterations often overlap among symptom-defined diseases (19). While some progress in genetic biomarkers has been made using disease-specific polygenic risk scores (PRS), the usage of genetics alone for determining brain disease subtypes has been mostly elusive (20, 21). However, one of the most promising fields to pursue this aim has been neuroimaging, with Magnetic Resonance Imaging (MRI) as arguably its most proficient method to date. This technique has been increasingly used to study not only the structure of the brain (structural *MRI*) but also to measure changes in the blood oxygen levels surrounding particular regions as a proxy of neuronal activation (*BOLD fMRI*) (22). One of the most prevalent uses of this technology has been *task-based fMRI*, in which an experimental design matrix, typically convolved with a mathematical function modeling the hemodynamic response (called hemodynamic response function, or HRF), is set to explain the observed signal using a General Linear Model (GLM). While this approach has a substantial amount of literature behind it and is highly flexible due to relying on a Linear Model assumption (23), it has some notorious drawbacks. First, the most common analyses rely

on *mass univariate tests*, which statistically assess differences in activation on each voxel separately, assuming independence even among contiguous regions in space. Second, it depends on an experimental task design, which, even though it can be a powerful tool for answering specific questions, is relatively hard to perform, difficult to generalize, and prone to habituation (24). An alternative that gained momentum over the last two decades has been *resting-state* fMRI, in which the subjects perform no particular task. Since it was first employed in 1995 (25), this approach allowed researchers to study the relationship between brain regions over time, which has been proven to be a useful tool to study both *functional connectivity* (Resting-State Functional Connectivity–RSFC), based on voxel correlation and yielding *undirected* connectivity networks) and *effective connectivity* (Resting-State Effective Connectivity–RSEC), based on causal modeling and yielding *directed* connectivity networks). Regardless of the analysis tool, most studies largely converged in reporting multiple robust resting-state networks across the brain, such as the primary sensorimotor network, the primary visual network, frontoparietal attention networks, and the well-studied default mode network (26). In addition, Seeley et al. proposed in 2007 the concept of *Intrinsic connectivity networks*, which refers to correlated brain regions that can be captured in either resting state or task-based neuroimaging data (27). Furthermore, recent studies interestingly show that the contribution of task performing to an individual's established connectivity networks is rather small (28), suggesting the possibility of utilizing already generated task-based fMRI data for RSFC as well (29).

The idea of the brain having stable connectivity between its different regions that can be altered in illness has been an influential hypothesis for disease subtyping. Given its potential generalizability and the robustness of the obtained results (26, 30), resting-state connectivity is currently the most used fMRI approach for both searching for and validating distinct mechanisms underlying brain disease, in an attempt to explain the aforementioned vast heterogeneity.

Unsupervised Machine Learning on Psychiatric Disease Subtyping

Automated pattern recognition (i.e., *machine learning*) can be used to unveil subtypes in psychiatric disease in an unsupervised way (i.e., without the presence of hardcoded labels indicating for example if a disease is present or not). Given the complexity of the data at play, this set of approaches has been proven extremely useful in various settings and data domains, mainly for *clustering* and *dimensionality reduction* (13, 28). While the former deals with the process of finding subtypes in itself, the latter encapsulates a set of methods to project the data into lower-dimensional manifolds (31), in an attempt to reduce dataset size while retaining the most valuable information, which can substantially aid downstream model training.

In the case of functional MRI, unsupervised machine learning has been extensively used given the unstructured nature of the data. Its main uses include but are not restricted to parcellation of the brain into discrete functional subunits (unraveling of brain connectivity networks), the study of brain connectivity dynamics (how those networks develop over time), and grouping subjects according to their connectivity features (used for disease subtyping in itself). While the first two mentioned uses fall into the *dimensionality reduction* category, the third is inherent to *clustering*, and it will be part of the focus of this review.

Over the years, many clustering algorithms have been proposed. While a thorough classification of them is out of the scope of this review, an introductory, coarse grain subdivision of those applied in the analyzed studies, based on their general properties, can be found in **Table 1**.

With Great Power Comes Great Responsibility

While extremely useful when properly used, there are some inherent issues to clustering that are worth discussing before delving into the literature. For starters, clustering is in itself an ill-defined problem (34). This means that, unlike in other machine learning domains such as classification, there is neither a unique well-defined solution nor a unique definition of what a cluster is. That said, different algorithms will make different assumptions on the data that will intrinsically lead to distinct (although potentially overlapping) solutions. The choice may then rely on knowing these assumptions hold on a particular dataset, or on the empirical interpretation of a particular set of retrieved components using external variables (such as using fMRI to validate symptom or biomarker clusters, as will be presented later).

In addition, many popular clustering algorithms (although not all of them) require users to define the number of clusters they expect beforehand (typically codenamed k). While there are some exceptions (such as handwritten digit recognition, for example, where there are exactly 10 classes to detect), clustering is about *understanding data*, and recognizing the best number of components to define is, in most cases, a problem in itself. To solve it, researchers often rely on heuristics that compare the solutions achieved within a range of different values, exploiting a certain definition of *cluster* that the algorithm at hand uses. Besides, there is no guarantee that there are clusters at all in the data. Therefore, it is important to test the null hypothesis of *no-clusters* in our setting as well. This can be done by adding $k=1$ to the range of values to test or using statistical methods (35).

Last but not least, there is the problem of *generalizability*, arguably one of the holy grails of machine learning as a whole. The whole point of unveiling disease subtypes from our data is to extend the results to at least a broader subset of the general population. If a solution is only valid within the boundaries of a particular study but breaks apart on different datasets, we say that the model *overfits* the data it's been trained on. To counter this issue, it is common practice to run these algorithms multiple times with different subsamplings of the dataset (by removing random sets of samples using predefined schemes, such as cross-validation, bootstrap, or Jackknife), and to assess how much the clustering solution is affected. If clusters are highly stable across samples (as measured by established metrics, such as the Adjusted Rand Index or the Jaccard Index), the solution is said to be *robust* (34, 36). While these approaches are extremely

TABLE 1 | Coarse classification of clustering algorithms.

Algorithmic family	Distance-based clustering	Graph-based clustering	Model-based clustering
Description	A similarity/distance matrix between samples is computed, and the raw distance between samples is used for grouping similar objects together.	The similarity/distance matrix is thresholded to establish deterministic connections (edges) between samples, yielding a graph. Distance metrics at the graph level are used for determining clusters (called *communities*)	A parameterized model (typically a multimodal probability distribution) is fitted to the data. Training consists of finding the model parameters that best model the data.
Advantages	- Relatively low time complexity - High Computing Efficiency (they scale well to large datasets)	- Variety of highly efficient algorithms to deal with graphs (32) - Can capture the geometry of complex manifolds, a feature of interest in realistic datasets (33)	- High flexibility - Well-defined metrics for model selection (one can check how well a given model fits the data using likelihood based metrics). - Natural approach to soft clustering (probabilities are reported)
Limitations	- Sensitive to the selected distance metric - Number of clusters usually needs to be manually preset - Low flexibility	- Time complexity increases dramatically with the number of edges in the graph (proportional to the number of samples). - Sensitive to how the graph is constructed	- High time complexity (don't scale well for large datasets) - Flexibility comes at a cost (one must think carefully about which type of model to apply).
Examples (mentioned across this review)	K-means, Hierarchical Agglomerative Clustering, fuzzy c-means, Spectral clustering, Q-Factor analysis	Walktrap, Modularity maximization (Newmann's)	Gaussian Mixture Models (GMMs), Variational Bayesian GMMs

useful to test generalizability inside our data distribution, further validation steps are usually required to extend a solution to other settings, such as contrasting results to data obtained on different hospitals, or from different ethnicities [involving, for example, schemes such as leave-one-site-out cross-validation and external validation (37)]. The bottom line is: *If a subtyping study aims to draw conclusions for a certain population, generalizability to that population should be thoroughly tested.*

For a detailed review on machine learning for clinical psychiatry with a special focus on testing generalizability, please refer to (13, 38). For details on the existing unsupervised learning methods for disease subtyping, see Marquand et al. (39). For details on machine learning methods for resting-state fMRI data, refer to Khosla et al. (26).

This review will analyze the reported use to date of fMRI data for unveiling subtypes in several psychiatric disorders, and as a tool for validating subtypes reported after the analysis of other data modalities (such as symptom information, genetics, or structural MRI). The strengths and weaknesses of each approach will be discussed.

METHODS

This study followed the Preferred Reporting Items for Systematic reviews and Meta-Analysis (PRISMA) statements (40). A complete flow chart of the process is shown in **Figure 1**. The research question intended to delve into was defined using the PICo guidelines for qualitative systematic reviews (41): *What is the state of the art in the usage of unsupervised subtyping for explaining the heterogeneity in psychiatric disease symptomatology? What role does functional MRI play in this process?*

Search Methods for Article Retrieval

A systematic search of original articles was carried out on the PubMed database, including all non-review articles from the date of database creation up to 25 May 2020. The string "(unsupervised learning OR clustering OR dimensionality reduction OR subtyping) AND functional MRI" was entered on the search engine to retrieve all available papers in which functional MRI was used either for brain disease subtyping or for validation of brain disease subtypes obtained *via* other methods, which should include at least one of symptom information and structural MRI data.

Article Filtering

All retrieved studies were downloaded and analyzed using PubMed metadata to filter review articles ("D016428:Journal Article", but "D016454:Review" absent in the "*publication_types*" metadata field). The remaining studies were analyzed using the ASReview (*Automatic Systematic Reviews*) python package (42). This active-learning-based recommender system trains a classifier on the provided papers' abstracts and presents the user with the most relevant articles to review. While all abstracts included in this step were carefully studied, this tool has been proven useful for prioritization. Studies whose abstracts met the exclusion criteria (see below) were discarded. The rest was selected for full-text review.

Inclusion/Exclusion Criteria

We retained all original non-review studies in which functional MRI was used either for brain disease subtyping directly or

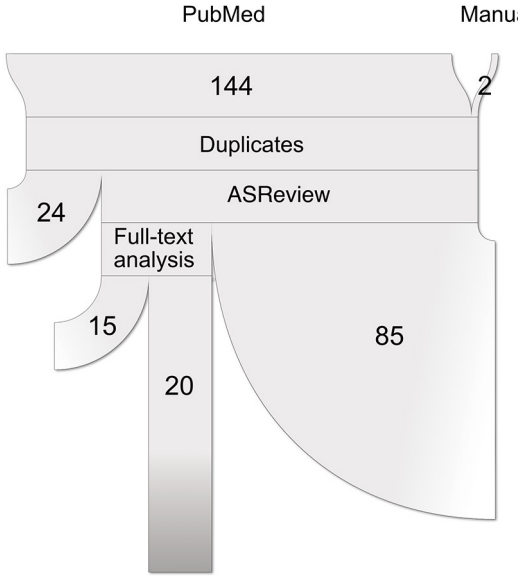

FIGURE 1 | Paper selection pipeline. PRISMA flowchart (represented as a ribbon plot, which flows from top to bottom) that schematizes the employed pipeline. A total of 144 articles were retrieved from PubMed using the string "*(unsupervised learning OR clustering OR dimensionality reduction OR subtyping) AND functional MRI*". Two articles were included after the manual search, yielding a total of 146 input studies. After several systematic filters, which included the exclusion of reviews, duplicated articles, and relevance to the defined inclusion criteria, a total of 20 articles were included in the review.

for validation of brain disease subtypes obtained *via* other methods, including at least one of symptom information and structural MRI data. Disease subtyping had to be carried out in an unsupervised way (no labels based on prior information except for case/controls). Precise definitions of the methods and their validation had to be included. As, given the heterogeneity of results, we think that cluster validation is currently one of the most important discussion topics in the field, articles trying to replicate or validate the results of included studies were also incorporated.

Data Extraction for Systematic Analysis

For each article included in the final review, a set of systematically collected pieces of information was extracted and added as an entry to a table (see **Tables 2**–**4**). This information includes: (a) *publication year*, (b) reference, (c) *pathology*, (d) *data domain used for clustering*, (e) sample size (clustering), (f) data domain utilized for validation/interpretation, (g) sample size (validation/interpretation), (h) feature selection / dimensionality reduction algorithms utilized, (i) clustering algorithm(s) employed, (j) cluster number selection criteria, (k) robustness assessment, (l) inclusion of healthy controls at clustering time[1] (m) testing against continuum (null hypothesis - absence of clustering structure in the data), (n) number of reported subtypes, (o) featured brain areas/networks that were recovered using fMRI.

[1]Both direct inclusion of healthy controls or indirect referencing to normative samples (i.e. by clustering differences between diagnosed patients and matched controls) were considered.

Characteristics of the Included Studies

The 20 retrieved studies were classified into one of three categories based on the nature of the analyzed subtypes and the usage of functional MRI (**Figure 2A**). The classes are: (a) *fMRI used for validation of subtypes obtained via unsupervised learning of symptom-related data*, (b) *fMRI used for validation of subtypes obtained via unsupervised learning of biomarkers other than fMRI (including structural MRI)*, and (c) *fMRI used for brain disease subtyping itself*. Over the next three sections, we will analyze these three cases separately, summarizing the results that the respective studies reported and discussing the assumptions they make and the advantages and disadvantages that they imply.

Regarding the pathological entities under study, most of the articles analyzed patients diagnosed with major depression disorder and schizophrenia (35 and 30%, respectively). Psychosis, attention-deficit/hyperactivity disorder, autism disorder, and the consequences of early violence were also included (**Figure 2B**).

RESULTS

fMRI Used for Validation of Subtypes Obtained *via* Unsupervised Learning of Symptom-Related Data

The unsupervised classification of psychiatric symptoms is not new: to our knowledge, the first papers were published back in the 1970s (12, 14, 15). The novelty of the studies presented here relies on interpreting and validating symptom clusters in terms of their underlying functional mechanisms. By comparing functional MRI data coming from patients on different clusters (or between particular clusters and healthy controls), researchers can potentially explain which mechanisms may be at play when yielding distinct sets of symptoms. The following paragraphs will explore the five papers that fall into this category.

Major Depression Disorder

In a pioneering study, Taubner et al. (43) addressed the symptomatic heterogeneity in a cohort of 20 patients with severe depression by clustering the personality features obtained from the Shedler-Westen Assessment Procedure (SWAP-200). As this assessment relies on clinical judgment rather than on a patient questionnaire, it is usually considered less noisy than other alternatives (44). Besides, as it is purely based on observed symptoms, it does not rely on any theoretical assumption about the mechanisms underlying depression.

In their setup, they applied a well-established method called Q-Factor analysis (45) to uncover a potential clustering structure in their data. This method aims to decompose the data matrix (of samples by features) into different components (called "factors"). The "Q" in the name indicates that factors refer to groups of individuals rather than to groups of features, as is the case in standard factor analysis. By employing an elbow method (45) on the variance explained by their factors, researchers decided to retain the two most prominent components in their data.

TABLE 2 | Retrieved articles in which fMRI was used to interpret symptom-based clusters.

Publication year	Reference	Pathology	Data used for clustering	sample size (symptoms)	Data used for validation	sample size (fMRI)	Dimensionality reduction	Clustering	Cluster number selection	Robustness testing	Healthy Controls included	Testing against continuum	Reported subtypes	Featured brain areas/ *networks*
2013	Taubner et al. (43)	MDD	SWAP-200 (44)	20	task fMRI (dysfunctional relationships)	20	Raw features	Q-Factor analysis (45)	variance explained (elbow method) (45)	No	No	No	2	orbitofrontal cortex, ventral striatum, temporal pole, middle frontal gyrus
2015	Geisler et al. (46)	SCZ	behavioral and cognitive scores	129	task fMRI SIRP (47)	165	PCA	K-means (36)	previous literature (48)	No	No	No	4	planum temporale, parietal operculum, precuneus cortices
2018	Dickinson et al. (49)	SCZ	PANS scores (50, 51)	549	rsfMRI	182	Raw features	GMMs (52, 53)	BIC (35)	1,000 model initializations (no left-out)	No	Yes	3	*frontoparietal working memory network*
2018	Maglanoc et al. (54)	MDD	BDI–BAI (54, 55)	1,084	rsfMRI sFC dFC	251	Raw features	GMMs (52, 53)	BIC (35)	100 model initializations (no left-out)	Yes	No	5	*default mode network, frontotemporal network*
2020	Chen et al. (56)	SCZ	PANS scores (50, 51)	1,545	rsfMRI	84	NMF (57)	fuzzy C-means (58)	fuzzy silhouette index, Xie/Beni index, partition entropy (31)	bootstrap resampling, leave-one-site-out cross-validation	No	Yes	2	ventromedial frontal cortex, temporoparietal junction, precuneus

TABLE 3 | Retrieved articles in which fMRI was used to interpret biomarker-based clusters.

Publication year	Reference	Pathology	Data used for clustering	Sample size (symptoms)	Data used for validation	Sample size (fMRI)	Dimensionality reduction	Clustering	Cluster number selection	Robustness testing	Healthy Controls included	Testing against continuum	Reported subtypes	featured brain areas/ ***networks***
2016	Clementz et al. (58)	Psychosis	biomarker panels	1,872	–	–	PCA (57)	K-means (36)	GAP Statistic (59)	Jackknife (34)	No	Yes	3	–
2016	Meda et al. (60)	Psychosis	–	–	rsfMRI	1,125	–	–	–	–	No	–	–	*cuneus-occipital, fronto-parietal, cerebellar-occipital, default mode, bilateral temporo-parietal, fronto-parietal*
2018	Chen et al. (61)	ASD	sfMRI (VBM)	356	rsfMRI	356	NMF (57)	K-means (36)	Silhouette index (62)	random splitting (34)	Yes, Indirectly	No	3	*default mode, frontoparietal, cingulo-opercular, sensory-motor, occipita*l
2019	Kaczkurkin et al. (63)	MDD	sfMRI (cortical thickness)	1,141	rsfMRI	40	raw features	HYDRA (64)	Adjusted Rand Index (62)	cross-validation (34)	Yes	No	3	frontal regions, right amygdala, right hippocampus

TABLE 4 | Retrieved articles in which fMRI was used to cluster subjects into biotypes.

Publication year	Reference	Pathology	Data used for clustering	Sample size (fMRI)	Data used for validation	Sample size (validation)	Dimensionality reduction	Clustering	Cluster number selection	Robustness testing	Healthy Controls included	Testing against continuum	Reported subtypes	featured brain areas/ *networks*
2014	Du et al. (65)	SCZ	functional connectivity	93	–	–	Recursive feature elimination	K-means, HAC (36)	based on previous knowledge	algorithm reinitialization - no data perturbation	Yes	No	5	frontal, parietal, precuneus, cingulate, supplementary motor, cerebellar, insular, and supramarginal cortices
2014	Brodersen et al. (66)	SCZ	effective connectivity	41	PANSS symptom scale	41	raw features - weights of DCM models	VBGMM (36)	automatic	not reported	Yes	Yes	3	visual–parietal–prefrontal working-memory network
2014	Gates et al. (67)	ADHD	effective connectivity	80	–	–	raw features - weights of DCM models	Walktrap (68)	automatic	network permutation	Yes	Yes	5	dorsolateral prefrontal and frontal cortices, intraparietal sulcus, inferior parietal lobule
2014	Yang et al. (69)	SCZ	functional connectivity	51	PANSS symptom scale	51	raw functional connectivity features	maximal clique (70)	automatic	cross-validation	Yes	Yes	2	precuneus-angular gyri
2015	Costa Dias et al. (71)	ADHD	functional connectivity	106	behavioral measures	101	meta-analytic masking (NeuroSynth) (72)	Walktrap (68)	automatic	random perturbation	Yes	Yes	3	nucleus accumbens, default mode network
2017	Drysdale et al. (73)	MDD	functional connectivity	220	HAM-D scores (symptoms)	1188	CCA (functional connectivity - symptoms) (74)	HAC (36)	CH index (75)	random splitting (34) external validation in independent samples	No	No	4	limbic and frontostriatal networks
2017	Price et al. (67)	MDD	effective connectivity	80	clinical data	80	raw features - weights of DCM models	Walktrap (68)	automatic	network permutation	No	Yes	2	default mode network, dorsal anterior cingulate nodes
2018	Lin et al. (76)	ADHD	functional connectivity	80	behavioral measures	80	CCA (functional connectivity - symptoms) (74)	K-means, spectral clustering (36)	jaccard, silhouette, gap	-	No	Yes	1	default-mode, cingulo-opercular and subcortical networks
2018	Tokuda et al. (77)	MDD	functional connectivity - biomarker data	134	CATS score, response to medication	134	raw features	custom multi-view co-clustering	automatic	cross-validation	Yes	Yes	5	default mode network, angular gyrus node

(Continued)

TABLE 4 | Continued

Publication year	Reference	Pathology	Data used for clustering	Sample size (fMRI)	Data used for validation	Sample size (validation)	Dimensionality reduction	Clustering	Cluster number selection	Robustness testing	Healthy Controls included	Testing against continuum	Reported subtypes	featured brain areas/ *networks*
2019	Dinga et al. (78)	MDD	functional connectivity	187	HAM-D scores (symptoms)	187	CCA (functional connectivity - symptoms) (74)	HAC (36)	CH - silhouette indices (75)	cross-validation	No	Yes (79)	1	–
2020	Sellnow et al. IPV (80)		emotion processing task fMRI	114	behavioral measures	114	meta-analytic masking (NeuroSynth) (72)	K-means (36)	cluster validity index (75)	cross-validation	No	Yes	3	medial prefrontal cortex, the anterior insula, hippocampus

Furthermore, functional MRI data from an individually tailored task paradigm using dysfunctional relationship patterns were obtained from each patient whose data was used for clustering, and a whole-brain correlational analysis was done comparing the fMRI GLM parameters with the individual values extracted within the SWAP-200 factors. This way, they cataloged their two retrieved components as indicators of "Depressive personality" or "Emotional-Hostile-Externalizing Personality", based on the analysis of the 20 SWAP-200 features that contributed the most to their partition. Moreover, the second component was linked to abnormal connectivity in the orbitofrontal cortex [strongly associated with cognitive processing and decision making (81)], the ventral striatum (a critical component of the reward system), and the temporal pole (involved in social emotion processing).

Even though they use simple, established methods, their sample size may be too low to derive reliable and generalizable conclusions. The authors call the study a hypothesis-generating experiment that might be followed up in the future. However, the recovery of previously reported, relevant activation networks seems promising.

A different approach, with a larger sample size ($n = 1{,}084$), was employed by Maglanoc et al. in 2018 (54). In this study, researchers used symptom data derived from Beck's depression and Beck's anxiety inventories (BDI and BAI, respectively) (55, 82), and combined individuals with and without a history of depression. These scoring systems, unlike the aforementioned SWAP-200, are self-assessed. Their reliability and competence to discriminate between subjects with and without anxiety and depression, however, has been extensively tested (83).

To cluster the symptom data, researchers applied a likelihood-based approach inspired by Gaussian Mixture Models (52, 53). One of the main advantages of this method is that it allows tuning the most suitable number of clusters in the data with a well-defined metric (the most common being the Akaike Information Criterion (AIC) and the Bayesian Information Criterion (BIC) (36)), by letting users select the solution that maximizes the likelihood of the trained model given the data. Several drawbacks should be considered, though, as this algorithm assumes the data is structured in a way in which clusters of patients in the feature space follow Gaussian distributions, which is not necessarily the case. Moreover, this approach will always report a solution (there is always a combination of parameters that maximizes the likelihood given the assumptions of the model, regardless of how good the fit to the actual data is). In this study, although a *robustness* analysis is carried out and the reported stability indices across 100 iterations are high, it is unclear if perturbations to the data were applied at all, or if the authors merely re-ran the algorithm on the same dataset. In the latter case, we would recommend taking their stability claims with caution.

Following the method described above, this study reported a five-component solution where clusters seem to differ mainly by disease severity. The authors noted, however, that severity alone did not explain the retrieved components, as (in concordance with their hypothesis) different clusters were enriched in distinct sets of symptoms.

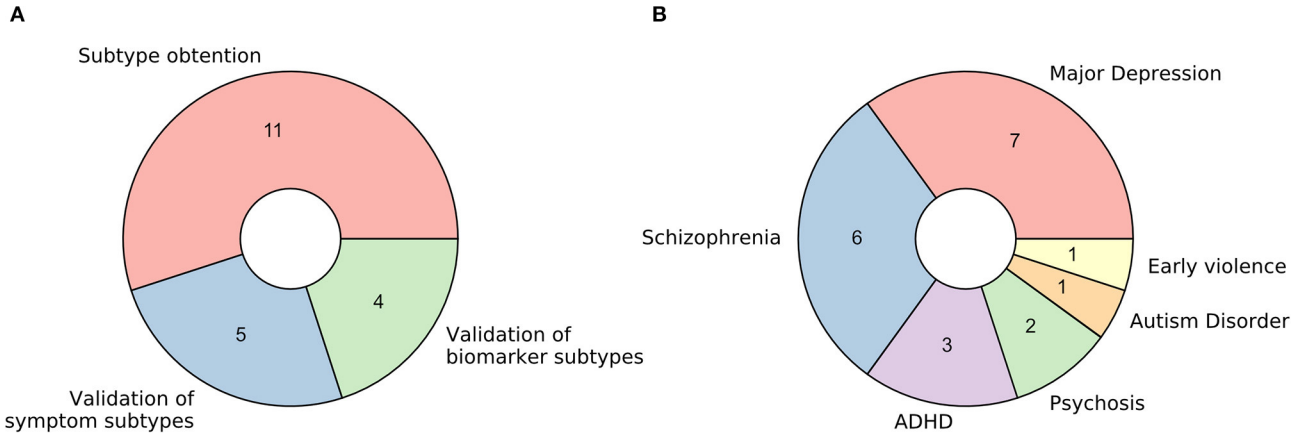

FIGURE 2 | Characteristics of retrieved studies. **(A)** Donut plot representing the number of selected studies for each of the three defined categories: (a) *fMRI used for validation of subtypes obtained via unsupervised learning of symptom-related data*, (b) fMRI *used for validation of subtypes obtained via unsupervised learning of biomarkers other than fMRI (including structural MRI)*, and (c) *fMRI used for brain disease subtyping directly.* **(B)** Donut plot representing the most prevalent brain disorders that the included studies analyzed.

Finally, the authors attempted to interpret the retrieved components using resting-state functional MRI from a subset of the initial subjects ($n = 251$), from which they obtained both dynamic and static functional connectivity networks (dFC and sFC, respectively). While this did not lead to any conclusion for dFC networks, significant results for two of the clusters were found for sFC in the default mode and the frontotemporal networks, both of which are extensively associated with depression in the literature (84, 85).

Schizophrenia

The other three studies in this section focused on clustering subjects with Schizophrenia. Having in mind how evident cognitive decay is in patients with the disease (86), Geisler et al. (46) decided in 2015 to search for subtypes on a set of 18 features derived from behavioral and cognitive scores, instead of pure clinical variables. This built on previous research on Schizophrenia subtyping, where it had been reported that clusters based on pure clinical features were longitudinally unstable: psychotic symptoms and disorganization, in particular, are highly variable across time, which causes subjects to change labels often when models are trained using diagnostic systems directly (48).

The dimensionality of the dataset as mentioned above ($n = 129$) was reduced using a linear principal component analysis (PCA), which works by projecting the data into its subsequently orthogonal most prominent modes of variation. A four-cluster solution was later obtained running the K-means algorithm (39) on the first eight components of this reduced space. While a standard pipeline in data science, successfully applied in a plethora of domains, researchers selected both the number of principal components to keep and the number of clusters (as K-means requires the user to define this beforehand) to match previous literature (47), without a concrete analysis of how this selection would affect their solution. In these cases, as was suggested above for Maglanoc et al., there are several pipelines to follow and determine the number of groups present in the data in a systematic way (36). As many already presented unsupervised algorithms, K-means will always report a solution for the given number of clusters, and special care needs to be taken to avoid subtypes that might be overfitting the dataset. Consequently, while the authors were able to interpret their four obtained clusters in terms of their mean feature values, it remains unclear whether this corresponds to the optimal cluster solution in terms of robustness and generalizability.

Once obtained, the clusters' correlates with both structural and task functional MRI [during a blocked working memory paradigm called SIRP (87)] were explored and compared to healthy controls ($n = 165$). This yielded specific patterns of cortical thickness changes in the hippocampus, the lingual gyrus, the occipital face, and Wernicke's areas for different clusters, all previously linked to schizophrenia in the literature (49, 88, 89). Interestingly, task fMRI correlates were found for two of the clusters. One of them, defined by face episodic memory, slowed processing speed, and increased verbal fluency, showed an increased neural activity in the planum temporale [one of the main reported brain areas for language processing (90)]. The other, defined by a deficit in general intellectual function, was found to be correlated with increased neural activity in the parietal operculum and precuneus cortices [both linked to schizophrenia in the literature (91, 92)].

In 2018, Dickinson and colleagues published an article (49) in which they attempted a different approach by clustering data coming from the Positive And Negative Syndrome Score (PANSS), a widely-used standardized schizophrenia-specific symptom scale proposed by Kay et al. in 1987 (88, 89). Using a sample of 549 individuals comprising only diagnosed patients, they attempted unsupervised subtyping using the two-step SPSS clustering algorithm (90, 91), which fits a likelihood-based model to the data in a way that allows the handling of both categorical and continuous variables in the same

model. By minimizing the aforementioned Bayesian Information Criterion (BIC) across different numbers of clusters (92), the authors obtained an optimal solution with three components, characterized as deficit (with enduring negative symptoms and diminished emotionality), distress (with high emotionality, anxiety, depression, and stress sensitivity), and low-symptomatic. While the algorithm was run 1,000 times with random reordering of the data, no pipeline with cross-validation (leave out sample) approach was reported. This carries the risk of biasing the *robustness* estimates, as readers cannot know if the reported clusters would hold in an even slightly different dataset.

Meanwhile, a subsample of 182 patients balanced across clusters was exposed to functional MRI scans during a working memory task. Here, their three components showed differential activation of the frontoparietal working memory network, including the right dorsolateral prefrontal (DLPFC) and left parietal cortices, and the left anterior cingulate, all of which had been linked to schizophrenia before (50, 51, 93). The low-symptom group in term showed significantly greater activation in the right DLPFC than the two more symptomatic groups, a healthier pattern mainly linked to working memory and cognitive flexibility (94).

Lastly, a similar approach was followed by Chen et al. in 2020 (56). Using a bigger sample of 1,545 patients diagnosed with schizophrenia, they used Non-Negative Matrix Factorization (NMF) to reduce the dimensionality of patients' PANSS score data. NMF compresses the feature space into a user-defined number of factors by decomposing the data into two non-negative matrices: a basis matrix (called dictionary) with factors as columns, and a factor-loading matrix representing symptomatology of individual patients in the training set (57). Besides, the algorithm imposes an orthonormality constraint that promotes a sparse, more interpretable, representation (95). Using this approach, the extensive PANSS data was reduced to just four values (one per retrieved factor) per individual. These reduced data were then clustered into two components using the fuzzy C-means algorithm (96), which can be thought of as a soft version of the k-means mentioned above, in which each subject is assigned a probability of belonging to each cluster instead of a hard cluster label only. This helps to deal with outliers, usually yielding more robust solutions in real-world data (97).

It is important to highlight here the extensive validation pipeline that this study, in contrast to the previously mentioned in this section, applied in each described step. For dimensionality reduction, we highlight that several standard factor concordance indices (98, 99) were computed for a range of factors across 10,000 runs on random half-splits of the data. Clustering stability was tested by subsampling, bootstrap resampling, and leave-one-site-out replication on a deliberately heterogeneous external sample of 490 patients recruited from nine hospitals across Asia, Europe, and the US. In both steps of the pipeline, the most *robust* solutions of four factors and two clusters were kept.

In addition, the two clusters, when projected on the original PANSS data, were revealed to be mainly representing patients with more prominent positive and negative symptoms respectively. Using functional MRI data derived from a balanced sample of 84 patients, researchers applied a Support Vector Machine [a classification algorithm (100)] to sort subjects in both clusters using functional connectivity features. An overall feature importance analysis of this classifier was used to interpret the components on the functional side, showing the ventromedial frontal cortex, the temporoparietal junction, and the precuneus as the most critical networks whose connectivity differed between clusters. All of these networks have not only been linked to Schizophrenia before but also, in concordance with the authors' interpretation of their clusters, to discriminating between positive and negative symptoms (97–99).

fMRI Used for Validation of Subtypes Obtained via Unsupervised Learning of Biomarker Data

In this second section, we will discuss three studies (published across four papers) in which the obtaining of biotypes was attempted applying unsupervised learning techniques to sets of biomarkers other than functional MRI itself. This is a particularly important approach, born from the assumption that different biological manifestations of disease can lead to the same phenotypic outcome (as discussed in more detail below).

Psychosis

The first study is composed of two articles, published by Clementz et al. and Meda et al. in 2016 (58, 60), on identifying psychosis biotypes. While the first article deals with the obtaining of the biotypes themselves, the second analyses their functional correlates using resting-state functional connectivity.

The term psychosis refers to several pathologies that lead to a deteriorated perception of reality (101). In concordance with what was explained above, the authors claim that different etiologies underlying psychotic symptoms do not necessarily overlap with the available symptom-defined labels (schizophrenia, schizoaffective disorder, and bipolar disorder with psychosis), as symptomatic outcomes may represent the convergence of distinct biological entities. With this in mind, they gathered 1,872 samples from patients diagnosed with any of these diseases ($n = 711$), their first-degree relatives ($n = 883$), and comparable healthy subjects ($n = 278$). The data consisted of biomarker panels comprising neuropsychological markers, cognitive assessment tasks [such as stop signal and saccadic control (101, 102)], and auditory paired stimuli and oddball evoked brain responses assessed by electroencephalography (EEG). Patient data were used for clustering, while relatives and controls served for result validation. Authors further reduced the dimensionality of their dataset by running a Principal Component Analysis (PCA) per modality, selecting the number of components to keep using the elbow in the variance explained curve (92). This yielded a reduced set of 9 features, which were fed into a K-means algorithm from which authors reported a three-component solution. Cluster selection was carried out by maximizing the *gap* statistic (59), which is higher for solutions in which distances between data points within a cluster are consistently smaller than distances between clusters. Cluster robustness to perturbation was assessed *via Jackknife* (103), an approach in which the model is trained as many times

as individuals in the dataset, leaving each time a different individual behind.

As hypothesized, cluster assignment did not merely recapitulate the DSM derived labels: they observed that clusters (or biotypes) differed beyond outcome severity, and manifested distinct overall profiles, such as (1) *impaired cognitive control and low sensorimotor response*, (2) *impaired cognitive control but exaggerated sensorimotor response* and (3) *near-normal cognitive and sensorimotor characteristics*. Furthermore, differential cortical thickness of key brain areas was found via voxel-based morphometry (VBM) such as the frontal, cingulate, temporal, and parietal cortices, as well as the basal ganglia and thalamus.

In the follow-up study, individuals in an independent sample ($n = 1{,}125$) were assigned to the already defined clusters. When comparing patients to relatives and healthy controls, the authors found significantly reduced functional connectivity (both globally and across specific biotypes) in nine networks consistent with previous reports (104–109), and with areas known to be compromised in psychiatric disorders in general, including cognitive control, working memory, attention and introspective thought maintenance. Importantly, all these deficits are claimed to track cognitive control factors more closely, suggesting potential implications for both disease profiling and therapeutic intervention.

The remaining two studies used structural MRI to find disease subtypes and projected their findings into resting-state functional connectivity data afterward.

Autism Disorder

The first of the two, published by Chen et al. in 2018 (61), attempts to find Autism Disorder (ASD) subtypes in a sample of 356 diagnosed patients. Taking into account the evidence of atypical neuroanatomy within patients with ASD (110), and the fact that subjects exhibiting different clinical symptoms showed distinct brain structural abnormalities (111), the authors used features extracted from a voxel-based morphometry analysis on structural MRI. Interestingly, the clustering was not performed on these features directly. Instead, researchers computed the *structural difference* between each ASD diagnosed patient and a set of matched healthy controls ($n = 403$), and then applied the aforementioned Non-negative Matrix Factorization algorithm for dimensionality reduction into 60 components representing differences in brain structure between cases and controls. By applying a simple K-means algorithm, authors were able to retrieve a three-component solution. Cluster number selection was carried out by maximizing the silhouette index (62), a statistic that, as many presented already, reflects how concentrated the values of the resulting components are within their respective clusters. While robustness analyses were carried out (by running the algorithm 10 times with random 80% subsets of the data), it is worth mentioning that authors do not report having tested the presence of clusters at all in the data (i.e., number of clusters equals to one).

When validating and interpreting their results, authors first reported differences in disease severity between clusters, as assessed by the Autism Diagnostic Observation Schedule (ADOS) score (112). Besides, when comparing the resting-state functional connectivity networks for each patient in each cluster to healthy controls, they found statistically significant differences in two of the clusters. In both cases, ASD patients showed diminished connectivity in the default mode network, the frontoparietal network, the cingulo-opercular network, the sensory-motor network, and the occipital network, all of which had been linked to autism disorder before (113–117). While more validation studies are needed, this paper provides evidence toward ASD not being a neuroanatomically homogeneous disease.

Internalizing Disorders

The last study in this section focused on finding structural subtypes in subjects with internalizing disorders, which are characterized by anxiety, depressive, and somatic symptoms. In this study, Kaczkurkin et al. (63) took a different approach to disease subtyping. Instead of clustering diagnosed patients in a fully unsupervised way, they used a semi-supervised approach called HYDRA (64), which uses the binary case-control labels to find different disease subtypes regarding their difference to controls. This way, the approach is conceptually similar to the paper by Chen et al. cited immediately above, although the difference between cases and controls is not processed directly, but a part of the clustering algorithm.

Thus, using HYDRA in volumetric and cortical thickness data from 1,141 individuals (715 cases and 426 controls), they found a two-cluster solution when maximizing robustness as assessed by the Adjusted Rand index (ARI) during a 10-fold cross-validation scheme (which consists of running the algorithm 10 times, each leaving a different random tenth of the data out). In addition, the functional connectivity of 40 subjects balanced across these two defined categories was obtained in the frequency space (118), which has the advantage of enabling the direct comparison of structural and functional measures using the same atlas (119). The functional measures reflect the average connectivity of a particular region of interest, in this case, delimited by differential structural features. By physically delimiting their functional search by the structural characteristics of their clusters, authors make the assumption that detected changes in connectivity would be directly influenced by the changes in structure, which is a debated concept that was not put directly in place by the studies proposed so far (120, 121). When interpreting the retrieved clusters, researchers reported that one of them was marked by reduced cortical thickness, and showed impaired cognitive performance and higher levels of psychopathology. On the functional side, moreover, this same cluster displayed abnormal connectivity in frontolimbic regions, which is consistent with poorer cognitive performance as reported in the literature (122).

fMRI Used for Brain Disease Subtyping Directly

The last results subsection will deal with studies in which biotype obtaining was attempted from functional MRI data itself. Eleven articles (ten original studies and a relevant replication) comprising four disorders were included, of which ten relied

on resting-state functional or effective connectivity and one in a task-based setting.

Schizophrenia and Related Disorders

Starting with Schizophrenia and its related disorders, in 2014, Du et al. (65) published an article in which the distinction between Schizophrenia (SZ) itself, psychotic bipolar disorder (BD), Schizoaffective disorder with depressive episodes (SADD), and Schizoaffective disorder with manic episodes (SADM), all of which share overlapping sets of symptoms and genetic landscapes (123, 124), was recapitulated using functional connectivity data clustering (65). This built upon the fact that, for all four, differences in functional connectivity between cases and controls had been reported, which had significantly raised the interest in delineating the functional implications of these diseases over the last few years (125, 126). In addition, the authors attempted to shed light on the controversy on whether SAD is an entity in itself or the manifestation of some degree of interaction between SZ and BD (127). To process their data, they used Independent Component Analysis [ICA, a standard technique for obtaining correlated brain networks (128)] to yield functional connectivity data from a sample of 93 subjects, balanced across all diagnosis categories (including healthy controls).

While pioneering the use of unsupervised learning on resting-state data, this paper illustrates one of the major issues with feature selection in clustering (129). Given that, *a priori*, this study deals with a high number of brain connectivity features and a relatively low number of samples, the authors proceeded to reduce the dimensionality of their data. However, instead of using an unbiased technique such as the aforementioned PCA or NMF, the authors fitted classifiers to discriminate between the five classes in a supervised manner and retained the most informative features. They accomplished this by using a standard technique called Recursive Feature Elimination (130), which measures how impactful the removal of certain features (in this case brain networks) is for a classifier to distinguish between entities. Even though they arrive at a nearly perfect 5-cluster solution (recapitulating their original four diseases and healthy controls), the problem arises from the fact that the features they used were selected to overfit the classification they already had, which makes the clustering trivial. Furthermore, we believe a warning of caution should be raised on the final conclusion of the study, which uses the distances between retrieved clusters (which had been artificially maximized) as evidence to support the hypothesis of Schizoaffective disorder being an independent etiological entity.

Another article that dealt with dissecting the mechanistic underpinnings of Schizophrenia and its potential subtypes was published by Brodersen et al. in (66, 86). In this proof-of-concept study, the authors employed Dynamic Causal Modeling (DCM) to retrieve a *directed connectivity* model from a balanced sample of 83 subjects, including diagnosed patients and healthy controls. While they present a plethora of demonstrative approaches in their study, here we will only discuss their unsupervised clustering, which implicated two separate pipelines: first, authors were able to recapitulate the classification between cases and controls with relatively high accuracy (∼71%) using only clustering on the whole sample. Second, and arguably more interesting to this review, the exclusion of the healthy controls led to a clustering solution of three components ($n = 41$), which seemed to differ mainly by symptom severity, as assessed by the aforementioned PANSS scale.

To reach these solutions, researchers applied a Variational Bayesian Gaussian Mixture Model, a variant of the likelihood approach presented above for Maglanoc et al. which runs automatic cluster selection by estimating how many components of a *prior* distribution are present in the data. While this algorithm is appealing for small studies, finite Gaussian Mixture Models as the ones presented above are still preferred in many settings, given their lower computational complexity and their fewer associated implicit biases (131).

While a mere pilot study where the main goal was to explore and define a working pipeline, the authors use these results as an argument to defend the exclusion of healthy controls in the unsupervised learning procedure, as the likelihood of the already-known binary factor is high (the variance in the data might in many cases be dominated by the disease-control distinction). However, we believe that a follow-up study should review if these premises hold in a bigger sample, and assess how generalizable and *robust* the solutions are using internal and external validation, as was highlighted throughout the review.

A different approach was taken by Yang et al. in 2014 (69) when investigating early-onset Schizophrenia (EOS) in a small sample of 52 individuals, balanced across medication-naïve diagnosed patients and age and gender-matched healthy controls. The authors used a pipeline called gRACIAR (generalized ranking and averaging independent component analysis by reproducibility) (132) to obtain both subject-specific functional connectivity networks (via Independent Component Analysis) and a meta graph concerning intersubject similarity within each functional connectivity network. Using a maximal-clique community detection algorithm, a clustering procedure that, unlike all presented above, works on a graph level (70), researchers reached a clustering solution for each of the retrieved networks. Importantly, the similarity thresholds for drawing the edges of the mentioned metagraph were selected based on the average solution robustness to permutation tests during cross-validation.

While no communities (the equivalent to clusters in graph theory) were retrieved for the majority of the explored networks, two of them yielded interesting results. First, a component involving the precuneus-angular gyri (PCU-AG, associated with the default mode network), was detected to significantly recapitulate the case-control separation, which suggested a novel association between these functional connectivity features and EOS. Second, a network involving bilateral superior temporal gyri and bilateral inferior frontal gyri yielded a solution enriched in diagnosed patients, which seemed to recapitulate the difference between positive and negative symptoms (as assessed for example with the PANSS scale).

While the retrieved clusters revealed little new about the disease substructure across subjects as a whole, this approach allowed for the discovery of associations within networks that had not been previously reported. Furthermore, the question

of whether more interesting clustering solutions from an EOS functional subtyping point of view could be retrieved with a bigger sample size remains.

Major Depression Disorder

Shifting to Major Depression Disorder, Drysdale et al. (73) reported in 2017 a four-cluster solution from resting-state functional connectivity data, using a training sample of 220 diagnosed patients. For dimensionality reduction, they applied an algorithm called Canonical Correlation Analysis (CCA), which, instead of selecting the most prominent modes of variation in one dataset as many of the approaches presented above (such as PCA or NMF), takes two data modalities and returns a space in which the correlation between them is maximized (74). In this case, the authors decided to apply it to a combination of the functional connectivity data, coming from fMRI, and the subjects' HAM-D scores [one of the most common self-assessed symptom scales for MDD (133)]. This type of analysis can be particularly useful for high-dimensional data where the major components of variability are not expected to be related to the problem at hand. In this case, the assumption is that there might be other sources of variance, such as sex, age, brain size, etc. that might overshadow the implications in functional connectivity of potential MDD subtypes. This way, a transformation of the biological data that correlates with psychiatric symptomatology is reported, making it likely that the downstream clustering will focus on relevant connectivity features.

After applying this pipeline, the authors retained the first two canonical variates (which one could see as analogous to principal components in this context) obtained from CCA, which they interpreted as anhedonia and anxiety-related by checking correlation with individual symptoms. Using a Hierarchical Agglomerative Clustering approach, they reached a four-component solution by maximizing the so-called Calinski-Harabasz (CH) index, a statistic similar to the Silhouette presented before, that measures how similar a datum is to its own cluster compared to others (75). Drysdale et al. (73), These components lay on each of four quadrants defined by two axes, interpreted by the authors as anhedonia and anxiety-related. Interestingly, both clusters associated with high anxiety profiles were linked to abnormal connectivity patterns in the frontal amygdala [fear-related behavior and reappraisal of negative emotional stimuli (134)] and abnormal hyper-connectivity in the reward system was especially pronounced in anhedonia-related clusters.

Aside from providing innovative methods and focusing thoroughly on the generalizability of the achieved results, this article incentivized active discussion in the field, especially after a replication attempt published by Dinga et al. in 2019 (78). When failing to reproduce the original results after applying nearly the same pipeline on a smaller independent cohort of 187 diagnosed individuals, the authors highlighted potential statistical weaknesses in the original study.

First, they claimed there was a statistical bias in the reported CCA results. While the original article alleged that both canonical variates' correlation with symptoms were statistically higher than random, the problem arose from a two-step process that Drysdale et al. applied. From the functional connectivity matrices obtained from fMRI, they selected voxels whose activations were most correlated with symptoms and *then* employed only those features on the CCA analysis. Furthermore, the first selection step was ignored in the statistical tests they ran [based on Wilk's lambda statistic, typically used for this purpose across the literature (135)], and permutation testing in the replication study showed that the significant correlations between symptoms and connectivity faded away when taking into account this pre-selection of voxels. This made it seem likely that the original procedure was selecting noise in the direction of the hypothesis. Moreover, CCA is known to be prone to overfitting (reporting correlates between modalities that are much stronger than they would be on an independent dataset). While Drysdale et al. did not evaluate this problem directly, 10-fold cross-validation in the replication revealed it was a significant issue, raising even more caution toward the reported CCA factors.

Lastly, even when Drysdale et al. assessed internal and external validation of their findings (by measuring cluster stability across 10,000 random splits of the data, and using an independent multisite dataset, respectively), they did not test the null hypothesis of whether there was an inherent clustering structure in the data against the possibility of a continuum (a single, unimodal distribution). When testing this using previously described methods (79), they found no significant evidence supporting a clustering structure. In summary, while some details of the proceedings were not the same as in the original, this article shows how important thorough statistical testing (which considers every step involved in all relevant pipelines) is in these complex scenarios of multiple data integration and how crucial replication attempts are. While Dinga et al. do not discard the possibility of subtypes of depression that are identifiable at a functional level, they raise a warning of caution about the lack of strong evidence supporting it, and call for more extensive methodological evaluation in an incipient field.

In another pioneering study, Price et al. were the first to our knowledge, in 2017, to use *effective* connectivity to build *directed* resting-state networks using causal modeling for MDD subtyping (67). The pipeline employed (called Group Iterative Multiple Model Estimation, or GIMME) has been shown to reliably recover both the presence and direction of connectivity among brain regions per individual in simulations (136). Using a sample of 80 diagnosed patients with Major Depression, the authors built a similarity matrix between model parameters among individuals, which they thresholded into a graph. Here, they reached a two-component solution via a clustering algorithm called Walktrap (68), which works under the assumption that short-distance random walks in a graph tend to stay in the same community. It is a *hard-clustering* algorithm, in the sense that a label is assigned to every patient, without any associated metric reflecting how confident the model is in each case. Furthermore, even though this approach arrives automatically to an optimal number of clusters in the data (according, that is, to its own definition of what a cluster is), neither *cluster robustness* analyses nor estimates of how generalizable their solution might be on external data were provided in this study. Besides, although innovative in their methodologies based on causal, directed

connectivity, their method is computationally demanding, which limits the resolution of the brain activation networks they can use when compared to methods based on functional connectivity.

Mapping back their retrieved components to functional connectivity, authors observed that one of the two retrieved groups showed a connectivity pattern across DMN nodes concordant with what was previously reported on average depressed patients (85). The other subgroup showed, however, a different pattern in this region, with increased dorsal anterior cingulate-driven connectivity paths. This group also had significantly higher comorbidity with an anxiety disorder and highly recurrent depression, which led to a poorer outcome of the disorder. Interestingly, altered connectivity in anterior cingulate regions (belonging to the DMN) has been more recently linked to persistent sadness and higher recurrence rates (137), which goes in concordance with these results.

In summary, while the employed sample size is small and further validation is highly encouraged, this study illustrates how graph theory and causal modeling can be used together to shed light on the mechanistic heterogeneity behind major depression in particular and brain disorders in general.

As previously mentioned, an issue that researchers often encounter when applying clustering algorithms to a problem is that, even when a relevant structure is present in the data, it can be overshadowed by variance factors that are ultimately unrelated to the problem. The most typical ways of dealing with this issue are to control for *known* confounders in our models, such as age or sex (138), to directly model and remove their variability (139), or to transform data in a way that maximizes its correlation with a highly informative variable [as previously presented for CCA and symptom scores (73)]. Tokuda et al. (77), however, introduced a custom algorithm that tackled the problem in a very different way: they arrived at multiple *solutions* (or *views*) simultaneously, which corresponded to *different modes of variation* in the data. This way, they could select *a posteriori* if any of them was actually related to subtypes of disease (in this case MDD) and still extract potentially useful insights about their samples from the rest. Furthermore, each of these *views* attempts to solve a so-called co-clustering problem, in which both subjects and features are grouped. This means that individual solutions won't be forced to adopt all the available information, ideally using only those features that are relevant to them. Moreover, the algorithm they propose is capable of simultaneously dealing with categorical and continuous variables, allowing researchers to integrate resting-state functional connectivity data with other data domains, such as BDI questionnaires, biomarker panels, genetics, and methylation data from a preselected set of related genes.

When applying this approach to a sample of 134 subjects, balanced across diagnosed patients and healthy controls, the authors reached a five-component solution after selecting the view that maximized the Cohen's D coefficient [a statistic that measures effect size (140)] between the two groups. Interestingly, two clusters were mainly composed of controls, whereas the other three included diagnosed patients almost exclusively. Moreover, these three MDD-related reported clusters were observed to differ significantly by functional connectivity between the Angular Gyrus (and other already reported brain areas in default mode network), child abuse trauma scale scores (CATS), and selective serotonin reuptake inhibitor treatment outcomes (although all of these were used directly for clustering). Cluster stability (*robustness*) was tested via leave-one-out cross-validation (similar to the aforementioned Jackknife) on the whole pipeline, but no external validation was accounted for. While the employed sample size is relatively small, and the results demand replication in independent datasets, this article proposes an innovative and assertive approach with a high potential for integrating distinct data domains.

Attention Deficit Hyperactivity Disorder

Another article that relied on effective directed connectivity, and applied the aforementioned GIMME algorithm, was published in 2014 by Gates et al. (120). In this study, the authors attempted to cluster a sample containing also 80 individuals, balanced across subjects diagnosed with attention-deficit/hyperactivity disorder (ADHD) and healthy controls.

After following a pipeline nearly identical to the one presented above for Price et al. (67), the study reported a solution with five components, two of which were almost exclusively composed of ADHD-diagnosed patients. First, researchers generated a network in which subjects were connected when the similarity between their directed connectivity patterns is high (*how* high was determined by measuring cluster *robustness* under a cross-validation scheme). For clustering, they used a *hard* community detection similar to the Walktrap mentioned above, which partitions the network into non-overlapping communities by maximizing a metric called *modularity* (that compares the number of edges within a community to those that connect it to other partitions) (141).

The obtained subgroups were reported to be highly distinguishable by their differential connectivity in regions such as the dorsolateral prefrontal and frontal cortices, the intraparietal sulcus, and the inferior parietal lobule, all of which had been previously linked to ADHD in the literature (142). Furthermore, the inclusion of healthy controls at clustering time, and their presence even in clusters highly dominated by diagnosed subjects, made it interesting to consider that the reported brain findings may reflect liability for ADHD in subgroups that are biologically at risk. Rather than ADHD *per se*, the controls in these groups may represent individuals at risk for ADHD who had sufficient protective factors in their development (or their genome) to avoid exhibiting the syndrome. Although inconclusive, this article, as many in this review, provides evidence toward the presence of biological subtypes in yet another psychiatric disease, which can be recovered at a functional level.

Using a functional connectivity pipeline on a sample of 106 children (aged 7–12 years), including both diagnosed patients and controls, Costa Dias et al. also attempted to find data-driven subtypes of ADHD in their article published in 2015 (71). One of the main highlights of this study is that, in order to reduce the original dimensionality of their functional connectivity data obtained from resting-state fMRI, the authors restricted the problem physically, by including only brain areas that had been previously reported as related to the disease.

To accomplish this, they built a mask using a meta-analytic tool called NeuroSynth (143), which yielded a set of brain regions that highly overlapped with the reward system. This constitutes a well-studied connectivity hub, which interacts with other brain networks to promote decision-making, and has been extensively shown to be altered in ADHD (72). From the resulting connectivity features, researchers extracted a meta-correlation matrix that was thresholded into a graph, and applied the same network-based modularity-based algorithm mentioned for the previous paper by Gates et al. Using this approach, authors arrived at a three-cluster solution, whose stability was assessed by randomly perturbing the aforementioned network 20 times. *Robustness* was then assessed using a metric called variation of information (VOI), which measures how much information differs between the two sets of community assignments, and varies from 0 (identical) to 1 (completely dissimilar) (144).

This article reported that connections between the nucleus accumbens and the default mode network were atypical in ADHD across all the three subgroups, a finding that was previously reported by the same group (145). The authors, however, arrived at this conclusion by comparing diagnosed patients to controls in each of the three reported communities. Furthermore, one of the main drawbacks of this study was that it seems to have failed to recapitulate disease manifestation along with the clustering solution, making it seem likely that the factors of variance captured by the applied methods do not correspond to the disease axis. Specifically, this would mean that the most prominent mode of variation in connectivity across the reward system does not correspond, at least in their sample, to the manifestation of the disease.

Having this issue in mind, Lin et al. published in 2018 (76) what constituted the last attempt to date (to our knowledge) to find biotypes of ADHD using resting-state fMRI. In this article, the authors used a sample of 80 diagnosed subjects and 123 matched healthy controls, to extract networks that, across the entire dataset, were differentially activated between both groups. This approach yielded differential activations predominantly between the default-mode, cingulo-opercular and subcortical networks, all of which had been previously reported as related to ADHD as a whole (62, 146). They then attempted to use this data to specifically contrast what they called a *dimensional biotype* (i.e. heterogeneity arises from variation over a continuum of the same entity) against a *categorical biotype* (different pathological entities explain the observed variability in the data, which converge in similar symptomatology).

To further deal with unwanted modes of variation, they applied a variant of the aforementioned canonical correlation analysis (CCA) to bring into the picture the maximum correlates between their differential functional connectivity and symptomatic scores. From this analysis, they were able to retrieve just one significant mode of covariation between both data modalities, which was interpreted as the first piece of evidence supporting a *dimensional biotype*. Moreover, they attempted to cluster the data using two distance-based clustering algorithms: K-means and spectral clustering, both of which yielded an optimal solution supporting the absence of discrete biotypes in the data. This was concluded after maximizing the *robustness* of the obtained results, as measured by already presented metrics, such as the Jaccard and silhouette indices, and the gap statistic (59).

While the overall conclusion of this paper supports the idea of ADHD being a single biological entity, we believe the presented evidence is inconclusive, and that a few concerns should be raised. For starters, while the sample size is said to be large enough to deal with the applied clustering algorithms given their number of features (34), this may not consider the complex feature selection/extraction that was employed. It is possible that even though it is technically possible to apply these algorithms to a sample this small, not enough variation is captured in their original dataset to represent with confidence potential categorical biotypes that might exist in the population. Second, the first step in their feature extraction pipeline involved the usage of only those networks that were differentially activated between cases and controls overall. While this can be useful, as mentioned, to dissect modes of variation that are related to the problem at hand, it also carries the risk of leaving behind brain connectivity features that might differ significantly between controls and particular subsets of patients (the biotypes). In other words, filtering by overall variation might bias the data toward features that correspond to a dimensional biotype.

Consequences of Early Trauma

The last study presented in this section, published by Sellnow et al. in 2020 (80), delves into the functional consequences of extreme stress in early childhood. Early stress events (such as interpersonal violence -IPV- or severe trauma) are one of the major causes of subsequent psychopathology, and no systematic studies had attempted to disentangle their underlying heterogeneity in neither the type nor the magnitude of their consequences (147).

To tackle this problem, the authors used a sample of 114 adolescent girls (aged 11–17), from which they obtained functional MRI data during an emotion processing task in a blocked design. After filtering the voxels of interest using a meta-analytic mask obtained from the aforementioned NeuroSynth (related to emotion processing), the GLM-first order coefficients were concatenated and clustered across individuals using the K-means algorithm. After selecting the best model using the already presented elbow method on the cluster validity index [a statistic that, like many introduced before, compares intra-cluster to inter-cluster density (34)], they reached a three-component solution, shown robust *via* leave-one-out cross-validation.

At a functional level, the retrieved clusters were distinguishable by engagement of the medial prefrontal cortex, the anterior insula, and the hippocampus, all involved in emotion processing (which is not surprising, given brain features had been filtered using a meta-analytic mask using this criterion). Interestingly, when analyzing the relationship between each cluster and external measures of interpersonal violence (IPV) and internalizing symptoms, the authors managed to report a 'healthier' component, in which exposure to violence had been lower, and two clusters with high symptom severity, that seemed to differ on the presence or absence of sexual assault. Furthermore, IPV exposed a negative correlation with symptom

reduction over Trauma-Focused Cognitive Behavioral Therapy (TFCBT), which led the authors to suggest the feasibility of their methodology to predict treatment outcomes based on functional information.

As many studies presented in this review, this last one attempts to set the ground for further exploration of an incipient field. One concern about their methods, though, is the high dimensionality of the used data. Having retained 3,970 voxels after filtering, and using a GLM with blocks of 4 different tasks, each of the 114 individuals ended up represented by 15,880 values. Although one could argue that these features are far from independent (after all, they represent the task-importance of voxels that are contiguous in space), this extremely high relationship between dimensions and samples can lead to overfitting, severely decreasing the generalizability of the models to external samples. This problem, often referred to as the "*curse of dimensionality*", is a very common drawback to many machine learning models which usually justifies the need for dimensionality reduction (148).

DISCUSSION

One Problem, Multiple Approaches: Top-Down, Bottom-Up, and Polytopic Learning

Throughout this article, we gave an overview of the most recent attempts to subtype psychiatric disease in a data-driven manner. Across 20 studies, we illustrated how functional MRI, arguably the most relevant proxy of brain function to date, was applied to both validation and interpretation of clusters retrieved with other techniques, and as part of the clustering pipelines themselves.

Furthermore, these categories are encapsulated within two broad ways of dealing with subtyping in data-driven medicine, which we would like to call *top-down* and *bottom-up* approaches. The former corresponds to what was presented in the first section of this review: the use of data comprehending the clinical and behavioral manifestation of disease, and the attempt to validate the retrieved components relying on the elemental biology. The latter is the opposite (second and third sections): clusters are defined based on the biology and validated at a clinical/behavioral level.

In this context, the first section of the results illustrated how unsupervised learning could be used to detect subgroups in psychiatric symptom data (**Table 2**). As briefly discussed in the introduction, this approach is likely to yield disease symptomatic states rather than biological entities, given that different sets of symptoms do not necessarily reflect distinct etiologies. Symptomatic profiles, moreover, are sensitive to treatment and environmental perturbations, among others. This may reflect in patients changing cluster assignments during the course of their disease, making the usage of this type of solution hard for diagnostic and prognostic models. Along the same lines, however, this type of approach can be very helpful to better evaluate the state of a patient at a given time, which constitutes an arguably different but equally relevant problem than the one we are presenting here.

The second and third sets of articles (**Tables 3**, **4**) focused on a *bottom-up* approach. When clustering biomarkers, the assumption is that the data capture the manifestation of the disorder at a lower level (hence *bottom*), yielding results that are potentially closer to uncovering pathological origins. This is particularly relevant when considering that distinct biological entities (which can have distinct optimal treatments) can converge to an equivalent symptomatic profile. For example, studies have shown how different genetic alterations that produced different structural consequences led to the same set of autistic-like behavioral traits in mice (49).

Among the methodologies overviewed in the second section, structural MRI clustering (encompassing 2/20 studies) and its projection into functional data deserve special mention, as several studies have shown that psychiatric disorders have structural implications (149). While diseases such as Autism or Schizophrenia are generally recognized as neurodevelopmental disorders with brain structure being affected, there are inconsistencies regarding the regional specificity of the neuroanatomical findings (149), making the importance of structural subtyping apparent. Furthermore, the search for functional correlates of these subtype-specific functional alterations relies on assuming that an altered structure may lead to an altered function. By combining the two data types, it is possible to test this hypothesis, retrieving multiple domains affected by the disorder that may be coupled with a non-trivial causal relationship.

Delving into the third and last set of articles (**Table 4**), we want to highlight that fMRI is the most direct measure of brain function we have to date. Although not ideal, it constitutes arguably the best available proxy for the biological manifestation of brain disease. This carries the potential to shed light on mechanistic biotypes reflecting distinct pathological entities that overlap at higher levels. Both task and resting-state approaches have been explored, although the vast majority (10/11) of studies opted for the latter given its more straightforward implementation and potentially broader conclusions and generalizability (39).

It shouldn't go unnoticed that many studies (4/20, all in the third section) integrate both symptom and biological data in several clever ways. This set of approaches, which lies arguably in the interface of the *top-down* and *bottom-up* presented above, belong to what has been called *polytopic learning* (39). By either combining both kinds of data for clustering directly (77) or relying on multimodal transformations such as CCA (73, 76, 78), researchers seek to bridge the gap between origin and manifestation of disease, in search of what have been described as *endophenotypes* (150). We think this has an incredible potential *a priori*, as illustrated by the many proofs of principle in this review. However, it implies extending the dimensionality of the datasets and, up to now, limiting sample sizes for reaching strong conclusions. However, the future, in this regard, looks promising.

Deep Validation of Retrieved Biotypes

As previously mentioned throughout this review, the interest in disease classification (and sub-classification) is far from

new. Aside from expanding basic knowledge, taxonomy as a whole serves the purpose of recognizing distinct, stable entities that may be treated differently, which can directly lead to improving people's lives. In this sense, unsupervised learning has the potential to help researchers discover these entities given the right data, models, and experimental designs. Whereas, in other medical subfields clinical application is more tangible (151, 152), psychiatry carries the weight of a perfect storm: on top of currently relying on fuzzy symptom-defined labels, relevant functional data collection is expensive, making sample sizes to date (as seen throughout this review) limitingly low.

This is far from discouraging though, as the field is still at an early stage where methodological exploration seems to be the rule. It does highlight, however, the importance of thoroughly validating the retrieved results on several equally relevant dimensions, in what some authors have called *deep validation* (153) of biotypes. This concept encompasses three main axes: (1) replication of clustering solutions in independent data, to assess methodological generalizability (2) application of a retrieved clustering solution to new independent data (without reclustering), to gauge whether the new assignments correspond to clinically meaningful outcomes, and (3) extension of clustering solutions defined in a cross-sectional manner to a longitudinal setting, to determine if baseline components yield, for example, differential trajectories of disease progression.

When exploring how these three concepts were touched upon across the systematically retrieved literature, we found that the first deep validation component, which goes in line with the notion of generalizability discussed above, was the most explored throughout the available corpus. Even in mostly proof-of-principle settings, 15 out of 20 studies engaged in robustness and generalizability analyses (**Tables 2–4**). Most of them, however, yielded intra-sample reports (by partitioning one available dataset instead of using truly external data) which can lead to inflated generalizability estimates (37). While nearly all studies (17/20, **Tables 2–4**) undertook an interpretation of their solution using clinically relevant measures, only four of them (56, 58, 60, 73) attempted to report generalizability across multiple data collection sites, using truly external data. Moreover, only two (60, 73) attempted the application of the retrieved biotypes to an independent sample (second deep validation component). Among these, interestingly, Drysdale et al. (73) reported significant differences in outcome after the patients were treated with transcranial magnetic stimulation (TCMS), which constitutes a perfect illustration of the potential utility of biotyping as mentioned above. Furthermore, only one of the retrieved studies to date has engaged in longitudinal validation (56). This one, unsurprisingly, used symptom data to cluster given its easier collection across time.

While the landscape we found is far from ideal, the lack of thorough, standard deep validation pipelines reflects, in our opinion, the scarcity of relevant available data in such an early stage of the field rather than deep methodological flaws.

Methodological Heterogeneity: Should We Strive for Standardization?

Whereas most of the papers followed overall similar formulas (data preprocessing, select relevant features or reduce the dimensionality of the dataset, and cluster the available samples), we observed vast methodological variability in every step along the way.

As differences in dimensionality reduction approaches were discussed throughout the corpus of the article, in this section we will focus on the coarse classification of clustering algorithms provided in **Table 1**. Here, we observed that the majority (12/20) of the studies employed distance-based methods. An equal number of papers applied algorithms that work at the graph level and model-based approaches (4/20 each). Whereas we think that, given the fuzzy nature of the available labels and how important the measure of uncertainty in the medical setting is (154), model-based approaches may be the most intuitive way to go, we found the preference for simpler, computationally cheaper models understandable given the incipient state of the field. It is refreshing to see, however, that even at this incipient stage several customized algorithms, designed specifically with the problem of biotyping in mind, have been presented (77, 120).

A topic that deserves special attention is the inclusion of healthy controls. Of the 20 retrieved studies, 6 decided to treat healthy controls as any other sample, one utilized them indirectly by clustering differences between matched subjects (61), and one treated them as a normative reference for semi-supervised learning (63) (**Tables 2–4**). As made evident by the variability in the literature [the strongest retrieved example being the three retrieved papers on ADHD (67, 71, 76)], this is not a closed topic and valid arguments on both sides exist. On the one hand, their inclusion may lead to an obvious first mode of variation in the data. This can lead to clustering algorithms finding the division between cases and controls as the dominant solution, which would yield no new insights on disease functioning. On the other hand, however, if sufficient data modalities are available and subtypes are prominent enough, the inclusion of healthy controls makes sense as a way to represent the true nature of the population. Finding clusters enriched in healthy controls can thus be interpreted as a mild form of validation. Moreover, individuals in disease-enriched clusters who were not diagnosed might correspond to early stages of disease, or be a consequence of the presence of protective factors that may lead to further investigation.

Finally, the available variability opens an important question: Should we strive for methodological standardization to remove potential dependencies of the results on the employed metrics? For now, we do not think so. First, because at such an early stage it is important to develop proofs of principle that work on the intended data, and no single algorithm has yet shown sufficient advantage. Second, because we think that the biggest source of inconsistency across the literature today comes from the data itself, not the algorithms employed. If the retrieved clusters are strong enough, researchers should be able to retrieve overlapping solutions regardless of the clustering

methodology. A word of caution here is, though, that as different algorithms make different assumptions, we should make sure they are met in the datasets we use. We strongly believe that the future of the field lies in concerted efforts to acquire more data.

Overview of the Field and Where to Go Next

Psychiatric disease subtyping is at the moment at an incipient, exploratory stage. While much remains to be answered and no irrefutable evidence of functionally relevant subtypes was presented, all the cited proofs of principle introduced valid, potential ways to move the field forward once the current limitations are overcome.

Aside from the algorithmic heterogeneity mentioned above, the number of different data modalities to choose from should not go unnoticed. Although we focused mainly on the functional aspect of disease and functional MRI as the most promising way of measuring it, psychiatric diseases can manifest at many levels, which can be captured across several different axes that can be included in any clustering effort. Other imaging techniques, such as the already discussed structural MRI or diffusion tensor imaging (DTI, useful for measuring white matter consistency across the brain) have also been used to detect relevant subtypes (38). Furthermore, the genetic components of many of these subtypes should not be ignored. As the dimensionality of this data is extremely high (millions of genetic variants per subject) and individual polymorphism contributions are generally small, however, genetic data is rarely useful for unsupervised learning. Supervised approaches, however, which aim to classify individuals among already defined labels, have shown more success (37). Lastly, in addition to questionnaires and more traditional clinical datasets, a data modality that gained momentum over the last few years is digitomics (electronic health records, mobile sensor data) (37, 155, 156). We think that, given sufficient sample sizes, the future lies in multimodal integration and, as stated previously, *polytopic learning*.

Furthermore, fMRI results may depend on external unmeasured factors, which often results in low signal-to-noise ratios and poor test-retest reproducibility (157). A relevant consequence of these limitations is that the sample sizes needed to capture the modes of variation in line with psychiatric subtypes are, to date, limitingly high. This demands concerted efforts to increase data collection, which are fortunately being accounted for, with new multi-site data collection consortia starting to collect functional data for psychiatric disease machine learning (158–160).

Although its details are out of the scope of this review, something that should not go unnoticed is that any effort in acquiring knowledge that aims to be transferable to the clinic needs to comply with standards of *fairness* (161). In this case, this reflects the need for models to be thoroughly tested across samples representative of the entire population to which they ought to be applied. As functional MRI hardware is expensive, bias in data collection toward richer societies is a significant risk (161). Fortunately, new technological advancements, such as portable MRI (162), also make the future look brighter in this regard: by reducing costs and the required infrastructure, solutions like this one can help bridge this gap and facilitate data collection across the world.

Moreover, the aforementioned limitations of fMRI, even if robust subtypes are available, make it a relatively poor clinical tool (163). This means that, even if robust subtypes at the functional level are detected, their application in clinical workflows might need to rely on technologies other than functional MRI. This could be achieved for example by training supervised classifier models to recognize these functionally defined subtypes based on data from other modalities, such as combinations of genetics, digitomics, and imaging (37).

Finally, all the retrieved studies aimed to find subtypes within already defined broad categories. Although several *transdiagnostic* efforts using other, readily available data modalities exist (38, 164), none to date have, to the best of our knowledge, applied functional MRI as part of their pipelines. As new, larger datasets are made available, the goal of shedding light on the functional aspects of trans diagnosis becomes reachable.

CONCLUSIONS

As mentioned throughout this article, further data-driven stratification of psychiatric diseases can help dissect the vast heterogeneity present in the field today. An improved diagnosis, presumably based on biological mechanisms that precede symptom manifestation, is not only a goal in itself but also key for improving disease prognosis and direct personalized treatment. Functional MRI, and brain connectivity, in particular, is positioned as the best tool to date to acquire insights into brain function, and the interest in using it for uncovering sub-entities of brain disease remains high. The presented results are however mixed, and much remains to be done in terms of increasing sample sizes, standardizing data collection, and providing models with strong assessments of generalizability and fairness, crucial for a future translation of any model to the clinic (13).

DATA AVAILABILITY STATEMENT

Publicly available datasets were analyzed in this study. This data can be found here: https://zenodo.org/record/3923919#X0ei3NP7TmE.

AUTHOR CONTRIBUTIONS

LM has organized the PRISMA workflow, gathered and scrutinized information, and written the entire manuscript

draft. RP has contributed to the inclusion/exclusion criteria, commented on the initial draft, suggested initial revisions to the manuscript's structure, and re-written several parts of the original draft. BP has greatly contributed to figure design. BP, NK, and BM-M have contributed with PRISMA assessment, proofreading of the document, and suggestions based on their expertise in the field. All authors contributed to the manuscript and approved the submitted version.

FUNDING

This project has received funding from the European Union's Horizon 2020 research and innovation programme under the Marie Skłodowska-Curie grant agreement No. 813533 and the Commitment grant No. 01ZX1904A (Modellierung von Komorbiditäts-Prozessen durch integratives, maschinelles Transfer-Lernen für psychiatrische Erkrankungen).

REFERENCES

1. Surís A, Holliday R, North CS. The Evolution of the classification of psychiatric disorders. *Behav Sci*. (2016) 6. doi: 10.3390/bs6010005
2. Shorter E. The history of DSM. In: Paris J, Phillips J, editors. *Making the DSM-5: Concepts and Controversies*. New York, NY: Springer New York. (2013). p. 3–19. doi: 10.1007/978-1-4614-6504-1_1
3. Spitzer RL, Endicott J, Williams JB. Research diagnostic criteria. *Arch Gen Psychiatry*. (1979) 36:1381–3. doi: 10.1001/archpsyc.1979.01780120111013
4. American Psychiatric Association. *Diagnostic and Statistical Manual of Mental Disorders*. Wahington DC: American Psychiatric Association (1980).
5. Steel Z, Marnane C, Iranpour C, Chey T, Jackson JW, Patel V, et al. The global prevalence of common mental disorders: a systematic review and meta-analysis 1980-2013. *Int J Epidemiol*. (2014) 43:476–93. doi: 10.1093/ije/dyu038
6. Rush AJ, Ibrahim HM. Speculations on the future of psychiatric diagnosis. *J Nerv Ment Dis*. (2018) 206:481–7. doi: 10.1097/NMD.0000000000000821
7. Moran P, Stokes J, Marr J, Bock G, Desbonnet L, Waddington J, et al. Gene × environment interactions in schizophrenia: evidence from genetic mouse models. *Neural Plast*. (2016) 2016:2173748. doi: 10.1155/2016/2173748
8. Syvälahti EK. Biological factors in schizophrenia. Structural and functional aspects. *Br J Psychiatry Suppl*. (1994) (23):9–14. doi: 10.1192/S0007125000292672
9. Paul R, Andlauer TFM, Czamara D, Hoehn D, Lucae S, Pütz B, et al. Treatment response classes in major depressive disorder identified by model-based clustering and validated by clinical prediction models. *Transl Psychiatry*. (2019) 9:187. doi: 10.1038/s41398-019-0524-4
10. Pandarakalam JP. Challenges of treatment-resistant depression. *Psychiatr Danub*. (2018) 30:273–84. doi: 10.24869/psyd.2018.273
11. Potkin SG, Kane JM, Correll CU, Lindenmayer JP, Agid O, Marder SR, et al. The neurobiology of treatment-resistant schizophrenia: paths to antipsychotic resistance and a roadmap for future research. *Focus*. (2020) 18:456–65. doi: 10.1176/appi.focus.18309
12. Vilar A, Pérez-Sola V, Blasco MJ, Pérez-Gallo E, Ballester Coma L, Batlle Vila S, et al. Translational research in psychiatry: The Research Domain Criteria Project (RDoC). *Rev Psiquiatr Salud Ment*. (2019) 12:187–95. doi: 10.1016/j.rpsmen.2018.04.002
13. Dwyer DB, Falkai P, Koutsouleris N. Machine learning approaches for clinical psychology and psychiatry. *Annu Rev Clin Psychol*. (2018) 14:91–118. doi: 10.1146/annurev-clinpsy-032816-045037
14. Paykel ES. Classification of depressed patients: a cluster analysis derived grouping. *Br J Psychiatry*. (1971) 118:275–88. doi: 10.1192/bjp.118.544.275
15. Farmer AE, McGuffin P, Spitznagel EL. Heterogeneity in schizophrenia: a cluster-analytic approach. *Psychiatry Res*. (1983) 8:1–12. doi: 10.1016/0165-1781(83)90132-4
16. Visscher PM, Wray NR, Zhang Q, Sklar P, McCarthy MI, Brown MA, et al. 10 Years of GWAS discovery: biology, function, and translation. *Am J Hum Genet*. (2017) 101:5–22. doi: 10.1016/j.ajhg.2017.06.005
17. Mullins N, Lewis CM. Genetics of depression: progress at last. *Curr Psychiatry Rep*. (2017) 19:43.
18. Meier SM, Trontti K, Purves KL, Als TD, Grove J, Laine M, et al. Genetic variants associated with anxiety and stress-related disorders: a genome-wide association study and mouse-model study. *JAMA Psychiatry*. (2019) 76:924–32. doi: 10.1001/jamapsychiatry.2019.1119
19. Brainstorm Consortium, Anttila V, Bulik-Sullivan B, Finucane HK, Walters RK, Bras J, et al. Analysis of shared heritability in common disorders of the brain. *Science*. (2018) 360:eaap8757. doi: 10.1126/science.aap8757
20. Fullerton JM, Nurnberger JI. Polygenic risk scores in psychiatry: Will they be useful for clinicians? *F1000Res*. (2019) 8:1293. doi: 10.12688/f1000research.18491.1
21. Murray GK, Lin T, Austin J, McGrath JJ, Hickie IB. Wray NR. Could polygenic risk scores be useful in psychiatry?: a review. *JAMA Psychiatry*. (2021) 78:210–9. doi: 10.1001/jamapsychiatry.2020.3042
22. Stroman PW. *Essentials of Functional MRI*. CRC Press. (2016). doi: 10.1201/b10960
23. Poline J-B, Brett M. The general linear model and fMRI: does love last forever? *Neuroimage*. (2012) 62:871–80. doi: 10.1016/j.neuroimage.2012.01.133
24. Monti MM. Statistical analysis of fMRI time-series: a critical review of the GLM approach. *Front Hum Neurosci*. (2011) 5:28. doi: 10.3389/fnhum.2011.00028
25. Wald L. *Faculty Opinions Recommendation of Functional Connectivity in the Motor Cortex of Resting Human Brain Using Echo-Planar MRI*. Faculty Opinions Ltd (2012). doi: 10.3410/f.714597885.790202808
26. Khosla M, Jamison K, Ngo GH, Kuceyeski A, Sabuncu MR. Machine learning in resting-state fMRI analysis. *Magn Reson Imaging*. (2019) 64:101–21. doi: 10.1016/j.mri.2019.05.031
27. Seeley WW, Menon V, Schatzberg AF, Keller J, Glover GH, Kenna H, et al. Dissociable intrinsic connectivity networks for salience processing and executive control. *J Neurosci*. (2007) 27:2349–56. doi: 10.1523/JNEUROSCI.5587-06.2007
28. Gratton C, Laumann TO, Nielsen AN, Greene DJ, Gordon EM, Gilmore AW, et al. Functional brain networks are dominated by stable group and individual factors, not cognitive or daily variation. *Neuron*. (2018) 98:439–52.e5. doi: 10.1016/j.neuron.2018.03.035
29. Satterthwaite TD, Xia CH, Bassett DS. Personalized neuroscience: common and individual-specific features in functional brain networks. *Neuron*. (2018) 98:243–5. doi: 10.1016/j.neuron.2018.04.007
30. Yang J, Gohel S, Vachha B. Current methods and new directions in resting state fMRI. *Clin Imaging*. (2020) 65:47–53. doi: 10.1016/j.clinimag.2020.04.004
31. *Dimension Reduction Techniques for Clustering*. Berlin; Heidelberg: Springer-Verlag (2011).
32. Liu Z, Barahona M. Graph-based data clustering via multiscale community detection. *Applied Network Science*. (2020) 5:1–20. doi: 10.1007/s41109-019-0248-7
33. Bronstein MM, Bruna J, LeCun Y, Szlam A, Vandergheynst P. Geometric deep learning: going beyond euclidean data. *IEEE Signal Process Mag*. (2017) 34:18–42. doi: 10.1109/MSP.2017.2693418
34. García-Escudero LA, Gordaliza A, Matrán C, Mayo-Iscar A, A. review of robust clustering methods. *Adv Data Anal Classif*. (2010) 4:89–109. doi: 10.1007/s11634-010-0064-5
35. Lawson RG, Jurs PC. New index for clustering tendency and its application to chemical problems. *J Chem Inf Comput Sci*. (1990) 30:36–41. doi: 10.1021/ci00065a010
36. Bouveyron C, Brunet-Saumard C. Model-based clustering of high-dimensional data: A review. *Comput Stat Data Anal*. (2014) 71:52–78. doi: 10.1016/j.csda.2012.12.008

37. Chekroud AM, Bondar J, Delgadillo J, Doherty G, Wasil A, Fokkema M, et al. The promise of machine learning in predicting treatment outcomes in psychiatry. *World Psychiatry*. (2021) 20:154–70. doi: 10.1002/wps.20882
38. Hermens DF, Hatton SN, White D, Lee RSC, Guastella AJ, Scott EM, et al. A data-driven transdiagnostic analysis of white matter integrity in young adults with major psychiatric disorders. *Prog Neuropsychopharmacol Biol Psychiatry*. (2019) 89:73–83. doi: 10.1016/j.pnpbp.2018.08.032
39. Marquand AF, Wolfers T, Mennes M, Buitelaar J, Beckmann CF. Beyond lumping and splitting: a review of computational approaches for stratifying psychiatric disorders. *Biol Psychiatry Cogn Neurosci Neuroimaging*. (2016) 1:433–47. doi: 10.1016/j.bpsc.2016.04.002
40. Preferred reporting items for systematic review and meta-analysis protocols (PRISMA-P) 2015: elaboration and explanation. *BMJ*. (2016) 354:i4086. doi: 10.1136/bmj.i4086
41. Linares-Espinós E, Hernández V, Domínguez-Escrig JL, Fernández-Pello S, Hevia V, Mayor J, et al. Methodology of a systematic review. *Actas Urol Esp*. (2018) 42:499–506. doi: 10.1016/j.acuroe.2018.07.002
42. van de Schoot R, de Bruin J, Schram R, Zahedi P, de Boer J, Weijdema F, et al. An open source machine learning framework for efficient and transparent systematic reviews. *Nature Machine Intelligence*. (2021) 3:125–33. doi: 10.1038/s42256-020-00287-7
43. Taubner S, Wiswede D, Kessler H. Neural activity in relation to empirically derived personality syndromes in depression using a psychodynamic fMRI paradigm. *Front Hum Neurosci*. (2013) 7:812. doi: 10.3389/fnhum.2013.00812
44. Lingiardi V, Shedler J, Gazzillo F. Assessing personality change in psychotherapy with the SWAP−200: a case study. *J Pers Assess*. (2006) 86:23–32. doi: 10.1207/s15327752jpa8601_04
45. Principal component analysis and factor analysis. In: Jolliffe IT, editor. *Principal Component Analysis*. New York, NY: Springer (2002) p. 150–66.
46. Geisler D, Walton E, Naylor M, Roessner V, Lim KO, Charles Schulz S, et al. Brain structure and function correlates of cognitive subtypes in schizophrenia. *Psychiatry Res*. (2015) 234:74–83. doi: 10.1016/j.pscychresns.2015.08.008
47. Hill SK, Ragland JD, Gur RC, Gur RE. Neuropsychological profiles delineate distinct profiles of schizophrenia, an interaction between memory and executive function, and uneven distribution of clinical subtypes. *J Clin Exp Neuropsychol*. (2002) 24:765–80. doi: 10.1076/jcen.24.6.765.8402
48. Arndt S, Andreasen NC, Flaum M, Miller D, Nopoulos P, A. longitudinal study of symptom dimensions in schizophrenia. Prediction and patterns of change. *Arch Gen Psychiatry*. (1995) 52:352–60. doi: 10.1001/archpsyc.1995.03950170026004
49. Dickinson D, Pratt DN, Giangrande EJ, Grunnagle M, Orel J, Weinberger DR, et al. Attacking heterogeneity in schizophrenia by deriving clinical subgroups from widely available symptom data. *Schizophr Bull*. (2018) 44:101–13. doi: 10.1093/schbul/sbx039
50. Chwa WJ, Tishler TA, Raymond C, Tran C, Anwar F, Pablo Villablanca J, et al. Association between cortical volume and gray-white matter contrast with second generation antipsychotic medication exposure in first episode male schizophrenia patients. *Schizophr Res*. (2020) 222:397–410. doi: 10.1016/j.schres.2020.03.073
51. Yildiz M, Borgwardt SJ, Berger GE. Parietal lobes in schizophrenia: do they matter? *Schizophr Res Treat*. (2011) 2011:581686. doi: 10.1155/2011/581686
52. Bouveyron C, Girard S, Schmid C. High-dimensional discriminant analysis. *Commun Stat Theor Methods*. (2007) 36:2607–23. doi: 10.1080/03610920701271095
53. Bergé L, Bouveyron C, Girard S. HDclassif: AnRPackage for model-based clustering and discriminant analysis of high-dimensional data. *J Stat Softw*. (2012) 46:1548–7660. doi: 10.18637/jss.v046.i06
54. Maglanoc LA, Landrø NI, Jonassen R, Kaufmann T, Córdova-Palomera A, Hilland E, et al. Data-driven clustering reveals a link between symptoms and functional brain connectivity in depression. *Biol Psychiatry Cogn Neurosci Neuroimaging*. (2019) 4:16–26. doi: 10.1016/j.bpsc.2018.05.005
55. Wang YP, Gorenstein C. Psychometric properties of the Beck Depression Inventory-II: a comprehensive review. *Braz J Psychiatry*. (2013) 35:416–31. doi: 10.1590/1516-4446-2012-1048
56. Chen J, Patil KR, Weis S, Sim K, Nickl-Jockschat T, Zhou J, et al. Neurobiological divergence of the positive and negative schizophrenia subtypes identified on a new factor structure of psychopathology using non-negative factorization: an international machine learning study. *Biol Psychiatry*. (2020) 87:282–93. doi: 10.1016/j.biopsych.2019.08.031
57. Naik GR. *Non-Negative Matrix Factorization Techniques: Advances in Theory and Applications*. Springer. (2015). doi: 10.1007/978-3-662-48331-2
58. Clementz BA, Sweeney JA, Hamm JP, Ivleva EI, Ethridge LE, Pearlson GD, et al. Identification of distinct psychosis biotypes using brain-based biomarkers. *Focus*. (2018) 16:225–36. doi: 10.1176/appi.focus.16207
59. Tibshirani R, Walther G, Hastie T. Estimating the number of clusters in a data set via the gap statistic. *J R Stat Soc*. (2001) 63:411–23. doi: 10.1111/1467-9868.00293
60. Meda SA, Clementz BA, Sweeney JA, Keshavan MS, Tamminga CA, Ivleva EI, et al. Examining functional resting-state connectivity in psychosis and its subgroups in the bipolar-schizophrenia network on intermediate phenotypes cohort. *Biol Psychiatry Cogn Neurosci Neuroimaging*. (2016) 1:488–97. doi: 10.1016/j.bpsc.2016.07.001
61. Chen H, Uddin LQ, Guo X, Wang J, Wang R, Wang X, et al. Parsing brain structural heterogeneity in males with autism spectrum disorder reveals distinct clinical subtypes. *Hum Brain Mapp*. (2019) 40:628–37. doi: 10.1002/hbm.24400
62. Dudek A. Silhouette index as clustering evaluation tool. In: *Studies in Classification, Data Analysis, and Knowledge Organization. Studies in Classification, Data Analysis, and Knowledge Organization*. Cham: Springer International Publishing (2020) p. 19–33. doi: 10.1007/978-3-030-52348-0_2
63. Kaczkurkin AN, Sotiras A, Baller EB, Barzilay R, Calkins ME, Chand GB, et al. Neurostructural heterogeneity in youths with internalizing symptoms. *Biol Psychiatry*. (2020)87:473–82. doi: 10.1101/614438
64. Varol E, Sotiras A, Davatzikos C, Alzheimer's Disease Neuroimaging Initiative. HYDRA: Revealing heterogeneity of imaging and genetic patterns through a multiple max-margin discriminative analysis framework. *Neuroimage*. (2017) 145:346–364. doi: 10.1016/j.neuroimage.2016.02.041
65. Du Y, Liu J, Sui J, He H, Pearlson GD, Calhoun VD. Exploring difference and overlap between schizophrenia, schizoaffective and bipolar disorders using resting-state brain functional networks. *Conf Proc IEEE Eng Med Biol Soc*. (2014) 2014:1517–20.
66. Brodersen KH, Deserno L, Schlagenhauf F, Lin Z, Penny WD, Buhmann JM, et al. Dissecting psychiatric spectrum disorders by generative embedding. *Neuroimage Clin*. (2014) 4:98–111. doi: 10.1016/j.nicl.2013.11.002
67. Price RB, Gates K, Kraynak TE, Thase ME, Siegle GJ. Data-driven subgroups in depression derived from directed functional connectivity paths at rest. *Neuropsychopharmacology*. (2017) 42:2623–32. doi: 10.1038/npp.2017.97
68. Berardo de Sousa F, Zhao L. Evaluating and comparing the IGraph community detection algorithms. In: *2014 Brazilian Conference on Intelligent Systems*. São Paulo (2014). p. 408–413.
69. Yang Z, Xu Y, Xu T, Hoy CW, Handwerker DA, Chen G, et al. Brain network informed subject community detection in early-onset schizophrenia. *Sci Rep*. (2014) 4:5549. doi: 10.1038/srep05549
70. Britto FCd, de Britto FC. *Community Detection in Graphs*. Universidade de São Paulo, Agencia USP de Gestao da Informacao Academica (AGUIA) (2021).
71. Costa Dias TG, Iyer SP, Carpenter SD, Cary RP, Wilson VB, Mitchell SH, et al. Characterizing heterogeneity in children with and without ADHD based on reward system connectivity. *Dev Cogn Neurosci*. (2015) 11:155–74. doi: 10.1016/j.dcn.2014.12.005
72. O'Doherty JP, Cockburn J, Pauli WM. Learning, reward, and decision making. *Annu Rev Psychol*. (2017) 68:73–100. doi: 10.1146/annurev-psych-010416-044216
73. Drysdale AT, Grosenick L, Downar J, Dunlop K, Mansouri F, Meng Y, et al. Resting-state connectivity biomarkers define neurophysiological subtypes of depression. *Nature Medicine*. (2017) 23:28–38. doi: 10.1038/nm0217-264d
74. Yang X, Liu W, Liu W, Tao D. A survey on canonical correlation analysis. *IEEE*. (2021) 33:2349–68. doi: 10.1109/TKDE.2019.2958342
75. Xu S, Qiao X, Zhu L, Zhang Y, Xue C, Li L. Reviews on determining the number of clusters. *Appl Math Inf Sci*. (2016) 10:1493–512. doi: 10.18576/amis/100428
76. Lin HY, Cocchi L, Zalesky A, Lv J, Perry A, Tseng WYI, et al. Brain-behavior patterns define a dimensional biotype in medication-naïve adults

with attention-deficit hyperactivity disorder. Psychol Med. (2017) 48:2399–408. doi: 10.1101/190660
77. Tokuda T, Yoshimoto J, Shimizu Y, Okada G, Takamura M, Okamoto Y, et al. Identification of depression subtypes and relevant brain regions using a data-driven approach. *Sci Rep.* (2018) 8:14082. doi: 10.1038/s41598-018-32521-z
78. Dinga R, Schmaal L, Penninx BWJH, van Tol MJ, Veltman DJ, van Velzen L, et al. Evaluating the evidence for biotypes of depression: Methodological replication and extension of. *Neuroimage Clin.* (2019) 22:101796. doi: 10.1016/j.nicl.2019.101796
79. Liu Y, Hayes DN, Nobel A, Marron JS. Statistical significance of clustering for high-dimension, low–sample size data. *J Am Stat Assoc.* (2008) 103:1281–93. doi: 10.1198/016214508000000454
80. Sellnow K, Sartin-Tarm A, Ross MC, Weaver S, Cisler JM. Biotypes of functional brain engagement during emotion processing differentiate heterogeneity in internalizing symptoms and interpersonal violence histories among adolescent girls. *J Psychiatr Res.* (2020) 121:197–206. doi: 10.1016/j.jpsychires.2019.12.002
81. Rushworth MFS, Noonan MP, Boorman ED, Walton ME, Behrens TE. Frontal cortex and reward-guided learning and decision-making. *Neuron.* (2011) 70:1054–69. doi: 10.1016/j.neuron.2011.05.014
82. Julian LJ. Measures of anxiety: State-Trait Anxiety Inventory (STAI), Beck Anxiety Inventory (BAI), and Hospital Anxiety and Depression Scale-Anxiety (HADS-A). *Arthritis Care Res.* (2011) 63:S467–72. doi: 10.1002/acr.20561
83. Maust D, Cristancho M, Gray L, Rushing S, Tjoa C, Thase ME. Chapter 13 - Psychiatric rating scales. In: Aminoff MJ, Boller F, Swaab DF, editors. *Handbook of Clinical Neurology*. Elsevier. (2012) p. 227–37. doi: 10.1016/B978-0-444-52002-9.00013-9
84. Wise T, Marwood L, Perkins AM, Herane-Vives A, Joules R, Lythgoe DJ, et al. Instability of default mode network connectivity in major depression: a two-sample confirmation study. *Transl Psychiatry*. (2017) 7:e1105. doi: 10.1038/tp.2017.40
85. Li BJ, Friston K, Mody M, Wang HN, Lu HB, Hu DW, et al. A brain network model for depression: from symptom understanding to disease intervention. *CNS Neurosci Ther.* (2018) 24:1004–19. doi: 10.1111/cns.12998
86. Elvevåg B, Goldberg TE. Cognitive impairment in schizophrenia is the core of the disorder. *Crit Rev Neurobiol.* (2000) 14:1–21. doi: 10.1615/CritRevNeurobiol.v14.i1.10
87. Michael AM, King MD, Ehrlich S, Pearlson G, White T, Holt DJ, et al. A data-driven investigation of gray matter-function correlations in schizophrenia during a working memory task. *Front Hum Neurosci.* (2011) 5:71. doi: 10.3389/fnhum.2011.00071
88. Kay SR, Fiszbein A, Opler LA. The Positive and negative syndrome scale (PANSS) for schizophrenia. *Schizophr Bull.* (1987) 13:261–76. doi: 10.1093/schbul/13.2.261
89. Aboraya A, Nasrallah HA. Perspectives on the Positive and Negative Syndrome Scale (PANSS): Use, misuse, drawbacks, and a new alternative for schizophrenia research. *Ann Clin Psychiatry.* (2016) 28:125–31.
90. Chiu T, Fang D, Chen J, Wang Y, Jeris C. A robust and scalable clustering algorithm for mixed type attributes in large database environment. In: *Proceedings of the Seventh ACM SIGKDD International Conference on Knowledge Discovery and Data Mining. KDD'01*. New York, NY: Association for Computing Machinery (2001) p. 263–8. doi: 10.1145/502512.502549
91. Norusis M, Inc SPSS, IBM SPSS. *Statistics 19 Advanced Statistical Procedures Companion*. Prentice Hall (2011).
92. Ding J, Tarokh V, Yang Y. Model selection techniques: an overview. *IEEE Signal Process Mag.* (2018) 35:16–34. doi: 10.1109/MSP.2018.2867638
93. Yoon JH, Minzenberg MJ, Ursu S, Ryan Walter BS, Wendelken C, Ragland JD, et al. Association of dorsolateral prefrontal cortex dysfunction with disrupted coordinated brain activity in schizophrenia: relationship with impaired cognition, behavioral disorganization, and global function. *Am J Psychiatry.* (2008) 165:1006–14. doi: 10.1176/appi.ajp.2008.07060945
94. Callicott JH. Physiological dysfunction of the dorsolateral prefrontal cortex in schizophrenia revisited. *Cereb Cortex.* (2000) 10:1078–92. doi: 10.1093/cercor/10.11.1078
95. Devarajan K. Nonnegative matrix factorization: an analytical and interpretive tool in computational biology. *PLoS Comput Biol.* (2008) 4:e1000029. doi: 10.1371/journal.pcbi.1000029
96. Bezdek JC, Ehrlich R, Full W. FCM: The fuzzy c-means clustering algorithm. *Comput Geosci.* (1984) 10:191–203. doi: 10.1016/0098-3004(84)90020-7
97. Peters G, Crespo F, Lingras P, Weber R. Soft clustering – Fuzzy and rough approaches and their extensions and derivatives. *Int J Approximate Resoning.* (2013) 54:307–22. doi: 10.1016/j.ijar.2012.10.003
98. Hubert L, Arabie P. Comparing partitions. *J Classif.* (1985) 2:193–218. doi: 10.1007/BF01908075
99. Meilă M. Comparing clusterings—An information based distance. *J Multivar Anal.* (2007) 98:873–95. doi: 10.1016/j.jmva.2006.11.013
100. Steinwart I, Christmann A. *Support Vector Machines*. Springer Science & Business Media (2008).
101. Arciniegas DB. Psychosis. *CONTINUUM: lifelong learning in neurology*. (2015) 21:715–36. doi: 10.1212/01.CON.0000466662.89908.e7
102. McMorris T. History of research into the acute exercise–cognition interaction. In: *Exercise-Cognition Interaction.* (2016). p. 1–28. doi: 10.1016/B978-0-12-800778-5.00001-3
103. Nisbet R, Miner G, Yale K, editors. Chapter 11 – Model evaluation and enhancement. In: *Handbook of Statistical Analysis and Data Mining Applications (Second Edition)*. Boston, MA: Academic Press (2018). p. 215–33. doi: 10.1016/B978-0-12-416632-5.00011-6
104. Calhoun VD, Sui J, Kiehl K, Turner J, Allen E, Pearlson G. Exploring the psychosis functional connectome: aberrant intrinsic networks in schizophrenia and bipolar disorder. *Front Psychiatry.* (2011) 2:75. doi: 10.3389/fpsyt.2011.00075
105. Khadka S, Meda SA, Stevens MC, Glahn DC, Calhoun VD, Sweeney JA, et al. Is aberrant functional connectivity a psychosis endophenotype? A resting state functional magnetic resonance imaging study. *Biol Psychiatry.* (2013) 74:458–66. doi: 10.1016/j.biopsych.2013.04.024
106. Meda SA, Gill A, Stevens MC, Lorenzoni RP, Glahn DC, Calhoun VD, et al. Differences in resting-state functional magnetic resonance imaging functional network connectivity between schizophrenia and psychotic bipolar probands and their unaffected first-degree relatives. *Biol Psychiatry.* (2012) 71:881–9. doi: 10.1016/j.biopsych.2012.01.025
107. Meda SA, Ruano G, Windemuth A, O'Neil K, Berwise C, Dunn SM, et al. Multivariate analysis reveals genetic associations of the resting default mode network in psychotic bipolar disorder and schizophrenia. *Proc Natl Acad Sci U S A.* (2014)111:E2066–75. doi: 10.1073/pnas.1313093111
108. Vargas C, López-Jaramillo C, Vieta E, A. systematic literature review of resting state network–functional MRI in bipolar disorder. *J Affect Disord.* (2013) 150:727–35. doi: 10.1016/j.jad.2013.05.083
109. Meda SA, Wang Z, Ivleva EI, Poudyal G, Keshavan MS, Tamminga CA, et al. Frequency-specific neural signatures of spontaneous low-frequency resting state fluctuations in psychosis: evidence from bipolar-schizophrenia network on intermediate phenotypes (B-SNIP) consortium. *Schizophr Bull.* (2015) 41:1336–48. doi: 10.1093/schbul/sbv064
110. Radua J, Via E, Catani M, Mataix-Cols D. Voxel-based meta-analysis of regional white-matter volume differences in autism spectrum disorder versus healthy controls. *Psychol Med.* (2011) 41:1539–50. doi: 10.1017/S0033291710002187
111. Katuwal GJ, Baum SA, Cahill ND, Michael AM. Divide and conquer: sub-grouping of ASD improves ASD detection based on brain morphometry. *PLoS ONE*. (2016) 11:e0153331. doi: 10.1371/journal.pone.0153331
112. Gotham K, Pickles A, Lord C. Standardizing ADOS scores for a measure of severity in autism spectrum disorders. *J Autism Dev Disord.* (2009) 39:693–705. doi: 10.1007/s10803-008-0674-3
113. Padmanabhan A, Lynch CJ, Schaer M, Menon V. The default mode network in autism. *Biol Psychiatry Cogn Neurosci Neuroimaging.* (2017) 2:476–86. doi: 10.1016/j.bpsc.2017.04.004
114. de Lacy N, Doherty D, King BH, Rachakonda S, Calhoun VD. Disruption to control network function correlates with altered dynamic connectivity in the wider autism spectrum. *Neuroimage Clin.* (2017) 15:513–24. doi: 10.1016/j.nicl.2017.05.024
115. Lin HY, Perry A, Cocchi L, Roberts JA, Tseng WYI, Breakspear M, et al. Development of frontoparietal connectivity predicts longitudinal symptom changes in young people with autism spectrum disorder. *Transl Psychiatry.* (2019) 9:86. doi: 10.1038/s41398-019-0418-5
116. Oldehinkel M, Mennes M, Marquand A, Charman T, Tillmann J, Ecker C, et al. Altered connectivity between cerebellum, visual, and

sensory-motor networks in autism spectrum disorder: results from the EU-AIMS longitudinal European autism project. *Biol Psychiatry Cogn Neurosci Neuroimaging*. (2019) 4:260–70. doi: 10.1016/j.bpsc.2018.11.010
117. Hernandez LM, Rudie JD, Green SA, Bookheimer S, Dapretto M. Neural signatures of autism spectrum disorders: insights into brain network dynamics. *Neuropsychopharmacology*. (2015) 40:171–89. doi: 10.1038/npp.2014.172
118. Cordes D, Haughton VM, Arfanakis K, Carew JD, Turski PA, Moritz CH, et al. Frequencies contributing to functional connectivity in the cerebral cortex in "resting-state" data. *AJNR Am J Neuroradiol*. (2001) 22:1326–33.
119. Zou QH, Zhu CZ, Yang Y, Zuo XN, Long XY, Cao QJ, et al. An improved approach to detection of amplitude of low-frequency fluctuation (ALFF) for resting-state fMRI: Fractional ALFF. *J Neurosci Methods*. (2008) 172:137–41. doi: 10.1016/j.jneumeth.2008.04.012
120. Gates KM, Molenaar PCM, Iyer SP, Nigg JT, Fair DA. Organizing heterogeneous samples using community detection of GIMME-derived resting state functional networks. *PLoS ONE*. (2014) 9:e91322. doi: 10.1371/journal.pone.0091322
121. Sarwar T, Tian Y, Yeo BTT, Ramamohanarao K, Zalesky A. Structure-function coupling in the human connectome: a machine learning approach. *Neuroimage*. (2021) 226:117609. doi: 10.1016/j.neuroimage.2020.117609
122. Pandya M, Altinay M, Malone DA, Anand A. Where in the brain is depression? *Curr Psychiatry Rep*. (2012) 14:634–42. doi: 10.1007/s11920-012-0322-7
123. Malaspina D, Owen MJ, Heckers S, Tandon R, Bustillo J, Schultz S, et al. Schizoaffective disorder in the DSM-5. *Schizophr Res*. (2013) 150:21–5. doi: 10.1016/j.schres.2013.04.026
124. Cosgrove VE, Suppes T. Informing DSM-5: biological boundaries between bipolar I disorder, schizoaffective disorder, and schizophrenia. *BMC Med*. (2013) 11:127. doi: 10.1186/1741-7015-11-127
125. Garrity AG, Pearlson GD, McKiernan K, Lloyd D, Kiehl KA, Calhoun VD. Aberrant "Default Mode" functional connectivity in schizophrenia. *Am J Psychiatry*. (2007) 163:450–7. doi: 10.1176/ajp.2007.164.3.450
126. Öngür D, Lundy M, Greenhouse I, Shinn AK, Menon V, Cohen BM, et al. Default mode network abnormalities in bipolar disorder and schizophrenia. *Psychiatry Res*. (2010) 183:59–68. doi: 10.1016/j.pscychresns.2010.04.008
127. Cheniaux E, Landeira-Fernandez J, Lessa Telles L, Lessa JLM, Dias A, Duncan T, et al. Does schizoaffective disorder really exist? A systematic review of the studies that compared schizoaffective disorder with schizophrenia or mood disorders. *J Affect Disord*. (2008) 106:209–17. doi: 10.1016/j.jad.2007.07.009
128. Du Y, Fan Y. Group information guided ICA for fMRI data analysis. *Neuroimage*. (2013) 69:157–97. doi: 10.1016/j.neuroimage.2012.11.008
129. Ahmad AU, Starkey A. Application of feature selection methods for automated clustering analysis: a review on synthetic datasets. *Neural Comput Appl*. (2018) 29:317–28. doi: 10.1007/s00521-017-3005-9
130. Chen XW, Jeong JC. Enhanced recursive feature elimination. In: *Sixth International Conference on Machine Learning and Applications (ICMLA 2007)*. (2007) p. 429–35. doi: 10.1109/ICMLA.2007.35
131. Corduneanu A, Bishop C. Variational Bayesian model selection for mixture distributions. In: *Proceedings Eighth International Conference on Artificial Intelligence and Statistics*. St. Louis, MO (2001) p. 27–34.
132. Yang Z, LaConte S, Weng X, Hu X. Ranking and averaging independent component analysis by reproducibility (RAICAR). *Hum Brain Mapp*. (2008) 29:711–25. doi: 10.1002/hbm.20432
133. Worboys M. The Hamilton Rating Scale for Depression: The making of a "gold standard" and the unmaking of a chronic illness, 1960–1980. *Chronic Illn*. (2013) 9:302–19. doi: 10.1177/1742395312467658
134. Wager TD, Davidson ML, Hughes BL, Lindquist MA, Ochsner KN. Prefrontal-subcortical pathways mediating successful emotion regulation. *Neuron*. (2008) 59:1037–50. doi: 10.1016/j.neuron.2008.09.006
135. Wilks SS. On the independence of k sets of normally distributed statistical variables. *Econometrica*. (1935) 3:309–26. doi: 10.2307/1905324
136. Gates KM, Molenaar PCM. Group search algorithm recovers effective connectivity maps for individuals in homogeneous and heterogeneous samples. *Neuroimage*. (2012) 63:310–9. doi: 10.1016/j.neuroimage.2012.06.026
137. Schwartz J, Ordaz SJ, Kircanski K, Ho TC, Davis EG, Camacho MC, et al. Resting-state functional connectivity and inflexibility of daily emotions in major depression. *J Affect Disord*. (2019) 249:26–34. doi: 10.1016/j.jad.2019.01.040
138. Pourhoseingholi MA, Baghestani AR, Vahedi M. How to control confounding effects by statistical analysis. *Gastroenterol Hepatol Bed Bench*. (2012) 5:79–83.
139. Zhang Y, Jenkins DF, Manimaran S, Johnson WE. Alternative empirical Bayes models for adjusting for batch effects in genomic studies. *BMC Bioinformatics*. (2018) 19:262. doi: 10.1186/s12859-018-2263-6
140. Goulet-Pelletier JC, Cousineau D. A review of effect sizes and their confidence intervals, Part I: the Cohen's d family. *Quant Methods Psychol*. (2018) 14:242–65. doi: 10.20982/tqmp.14.4.p242
141. Orman GK, Labatut V. A comparison of community detection algorithms on artificial networks. *Sci Rep*. (2009) 6:30750. doi: 10.1007/978-3-642-04747-3_20
142. Liston C, McEwen BS, Casey BJ. Psychosocial stress reversibly disrupts prefrontal processing and attentional control. *Proc Natl Acad Sci USA*. (2009) 106:912–7. doi: 10.1073/pnas.0807041106
143. Yarkoni T, Poldrack RA, Nichols TE, Van Essen DC, Wager TD. Large-scale automated synthesis of human functional neuroimaging. *Nat Methods*. (2011) 8:665–70.
144. Meilă M. Comparing clusterings by the variation of information. In: *Learning Theory and Kernel Machines. Lecture Notes in Computer Science*. Berlin; Heidelberg: Springer (2003) p. 173–87. doi: 10.1007/978-3-540-45167-9_14
145. Dias TGC, Costa Dias TG, Wilson VB, Bathula DR, Iyer SP, Mills KL, et al. Reward circuit connectivity relates to delay discounting in children with attention-deficit/hyperactivity disorder. *Eur Neuropsychopharmacol*. (2013) 23:33–45. doi: 10.1016/j.euroneuro.2012.10.015
146. Oldehinkel M, Beckmann CF, Franke B, Hartman CA, Hoekstra PJ, Oosterlaan J, et al. Functional connectivity in cortico-subcortical brain networks underlying reward processing in attention-deficit/hyperactivity disorder. *Neuroimage Clin*. (2016) 12:796–805. doi: 10.1016/j.nicl.2016.10.006
147. Cisler JM, Begle AM, Amstadter AB, Resnick HS, Danielson CK, Saunders BE, et al. Exposure to interpersonal violence and risk for PTSD, depression, delinquency, and binge drinking among adolescents: data from the NSA-R. *J Trauma Stress*. (2012) 25:33–40. doi: 10.1002/jts.21672
148. Sniedovich M. *Dynamic Programming: Foundations and Principles, Second Edition*. CRC Press. (2010).
149. Peter F, Andrea S, Nancy A. Forty years of structural brain imaging in mental disorders: is it clinically useful or not? *Dialogues Clin Neurosci*. (2018) 20:179–86. doi: 10.31887/DCNS.2018.20.3/pfalkai
150. Iacono WG. Endophenotypes in psychiatric disease: prospects and challenges. *Genome Med*. (2018) 10:11. doi: 10.1186/s13073-018-0526-5
151. Zhang J, Gajjala S, Agrawal P, Tison GH, Hallock LA, Beussink-Nelson L, et al. Fully automated echocardiogram interpretation in clinical practice. *Circulation*. (2018) 138:1623–35. doi: 10.1161/CIRCULATIONAHA.118.034338
152. Brag J. Artificial intelligence in medical imaging. In: Nordlinger B, Villani C, Rus D, editors. *Healthcare and Artificial Intelligence*. Cham: Springer International Publishing (2020) p. 93–103. doi: 10.1007/978-3-030-32161-1_14
153. Walter M, Alizadeh S, Jamalabadi H, Lueken U, Dannlowski U, Walter H, et al. Translational machine learning for psychiatric neuroimaging. *Prog Neuropsychopharmacol Biol Psychiatry*. (2019) 91:113–21. doi: 10.1016/j.pnpbp.2018.09.014
154. Hunter DJ. Uncertainty in the era of precision medicine. *N Engl J Med*. (2016) 375:711–3. doi: 10.1056/NEJMp1608282
155. Wang Y, Zhao Y, Therneau TM, Atkinson EJ, Tafti AP, Zhang N, et al. Unsupervised machine learning for the discovery of latent disease clusters and patient subgroups using electronic health records. *J Biomed Inform*. (2020) 102:103364. doi: 10.1016/j.jbi.2019.103364
156. Sükei E, Norbury A, Mercedes Perez-Rodriguez M, Olmos PM, Artés A. Predicting emotional states using behavioral markers derived from passively sensed data: data-driven machine learning approach. *JMIR Mhealth Uhealth*. (2021) 9:e24465. doi: 10.2196/preprints.24465

157. Herting MM, Gautam P, Chen Z, Mezher A, Vetter NC. Test-retest reliability of longitudinal task-based fMRI: Implications for developmental studies. *Dev Cogn Neurosci*. (2018) 33:17–26. doi: 10.1016/j.dcn.2017.07.001
158. Improving mental health through precision and prevention. Available online at: https://www.psych.mpg.de/2745686/dzpg (accessed Sep 21, 2021).
159. PRONIA - FP7 Research Project. Available online at: https://www.pronia.eu/ (accessed Sep 21, 2021).
160. Seidman L. Administrative supplement harmonization of at risk multisite observational networks for youth (HARMONY).
161. Mehrabi N, Morstatter F, Saxena N, Lerman K, Galstyan A. A survey on bias and fairness in machine learning. *arXiv [Preprint]. arXiv: 1908.09635* (2019).
162. Wald LL, McDaniel PC, Witzel T, Stockmann JP, Cooley CZ. Low-cost and portable MRI. *J Magn Reson Imaging*. (2020) 52:686–96. doi: 10.1002/jmri.26942
163. Matthews PM, Honey GD, Bullmore ET. Applications of fMRI in translational medicine and clinical practice. *Nat Rev Neurosci*. (2006) 7:732–44. doi: 10.1038/nrn1929
164. Pelin H, Ising M, Stein F, Meinert S, Meller T, Brosch K, et al. Identification of transdiagnostic psychiatric disorder subtypes using unsupervised learning. *Neuropsychopharmacology*. (2021) 46:1895–905. doi: 10.1101/2021.02.04.21251083

Conflict of Interest: The authors declare that the research was conducted in the absence of any commercial or financial relationships that could be construed as a potential conflict of interest.

Publisher's Note: All claims expressed in this article are solely those of the authors and do not necessarily represent those of their affiliated organizations, or those of the publisher, the editors and the reviewers. Any product that may be evaluated in this article, or claim that may be made by its manufacturer, is not guaranteed or endorsed by the publisher.

frontiers in Psychiatry

ORIGINAL RESEARCH
published: 24 December 2021
doi: 10.3389/fpsyt.2021.718539

Treatment-Specific Hippocampal Subfield Volume Changes With Antidepressant Medication or Cognitive-Behavior Therapy in Treatment-Naive Depression

*Hua-Hsin Tai[1], Jungho Cha[1], Faezeh Vedaei[2], Boadie W. Dunlop[3], W. Edward Craighead[3], Helen S. Mayberg[1] and Ki Sueng Choi[1]**

[1] Nash Family Center for Advanced Circuit Therapeutics, Icahn School of Medicine at Mount Sinai, New York, NY, United States, [2] Thomas Jefferson University, Philadelphia, PA, United States, [3] Department of Psychiatry and Behavioral Sciences, Emory University School of Medicine, Atlanta, GA, United States

Background: Hippocampal atrophy has been consistently reported in major depressive disorder with more recent focus on subfields. However, literature on hippocampal volume changes after antidepressant treatment has been limited. The first-line treatments for depression include antidepressant medication (ADM) or cognitive-behavior therapy (CBT). To understand the differential effects of CBT and ADM on the hippocampus, we investigated the volume alterations of hippocampal subfields with treatment, outcome, and chronicity in treatment-naïve depression patients.

Methods: Treatment-naïve depressed patients from the PReDICT study were included in this analysis. A total of 172 patients who completed 12 weeks of randomized treatment with CBT ($n = 45$) or ADM ($n = 127$) were included for hippocampal subfield volume analysis. Forty healthy controls were also included for the baseline comparison. Freesurfer 6.0 was used to segment 26 hippocampal substructures and bilateral whole hippocampus from baseline and week 12 structural MRI scans. A generalized linear model with covariates of age and gender was used for group statistical tests. A linear mixed model for the repeated measures with covariates of age and gender was used to examine volumetric changes over time and the contributing effects of treatment type, outcome, and illness chronicity.

Results: Of the 172 patients, 85 achieved remission (63/127 ADM, 22/45 CBT). MDD patients showed smaller baseline volumes than healthy controls in CA1, CA3, CA4, parasubiculum, GC-ML-DG, Hippocampal Amygdala Transition Area (HATA), and fimbria. Over 12 weeks of treatment, further declines in the volumes of CA1, fimbria, subiculum, and HATA were observed regardless of treatment type or outcome. CBT remitters, but not ADM remitters, showed volume reduction in the right hippocampal tail. Unlike ADM remitters, ADM non-responders had a decline in volume in the bilateral hippocampal tails. Baseline volume of left presubiculum (regardless of treatment type) and right fimbria and HATA in CBT patients were correlated with a continuous measure of clinical improvement. Chronicity of depression had no effect on any measures of hippocampal subfield volumes.

OPEN ACCESS

Edited by:
Hang Joon Jo,
Hanyang University, South Korea

Reviewed by:
Paul Croarkin,
Mayo Clinic, United States
Mohammad M. Herzallah,
Al-Quds University, Palestine

***Correspondence:**
Ki Sueng Choi
kisueng.choi@mssm.edu

Specialty section:
This article was submitted to Neuroimaging and Stimulation, a section of the journal Frontiers in Psychiatry

Received: *01 June 2021*
Accepted: *08 November 2021*
Published: *24 December 2021*

Citation:
Tai HH, Cha J, Vedaei F, Dunlop BW, Craighead WE, Mayberg HS and Choi KS (2021) Treatment-Specific Hippocampal Subfield Volume Changes With Antidepressant Medication or Cognitive-Behavior Therapy in Treatment-Naive Depression. Front. Psychiatry 12:718539. doi: 10.3389/fpsyt.2021.718539

Conclusion: Two first-line antidepressant treatments, CBT and ADM, have different effects on hippocampal tail after 12 weeks. This finding suggests that remission achieved via ADM may protect against progressive hippocampal atrophy by altering neuronal plasticity or supporting neurogenesis. Studies with multimodal neuroimaging, including functional and structural analysis, are needed to assess further the impact of two different antidepressant treatments on hippocampal subfields.

Keywords: hippocampal atrophy, depression, antidepressant medication, cognitive behavioral theory, hippocampal tail

INTRODUCTION

Major depressive disorder (MDD) affects more than 16.1 million American adults (6.7% of the US population) older than 18 each year (1) and is a significant public health concern throughout the world (2) First-line treatments for MDD include antidepressant medication (ADM) or cognitive-behavior therapy (CBT). Both treatments have roughly equivalent efficacy for achieving remission, which is the goal of acute-phase treatment for depression (3). Both treatments yield heterogeneous responses, with a large proportion of patients still having symptoms even after treatment. Several studies have reported that these variabilities in treatment responsiveness have been associated with specific clinical characteristics of MDD, such as the age of onset, comorbidity, duration of illness, past treatment, recurrence, or anxiety (4). Many studies, including the STAR*D trial, the largest controlled study of sequential MDD treatments, have investigated the effectiveness of different treatments for patients who fail to get sufficient relief from their initial ADM. Results of these studies indicate a declining probability of response with each additional treatment failure. However, the structural neurology underlying outcomes to treatments and their change with different types of treatment has received only little study to date.

The hippocampus (HC) is an important brain region involved in memory and emotion regulation. Smaller HC volumes have been consistently reported in MDD (5, 6). Despite well-documented whole HC atrophy in depression, there is mixed evidence concerning subregional morphology in HC volumes. Many studies show MDD patients have smaller volumes of HC subregions in the bilateral subiculum, Cornu Ammonis (CA)1, CA2, CA3, and tail regions (7, 8). In contrast, a recent study by Cao et al. did not find any difference in HC subfield volumes in MDD patients when compared to healthy controls (9). Additionally, MacQueen et al. examined the posterior HC volumes, reporting larger bilateral HC tail volumes at pre-treatment in eventual remitters than non-remitters treated with ADM (10). Following the MacQueen study, two recent studies with large cohorts replicated that larger HC tail volume is associated with remission achieved with ADM treatment (11, 12).

In the past decade, neuroimaging studies techniques have improved substantially, providing new insights into HC functional and structural brain alterations resulting from different treatments. Sheline et al. showed that ADM treatment counteracts the volume reduction in MDD patients (13). Additionally, other studies found that ADM stimulates neurogenesis in the dentate gyrus of adult rodents by increasing the number of neural progenitor cells (NPCs) (14, 15). A recent meta-analysis of treatment effects by Enneking et al. compared different modalities of effective treatments, including ADM, CBT, and electroconvulsive therapy (ECT) for MDD patients (16). ECT had the most robust volume changes in subcortical structures, including the hippocampus-amygdala complex, anterior cingulate cortex, and striatum. However, there was not sufficient evidence to determine the structural brain effects resulting from CBT treatment.

To date, there have been no studies directly comparing different subfield volume changes of the HC after two first-line treatments, CBT versus ADM. In order to understand treatment-specific effects on the HC, we analyzed longitudinal neuroimaging dataset collected at baseline and after 12 weeks of treatment in adults with MDD. We investigated differential changes patterns associated with (1) specific treatment (CBT versus ADM), (2) clinical outcome (remitter vs. nonremitter), and (3) chronicity (chronic vs. nonchronic).

METHODS

Participants

MDD patients from the Predictors of Remission to Individual and Combined Treatments (PReDICT) study were included in this analysis (17). Briefly, in the PReDICT study adults aged 18–65 with moderate to severe, non-psychotic and treatment-naïve MDD were randomly assigned to 12 weeks of treatment with either CBT (16 1-h individual sessions) or one of two ADM, duloxetine (30–60 mg/day) or escitalopram (10–20 mg/day), in a 1:1:1 manner. Patients enrolled met DSM-IV criteria for MDD and had never previously received $\geq$4 weeks of ADM treatment or $\geq$4 sessions of an evidence-based psychotherapy for MDD or dysthymia. To ensure patients had at least moderate severity MDD, patients had to score $\geq$18 at screening and $\geq$15 at baseline on the 17-item Hamilton Depression Rating Scale (HDRS-17) (18). Patients were excluded if they met DSM-IV lifetime criteria for a psychotic disorder, bipolar disorder, or dementia, or if they had a current (past-year) diagnosis of eating disorder, dissociative disorder, or obsessive-compulsive disorder. Additionally, patients with any current

primary DSM-IV disorder other than MDD were excluded (17). All participants provided written informed consent before beginning study procedures and the study was approved by the Emory Institutional Review Board.

A total of 172 patients (127 ADM and 45 CBT) completed the 12 weeks of treatment and had usable structural magnetic resonance imaging (MRI) scans at baseline and week 12. For comparison purposes, we analyzed MRI data from 40 healthy control subjects without a current or past history of psychiatric or neurological disorder who were scanned once as part of separate imaging studies conducted on the same scanner at Emory University.

Clinical Outcomes and Chronicity

Patients were divided by their clinical outcomes and chronicity of their major depressive episode. Patients were split into four outcome groups based on the HDRS-17 change over the 12 weeks of treatment. Remitters had an HDRS-17 score $\leq$7 at both weeks 10 and 12. Responders without remission had a $\geq$50 % decrease from baseline but did not meet the remission definition. Partial responders had a 30–49% decrease in HDRS-17 score. Non-responders had a <30% decrease. Additionally, patients were divided into two groups (chronic and non-chronic) using a cut-point of 104 weeks (i.e., 2 continuous years) for their major depressive episode length at the time of screening. Patients were also subdivided by the reported number of depressive episodes (1, 2, and $\geq$3).

MRI Acquisition

MRI scanning was performed using a 3T Siemens TIM Trio (Siemens Medical Systems, Erlangen, Germany) at Emory University. Two longitudinal high-resolution T1-weighted magnetization-prepared rapid gradient echo (MPRAGE) scans were acquired at the start of the study (baseline) and after 12 weeks of treatment. The acquisition parameters are the following: sagittal slice orientation; slice thickness = 1.0 mm; in-plane resolution = 1.0 × 1.0 mm; matrix = 240 × 240; repetition time = 2,300 ms; inversion time = 900 ms; flip angle = 9°.

Hippocampal Subfield Volume Calculation

The hippocampal subfield segmentation module implemented in Freesurfer 6.0 was used to estimate a total of 26 different segmented subfields, 13 for each side of the brain (19). A further description of the algorithm can be found in Iglesias et al. (20). The segmented hippocampal subfield masks were carefully checked visually, and no substantial error was detected. The volumes of the hippocampal subfield were extracted based on the segmented masks. In addition, the whole HC volume of each hemisphere was also extracted. The volumes in all discussed analyses use the following normalization formula to account for different total brain volumes of subregions between subjects (**Equation 1**). The estimation of total intracranial volume of each subject was calculated using the standard Freesurfer pipeline. Further discussion of subfield volumes in this paper will assume the use of the normalized volume unless otherwise noted.

Equation 1. Brain Volume Normalization:

$$\%Normalized\ Volume\ of\ Interest = \frac{Hippocampal\ Subfield}{Total\ Intracranail\ Volume} * 100$$

Statistical Analysis

For the current analyses, the two antidepressants were combined to form one ADM group. This was done to increase statistical power and is justified based on the absence of any literature demonstrating differences in clinical efficacy or neurological volume effects between these medications (**Supplementary Table 1**). All statistical analyses were conducted using Jamovi software (21). A general linear model was used to compare the group difference at baseline including: (1) healthy controls vs. treatment-naive MDD, and (2) CBT-treated vs. ADM-treated remitters. A linear mixed model with repeated measures was used to examine the longitudinal volume changes of the HC subfield regardless of treatment, outcome, or chronicity. Furthermore, a linear mixed model with interaction evaluated: (1) treatment-specific effect—time × treatment (CBT-treated vs. ADM-treated remitters); (2) treatment-specific outcome effect—time × outcome (remitters vs. non-responders); and (3) chronicity effect—time × chronicity (chronic vs. nonchronic). Following any significant interaction findings, a *post-hoc* paired *t*-test was performed to validate the results. Lastly, a correlation analysis was performed between HC subfield volume at baseline and volume changes (**Equation 2**) over time and HDRS-17 changes (**Equation 3**). All statistical analyses included age and gender as covariates. Two statistical significance thresholds were applied to all analyses: (1) $p_{Uncorrected}$ <0.05 and (2) $p_{Bonferroni}$ <0.05, which takes 26 different regions (considering both left and right brain), to get $p_{Uncorrected}$ <0.0019. Both alphas are reported to capture potentially significant factors.

Equation 2. Brain Volume Change:

$$\Delta BV = BV_{Baseline} - BV_{Wk12}$$

where $BV_{Baseline}$ is the %Normalized Volume of Interest at baseline and BV_{Wk12} is the % Normalized Volume of Interest at week 12.

Equation 3. HDRS-17 Change:

$$\Delta HDRS = \frac{HDRS_{Baseline1} - HDRS_{Wk2}}{HDRS_{Baseline}} * 100$$

where $HDRS_{Baseline}$ is the HDRS-17 score at baseline and $HDRS_{Wk12}$ is the HDRS-17 score at week 12.

A legend for the 26 different subfields (left and right) is as follows (**Figure 1**): (1) hippocampal tail, (2) subiculum, (3) CA1, (4) hippocampal fissure, (5) presubiculum, (6) parasubiculum, (7) molecular layer, (8) Granule Cell Molecular Layer of the Dentate Gyrus (GC-ML-DG), (9) CA3, (10) CA4, (11) fimbria, (12) Hippocampal Amygdala Transition Area (HATA), and (13) unilateral whole hippocampus.

TABLE 1 | Demographics and baseline characteristics of participants with MDD.

Characteristic	Study group	
	Healthy controls	MDD
N	40	172
Female	24 (60.0)	104 (60.5)
Age, mean (SD), yrs[A]	36.5 (8.76)	39.0 (11.5)
Outcome, treatment N		
Remitter, total/ADM/CBT[A]	-	85 / 63 / 22
Responder, total/ADM/CBT[A]	-	36 / 29 / 7
Partial-responder, total/ADM/CBT[A]	-	25 / 17 / 8
Non-responder, total/ADM/CBT[A]	-	26 / 18 / 8
No. lifetime episodes		
1	-	90 (52.3)
2	-	26 (15.1)
≥3	-	56 (32.6)
Chronic episode (≥2 yrs)	-	57 (33.1)
Symptom severity, HDRS-17 score	**Baseline MDD**	**Week 12 MDD**
All participants, mean (SD)[A]	18.9 (3.32)	7.22 (5.72)
Remitter, mean (SD)[A]	18.7 (3.51)	2.82 (2.21)
Responder, mean (SD)[A]	20.2 (3.11)	7.64 (2.31)
Partial-responder, mean (SD)[A]	18.3 (2.43)	11.7 (1.95)
Non-responder, mean (SD)[A]	18.6 (3.45)	16.7 (4.12)

MDD, Major depressive disorder; HDRS-17, Hamilton Depression Rating Scale; ADM, Antidepressant medications; CBT, Cognitive behavioral therapy.
[A]*Unless otherwise indicated, data are expressed as number (percentage) of participants.*

RESULTS

Clinical Characteristics and Treatment Outcomes

The demographic and clinical characteristics of the participants are presented in **Table 1**. There was no significant difference in age between the healthy controls (36.5 ± 8.57 years) and the MDD group (39 ± 11.5 years). There were also no significant differences in age among the four treatment outcome groups. At the baseline, MDD patients had an HDRS-17 score of 18.9 ± 3.32. After 12 weeks treatment, MDD patients had a HDRS-17 score of 7.22 ± 5.72, which was significantly reduced (t (171) = 24.7, $p < 0.001$) and 85 patients (49.4%) had remitted. Detailed HC subfield volumes are presented in **Supplementary Table 2**.

Baseline Hippocampal Subfield Volume Differences Between Healthy Controls and Treatment Naive MDD Patients

Fifteen hippocampal subfields out of 26 regions were significantly smaller in MDD patients compared to healthy controls ($p_{Uncorrected} < 0.05$) at baseline: (1–2) bilateral CA1, (3–4) bilateral CA3, (5–6) bilateral CA4, (7–8) bilateral parasubiculum, (9–10) bilateral GC-ML-DG, (11–12) bilateral Molecular layer, (13–14) bilateral HATA, (15) right Fimbria (**Supplementary Table 3**). Interestingly, the bilateral whole HC volumes were also smaller in MDD patients although this finding did not survive after Bonferroni correction (**Supplemantary Table 3**). With Bonferroni multiple comparison correction ($p_{Bonferroni} < 0.05$), only eight subregions out of 15 significant substractures survived including bilateral CA3, CA4, parasubiculum, left HATA, and right GC-ML-DG (**Figure 2**).

Baseline Hippocampal Subfield Volume Differences Between ADM- and CBT-Treated Patients

There were no statistical baseline differences in hippocampal subfield volumes between ADM-treated ($n = 127$) and CBT-treated (n = 45) patients. However, ADM-treated remitters ($n = 63$) showed smaller hippocampal baseline volumes in right fimbria ($p_{Uncorrected} = 0.019$) and HATA ($p_{Uncorrected} = 0.042$) than CBT-treated remitters ($n = 22$) (**Figures 3A,B**).

Baseline Hippocampal Subfield Volume Associated With Outcome

Left presubiculum volume at baseline showed a significant relationship with the percentage change of HDRS-17 scores. Larger HC volume in the left presubiculum was positively associated with clinical improvement ($R^2 = 0.056$, $p = 0.038$). In addition, the CBT-treated group ($n = 45$) showed a positive relationship between clinical improvement and volume of the right fimbria ($R^2 = 0.182$, $p = 0.022$) and HATA ($R^2 = 0.169$, $p = 0.032$), but no such relationship was obtained for the ADM-treated patients ($n = 127$) (**Figure 1**). *Post-hoc* analysis by group found that remitters had larger volumes at baseline in the left presubiculum ($p_{Uncorrected} = 0.019$) and parasubiculum ($p_{Uncorrected} = 0.04$) than non-responders regardless of treatment. Within ADM-treated patients, there were no volumes that showed statistically significant differences between remitters and non-responders, but within CBT-treated patients, remitters had larger baseline volumes than non-responders in the whole right HC ($p_{Uncorrected} = 0.025$) and various subregions including left GC-ML-DG ($p_{Uncorrected} = 0.032$) and CA4 ($p_{Uncorrected} = 0.04$), and right CA1 ($p_{Uncorrected} = 0.011$), GC-ML-DG ($p_{Uncorrected} = 0.02$), molecular layer ($p_{Uncorrected} = 0.029$), HATA ($p_{Uncorrected} = 0.029$). Additional statistical results of these comparisons are presented in **Supplementary Table 4**.

Baseline Hippocampal Subfield Volume Associated With Chronicity, Number of Episodes, or Symptom Severity

There were no statistical differences in any HC subfields between chronic and non-chronic groups or by number of past episodes at baseline. Additionally, there were no interaction effects of time and chronicity (**Supplementary Table 5**). Lastly, there was no significant findings between symptom severity (HAMD score) and baseline volumes.

Hippocampal Subfield Volume Changes Across Treatments (Time Effects)

Regardless of treatment (ADM or CBT), MDD patients demonstrated longitudinal HC volume reduction over 12 weeks in six subregions, including bilateral HATA, left subiculum, left CA1, left Fimbria, and right tail ($p_{Uncorrected} < 0.05$). Notably,

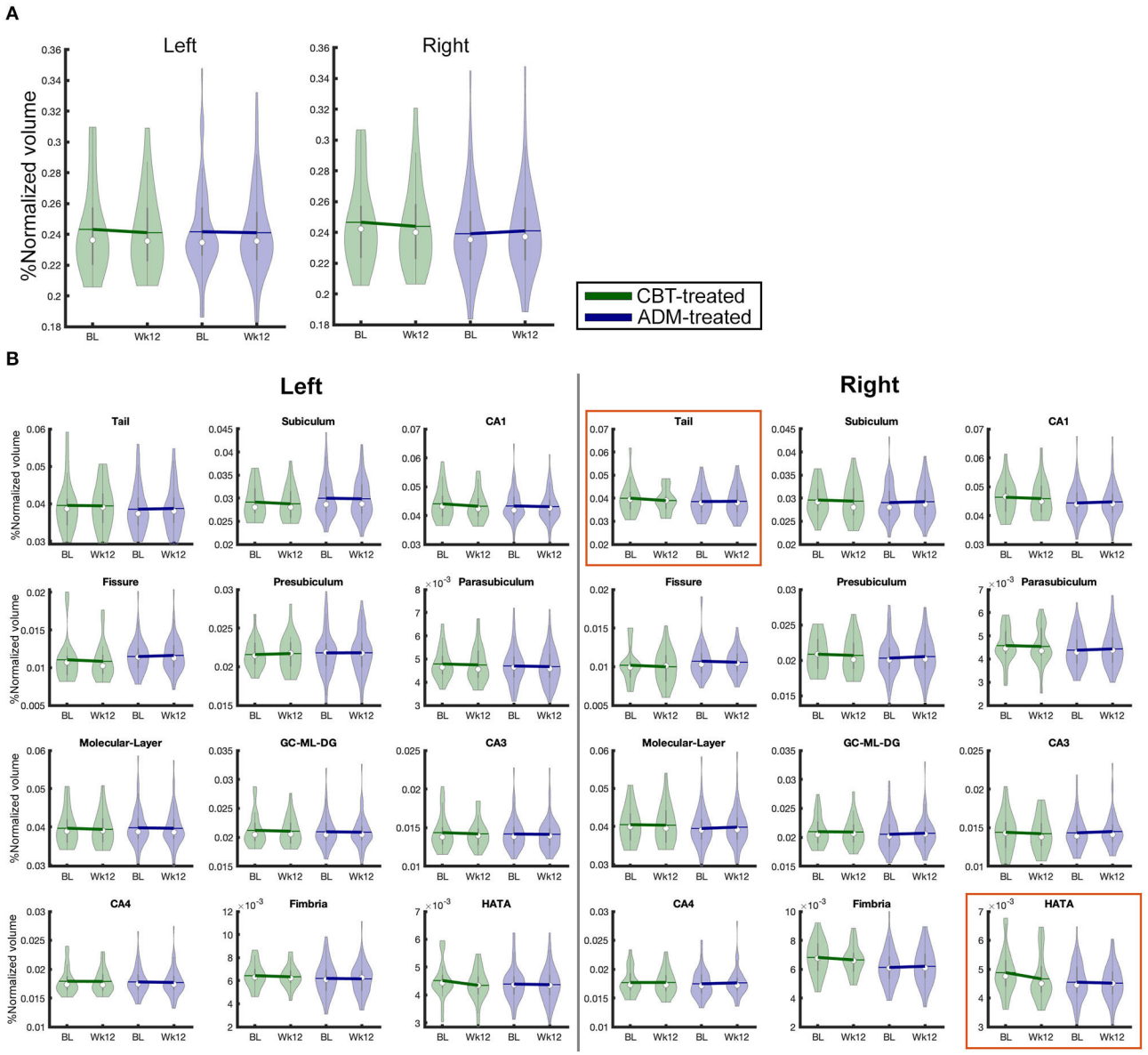

FIGURE 1 | Total volumes of 26 hippocampal subfield used in analysis broken by treatment group and time. BL, Baseline; Wk12, Week 12; CBT, cognitive behavioral therapy; ADM, antidepressant medications. **(A)** whole hippocampus, **(B)** hippocampal subfields.

bilateral HATA and left CA1 were smaller compared to healthy controls at baseline and continued to decrease over 12 weeks with treatment (**Figure 2**). Only the left HATA survived after multiple comparison corrections ($p_{Bonferroni} < 0.05$). The left whole HC volume also decreased over time ($p_{Uncorrected} < 0.05$). **Figure 2** presents HC volume changes over 12 weeks of treatment and **Supplementary Table 4** presents detailed statistical results.

Treatment-Specific Hippocampal Subfield Volume Changes (Treatment Effects)

Only remitters are included in treatment-specific change analyses because finding pathological changes in the remitters could help explain the clinical outcomes as they showed the largest improvement. Interestingly, there were differential treatment-specific HC subfield volume changes in the right HC tail ($p_{Uncorrected} = 0.035$) and HATA ($p_{Uncorrected} = 0.03$): remitters to CBT demonstrated decreased volumes over time, whereas ADM remitters showed no volume changes (**Supplementary Table 6**). **Figure 3** presents treatment-specific volume changes in the right HC tail and HATA.

Hippocampal Subfield Volume Changes Associated With Outcome (Outcome Effects)

There was no statistical relationship between clinical improvement (percent change of HDRS-17 scores) and HC subfield volume changes. In addition, there were no significant

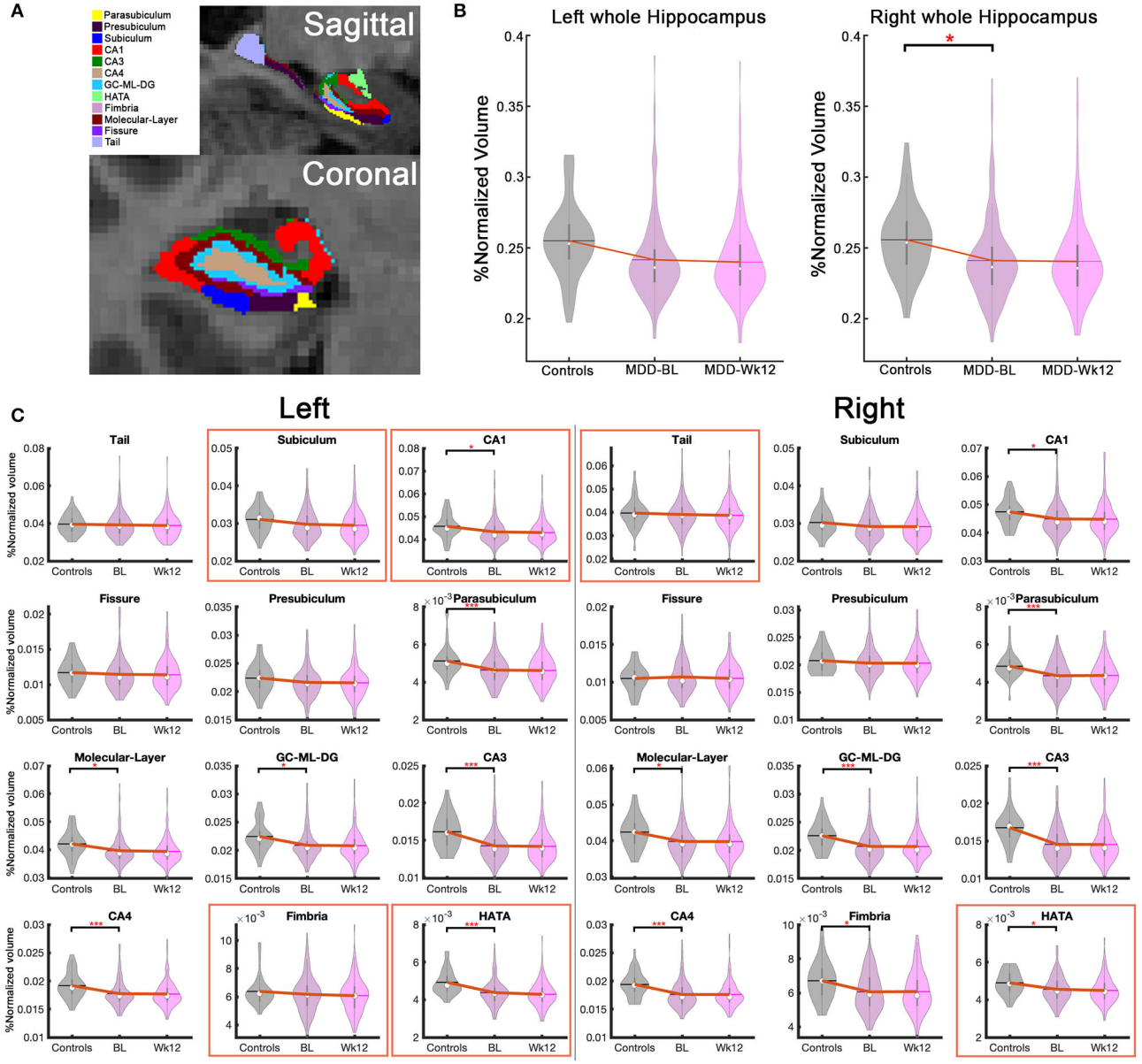

FIGURE 2 | Hippocampal subfield volume differences between treatment-naive MDD and Healthy controls, and hippocampal volume changes over 12 weeks of treatments. **(A)** Hippocampal subfield volumes in coronal and sagittal images. **(B)** Bilateral whole hippocampus volume changes. Right whole hippocampus volume at baseline was significantly smaller than healthy controls ($p_{Uncorrected} < 0.05$) **(C)** 26 hippocampal subfield volume in healthy controls, baseline and week 12 in treatment-naive MDD patients. Fifteen substructures including bilateral CA1, CA3, CA4, parasubiculum, GC-ML-DG, molecular layer, HATA, and right fimbria are shown significant volume reduction in the MDD patients compared to healthy controls ($p_{Uncorrected} < 0.05$). The bilateral CA3, bilateral CA4, bilateral Parasubiculum, left HATA, and right GC-ML-DG results survived multiple comparison corrections ($p_{Bonferroni} < 0.05$). Notably, six subregions (red box), including bilateral HATA, left subiculum, left CA1, left Fimbria, and right tail, showed a volume reduction between baseline and week 12 ($p_{Uncorrected} < 0.05$). The left HATA is highly significant ($p_{Bonferroni} < 0.05$). *$p_{Uncorrected} < 0.05$, ***$p_{Bonferroni} < 0.05$, BL, baseline; Wk12, week 12.

interaction effects in time-by-outcome among four different outcome groups, including remitters, responders, partial responders, and non-responders. However, the left HC tail ($p_{Uncorrected} = 0.03$) had a significant interaction effect between remitters and non-responders regardless of treatment. Left HC tail volume in non-responders significantly decreased over time, but no volume change occurred in remitters (**Supplementary Table 7**). *Post-hoc* analysis in each treatment group revealed that the left tail volume reduction was only significant in the ADM-treated patients. There were no significant interaction effects between time and outcomes in the CBT group. Interestingly, the *post-hoc* analysis also found volume reduction in the right HC tail ($F = 6.37$, $p_{Uncorrected} = 0.01$) with the ADM-treated patients (**Figure 4**).

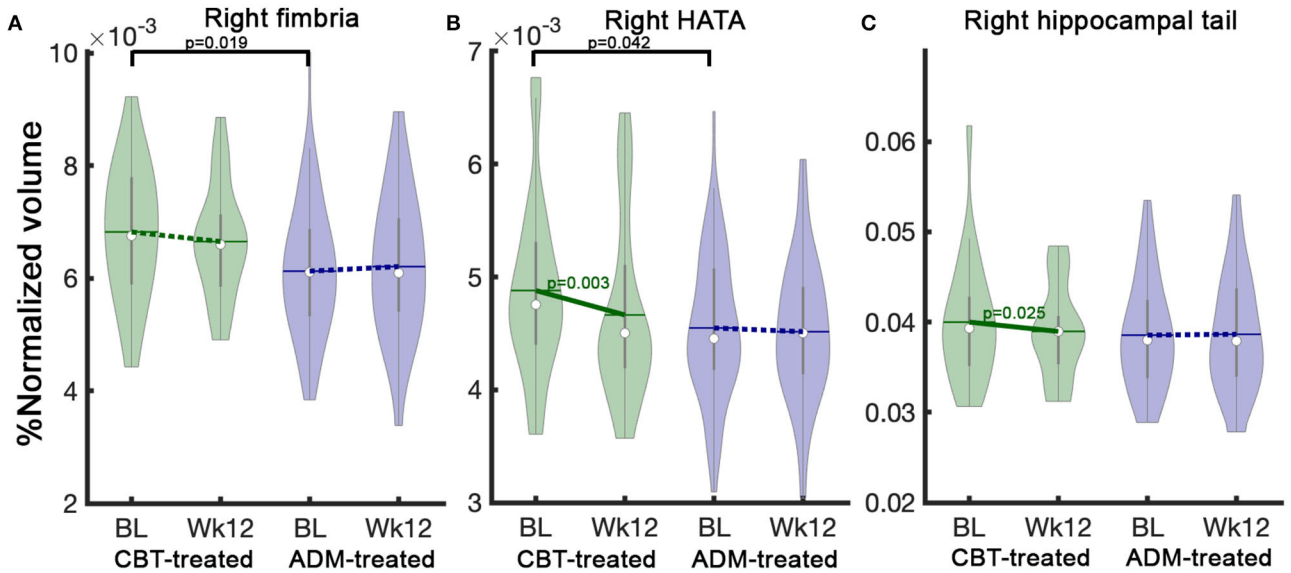

FIGURE 3 | Treatment specific hippocampal volume differences between CBT-treated and ADM-treated remitters at baseline and changes after 12 weeks of treatment. CBT-treated remitters showed larger HC volumes at baseline in **(A)** Right fimbria and **(B)** Right HATA. Notably, CBT-treated patients show significant volume reductions over 12 weeks of treatment in **(B)** Right HATA and **(C)** Right hippocampal tail. In contrast, ADM-treated patients showed no changes. The solid line represents *p*-values from the *post-hoc* paired *t*-test between baseline and week 12 volume. BL, baseline, Wk12, week 12. CBT, cognitive behavioral therapy; ADM, antidepressant medication.

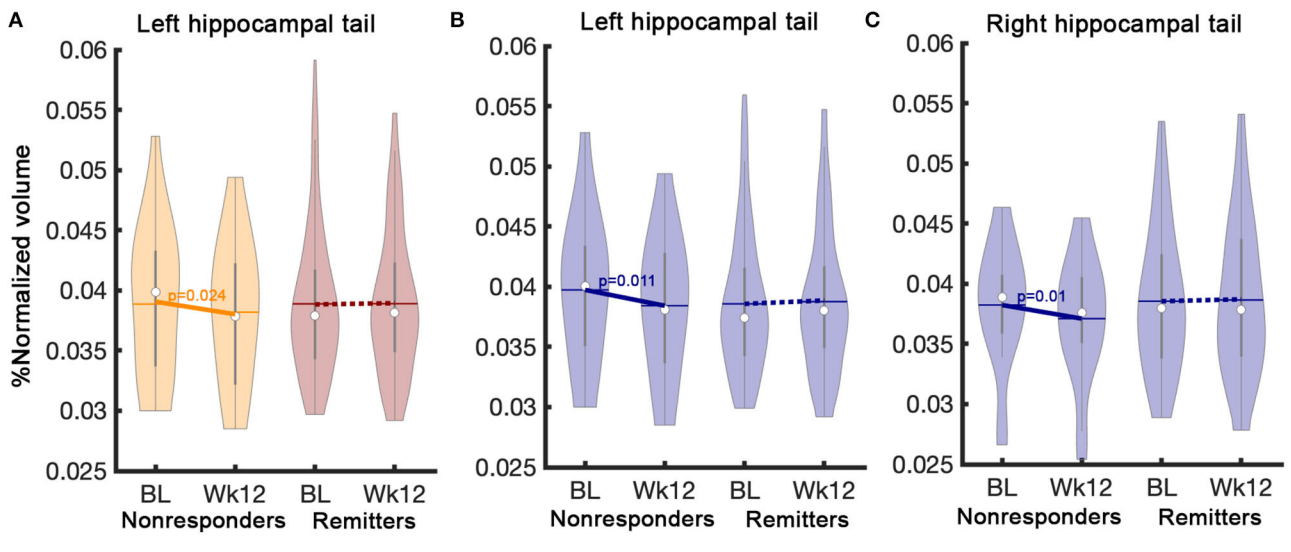

FIGURE 4 | Interaction effects between time and outcome (remitters vs. non-responders). A significant interaction effect between remitters ($n = 85$) and non-responders ($n = 26$) regardless of treatment was found **(A)** in the left hippocampal tail. *Post-hoc* analysis in the ADM-treated patients show differential volume changes between remitters ($n = 63$) and non-responder ($n = 18$) **(B)** in the left and **(C)** right hippocampal tails. The solid line represents *p*-values from the *post-hoc* paired *t*-test between baseline and week 12 volume. BL, Baseline; Wk12, Week 12; CBT, cognitive behavioral therapy; ADM, antidepressant medication.

DISCUSSION

The main aim of this study was to explore the differential effects of treatment types, treatment outcomes, and chronicity of depression on hippocampal substructures using a longitudinal neuroimaging dataset from baseline and following 12 weeks of treatments. This study is the first to directly compare the effects of antidepressant medication vs. cognitive behavior therapy in hippocampal subfield volume changes in a large cohort of treatment-naive MDD ($n = 172$) patients. Differential treatment-specific volume changes were found in HC subregions between remitters to ADM and CBT. CBT remitters showed a volume reduction in the right hippocampal tail, which did not occur in ADM-treated remitters. In contrast, non-responders in

ADM-treated patients showed volume reductions in the bilateral hippocampal tails while remitters in ADM-treated patients had unchanged volumes. This finding suggests the importance of hippocampal tail volumes in considering the effects of ADM treatment, consistent with prior research (10). ADM may protect against progressive hippocampal atrophy by altering neuronal plasticity or supporting neurogenesis (22). The other notable results from this study are: (1) various hippocampal subregion volumes are smaller in patients with MDD compared to healthy controls, which is consistent with previous findings (6); (2) six hippocampal subregion volumes demonstrated decreases after 12 weeks of treatment regardless of treatment or outcome, particularly the highly significant finding of left HATA volume reduction; (3) larger baseline right fimbria and HATA volumes in the CBT-treated patients were positively associated with clinical improvement.

Consistent with previous reports, the MDD patients in our study showed significantly smaller bilateral whole HC volumes at baseline compared to healthy controls (5). Additionally, our results indicate various HC subregions are smaller in MDD compared to healthy controls. Roddy et al. recently suggested that hippocampal subregion atrophy starts with principal substructures, including CA regions, and possibly progresses to an expanding pattern of substructure involvement including subiculum, dentate, and molecular layer. Furthermore, they reported no peripheral HC substructure involvement, including HATA, tail, presubiculum, and parasubiculum. However, our results show significant volume reductions in both principal and peripheral regions in treatment-naive depression and no relation of these changes to chronicity of depressive episode.

Two recent studies reported the importance of hippocampal tail volumes in the prediction of remission with antidepressant medication (11, 12). Maller et al. showed that MDD patients had larger hippocampal tail volumes than healthy controls at baseline, and this larger volume was associated with both a diagnosis of MDD and a greater chance of remission to ADM (11). In contrast, Nogovitsyn et al. reported smaller hippocampal tail volumes in MDD patients than healthy controls, and the size of hippocampal tail volumes in depression patients was positively associated with remission status, including early and later remission with antidepressant medication. Although the two studies reported opposite results in baseline hippocampal tail volumes in MDD vs. control subjects, both studies agreed that larger hippocampal volume was associated with remission in ADM-treated patients. Our analysis did not show a difference in hippocampal tail size compared to healthy controls at baseline. Furthermore, there were no differences between remitters and non-responders in hippocampal tails at baseline. However, these two studies also showed that the HC tail did not change over time in ADM remitters suggesting that hippocampal tail volumes were sensitive to ADM treatment. Additionally, previous studies demonstrated HC volume increase with 8 weeks of citalopram treatment as well as with 3 years of treatment with various antidepressant medications (23, 24). These findings may reflect the effects of ADM on suppressing toxic stress and enhancing neurogenesis and synaptic plasticity as previously reported (25–28).

We found that the right fimbria and HATA volumes at baseline were positively associated with clinical improvement specifically in CBT-treated patients. The fimbria is an important white matter relay connecting the HC to the paraventricular nucleus of hypothalamus and other limbic regions. A previous study demonstrated that deep brain stimulation of fimbria-fornix enhanced learning and memory capability (29). Additionally, HATA atrophy might affect the integrity of the hippocampal-amygdala network that is critical to cognition. This suggests that patients with significant decline in fimbria and HATA volume are less responsive to CBT and, therefore, may warrants further research in MDD patients. Nevertheless, the benefits achieved with CBT treatment of MDD is likely related to other neural effects rather than hippocampal tail volume changes.

Hippocampal atrophy with chronicity has been consistently reported in depression. Previously Sheline et al. reported that longer untreated periods in recurrent depression are associated with volume decline in the HC (14). Unlike their report, we found no baseline differences between chronic and non-chronic groups and no significant differences in volumes changes during treatment between these subgroups. This discrepancy may be due to reduced statistical power stemming from group comparisons using a two year cut off instead of a correlation analysis employing a continuous measure of episode duration. We used group analysis because retrospective self-report for duration of illness is often highly inaccurate, so categorical classification is a more conservative approach to the data (30). Our analysis also showed no statistical relationship between depression severity and volume reduction at baseline as previously reported by Frodl et al. (31) and Nils et al. (32). Furthermore, we found no significant relationship between baseline severity and volume changes after 12 weeks of treatment (**Supplementary Table 8**).

Interestingly, after 12-weeks of antidepressant treatment, six HC substructures show significant longitudinal volume reduction regardless of treatment and outcomes. Left HATA and left CA1 were smaller at baseline compared to healthy controls, and they continued to decrease over 12 weeks of treatment. In contrast, the remainder of the abnormal substructures at baseline compared to healthy controls show no longitudinal changes. This finding is consistent with our chronicity findings which show no differences between chronic and non-chronic groups. These findings suggest there is no progressive atrophy in these HC substructures once atrophy happens in depressed patients, which may suggest a floor effect in HC subfields.

A recent study using the same imaging dataset, but analyzing functional magnetic resonance imaging (fMRI), in treatment-naive depressed patients treated with ADM or CBT identified that the functional connectivity of the subcallosal cingulate cortex (SCC) with three brain regions (ventromedial frontal, ventrolateral frontal/anterior insula, and dorsal midbrain) differed between remitters to CBT or ADM (5). Greater hyperconnectivity between the SCC, one of the critical hub regions in depression networks, and these three regions

predicted remission with ADM; in contrast, hypo-connectivity predicted remission with CBT (5). Further studies may consider volumetric analysis. Combining the multiple structural data with volumetric-connectivity associations could create a more multifactorial approach for better understanding MDD. Additionally, direct comparison with recurrent or treatment-resistant depression cohorts could also be considered to evaluate the effects of past treatments and disease progression toward treatment-resistant depression.

Our study has limitations, including different sample sizes between ADM- and CBT-treated patients and HC subfield segmentation with a 1mm resolution using a single modality. There were more remitters in the ADM group ($n = 63$) than CBT ($n = 22$) due to two different antidepressant medications (duloxetine and escitalopram) in our protocol. Additionally, the sample size of CBT non-responders ($n = 8$) is relatively small, limiting the statistical inferences that can be drawn regarding outcome effects. In addition to the sample size, the recent version of Freesurfer (Freesurfer 6.0) allows both T1 and T2 images to improve HC subfield segmentation performance. However, our analysis only used T1 images because there were no reliable T2 images available. Importantly, interaction effects, including treatment- and outcome-specific findings, did not survive after Bonferroni multiple comparison corrections. The small magnitude of changes in HC subfield volume limited our ability to find significance after multiple comparison corrections.

To the best of our knowledge, there have been no direct comparisons of hippocampal subfield morphological changes between antidepressant medication and cognitive behavior therapy with treatment outcomes in a large sample. This study advances our understanding of first-line antidepressant treatment effects on hippocampal substructures. In particular, we demonstrate differential treatment-specific effects on hippocampal tail volume changes after 12 weeks of treatments. Remitters with antidepressant medication had preserved hippocampal tail volume but CBT remitters did not. We further show hippocampal tail volume reduction in non-responders with antidepressant medication. The observation that no hippocampal tail volume changes in remitters with antidepressant medication may reflect the action of suppressing stress toxic effects and increasing neurogenesis factors, consistent with animal studies (33).

DATA AVAILABILITY STATEMENT

The data that support the findings of this study are available from the corresponding author, upon reasonable request.

ETHICS STATEMENT

The studies involving human participants were reviewed and approved by the Emory Institutional Review Board and the Grady Hospital Research Oversight Committee. The patients/participants provided their written informed consent to participate in this study.

AUTHOR CONTRIBUTIONS

H-HT, JC, and KC: neuroimaging analysis, statistical analysis, and co-writing paper. FV: neuroimaging analysis. BD: co-writing protocols, inclusion/recruitment, clinical assessment, and co-writing paper. WC: co-writing protocols, grant recipient, inclusion/recruitment, and clinical assessment. HM: co-writing protocols, grant recipient (principal investigator), and co-writing paper. All authors contributed to the article and approved the submitted version.

FUNDING

This work was supported by the National Institutes of Health (HM, P50 MH077083; WC, RO1MH080880; and David S. Stephens, UL1 RR025008, M01 RR0039).

SUPPLEMENTARY MATERIAL

The Supplementary Material for this article can be found online at: https://www.frontiersin.org/articles/10.3389/fpsyt.2021.718539/full#supplementary-material

Supplementary Table 1 | Hippocampal subfield volume change associated with different medication treatment. Cornu Ammonis (CA), Granule Cell Molecular Layer of the Dentate Gyrus (GC-ML-DG), Hippocampal Amygdala Transition Area (HATA).

Supplementary Table 2 | Volumes are given as mean ± SD in cubic millimeters (mm^3); eTIV, estimated total intracranial volume; Cornu Ammonis (CA), Granule Cell Molecular Layer of the Dentate Gyrus (GC-ML-DG), Hippocampal Amygdala Transition Area (HATA).

Supplementary Table 3 | Baseline effect between healthy controls and Baseline MDD. Cornu Ammonis (CA), Granule Cell Molecular Layer of the Dentate Gyrus (GC-ML-DG), Hippocampal Amygdala Transition Area (HATA).

Supplementary Table 4 | Baseline effect between Baseline and Week 12. Cornu Ammonis (CA), Granule Cell Molecular Layer of the Dentate Gyrus (GC-ML-DG), Hippocampal Amygdala Transition Area (HATA).

Supplementary Table 5 | Chronicity effect between Baseline and Week 12. Cornu Ammonis (CA), Granule Cell Molecular Layer of the Dentate Gyrus (GC-ML-DG), Hippocampal Amygdala Transition Area (HATA).

Supplementary Table 6 | Treatment effect between Baseline and Week 12. Cornu Ammonis (CA), Granule Cell Molecular Layer of the Dentate Gyrus (GC-ML-DG), Hippocampal Amygdala Transition Area (HATA).

Supplementary Table 6a | Baseline differences of different treatments. Cornu Ammonis (CA), Granule Cell Molecular Layer of the Dentate Gyrus (GC-ML-DG), Hippocampal Amygdala Transition Area (HATA).

Supplementary Table 7 | Outcome effect between Baseline and Week 12. Cornu Ammonis (CA) Granule Cell Molecular Layer of the Dentate Gyrus (GC-ML-DG), Hippocampal Amygdala Transition Area (HATA).

Supplementary Table 8 | HDRS score changes with volume change. Cornu Ammonis (CA), Granule Cell Molecular Layer of the Dentate Gyrus (GC-ML-DG), Hippocampal Amygdala Transition Area (HATA), Hamilton Depression Rating Scale (HDRS).

REFERENCES

1. Facts & Statistics |Anxiety and Depression Association of America, ADAA." n.d. *Anxiety & Depression Association of America*. Available online at: https://adaa.org/understanding-anxiety/facts-statistics (accessed April 7, 2021).
2. "Depression". *World Health Organization*. (2020). Available online at: https://www.who.int/news-room/fact-sheets/detail/depression (accessed January 30, 2020).
3. Weitz ES, Hollon SD, Twisk J, van Straten A, Huibers MJ, David D, et al. Baseline depression severity as moderator of depression outcomes between cognitive behavioral therapy vs pharmacotherapy: an individual patient data meta-analysis. *JAMA Psychiatry*. (2015) 72:1102–9. doi: 10.1001/jamapsychiatry.2015.1516
4. Yang Z, Oathes DJ, Linn KA, Bruce SE, Satterthwaite TD, Cook PA, et al. Cognitive behavioral therapy is associated with enhanced cognitive control network activity in major depression and posttraumatic stress disorder. *Biol Psychiatry*. (2018)3:311–19. doi: 10.1016/j.bpsc.2017.12.006
5. McKinnon MC, Yucel K, Nazarov A, MacQueen GM. A meta-analysis examining clinical predictors of hippocampal volume in patients with major depressive disorder. *J Psychiatry Neurosci*. (2009) 34:41–54.
6. Videbech P, Ravnkilde B. Hippocampal volume and depression: a meta-analysis of MRI studies. *Am J Psychiatry*. (2004) 161:1957–66. doi: 10.1176/appi.ajp.161.11.1957
7. Cole J, Toga AW, Hojatkashani C, Thompson P, Costafreda SG, Cleare AJ, et al. Subregional hippocampal deformations in major depressive disorder. *J Affective Disord.* (2010) 126:272–77. doi: 10.1016/j.jad.2010.03.004
8. Maller JJ, Daskalakis ZJ, Fitzgerald PB. Hippocampal volumetrics in depression: the importance of the posterior tail. *Hippocampus*. (2007) 17:1023–27. doi: 10.1002/hipo.20339
9. Cao B, Passos IC, Mwangi B, Amaral-Silva H, Tannous J, Wu MJ. Hippocampal subfield volumes in mood disorders. *Mol Psychiatry*. (2017) 22:1352–58. doi: 10.1038/mp.2016.262
10. MacQueen GM, Yucel K, Taylor VH, Macdonald K, Joffe R. Posterior hippocampal volumes are associated with remission rates in patients with major depressive disorder. *Biol Psychiatry*. (2008) 64:880–83. doi: 10.1016/j.biopsych.2008.06.027
11. Maller JJ, Broadhouse K, Rush AJ, Gordon E, Koslow S, Grieve SM. Increased hippocampal tail volume predicts depression status and remission to antidepressant medications in major depression. *Mol Psychiatry*. (2018) 23:1737–44. doi: 10.1038/mp.2017.224
12. Nogovitsyn N, Muller M, Souza R, Hassel S, Arnott SR, Davis AD. Hippocampal tail volume as a predictive biomarker of antidepressant treatment outcomes in patients with major depressive disorder: a CAN-BIND report. *Neuropsychopharmacology*. (2020) 45:283–91. doi: 10.1038/s41386-019-0542-1
13. Sheline YI, Gado MH, Kraemer HC. Untreated depression and hippocampal volume loss. *Am J Psychiatry*. (2003) 160:1516–8. doi: 10.1176/appi.ajp.160.8.1516
14. Czeh B, Michaelis T, Watanabe T, Frahm J, de Biurrun G, van Kampen M, et al. Stress-induced changes in cerebral metabolites, hippocampal volume, and cell proliferation are prevented by antidepressant treatment with tianeptine. *Proc Natl Acad Sci*. (2001) 98:12796–801. doi: 10.1073/pnas.211427898
15. Li YF, Zhang YZ, Liu YQ, Wang HL, Yuan L, Luo ZP. Moclobemide up-regulates proliferation of hippocampal progenitor cells in chronically stressed mice. *Acta Pharmacol Sin*. (2004) 25:1408–12.
16. Enneking V, Leehr EJ, Dannlowski U, Redlich R. Brain structural effects of treatments for depression and biomarkers of response: a systematic review of neuroimaging studies. *Psychol Med*. (2020) 50:187–209. doi: 10.1017/S0033291719003660
17. Dunlop BW, Binder EB, Cubells JF, Goodman MM, Kelley ME, Kinkead B. Predictors of remission in depression to individual and combined treatments (PReDICT): study protocol for a randomized controlled trial. *Trials*. (2012) 13:106. doi: 10.1186/1745-6215-13-106
18. Hamilton M. A rating scale for depression. *J Neurol Neurosurg Psychiatry*. (1960) 23:56–62. doi: 10.1136/jnnp.23.1.56
19. Reuter M, Schmansky NJ, Rosas HD, Fischl B. Within-subject template estimation for unbiased longitudinal image analysis. *Neuroimage*. (2012) 61:1402–18. doi: 10.1016/j.neuroimage.2012.02.084
20. Iglesias JE, Augustinack JC, Nguyen K, Player CM, Player A, Wright M. A computational atlas of the hippocampal formation using *ex vivo*, ultra-high resolution MRI: application to adaptive segmentation of *in vivo* MRI. *Neuroimage*. (2015) 115:117–37. doi: 10.1016/j.neuroimage.2015.04.042
21. Love J, Damian D, Selker R. *The Jamovi Project*. (2021) (version 1.6). Computer. Available online at: www.jamovi.org.
22. Meshi D, Drew MR, Saxe M, Ansorge MS, David D, Santarelli L, et al. Hippocampal neurogenesis is not required for behavioral effects of environmental enrichment. *Nat Neurosci*. (2006) 9:729–31. doi: 10.1038/nn1696
23. Arnone D, McKie S, Elliott R, Juhasz G, Thomas EJ, Downey D, et al. State-dependent changes in hippocampal grey matter in depression. *Mol Psychiatry*. (2013) 18:1265–72. doi: 10.1038/mp.2012.150
24. Frodl T, Jäger M, Smajstrlova I, Born C, Bottlender R, Palladino T. Effect of hippocampal and amygdala volumes on clinical outcomes in major depression: a 3-year prospective magnetic resonance imaging study. *J Psychiatry Neurosci*. (2008) 33:423–30.
25. Santarelli L. Requirement of hippocampal neurogenesis for the behavioral effects of antidepressants. *Science*. (2003) 301:805–9. doi: 10.1126/science.1083328
26. Manji HK, Moore GJ, Chen G. Clinical and preclinical evidence for the neurotrophic effects of mood stabilizers: implications for the pathophysiology and treatment of manic–depressive illness. *Biol Psychiatry*. (2000) 48:740–54. doi: 10.1016/S0006-3223(00)00979-3
27. Magariños AM, Deslandes A, McEwen BS. Effects of antidepressants and benzodiazepine treatments on the dendritic structure of CA3 pyramidal neurons after chronic stress. *Eur J Pharmacol*. (1999) 371:113–22. doi: 10.1016/S0014-2999(99)00163-6
28. Van der Hart MG, Czéh B, de Biurrun G, Michaelis T, Watanabe T, Natt O, et al. Substance P receptor antagonist and clomipramine prevent stress-induced alterations in cerebral metabolites, cytogenesis in the dentate gyrus and hippocampal volume. *Mol Psychiatry*. (2002) 7:933–41. doi: 10.1038/sj.mp.4001130
29. Hao S, Tang B, Wu Z, Ure K, Sun Y, Tao H, et al. Forniceal deep brain stimulation rescues hippocampal memory in rett syndrome mice. *Nature*. (2015) 526:430–34. doi: 10.1038/nature15694
30. Dunlop BW, Granros M, Lechner A, Mletzko-Crowe T, Nemeroff CB, Mayberg HS, et al. Recall accuracy for the symptoms of a major depressive episode among clinical trial participants. *J Psychiatr Res*. (2019) 116:178–84. doi: 10.1016/j.jpsychires.2019.03.008
31. Frodl T, Meisenzahl EM, Zetzsche T, Born C, Groll C, Jäger M, et al. hippocampal changes in patients with a first episode of major depression. *Am J Psychiatry*. (2002) 159:1112–18. doi: 10.1176/appi.ajp.159.7.1112
32. Opel N, Redlich R, Zwanzger P, Grotegerd D, Arolt V, Heindel W, et al. Hippocampal atrophy in major depression: a function of childhood maltreatment rather than diagnosis? *Neuropsychopharmacology*. (2014) 39:2723–31. doi: 10.1038/npp.2014.145
33. Schmidt HD, Duman RS. The role of neurotrophic factors in adult hippocampal neurogenesis, antidepressant treatments and animal models of depressive-like behavior. *Behav Pharmacol*. (2007) 18:391–418. doi: 10.1097/FBP.0b013e3282ee2aa8

Conflict of Interest: BD has received research support from Acadia, Compass, Aptinyx, NIMH, Sage, and Takeda, and has served as a consultant to Greenwich Biosciences, Myriad Neuroscience, Otsuka, Sage, and Sophren Therapeutics.

The remaining authors declare that the research was conducted in the absence of any commercial or financial relationships that could be construed as a potential conflict of interest.

Publisher's Note: All claims expressed in this article are solely those of the authors and do not necessarily represent those of their affiliated organizations, or those of the publisher, the editors and the reviewers. Any product that may be evaluated in this article, or claim that may be made by its manufacturer, is not guaranteed or endorsed by the publisher.

Advantages of publishing in Frontiers

OPEN ACCESS
Articles are free to read for greatest visibility and readership

FAST PUBLICATION
Around 90 days from submission to decision

HIGH QUALITY PEER-REVIEW
Rigorous, collaborative, and constructive peer-review

TRANSPARENT PEER-REVIEW
Editors and reviewers acknowledged by name on published articles

Frontiers
Avenue du Tribunal-Fédéral 34
1005 Lausanne | Switzerland

Visit us: www.frontiersin.org
Contact us: frontiersin.org/about/contact

REPRODUCIBILITY OF RESEARCH
Support open data and methods to enhance research reproducibility

DIGITAL PUBLISHING
Articles designed for optimal readership across devices

FOLLOW US
@frontiersin

IMPACT METRICS
Advanced article metrics track visibility across digital media

EXTENSIVE PROMOTION
Marketing and promotion of impactful research

LOOP RESEARCH NETWORK
Our network increases your article's readership